Tomas Bata University in Zlín
Faculty of Technology

Habilitation Thesis

Conducting Polymer Scaffolds – the Technology of Preparation and Cytocompatibility

Vodivé polymerní scaffoldy – technologie přípravy a cytokompatibilita

Ing. Zdenka Capáková, Ph.D.

Technology of Macromolecular Compounds

Zlín, 2021

Keywords: *biomaterials, cytocompatibility, conducting polymers, stimuli-responsive materials.*

Klíčová slova: *biomateriály, cytokompatibilita, vodivé polymery, stimuli-responsivní materiály.*

A full text of the habilitation thesis is available in the library of Tomas Bata University in Zlín.

ACKNOWLEDGMENTS

In my life, both personal and professional, I have met many people who have influenced me and to whom my thanks belongs. Although, it is not possible to name them all. I am immensely grateful to Petr Humpolíček for his patience and his guidence throughout my whole research career. I am also indebted to willing person Věra Kašpárková for her help and kindness. Moreover, my thanks also tend to Jaroslav Stejskal and Patrycja Bober for sharing of their immense knowledge in the field of conductive polymers.

I would like to thank also to my family, my parents and siblings for supporting me all my life. An infinite number of thanks belong to the exeptional person, my partner Jan Vícha for motivation, dicussions and encouragement.

I would like to express my gratitude also to prof. Ing. Petr Sáha, CSc., doc. Dr. Ing. Vladimír Pavlínek and prof. Ing. Vladimír Sedlařík, Ph.D. for the opportunity to be part of the Centre of Polymer Systems on Tomas Bata University.

ABSTRACT

This habilitation thesis summarises studies performed on conducting polymers, especially polyaniline and polypyrrole, during more than ten years of research. In the course of time, various procedures for polymer synthesis and a number of modification techniques were employed, giving rise to a wide variety of conducting materials or their composites. Prepared conducting polymers and their composites were deeply characterized in terms of their material properties, with special interest paid to their surface properties. The thesis also sums up unique and original results documenting improvements in the cytocompatibility of these conducting polymers and composites. Especially the composites with biopolymers are unique in terms of their cytocompatibility. The new knowledge gained in this field resulted in the preparation of cytocompatible conducting scaffolds with target applications in tissue engineering.

ABSTRAKT

Habilitační práce shrnuje více než desetiletou práci uchazečky v oblasti studia elektricky vodivých polymerů, zejména pak polyanilinu a polypyrrolu. Za oněch deset let využila uchazečka ve své práci řadu postupů syntézy vodivých polymerů a jejich modifikací. Výsledkem je široká škála připravených vodivých polymerů a jejich kompozitů. Připravené materiály byly detailně studovány z hlediska materiálových, především povrchových, vlastností. Teze sumarizují především oblast originální uchazeččiny práce zaměřené na zlepšení buněčné kompatibility vodivých polymerů a jejich kompozitů. Obzvláštní pozornost zasluhují kompozity s biopolymery, které vykazují unikátní biologické vlastnosti. Nové znalosti, které vzniky díky práci uchazečky, vyústily v přípravu tkáňových lešení vhodných pro oblast tkáňového inženýrství.

TABLE OF CONTENT

ACKNOWLEDGMENTS **3**
ABSTRACT **4**
ABSTRAKT **5**
TABLE OF CONTENT **6**
LIST OF PUBLICATIONS RELATED TO THESIS **7**
INTRODUCTION **9**
1 BIOMATERIALS **10**
1.1 POLYMERS **11**
1.1.1 CLASSIFICATION OF POLYMERS BASED ON THEIR ORIGIN 12
1.2 PROPERTIES OF BIOMATERIALS **12**
1.2.1 MATERIAL PROPERTIES 13
1.2.2 BIOLOGICAL PROPERTIES – BIOCOMPATIBILITY 14
2 BIOELECTRICITY **17**
2.1 ELECTRICALLY CONDUCTING POLYMERS **18**
2.1.1 PREAPARATION OF CONDUCTING POLYMERS 19
2.1.2 MODIFICATIONS OF POLYMERS 22
3 CYTOCOMPATIBILITY OF CONDUCTING POLYMERS **28**
3.1 PANI - POWDERS **28**
3.2 PANI – COLLOIDAL DISPERSIONS **29**
3.3 PANI – FILMS **32**
3.4 PANI – FILMS PREPARED IN COLLOIDAL MODE **34**
3.5 PANI AND PPY – COMPARISON OF BIOCOMPATIBILITY **35**
4 SCAFFOLDS – PREPARATION AND CYTOTOXOMPATIBILITY **38**
5 CONTRIBUTION TO SCIENCE AND PRACTICE **43**
6 FUTURE PERSPECTIVE **46**
LIST OF FIGURES **47**
LIST OF TABLES **48**
LIST OF SYMBOLS AND ABBREVIATIONS **49**
REFERENCES **51**
CURRICULUM VITAE **60**

LIST OF PUBLICATIONS RELATED TO THESIS

Article I. Rejmontova, P.; **Capakova, Z**.; Mikusova, N.; Marakova, N.; Kasparkova, V.; Lehocky, M.; Humpolicek, P. Adhesion, Proliferation and Migration of NIH/3T3 Cells on Modified Polyaniline Surfaces. Int. J. Mol. Sci. 2016, 17 (9), 1439. https://doi.org/10.3390/ijms17091439.

Article II. Della Pina, C.; **Capakova, Z**.; Sironi, A.; Humpolicek, P.; Saha, P.; Falletta, E. On the Cytotoxicity of Poly(4-Aminodiphenylaniline) Powders: Effect of Acid Dopant Type and Sample Posttreatment. Int. J. Polym. Mater. Polym. Biomat. 2017, 66 (3), 132–138. https://doi.org/10.1080/00914037.2016.1190928.

Article III. Humpolicek, P.; **Kucekova, Z**.; Kasparkova, V.; Pelkova, J.; Modic, M.; Junkar, I.; Trchova, M.; Bober, P.; Stejskal, J.; Lehocky, M. Blood Coagulation and Platelet Adhesion on Polyaniline Films. Colloid Surf. B-Biointerfaces 2015, 133, 278–285. https://doi.org/10.1016/j.colsurfb.2015.06.008.

Article IV. Kasparkova, V.; Humpolicek, P.; Stejskal, J.; Kopecka, J.; **Kucekova, Z**.; Moucka, R. Conductivity, Impurity Profile, and Cytotoxicity of Solvent-Extracted Polyaniline. Polym. Adv. Technol. 2016, 27 (2), 156–161. https://doi.org/10.1002/pat.3611.

Article V. Kucekova, Z.; Humpolicek, P.; Kasparkova, V.; Perecko, T.; Lehocky, M.; Hauerlandova, I.; Saha, P.; Stejskal, J. Colloidal Polyaniline Dispersions: Antibacterial Activity, Cytotoxicity and Neutrophil Oxidative Burst. Colloid Surf. B-Biointerfaces 2014, 116, 411–417. https://doi.org/10.1016/j.colsurfb.2014.01.027.

Article VI. Kasparkova, V.; Jasenska, D.; **Capakova, Z**.; Marakova, N.; Stejskal, J.; Bober, P.; Lehocky, M.; Humpolicek, P. Polyaniline Colloids Stabilized with Bioactive Polysaccharides: Non-Cytotoxic Antibacterial Materials. Carbohydr. Polym. 2019, 219, 423–430. https://doi.org/10.1016/j.carbpol.2019.05.038.

Article VII. Kasparkova, V.; Humpolicek, P.; **Capakova, Z**.; Bober, P.; Stejskal, J.; Trchova, M.; Rejmontova, P.; Junkar, I.; Lehocky, M.; Mozetic, M. Cell-Compatible Conducting Polyaniline Films Prepared in Colloidal Dispersion Mode. Colloid Surf. B-Biointerfaces 2017, 157, 309–316. https://doi.org/10.1016/j.colsurfb.2017.05.066.

Article VIII. Humpolicek, P.; Kasparkova, V.; Pachernik, J.; Stejskal, J.; Bober, P.; **Capakova, Z**.; Radaszkiewicz, K. A.; Junkar, I.; Lehocky, M. The Biocompatibility of Polyaniline and Polypyrrole: A Comparative Study of Their Cytotoxicity, Embryotoxicity and Impurity Profile. Mater. Sci. Eng. C-Mater. Biol. Appl. 2018, 91, 303–310. https://doi.org/10.1016/j.msec.2018.05.037.

Article IX. Capakova, Z.; Radaszkiewicz, K. A.; Acharya, U.; Truong, T. H.; Pachernik, J.; Bober, P.; Kasparkova, V.; Stejskal, J.; Pfleger, J.; Lehocky, M.; Humpolicek, P. The Biocompatibility of Polyaniline and Polypyrrole 2(1): Doping with Organic Phosphonates. Mater. Sci. Eng. C-Mater. Biol. Appl. 2020, 113, 110986. https://doi.org/10.1016/j.msec.2020.110986.

Article X. Rejmontova, P.; Kovalcik, A.; Humpolicek, P.; **Capakova, Z**.; Wrzecionko, E.; Saha, P. The Use of Fractionated Kraft Lignin to Improve the Mechanical and Biological Properties of PVA-Based Scaffolds. RSC Adv. 2019, 9 (22), 12346–12353. https://doi.org/10.1039/c8ra09757g.

Article XI. Munster, L.; **Capakova, Z**.; Fisera, M.; Kuritka, I.; Vicha, J. Biocompatible Dialdehyde Cellulose/Poly(Vinyl Alcohol) Hydrogels with Tunable Properties. Carbohydr. Polym. 2019, 218, 333–342. https://doi.org/10.1016/j.carbpol.2019.04.091.

Article XII. Muchová, M.; Münster, L.; **Capáková, Z**.; Mikulcová, V.; Kuřitka, I.; Vícha, J. Design of Dialdehyde Cellulose Crosslinked Poly(Vinyl Alcohol) Hydrogels for Transdermal Drug Delivery and Wound Dressings. Materials Science and Engineering: C 2020, 116, 111242. https://doi.org/10.1016/j.msec.2020.111242.

Article XIII. Humpolicek, P.; Radaszkiewicz, K. A.; **Capakova, Z**.; Pachernik, J.; Bober, P.; Kasparkova, V.; Rejmontova, P.; Lehocky, M.; Ponizil, P.; Stejskal, J. Polyaniline Cryogels: Biocompatibility of Novel Conducting Macroporous Material. Sci Rep 2018, 8, 135. https://doi.org/10.1038/s41598-017-18290-1.

Article XIV. Bober, P.; **Capakova, Z**.; Acharya, U.; Zasonska, B. A.; Humpolicek, P.; Hodan, J.; Hromadkova, J.; Stejskal, J. Highly Conducting and Biocompatible Polypyrrole/Poly(Vinyl Alcohol) Cryogels. Synth. Met. 2019, 252, 122–126. https://doi.org/10.1016/j.synthmet.2019.04.015.

INTRODUCTION

Thousands of surgical procedures are performed globally on a daily basis due to the need to replace or repair of tissues which have been damaged by disease or injury. This is made possible by the enormous progress in material science, which has led to the preparation of biocompatible materials suitable for the fabrication of medical devices – otherwise known as biomaterials. Biomaterial science has matured in the last few decades and become a highly interdisciplinary field. An important part of biomaterial science is the field of polymer science. The development of biocompatible polymers and their utilization as biomaterials have significantly contributed to progress in modern medicine. The chief advantage of using polymers is the ability to control their shape and size, as well as their functionalities and mechanical properties, in order to fabricate products with the desired properties for a specific use. However, considering the complexity of the human body, the field of biomaterials is still open to new discoveries and inventions. Hence, new biomaterials with new applications are continually being developed in the biomedical area. This includes the synthesis, fabrication, design, and selection of such materials. The increasing demand for the development of superior biomaterials with new applications has resulted in efforts to create smart biomaterials.

Smart biomaterials are sophisticated materials which are able to respond to various external chemical and physical stimuli, and to changes in physiological parameters. They can be sensitive to pH, temperature, redox potential, stress, and electrical fields. The development of such stimuli-responsive materials with properties tailored to specific applications is a very challenging task for researchers worldwide. Electro-conducting materials are classified as one such smart biomaterial. They allow for current conduction and thus the modification of cell behaviour. Conducting polymers are an excellent choice for the preparation of such smart materials. However, a lack of fundamental understanding of the impact of various forms of conducting polymers on cell behaviour has been the major limitation on their utilization in biomaterials sciences. Hence, the biological characterization of various conducting polymers and their composites, prepared by a variety of means, is the main topic of this work, this thesis, and my research career. My interest focuses especially on two of them: polyaniline and polypyrrole.

1 BIOMATERIALS

Nowadays, modern medicine is unthinkable without the use of biomaterials. Thanks to the utilization of various biomaterials, the quality of healthcare has rapidly increased. Biomaterials are used in a broad range of applications, from disposable medical devices (e.g. blood bags), through contact lenses, to medical implants. Although humans have used biomaterials since the dawn of history, their development has accelerated over the last 50 years. However, there is still demand for new biomaterials with better properties. Indeed, it is not sufficient for a biomaterial merely to be biocompatible and to serve as a simple replacement; it should also have additional advanced properties, such as health-promoting function(s).

Biomaterials can be defined in several ways. Indeed, definitions have been evolving in the same manner as biomaterials themselves. Originally (in 1987), the European Society for Biomaterials Consensus Conference II proposed the following simple definition "*A biomaterial is a material intended to interface with biological systems to evaluate, treat, augment or replace any tissue, organ or function of the body*"[1]. Currently, one of the most broadly accepted definitions states that "*A biomaterial is any substance or combination of substances, other than drugs, synthetic or natural in origin, which can be used for any period of time, which augments or replaces partially or totally any tissue, organ or function of the body, in order to maintain or improve the quality of life of the individual*"[2,3]. However, both these definitions agree that a biomaterial is essentially a material which interacts with the human body. The material can be both natural and synthetic and it can come into contact with organisms in a direct or indirect way. Consequently, the material which is in contact with the body can influence its physiology or more generally its biological function. Therefore, biocompatibility is its first and most crucial characteristic, which is to say that biomaterials cannot elicit any harmful effects in or on organisms.

Each of a substance's material properties, however, is able to affect the substance's overall biocompatibility. All of them together, including chemical composition and surface, mechanical and physical properties, must therefore be considered in this context. Unfortunately, there is no exact "recipe" for preparing materials with a combination of properties which would ensure biocompatibility. Which properties are desirable depends on where the biomaterial is to be applied and on its expected function. The basic classification of material properties affecting host response covers surface and bulk properties and will be described in more detail below.

Metals, ceramics, glass, and polymers or their composites can be utilised as biomaterials[4,5]. Metals and their alloys are widely used as load bearing implants

or internal fixation materials, such as screws, wires etc. The biggest advantages are their strength and easy sterilization[5]. However, among their disadvantages includes corrosion due to chemical reaction with body enzymes or acids[6]. Ceramics are also known for their strength, stiffness, and hardness[7]. They generally find applications in the repair of the skeletal system, i.e. bones, joints, and teeth[8]. Biomaterials based on glass are also intended for use in the skeletal system, e.g. for the correction of bone defects or as composites in dentistry[9]. All the above mentioned materials find application mainly in hard tissues, and their mechanical properties are not suitable for soft tissue engineering. The sophisticated nature of soft tissue can, however, be mimicked by polymers,[10] whose utilization in biomedical sciences is more diverse than that of metallic, ceramic, or glass materials.

1.1 Polymers

The term polymer was introduced in 1833 by the Swedish chemist Jöns Jacob Berzelius[11] who described compounds with identical empirical formulas but different properties[12]. However, as organic chemistry developed, his characterization was shown to be too simplistic. The modern conception of polymers is connected with the German chemist Hermann Staudinger, who proposed that macromolecules are covalently bonded monomers composed of more than 1000 atoms[12,13]. Later in 1953, Staudinger was awarded the Nobel Prize for his contribution to chemistry[14].

Since Staudinger's times, progress in the development of polymeric materials has been great. Now, polymers play an important role in almost every area of modern life, touching almost every aspect of our lives. For example, water bottles, food packaging, toys, textile fibres, tires, and even computers and mobile telephones all contain polymers[15–17]. Polymeric material can have unique properties which depend on many factors, such as the type of bonded molecules and the nature of the bonds, the size of the macromolecules, and the strength of the intermolecular bonds[18,19]. They can have great flexibility and can bend and stretch (e.g. rubber) or be hard and tough (e.g. epoxies). Also, they can be produced in various desired shapes[5].

Nowadays, polymers are also the most widely-used materials in medicine[5], where they can be used both as medical devices and in tissue engineering. Implantable devices, catheters, vascular grafts, and drug delivery systems can serve as examples[20]. Currently, polymers are one of the cornerstones of tissue engineering[10].

Polymers can be classified in different ways – for example, according to their origin, structure, monomer, molecular forces, tacticity, and mode of polymerization[21,22]. Classification based on the source of origin is the most relevant for this thesis and therefore this class will be discussed further.

1.1.1 Classification of polymers based on their origin

As the name suggests, the origin of natural polymers lies in natural materials, mostly in plants and animals, but such polymers can also be of microbial origin. Natural polymers are also essential for human beings. According to the book Polymer Chemistry[23], they can be further classified under:

- polysaccharides,
- proteins and polypeptides,
- polynucleotides,
- polyesters,
- polyisoprenes.

In general, natural polymers exhibit good biocompatibility, but they can also easily undergo degradation processes. Moreover, they are variable in their properties depending on the source of their origin. This somewhat limits their practical application[24].

Semi-synthetic polymers are derived from natural polymers, which have undergone further chemical modification to improve their properties. They include, for example, cellulose nitrate and cellulose acetate[25].

Synthetic polymers comprise a large group of man-made polymers. They are commonly used in various industrial branches, such as packaging, the car industry, and mobile phones, as well as in medicine and pharmacy. Among their advantages are their versatility, the capacity to be fabricated in various shapes, and the possession of good mechanical properties, strength, or chemical inertness[26]. On the other hand, they are not without disadvantages. In this respect, poor biocompatibility and negative impacts on the environment can be mentioned. However, these shortcomings can be suppressed thanks to their modifications[27,28]. This topic will be discussed further in the work.

Within my research, synthetic (poly(vinyl alcohol) (PVA), N-poly(vinylpyrrolidone) (PVP) as well as natural (chitosan, cellulose or hyaluronic acid) polymers have been investigated. A special category of synthetic polymers are conducting polymers, mainly polyaniline (PANI) and polypyrrole (PPy), which will be discussed in more detail in part 2.1.1 of this thesis.

1.2 Properties of biomaterials

The properties of biomaterials can be classified into the two main groups: 1) material properties and 2) biological properties[29]. As already mentioned, these two groups are closely connected and affect each other. No matter whether we are considering chemical composition, or mechanical or physical properties, all such properties can directly influence the biocompatibility of the material.

1.2.1 Material properties

Material properties play an important role in the development of new biomaterials. No matter whether we are talking about physical, chemical or mechanical properties, all are able to directly influence the host response. Material properties cover both surface and bulk properties[30]. This topic is described in more detail in teaching materials prepared by myself within the framework of project No. CZ.02.2.69/0.0/0.0/16_018/0002720 .

1.2.1.1 Surface properties

The surface is the first "part" of any material which comes into contact with the organism (i.e., when considering materials used in direct contact with the body). The very first phenomenon which occurs after contact between the biomaterial and the host organism is protein adsorption onto the material surface. The type as well as amount of adsorbed proteins affects the adhered cells in respect of their physiology and cellular signalling pathways. Therefore, protein adsorption plays an important role in the future fate of cell adhesion, proliferation, and differentiation, etc. The surface immobilization of proteins is explained by a process called the Vroman effect[31].

Protein adsorption is influenced by a broad range of factors including the physical as well as chemical properties of the material surface[29]. For example, surface properties such as free energy, charge, wettability, functional groups, or topography affect protein adsorption and, therefore, the final biocompatibility of the material. In the case of conducting polymers, conductivity should also be included.

1.2.1.2 Bulk properties

After the cells have adhered to the surface of material, the physical, chemical and material properties of the bulk material directly influence the dynamic interactions at the interface between the cells and the biomaterial, which subsequently affect cell fate.

Generally, the first prerequisite for successful cell adhesion is conditioned by the requirement that biomaterials should mimic the properties of native tissue, according to the exact location of the intended use[30]. Therefore, it is very important to consider whether the biomaterial will be utilized in soft or hard tissue, etc. As their names suggest, soft or elastic materials are desirable for soft tissues. By contrast, rigid and tight materials are more suitable for hard tissues.

Bulk properties of materials directly influence dynamic interactions at tissue/biomaterial interfaces. Among the most important are two interrelated characteristics - mechanical properties and the architecture (porosity) of the material. The size, shape, orientation, and distribution of pores influence the mechanical properties of the bulk, as they define the structure and

dimensions[32,33]. It is desirable to mimic the physicochemical properties of native tissues that the biomaterials are intended to replace or augment.

Nevertheless, even if the "perfect material" – one exhibiting "perfect" chemical physical and structural properties – were to be created, biological compatibility would still have to be ensured. Thus, biocompatibility testing is, and always will be, necessary.

1.2.2 Biological properties – biocompatibility

The most common term characterising the suitability of the biological properties of biomaterials is biocompatibility[34]. The first definition of biocompatibility came from Williams, who defined biocompatibility in 1987 as "*the ability of a material to perform with an appropriate host response in a specific situation*"[35]. However, over time, this simple definition proved insufficient, which led to a re-definition of the term in 2008 by Williams himself. This definition is commonly used until today. Its exact wording is: "*The ability of a material to perform its desired function with respect to a medical therapy, without eliciting any undesirable local or systemic effects in the recipient or beneficiary of that therapy, but generating the most appropriate beneficial cellular or tissue response in that specific situation, and optimizing the clinically relevant performance of that therapy*"[36].

The biocompatibility of a material is a very complex characteristic, which involves various biological properties. A biocompatible material has to fulfil several conditions, e.g. it has to be non-cytotoxic, non-immunogenic, non-irritant, non-inflammatory, and non-carcinogenic[37]. To test the biocompatibility of a material, a series of different tests has to be performed. The exact types of tests depend on the anticipated future utilization of the material. There are numerous aspects determining the extent of biological testing. Here, we can mention, for example, the nature of biomaterial contact with the organism, which is classified as external contact, surface contact, or implantation. The duration of the contact (limited, prolonged, or permanent) is another important aspect of biocompatibility. Indeed, there is a legislative framework defining specifications which the material or device has to meet[38].

The evaluation of cytotoxicity, in contrast, has to be accomplished no matter what the intended utilization of the biomaterial is. It is one of the first tests performed for every biomaterial[38].

After the evaluation of cytotoxicity, the material undergoes other types of biological testing, which may include carcinogenicity, chronic toxicity, genotoxicity, immune response, skin sensitization and irritation, intracutaneous reactivity, and reproductive toxicity, among others.

1.2.2.1 Biocompatibility testing

The biocompatibility testing of a material or product is a long procedure. As already mentioned above, it involves a broad range of biological tests, which starts with *in vitro* testing, continues with *in vivo* testing, and ends with clinical testing[39]. During my research career, I have specialized on *in vitro* tests, which are briefly introduced in the following sections. For *in vitro* testing, a number of cell lines can be utilized[34]. There are several cell lines available for such testing and which can differ in tissue origin, genus origin, and life span, etc. The correct choice of cell line depends mainly on the expected utilization of the tested material. Within my research various cell lines have been used. Mouse embryonic fibroblast (NIH/3T3) and human immortalized keratinocytes (HaCaT) are representatives of healthy cells, whilst human cells from lung carcinoma (A549) and hepatocellular carcinoma (HepG2) have mainly been used as cancer cell lines. In addition, stem cells such as human mesenchymal stem cells derived from bone marrow have also been utilised within my research.

Each *in vitro* biocompatibility test which I conduct starts with basic screening – the cytotoxicity test. As previously mentioned, cytotoxicity testing is crucial for every material, irrespective of its planned form of contact with the organsim. It can be stated that the results of cytotoxicity testing predetermine the future fate of the material. If the test is successful, the material can be further tested for other biological properties. If not, the material has to be further modified to reduce or eliminate its cytotoxicity.

Cytotoxicity can be determined through direct or indirect contact (agar diffusion) between the material and the organism and via the testing of aqueous extracts of the material according to protocol ISO 10 993, part 5[40]. The latter has to be considered because of the constant blood flow in the human body, which may cause the leaching of possible toxic substances from the material. Of these methods, testing in direct contact is the most sensitive as it is capable of detecting even weak cytotoxic effects. The choice of the method depends mainly on the nature of material. In my research, I have mostly conducted cytotoxicity tests on extracts and on materials in direct contact.

The level of material cytotoxicity can be tested quantitatively (e.g. by measuring of cell growth, metabolic activity) or qualitatively (by observing changes in cell morphology)[41]. The latter is important as the material can cause cytotoxicity in several ways; for instance, it can inhibit cell growth, it can trigger cell death, or it can provoke changes in cell structure resulting in changes in their morphology. Flow cytometry can be used to detect these parameters.

Flow cytometry is a technique used to detect the chemical and physical characteristics of cells – not only in research, but also in clinical practice. Flow cytometer is equipped with multiple lasers, which allow the detection of various cell characteristics based on the cell labelling; parameters such as cell viability,

type of cell death, enzymatic activity, the presence of antigens, and protein modifications, among others, can be determined[42]. This methodology was established by me at TBU.

Cell cultures for *in vitro* testing are grown as monolayers on tissue culture plastic and cells are thus not affected by flow or mechanical stress. Hence, although tests on cultures are fundamental for biocompatibility testing, they do not sufficiently mimic real *in vivo* conditions due to the absence of blood circulation, pressure, or shear stress. Hence, bioreactors, which resemble *in vivo* conditions, are employed for testing in my research. The mimicking of *in vivo* conditions can be achieved by the controlling of external parameters, such as shear stress, fluid flow, pressure, and other stimuli[43].

Another method for mimicking the influence of biomaterials on native tissues applied in my research is the use of reconstructed tissue models[44]. These models are made of specific cells and are produced as three dimensional, highly differentiated tissues with mitotic and metabolic activity simulating real tissues. They can include various tissues, such as skin[45], ocular, oral[46], intestinal[47], alveolar[48], and vaginal[49]. I worked with these models during an internship at MatTek corporation, which is a global leader in reliable *in vitro* human tissue model innovations. Currently, in our cell laboratory, we are working on research leading towards the production of our own reconstituted skin tissues.

2 BIOELECTRICITY

The effect of electric fields on the behaviour of cells and tissues, especially muscle and nerve, has been of interest for a long time[50,51]. The impact of electricity on muscle contractions was demonstrated as early as 1791 by Luigi Galvani[52]. In his work, he uncovered the fact that electricity occurs in living tissues. Later, in the 19th century, Emil du Bois-Reymond, following up the work of Galvani, reported the presence of electricity in wounds[53]. The electrical phenomena occurring in or generated by living organisms are termed bioelectricity. Interest in bioelectricity grew in the 20th century and led to the design of many commonly used medical devices. Today, it is well-known that electricity plays a role in many cellular processes, such as cell differentiation, cell division, and cell migration, and in signalling systems[54].

It is worth mentioning that the conduction of electric current, which is a stream of charged particles, can be accomplished either *via* the flow of electrons or the flow of ions, the latter being typical for bioelectric current[55]. This means that ions are the charge carriers in living tissues and organisms. This relates to one of the advantages of conducting polymers compared to other conducting materials such as metals. Conducting polymers (which will be discussed further) exhibit mixed conductivity – ionic and electronic – and can thus better "communicate" with living objects[56].

Bioelectricity is a result of electrical signalling proceeding through ion channels and pumps at or within the plasma membrane. Plasma membranes have the ability to create and maintain different charges on their opposite sides. This is because of differences between the ion concentrations in cytosol and outside the cell[57]. Several types of ions influence electric potential, but potassium, sodium and chloride ions are especially noteworthy. Intracellular fluid contains more positively charged potassium ions than extracellular fluids. By contrast, more positively charged sodium and negatively charged chloride ions are present outside cells. The semi-permeability of the plasma membrane plays an important role in this process, as sodium ions are not able to diffuse directly through the membrane but have to employ ion channels or active transport, in which an ion pump is involved[58]. The different concentrations of ions determine the potentials of cells and tissues. The strength of bioelectric potentials can vary from units to hundreds of millivolts in various tissues. Generally, undifferentiated cells exhibit a lower potential compared to fully differentiated ones. However, differences are also found among various types of differentiated cells. For example, the highest membrane potential can be found in muscle cells, where it is around -90 mV. In nerve cells, the typical value is around -70 mV, and for epithelial cells it is approximately -50 mV[59].

The effect of external electric fields on cell behaviour was demonstrated in a number of works. In this context, wound healing is the most discussed topic.

An essential process involved in wound healing is cell migration. Defective migration can lead to the formation of chronic wounds. An important aspect of migration is the direction in which migration takes place. In the last few decades it has been shown that an endogenous electric field can increase the rate of healing and provide cues that direct cells[60]. The effect of electrical fields on various cell lines has been the subject of numerous studies. It was confirmed, for example, that keratinocytes[61], fibroblasts[62], endothelial cells[63], lymphocytes [64], macrophages[65] and neuronal cells[66,67] are able to respond to weak electric fields that are externally applied.

2.1 Electrically conducting polymers

There is currently an enormous effort to develop biomaterials with "added value" – in literature, called "smart" or "intelligent" materials. Smart materials should have tailored properties and controlled functions which directly influence cell behaviour. These biomaterials should be able to respond to various environmental stimuli by changing their properties, such as biomechanical or drug-releasing features[68]. This means, for example, that they can be temperature or pH sensitive, or enzymatically active. As reported in the previous chapter, electric fields are able to influence cell behaviour. Therefore, conducting polymers could be useful with respect to the preparation of such smart biomaterials.

The materials with the best electrical conductivity are metals, of which the highest conductivity was measured for silver (6.3 S m^{-1} at 20 °C)[69]. However, the limited compatibility of some metals with living systems is often encountered in tissue engineering. The limitations are mainly connected to 1) their mechanical properties making them incompatible with soft tissues, and 2) the fact that the electric current is carried by electrons and not by ions. In light of these facts, conducting polymers are suitable candidates for the replacement of metals in the area of tissue engineering[50].

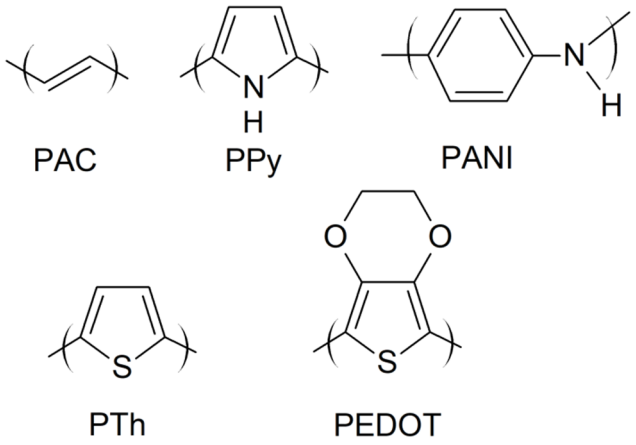

Fig. 1. *Examples of conductive polymers. PAC – polyacetylene, PPy – polypyrrole, PANI – polyaniline, PTh – polythiophene, PEDOT –poly(3,4-ethylenedioxythiophene).*

Polyacetylene (PAC), polypyrrole (PPy), polyaniline (PANI), and polythiophene (PTh) and its derivatives, such as poly(3,4-ethylenedioxythiophene) (PEDOT) belong to the family of conducting polymers (Fig. 1). Among these polymers, PAC exhibits the highest conductivity. On the other hand, PAC exhibits very low stability in air [70]. Therefore, this polymer is not suitable for further processing. With respect to processability, PANI and PPy are the best studied conducting polymers. They exhibit several advantages for applications in tissue engineering[71]. Among the most important is their mixed ionic and electronic conductivity, already mentioned in the previous chapter. Also their chemical, electrical and physical properties can be tailored for specific applications by using various dopants or by the incorporation of biological active substances such as enzymes and proteins, etc. The dopant agents are able to affect the conductivity of these polymers as well as their stability[72].

Conducting polymers can be prepared in two ways, chemically or electrochemically[73]. Thin films with a well-controlled thickness and morphology are commonly obtained by electrochemical synthesis, while various forms of these polymers can be produced by chemical synthesis. Depending on the polymer type, powders, films, colloidal suspensions, or hydrogels/cryogels can be prepared[74]. Therefore, chemical synthesis provides a wide range of suitable conducting materials for various applications. On the other hand, the electrochemical route leads to lower concentrations of unwanted by-products formed in the polymer during synthesis.

As mentioned above, most attention is devoted to two conducting polymers, PANI and PPy. This has also been true of my research. Therefore, a short description of their chemical preparation and properties is presented in the next chapter.

2.1.1 Preaparation of conducting polymers

The conducting polymers were for the first time produced several decades ago[74]. Today, they can be prepared by many methods. The most common is the oxidative polymerization[75]. Here, we will focus on the preparation of conducting polymers which are in the interest of this thesis – PANI and PPy.

2.1.1.1 Polyaniline

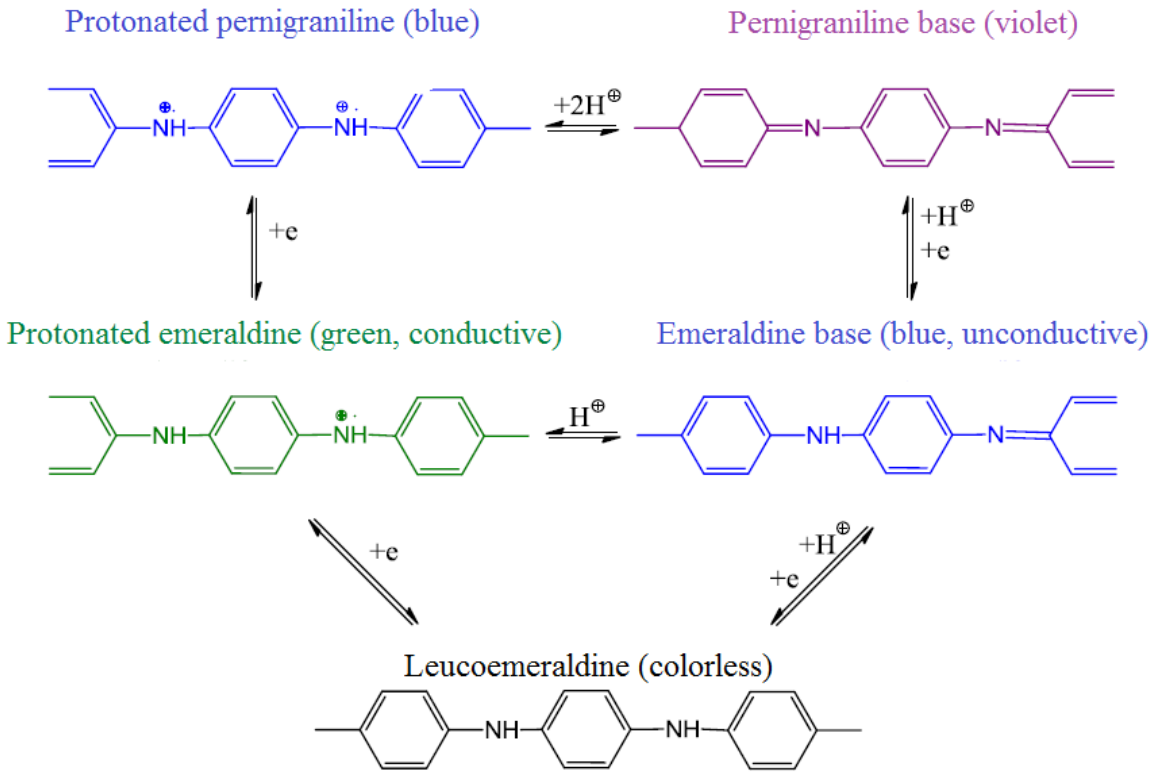

Fig. 2. *Oxidation forms of PANI.*

Polyaniline is an intensively studied conducting polymer. It has excellent electrical and optical properties, is easy to synthesize in high yields, and achieves good conductivity. However, its conductivity highly depends on its oxidation state (Fig. 2). Three types of polyaniline, differing in the degree of oxidation/reduction, are known: 1) the fully reduced form – leucoemeraldine, 2) the semi-oxidized form – emeraldine, and 3) the fully oxidized form - pernigraniline[76]. Emeraldine is the most stable and the most highly conducting PANI form.

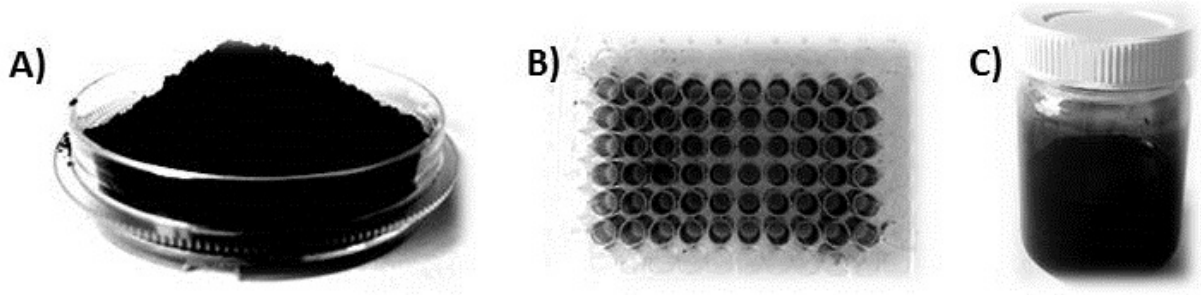

Fig. 3. *PANI in the formo f A) powder, B) film, C) colloidal dispersion.*

Pristine PANI can be manufactured in the form of a powder, film or colloidal dispersion (Fig. 3) depending on the preparation procedure. The standard

preparation of all three forms is well described in IUPAC technical reports[77,78]. Now, we will briefly focus on these procedures.

The preparation of PANI powders builds on the work in an *IUPAC technical report* written by Stejskal and Gilbert in 2002[77], in which PANI powder was prepared at various laboratories and the results were compared. The standard procedure is based on the oxidation of monomer aniline hydrochloride (AH) by an oxidation agent, namely ammonium peroxydisulfate (APS), in aqueous medium at laboratory temperature using concentrations of 0.2 M for AH and 0.25 M for APS. Both precursors are prepared in aqueous solutions, which are mixed together, stirred, and left to polymerize overnight. Thereafter, the polymerization mixture is filtered and the PANI precipitate is collected on the filter and washed with 0.2 M HCl and subsequently with acetone, before being dried. The greenish powder of PANI hydrochloride (emeraldine) is obtained by this procedure. According to the IUPAC technical report, the electrical conductivity of PANI prepared by this method was 4.4 ± 1.7 S cm^{-1} (the average of 59 samples).

The preparation of colloidal dispersions and thin films was also described in an IUPAC technical report three years later, in 2005. This report was written by Stejskal and Sapurina[78]. Similarly to the previous report, the procedure was conducted by various laboratories in six countries.

PANI films were prepared using the same concentrations of precursors used for PANI powder; i.e. 0.2 M AH and 0.25 M APS solutions were mixed together and the mixture poured onto the glass substrate at laboratory temperature. The polymerization was completed in 10 minutes and the substrates were washed with 0.2 M HCl and acetone and then dried in air. The great advantage of PANI films is their ability to cover various materials, such as silicon, polymers (e.g. polystyrene), or noble metals, which can all be used as substrates for the films. The thickness of the films prepared by this procedure is 125 ± 9 nm and they achieve a conductivity of 2.6 ± 0.7 S cm^{-1}.

The preparation of colloidal PANI dispersions is based on a similar method, as samples are synthetized using 0.2 M AH and 0.25 APS solutions. However, in addition, a suitable stabilizer has to be used to prepare the colloidal form of this polymer. Here, a water-soluble polymer is employed, specifically poly(*N*-vinylpyrrolidone) (PVP, M_r = 360 000). Briefly, the AH is dissolved in an aqueous solution of 2 mass % PVP, instead of water. This solution is mixed with a solution of APS, stirred, and left to polymerize. The polymerization is finished in several minutes. The average size of particles formed in colloidal dispersions prepared by this method is 241 ± 50 nm and the polydispersity is 0.26 ± 0.12.

2.1.1.2 Polypyrrole

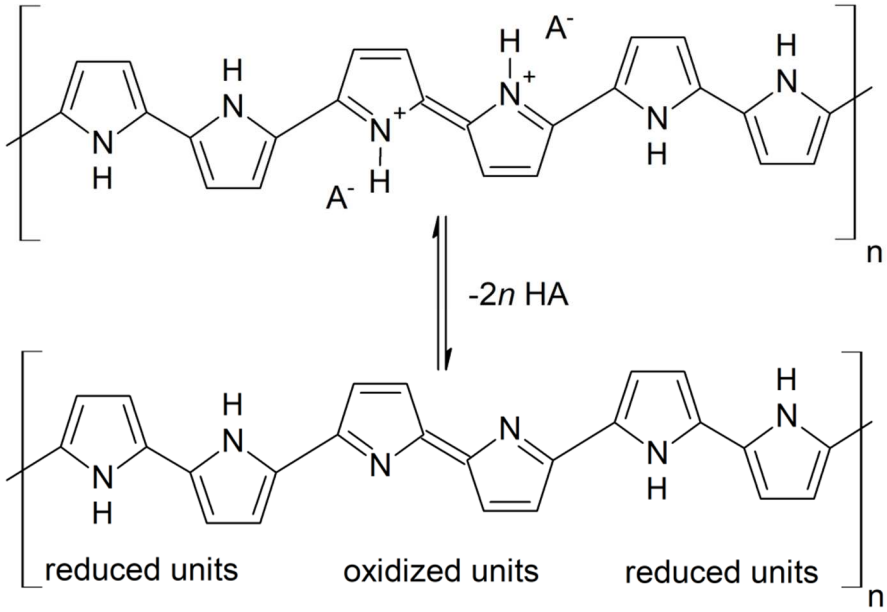

Fig. 4. *The molecular structure of protonated and deprotonated PPy.*

Similarly to PANI, the advantage of PPy is its easy preparation, environmental stability, and electrochemical activity[79]. PPy can be prepared in the form of powder[80], film[81] or colloid[82].

The oxidation of pyrrole can be performed by electrochemical[83] or chemical[84] means. The properties of PPy change depending on the degree of oxidation. The molecular structures of protonated and deprotonated PPy are depicted in fig. 4. For example, PPy films change colour from blue to dark black as the degrees ofoxidation and film thickness increase[85]. PPy conductivity ranges from units to tens of S cm^{-1} depending on the mode of preparation[86]. The most common procedure to synthesise polypyrrole is *via* the oxidation of pyrrole by iron (III) chloride[87,88]. The typical conductivity of PPy prepared in this way is 10^{-2} S cm^{-1} [89]. Additionally, ferric sulfate[90], ammonium persulfate[91], hexycyanoferrate[92], or ferric percholate[93] can be used as oxidizing agents.

2.1.2 Modifications of polymers

Any change in the polymer preparation process will result in changes in the properties of the final polymer. Preparation conditions can affect the molecular weight, morphology, conductivity, molecular structure, and also the biocompatibility of the resulting product. Therefore, modifications of conducting polymers are often desirable.

With increasingly demanding requirements with respect to polymer properties, the functionalization of macromolecules has evolved, leading to the production of complex and functional polymers. Functionalization is aimed at

improving polymer properties, such as their biocompatibility and their mechanical and/or surface properties. Various modifications can be employed to improve the properties of these materials. In general, modifications can be accomplished 1) before polymerization[94], 2) during synthesis[95] and 3) post-polymerization[96]. Modifications before polymerization usually include the functionalization of the precursors. Regarding post-polymerization methods, various chemical and physical modifications have been developed. Among the most commonly used physical methods are plasma treatment, ion implantation, and UV irradiation. Chemical methods are presented by a broad range of modifications, which result in changes in the chemical constitution or configuration of macromolecules. The surfaces of materials can be modified with amide, carboxylic, and hydroxyl groups, among many others. However, in addition to the desired positive effects, many types of functionalization are also associated with undesirable side effects, leading, for example, to the degradation of the material[97].

As mentioned before, the functionalization of polymers can be valuable as it can lead to improvements in their properties that are not accessible by direct polymerization of the monomer. Important characteristics, such as wettability, yield, polymer morphology, stability, and mechanical properties, can be changed[97]. And naturally, all of these properties have a final impact on the biocompatibility of the material.

2.1.2.1 Modification of conducting polymers

The modification and functionalization of conducting polymers can lead to improvements in their properties with respect to their various applications. For example, the incorporation of functional groups can improve the biocompatibility of such polymers and open them up for utilization in tissue engineering and biomedical areas. As a further example, the wettability of PANI can be changed simply through reprotonation by an acid. In the study of Stejskal et al.[98], forty two various acids were used for the reprotonation of PANI. While the contact angle of pristine PANI hydrochloride is above 49° [99], the measured contact angles after reprotonation varied from 29° to 102°. Therefore, it can be concluded that reprotonation can both increase and decrease the wettability of conducting polymers.

Another aspect which can be changed by a modification procedure is the morphology of PANI, which can vary according to the acidity of the reaction mixture during polymerization, this allowing PANI to be prepared with globular, nanofibrilar, or nanotubular morphology[100]. For example, globular PANI is obtained by the oxidation of monomer in strongly acidic conditions, while nanotubular PANI is obtained if the polymerization is conducted in less acidic conditions (e.g. in the presence of sulfuric acid)[101].

In the case of PPy, the morphology can be controlled by polymerization conducted in the presence of different azo dyes. For example, in the studies by

Hu et al.[102] and Yang et al.[103] methyl orange was used to obtain nanotubes with circular profiles. In another work, the replacement of methyl orange with ethyl orange led finally to PPy with a globular morphology[104]. In contrast, Yan and Han[105] used Acid red 1 for the synthesis of PPy with rectangular nanotube morphology.

Last but not least, the final product (in this case, PANI) can be significantly affected by the polymerization temperature. Stejskal et al.[106] studied the influence of polymerization run at 20 and −50 °C on molecular weight and observed that it increased at the lower polymerization temperature. The effect of temperature during polymerization was also studied by Bláha et al.,[107] who found that the molecular structure, morphology, and crystallinity of PANI can be controlled through the polymerization temperature.

When dealing with conducting polymers, the aspect of conductivity should not be forgotten. The most common method of influencing the conductivity of these polymers is to dope them with various agents, which may increase the conductivity by several orders of magnitude[74,106,108]; however, changes in the preparation technique can also influence the conductivity. For example, the polymerization temperature can strongly affect the conductivity of PANI[107,109]. Polymerization in the presence of various reaction media or the addition of other polymers are other approaches that can lead to changes in electrical properties[110].

In my work, several types of conducting polymer modifications have been employed, with the main focus on improving the biocompatibility of the materials. Now, I will briefly discuss examples of this research, which clearly document changes in material characteristics after modification.

In **article I.** the effect of PANI surface modifications on surface energy and their impact on biocompatibility were studied. Pristine PANI hydrochloride (PANI-S) and its deprotonated form (PANI-B) were prepared according to the IUPAC protocol[78]. Sulfamic, phosphotungstic, and poly(2-acrylamido-2-methyl-1-propanesulfonic) (PAMPSA) acids were used for modifications. Two types of preparation routes were studied: 1) using the acids as doping agents or 2) direct incorporation of the acids into the reaction mixture. Sulfamic and phosphotungstic acid were used as doping agents for PANI-B films, resulting in reprotonated films named PANI-SULF and PANI-PT. Polymeric acid PAMPSA was added to the reaction mixture in different concentrations. The mole ratio of aniline hydrochloride to PAMPSA was adjusted to 1:1 (PANI-PAMPSA-1:1) or 2:1 (PANI-PAMPSA-2:1).

Table 1. Surface energy evaluation of different surfaces.

	Surface energy components (mN m^{-1})		
Sample	γ^{tot}	γ^{LW}	γ^{AB}
PANI-S	52.54	46.05	6.49
PANI-B	50.88	46.54	4.35
PANI-SULF	52.13	44.97	7.17
PANI-PT	51.89	47.39	4.50
PANI-PAMPSA-1:1	41.85	40.98	0.87
PANI-PAMPSA-2:1	56.35	43.91	12.45

Note: γ^{tot} - total surface energy, γ^{LW} - disperse part of surface energy, γ^{AB} - polar part of surface energy. Data obtained from article I.[111].

The effect of the modifications on surface energy is shown in Tab. 1. Samples PANI-S, PANI-B, PANI-SULF and PANI-PT produced similar results. However, the modification with PAMPSA resulted in changes in surface energies. The most significant differences, compared to pristine PANI-S, were observed for PANI-PAMPSA-1:1, where the total surface energy decreased by about 20 %. By contrast, PANI-PAMPSA-2:1 slightly increased the surface energy compared to pristine PANI-S.

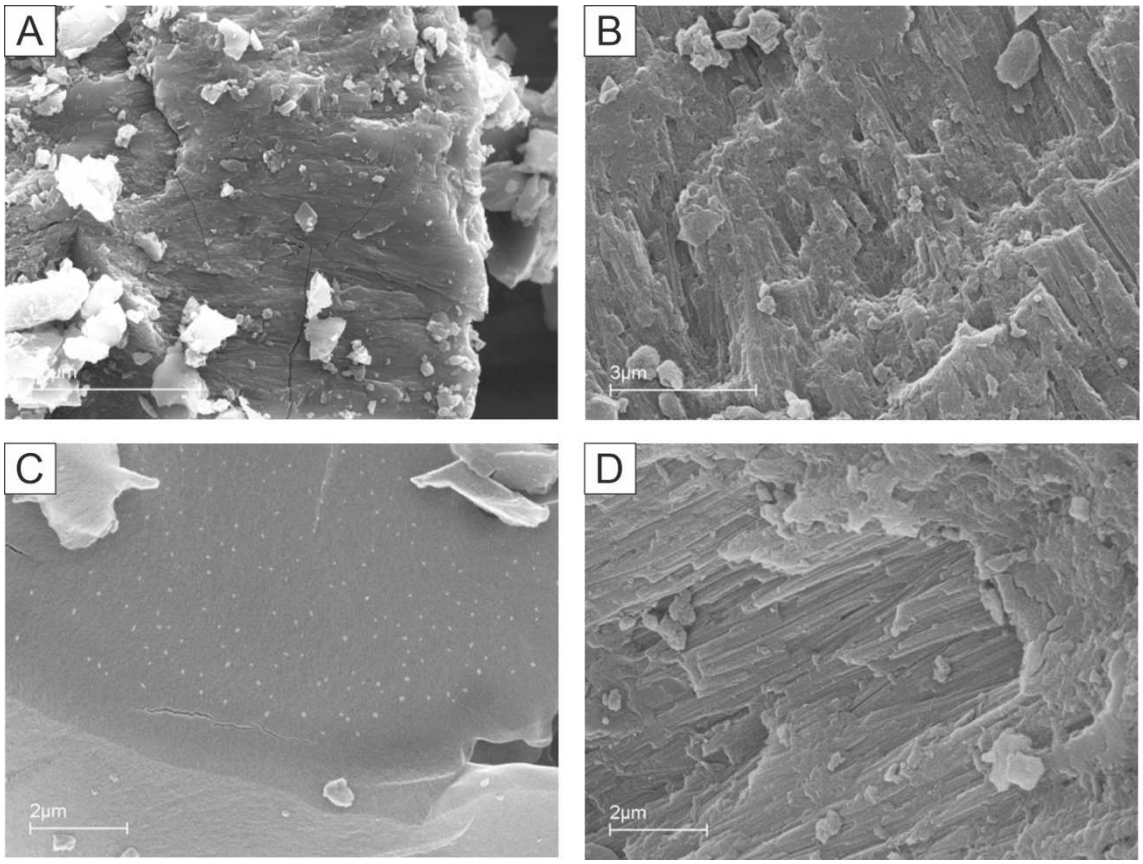

Figure 5. *SEM images of A) P4APA/HCl, B) P4APA/HCl after the post-treatment, C) P4APA/SA, B) P4APA/SA after the post-treatment. Adapted from article II.*[112].

Modification of the conducting polymer poly(4-aminodiphenylaniline) (P4APA) by acids was also studied in **article II**. Here, the effect of P4APA doping on the cytotoxicity, morphology, and molecular weight distribution of P4APA was examined. P4APA powder was prepared in the presence of HCl according to standard procedure; this sample was named P4APA/HCl. Similarly to the previous article, pristine P4APA/HCl was deprotonated with ammonium hydroxide. This deprotonated form was further subjected to a reprotonation process. The following acids were used as doping agents: phosphoric acid (H_3PO_4), salycilic acid (SA), dodecylbenzenesulfonic acid (DBSA), and camphorsulfonic acid (CSA). Furthermore, the samples were exposed to a post-treatment procedure in which they were purified by soaking in phosphate buffer saline (PBS) with pH 7.3. The results showed that the post-treatment procedure influenced both the morphology of the modified samples and the content of oligomers. Data from size exclusion chromatography showed the presence of aniline oligomers before post-treatment. Aniline dimer, hexamer, and octamer derivatives were present in all the powders. The post-treatment process allowed the removal of these oligomers, which are potentially cytotoxic species. In addition, from the SEM images (Fig. 5) it is obvious that the sample morphology changed. Before the post-treatment procedure, the samples exhibited an irregular morphology whilst after post-treatment, layer-by-layer oriented rod-like structures were observed.

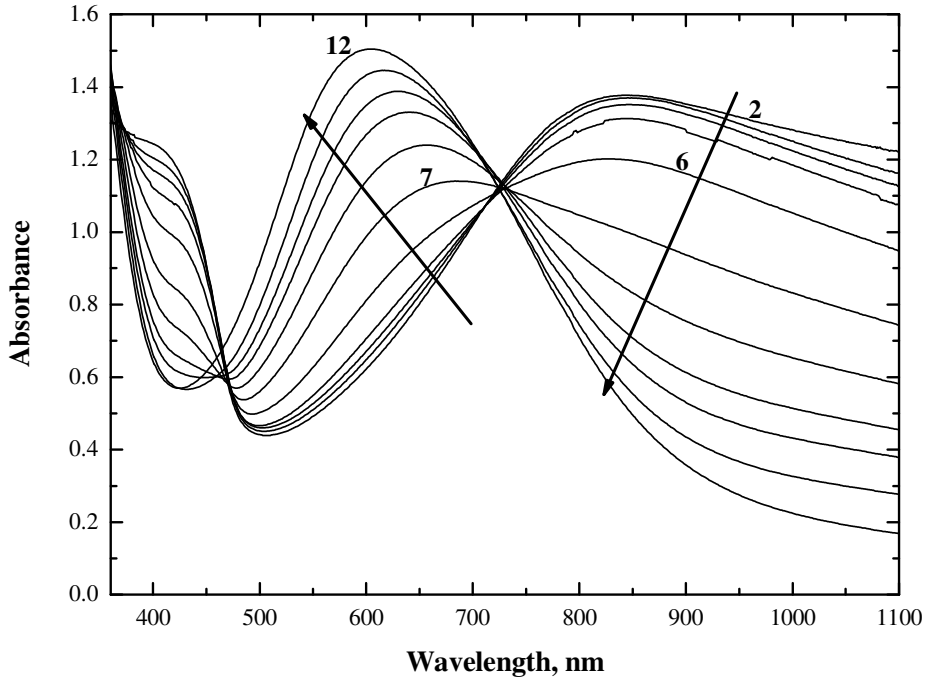

Fig. 6. *UV–vis spectra of PANI–PAMPSA films between pH 2–12. Adapted from article III.*[113].

Another important aspect related to bio-applications is the stability of polyaniline conductivity under physiological pH. Standard PANI is non-conducting in physiological pH. The transition from conducting PANI salt to non-conducting PANI base occurs at a pH of around 4[114]. This transition can be shifted to higher pH by various modifications. In **article III.** the pH stability of conductivity was improved by reprotonation of the PANI surface by PAMPSA. The acceptable level of conductivity for this modified polymer was retained at pH 6 (Fig. 6), which is a very notable improvement over pristine PANI.

3 CYTOCOMPATIBILITY OF CONDUCTING POLYMERS

The main effort of my research has been focused on the preparation of a stimuli-responsive biomaterial which can be used to prepare scaffolds with excellent mechanical properties together with good biocompatibility. At the beginning of my work, I chose conducting polymers as potentially stimuli-responsive materials. Considering all the issues mentioned so far, the utilization of conducting polymers in biomaterials requires deep knowledge about various aspects of their biocompatibility. However, at the start of my research, the impact of conducting polymers on cell behaviour had not been adequately studied and knowledge was insufficient. Therefore, it was first necessary to widen our grasp of this field to gather new and advanced knowledge on these materials.

First, the biological properties of pristine conducting polymers were at the centre of interest. Then, various modifications were employed to improve the biological response of these polymers. In addition, various forms of these polymers were prepared and tested. The research began with the testing of PANI powders and continued with colloidal dispersions and thin films, and the knowledge acquired was applied to the preparation of conducting polymer-based scaffolds. Over time, the level of biological testing was also notably extended and improved, from basic cytotoxicity studies conducted on standard cell lines to cell cultivations in bioreactors with stem cells.

3.1 PANI - powders

To the best of my knowledge, the biocompatibility of pure PANI powders was tested for the first time in 2012 by Humpolíček at al.[115]. Previous investigations were targeted on various PANI composites or complexes[116,117], but not on pristine PANI. Tests on PANI salt and base to determine levels of skin irritation, sensitization, and cytotoxicity were performed in the mentioned study, which showed that pristine PANI did not induce any sensitization or skin irritation either. However, both forms of PANI exhibited significant cytotoxic effects. This study showed that the modification of pure PANI is needed for it to be used in biological applications.

For the reasons given above, **article IV.** focuses on one of the possible ways of purifying PANI, and on the determination of leached impurities. The aim of this work was to overcome the limitations of PANI described by Humpolicek et al., 2012. PANI powder was therefore prepared by the same procedure and subsequently purified in a Soxhlet extractor using the following solvents: methanol, 1,2-dichloroethane, acetone, ethyl acetate, hexane, and 0.2 M aqueous hydrochloric acid. The impurities removed from PANI were determined by size

exclusion chromatography and their contents are shown in Tab. 2. The cytotoxicity of purified samples was evaluated using mouse embryonic fibroblasts (NIH/3T3 cell line). After purification with HCl and methanol, the cytotoxic effect of extracted samples was decreased compared to pristine PANI. In addition, it was found that the cytotoxicity of pristine PANI is mostly connected with the presence of low-molecular-weight fractions in the polymer. The knowledge summarised in the article led to an understanding of the causes of PANI cytotoxicity and contributed to further improvement in the purity of this polymer.

Table 2. The impurities removed from PANI after treatment with different solvents in a Soxhlet extractor (given in normalized peak area) determined by SEC and the extracted matter.

Solvent	Monomers and oligomers	Dissolved polymer	Total impurities	Extracted Matter (mg/ 100 mL)
0.2 M HCL	1445	15	1460	113
Methanol	840	80	920	87
Acetone	50	410	460	14
Dichloroethane	125	195	320	17
Ethyl acetate	80	480	560	9
Hexane	12	43	55	8

Note: Data obtained from article IV.[118].

3.2 PANI – colloidal dispersions

The powders studied in **manuscript IV.** are regrettably insoluble in aqueous media and common organic solvents. Therefore, it is difficult to process them to any suitable product useful in biomedical applications. Here, thin films or colloidal dispersions are much more desirable. Colloidal forms of conducting polymers can be easily dispersed in aqueous media, and the advantages of films lie in their ability to easily cover various substrates.

Knowledge about the biological activity of PANI was extended in the work published in **article V**. Here, the biological characteristics of colloidal PANI were reported for the first time. Colloidal dispersions were prepared according the standard protocol of the IUPAC by oxidation of aniline hydrochloride with ammonium persulfate in the presence of poly (N-vinylpyrrolidine) (PVP) as a stabilizer[78].

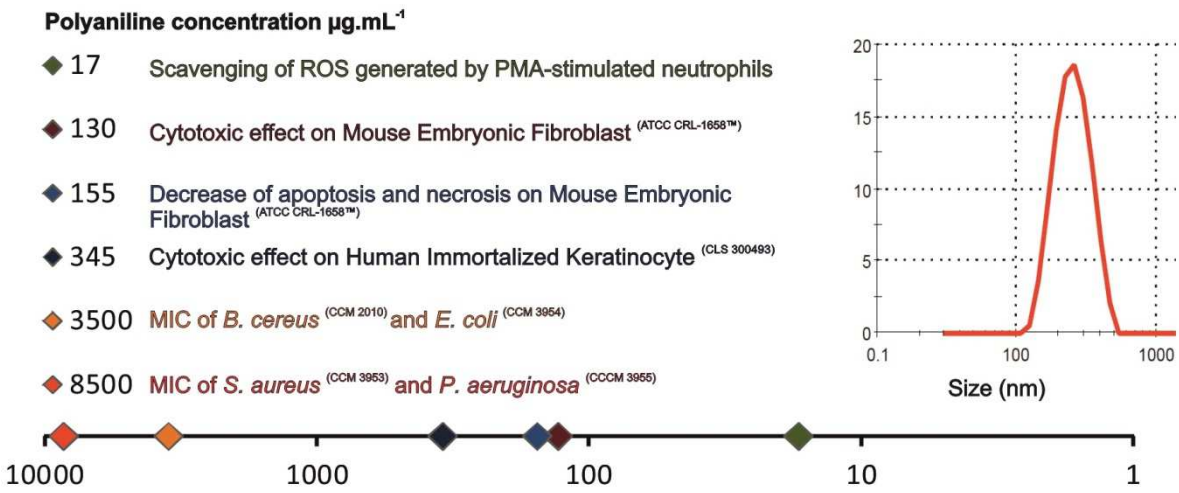

Fig. 7. *Dependence of biological properties on concentration of PANI in colloidal dispersion. Adapted from article V.*[119].

Particle size, PANI concentration, and biological properties were determined (Fig. 7). The biological testing of the colloid focused on its antibacterial activity, cytotoxic effect, the type of cell death, and oxidative burst in neutrophils and whole blood. The tests revealed that PANI dispersion was homogenous, with a nearly uniform single population of particles of size 226.5 ± 0.5 nm and a polydispersity index of 0.145 ± 0.004. These data showed particles with the expected size range, meaning that the dispersions were prepared correctly. The type of cell death, apoptosis or necrosis, was recognized by means of an annexin/propidium iodide assay on flow cytometry. The results indicated that the safe concentration of PANI in colloid for biological applications is of the order of 150 µg mL^{-1}. At the same time, this concentration did not provoke neutrophil activity, as measured through the detection of reactive oxygen species. These observations suggest that colloidal PANI is a potentially good candidate for biological applications.

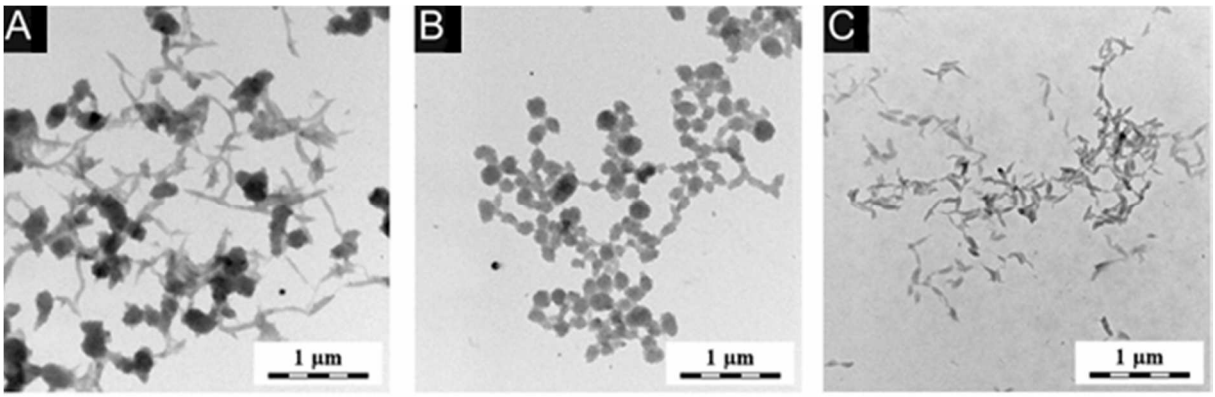

Fig. 8. *Transmission electron micrographs of PANI colloids stabilized with A) sodium hyaluronate of lower molecular weight, B) sodium hyaluronate of higher molecular weight, and C) chitosan. Adapted from article VI.*[120].

The advantageous properties of colloidal dispersions described in **Article V.** led to their further research and an effort to utilise such colloids in advanced applications. To improve their biological properties, the PANI colloids were stabilized with biocompatible polysaccharides. The preparation and characterization of the composite polysaccharide-PANI particles is described in the **article VI**. Sodium hyaluronate (HA) and chitosan (CH) were used for this experiment. Both biopolymers were used in two different molecular weights for the stabilization (HA: M=1 800 – 2 100 kDa and 50 kDa; CH: M = 50 –190 000 Da and 400 kDa). The material characterization involved the determination of UV-Vis spectra, the particle size distribution, and morphology which is shown in Fig. 8. The behaviour of the colloids in contact with prokaryotic and eukaryotic cells was studied and the cytotoxicity and antibacterial activity were determined. The cytotoxic effect depended mainly on the concentration of PANI in the respective colloidal samples. Colloids stabilized with higher molecular weight HA exhibited the best properties, with the absence of cytotoxicity observed for a PANI concentration of 465 μg mL^{-1} (Fig. 9), which was a significant improvement over pristine PANI. In addition, this colloid exhibited an antibacterial effect against *Staphylococcus aureus*. Thus, these formulations of PANI colloids can be considered as promising candidates for use as stimuli-responsive biomaterials.

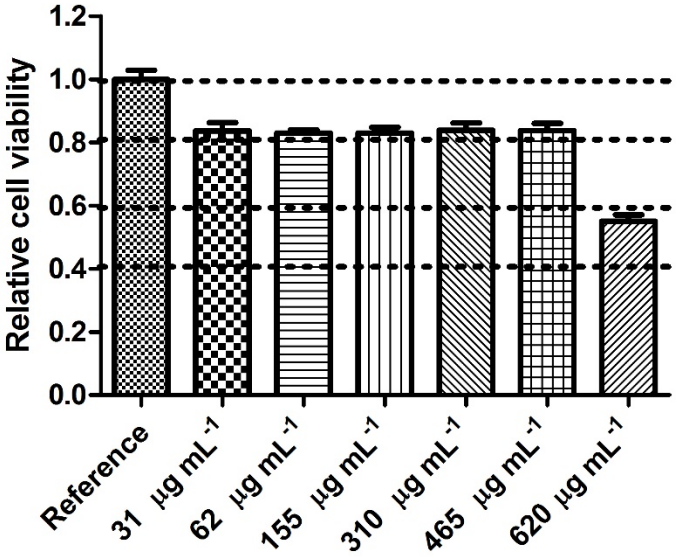

Fig. 9. *Cytotoxicity of colloidal PANI stabilized with sodium hyaluronate (molecular weights 1 800 – 2 100 kDa) for individual concentrations of PANI in colloid. Adapted from article VI.*[120].

3.3 PANI – films

Many potential applications for conducting polymers in medicine are related to the formation of surfaces. Here, biosensing or the control of the fate of adhered cells can be given as examples. PANI films were studied in **Article III**. Here, pristine PANI films were prepared according to the IUPAC procedure in the form of PANI salt and base[78]. Subsequently, the films were modified with PAMPSA. The polymeric acid PAMPSA was chosen as a representative of heparin-like substances. Heparin is the most common compound used as an anticoagulant and its efficacy is attributed to the structure of its polysaccharide backbone with a combination of sulfo and carboxyl groups [121]. The molecular structures of heparin and PAMPSA are shown in Fig. 10.

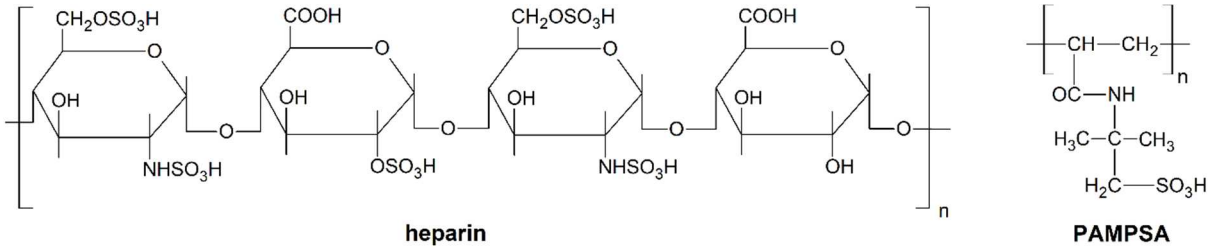

Fig. 10. *The molecular structure of heparin and PAMPSA.*

The prepared samples were tested for selected parameters of their hemocompatibility, namely blood coagulation and platelet adhesion. Two different procedures for the preparation of PANI/PAMPSA films were employed. The first consisted in the reprotonation of PANI base with PAMPSA (PANI-PAMPSA). In the second procedure, PAMPSA was used directly in the reaction mixture (PANI-1:1) under PANI synthesis. The films were also tested for their surface properties and contact angle measurements were performed. The contact angle increased in the samples with PAMPSA incorporated into the reaction mixture compared to standard PANI salt. In contrast, after the reprotonation of PANI base with PAMPSA, the contact angle decreased. As it is a commonly accepted fact that plasma proteins prefer hydrophobic surfaces to hydrophilic ones[122], these results correspond to the results on platelet adhesion on the film surfaces, where the lowest adhesion was observed for the most hydrophobic surface (PANI-PAMPSA). This surface not only reduced platelet adhesion, but also had a notable impact on blood coagulation. Moreover, the modification of PANI with PAMPSA improved the pH stability of PANI under physiological conditions by increasing the salt-base transition from pH 4 to pH 6. These findings suggest that this procedure can be a possible means of preparing PANI-based biomaterials.

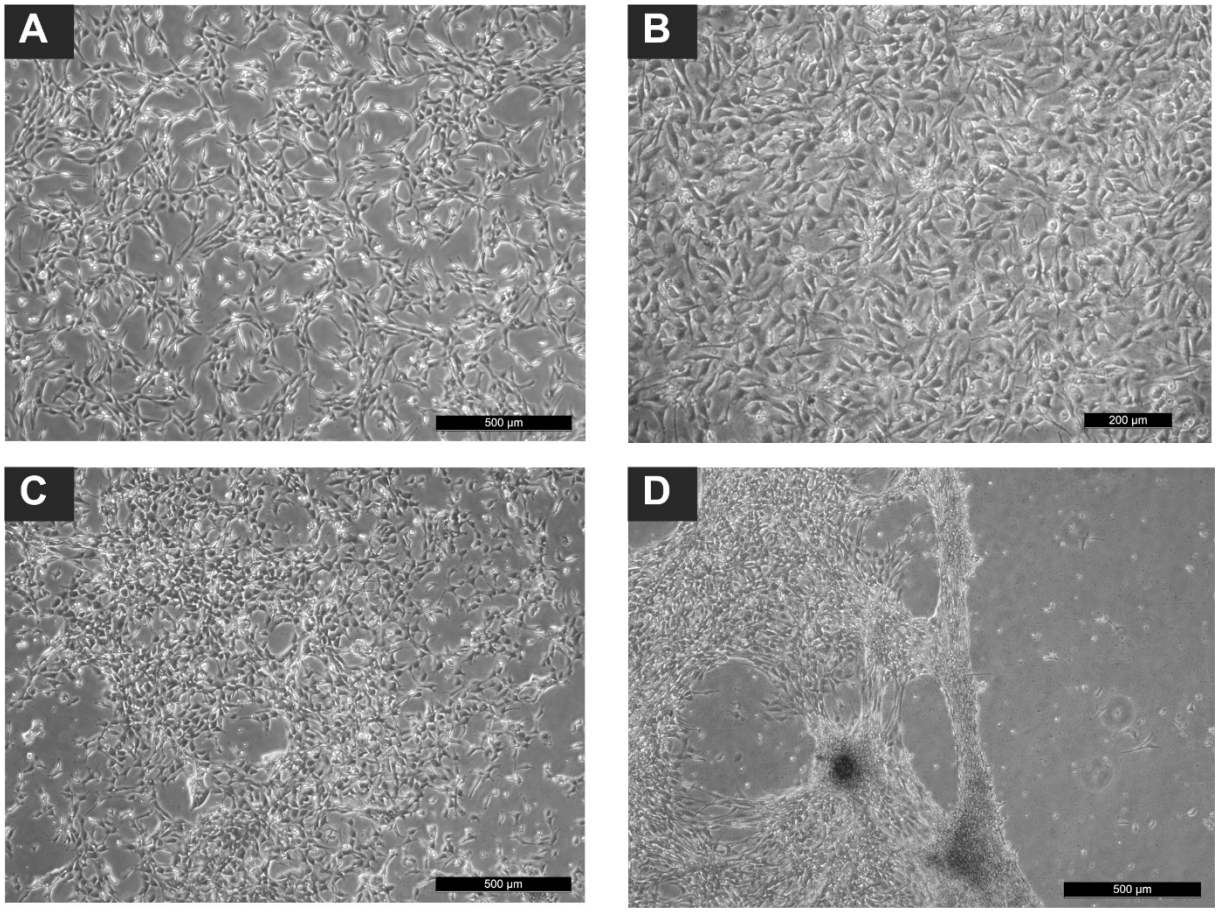

Fig. 11. *Cell growth on different PANI surfaces (after various times of proliferation). A) Reference (24 hrs), B) PANI salt (24 hrs), C) PANI modified with PAMPSA in the molar ratio of aniline hydrochloride to PAMPSA adjusted to 1:1 (144 hrs), D) PANI modified with PAMPSA in the molar ratio of aniline hydrochloride to PAMPSA adjusted to 2:1 (144 hrs). Adapted from article I.*[111].

PANI films modified with PAMPSA were also tested for cell compatibility. These tests are described in **Article I.** Besides PAMPSA, the PANI films were also doped with sulfamic and phosphotungstic acids. Cell adhesion, proliferation, and migration were determined on the modified surfaces. Unfortunately, in this study, the samples of PANI doped with PAMPSA did not show good cytocompatibility, as the cell attachment on this surface was weak (Fig. 11). Moreover, the cells also migrated more slowly on the PANI surface with PAMPSA compared to the other tested surfaces. The doping with sulfamic and phosphotungstic acids resulted in good cytocompatibility. Hence, these surfaces could possibly be utilized in tissue engineering.

3.4 PANI – films prepared in colloidal mode

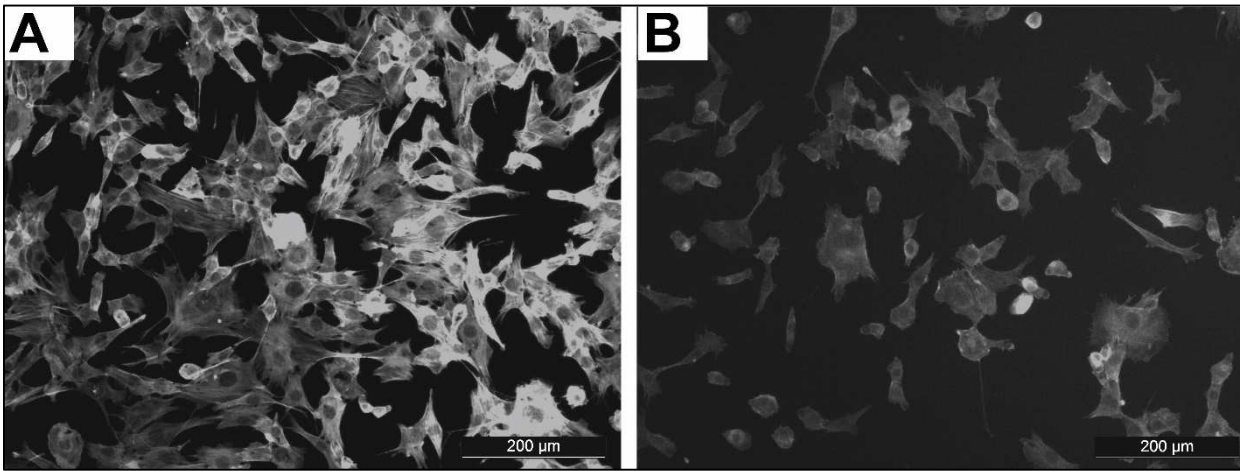

Fig 12. *The cytoskeleton organization of NIH/3T3 cells cultivated for 24 hours on the PANI films prepared in the presence of A) SDS, B) HCl. Adapted from article VII.*[123].

As shown in **article VI.**, the biocompatibility of colloidal PANI can be modified by using suitable stabilizers. Correspondingly, the properties of PANI films, such as surface morphology and electrical properties, can be controlled by using different stabilizers. In an effort to prepare conducting films with low cytotoxicity, PANI colloidal dispersions were prepared in the presence of four stabilizers and films were made thereof, as described in **article VII.** Poly-N-vinylpyrrolidone (PVP), sodium dodecylsulfate (SDS), Tween 20, and Pluronic F108 were chosen for this purpose. In addition, two types of reaction media were used during synthesis, water and 1M HCl, the latter to increase the acidity of the reaction mixture. The material properties of the films, such as surface energy, conductivity, and spectroscopic characteristics, were determined. Biological testing was conducted to determine cell adhesion, proliferation, morphology and migration. Regarding conductivity, higher values were achieved for films where HCl was used as a reaction medium during synthesis. In contrast, the reaction medium did not influence the surface energy. Cells were able to adhere on all surfaces, but their further growth and proliferation were not so uniform. Cells were not able to proliferate on surfaces modified with Pluronic F108 and Tween 20. The morphology of cells growing on films modified with PVP was significantly changed; the cytoskeleton did not form filopodia and the cells did not spread. On the other hand, samples modified with SDS showed good cytocompatibility, which can also be seen in the Fig. 12, where cells are spreading and have their typical triangular shape. Overall, the PANI-SDS films emerged as the samples with the best properties. Because of the presence of SDS, which is a known irritant, a skin irritation test was performed on a 3D reconstructed human tissue model. Surprisingly, the sample scored as a non-irritant material. In fact, it was shown that it had lower irritant

potential than the reference, i.e., PANI prepared without stabilizer. It can be concluded, therefore, that the preparation of PANI films in colloidal dispersion mode can lead to notable improvements in their biological properties.

3.5 PANI and PPy – comparison of biocompatibility

All of the above described papers deal only with PANI. The main reason for this lies mainly in the limited information about its biocompatibility available at the start of my career. Regarding the second investigated conducting polymer PPy, research dealing with its biocompatibility was sparse but some interesting data and studies could be found. For example, polyesters coated with PPy were tested for tissue reactions[124], the cellular response of PPy/biomolecule blends on silicone electrodes was investigated[125], and the doping of PPy was examined[126]. However, no study investigating the properties of pristine PPy was available. Consequently, it was not possible to compare the biocompatibility of PPy and PANI with respect to existing studies. Nevertheless, the general opinion among researchers was that PPy exhibited better biocompatibility with a lower cytotoxic effect than PANI[127,128]. This generally accepted view gave rise to **article VIII**., which compared these two polymers with respect to their biocompatibility. Both polymers were prepared according to standard procedures and their biological characteristics were determined in one laboratory to eliminate differences in testing. The cytotoxicities of the polymer extracts were determined using embryonic fibroblasts and embryonic stem cells. Embryotoxicity was also tested through the impact of the extracts on erythropoiesis and cardiomyogenesis within embryonic bodies. In addition, sample morphologies were captured by SEM and the extracts were analysed by mass spectroscopy. Both forms of PANI and PPy were tested, i.e., protonated salts and deprotonated bases. Observations showed that the differences in cytotoxicity were between the forms of the polymers (salt vs base) rather than between the individual polymers *per se* (PANI vs PPy) (Fig. 13). That is, while the same forms (salt or base) of each polymer showed almost identical cytotoxic and embryotoxic effects, it was the base forms of both polymers that exhibited better cytocompatibility than the protonated salts. Overall, therefore, direct comparison of both polymers using the same methodology evidenced that PPy and PANI exhibit similar degrees of biocompatibility. Hence, the generally accepted opinion that PPy is a less cytotoxic polymer was disputed.

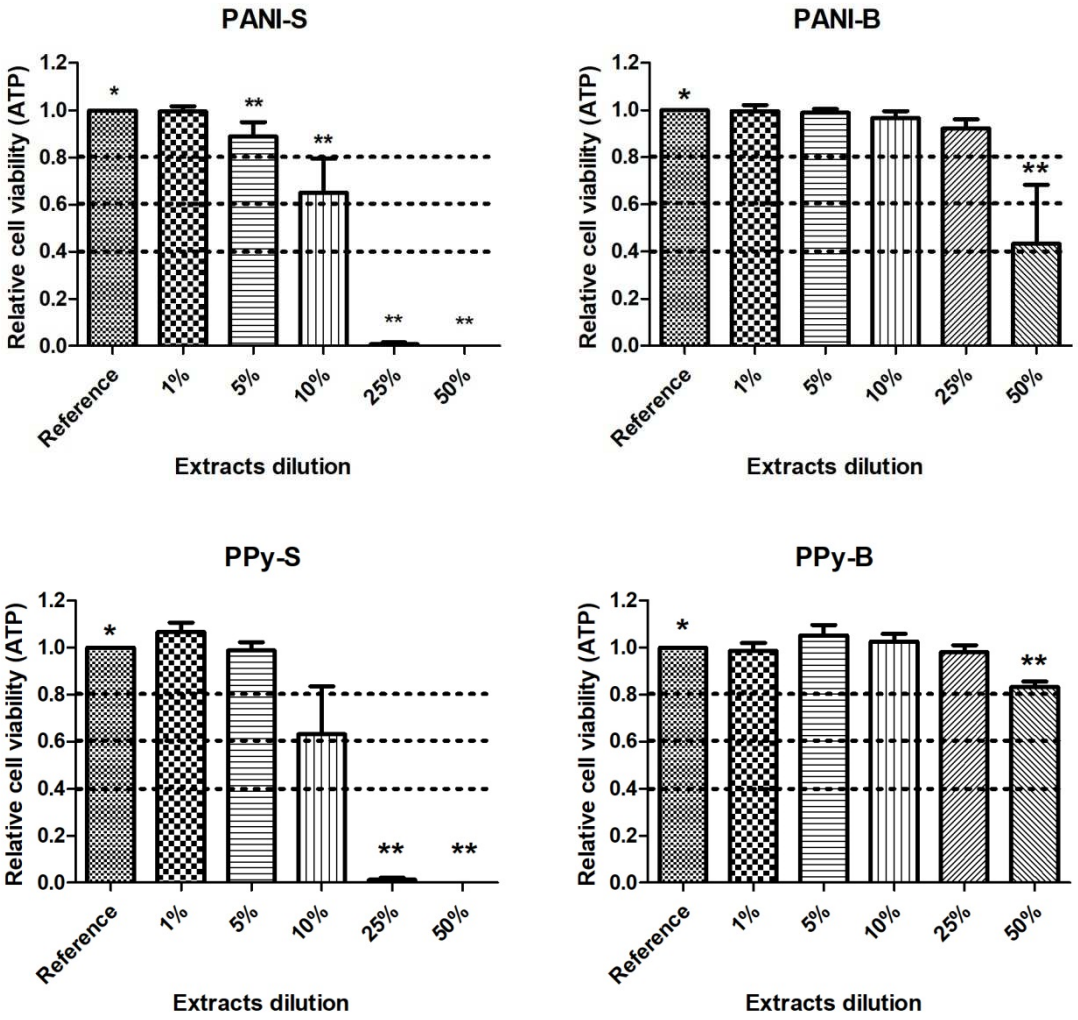

Fig. 13. *Cytotoxicity of extracts of PANI and PPy on ESc determined by the relative level of ATP compared to the reference. The different superscripts correspond to significant differences ($P \leq 0.05$) compared to the reference. The dashed lines highlight the limits of viability according to EN ISO 10993-5: viability > 0.8 corresponds to no cytotoxicity, > 0.6 – 0.8 mild cytotoxicity, > 0.4 – 0.6 moderate cytotoxicity and < 0.4 severe cytotoxicity. Adapted from article VIII.*[129].

The study published in **Article VIII.** was later extended by further work in which PANI and PPy were compared after doping with the same doping agents. This work is outlined in **Article IX**. As already mentioned, the use of conducting polymers in biomedical applications is complicated by the fact that their conductivity rapidly decreases at physiological pH. Researchers worldwide are currently engaged in efforts to increase the pH stability of such polymers by various methods [107,114,130]. In our work, "re-doping" with four types of organic phosphonates was employed. Dimethyl phosphonate (DMPH), diethyl phosphonate (DEPH), dibutyl phosphonate (DBPH), and diphenyl phosphonate

(DPPH) were used. The following properties of such "re-doped" samples were studied: their conductivity and their embryotoxicity and cytotoxicity towards embryonic stem cells. The results showed that the pH stability of phosphonate-doped PANI samples improved in comparison with pristine PANI salt (Fig. 14). In particular, PANI doped with DPPH exhibited significant improvement. Unfortunately, this sample also showed high cytotoxicity. On the other hand, the cytotoxicity of PANI doped with DBPH and DMPH was low compare to pristine PANI. In contrast to PANI, all types of phosphonates improved the cytotoxicity of PPy. It can be concluded, therefore, that PPy doped with phosphonates could serve as a conducting biomaterial.

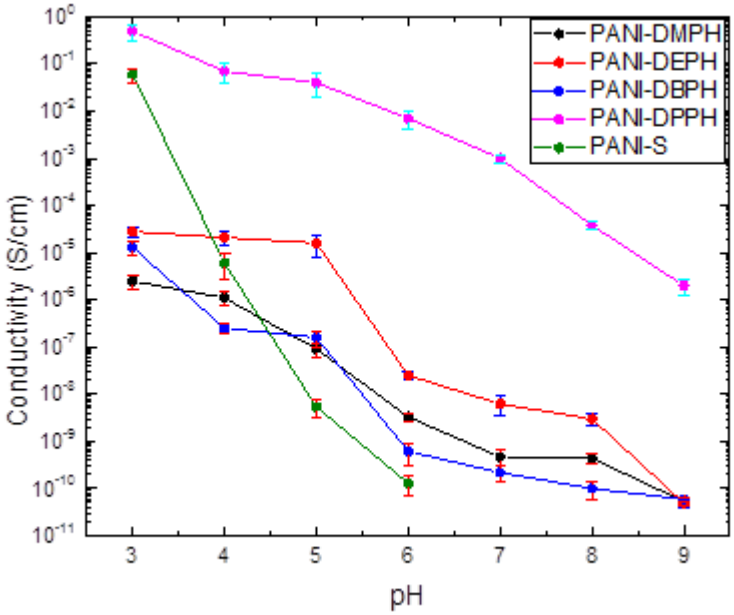

Fig. 14. *The conductivity of PANI doped with organic phosphonates under various pH and the comparison with pristine PANI-S. Adapted from article IX.*[131].

4 SCAFFOLDS – PREPARATION AND CYTOTOXOMPATIBILITY

Following our evaluation of the basic biological properties of conducting polymers, my attention was directed towards studying more advanced 3D systems, i.e., scaffolds. The aim of the work was to prepare scaffolds for tissue regeneration supported by conductivity. First, it was important to determine the optimal conditions for scaffold preparation, including the choice of a crosslinking agent or matrix. **Articles X., XI, and XII.** deal with this topic. PVA was the common denominator for these studies, being used either as matrix or as crosslinker. PVA is known for its physical properties suitable for biological applications[132], for its good water solubility[133], and for its biocompatibility;[134] therefore, it was chosen as a suitable candidate for scaffold preparation in our laboratory.

In **article X.** scaffolds based on PVA and fractionated kraft lignin were prepared and their material and biological properties evaluated. Kraft lignin was used to improve the stiffness of PVA hydrogels and to increase their antibacterial activity. The following properties were determined to characterise the material: the mechanical and thermal stability, the hydrogel network architecture, and the swelling ratio. Cytocompatibility studies determined the cytotoxicity of hydrogels in direct contact, the cytotoxicity of extracts, and cell ingrowth through the scaffolds in bioreactors. In addition, antibacterial properties were also studied. The mechanical stability was sufficient for all scaffolds with a concentration of kraft lignin up to 10 wt%. The tested cell line was able to grow with unchanged morphology in direct contact with all samples. However, the cytotoxicity of extracts was highly dependent on the concentration of kraft lignin in the scaffolds, with cell viability decreasing as the concentration of kraft lignin increased. Moreover, cell ingrowth in the bioreactor showed that only the scaffold with 1 wt% kraft lignin was suitable for applications in tissue engineering.

Another study on PVA-based hydrogels was published in **Article XI**. Here, PVA was used as a matrix for hydrogel, which was crosslinked by a modified polysaccharide – specifically, dialdehyde cellulose (DAC). DAC represents a less toxic, sustainable, and more effective alternative to highly toxic synthetic crosslinkers such as glutaraldehyde, which is widely used for the preparation of PVA hydrogels [135,136]. Three different concentrations of DAC were used to crosslink PVA and to prepare hydrogels with various mechanical and rheological properties, porosities, and surface areas. The material characteristics of PVA/DAC hydrogels were tunable, resulting in a range of hydrogels from stiff gels suitable for cartilage replacement to soft and highly porous viscoelastic hydrogels ideal for drug-delivery applications. They were also found to be superior to those of analogical material prepared using glutaraldehyde. The *in vitro* biological evaluation of hydrogel extracts using keratinocytes and

fibroblasts revealed no cytoxicity on the part of the prepared materials. Similarly, no negative effects of hydrogels on the cell growth or morphology of fibroblasts were observed. Hydrogels were subsequently loaded with biologically active substances, including the anticancer drug phenanthriplatin (PhPt). In addition to drug release, the cytotoxicity of PhPt-loaded hydrogel toward fibroblasts and malignant lung cells (A549) was evaluated. Notably, a synergistic effect of the loaded drug and hydrogel was observed in cytotoxicity towards the A549 cell line, though no such behavior was visible for fibroblasts. Thus, overall, PVA/DAC hydrogels represent tunable and biocompatible materials ideal for further study.

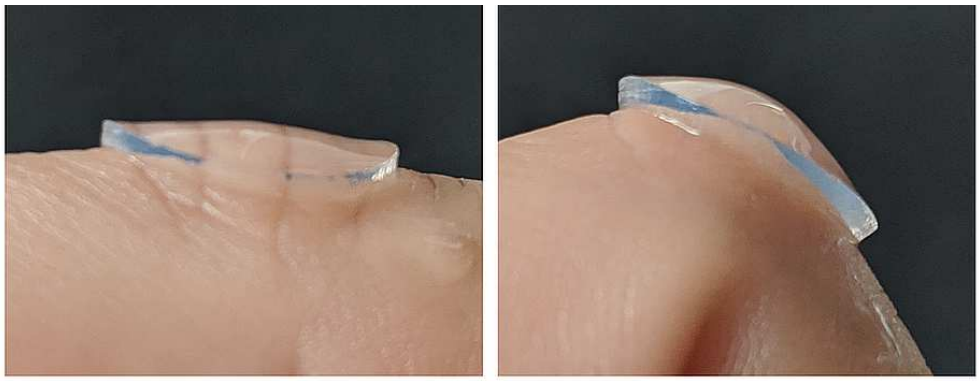

Fig. 15. *Bioadhesivity of PVA/DAC hydrogels. Adapted from article XII.*[137].

In **Article XII,** knowing the influence of DAC on the properties of PVA-based hydrogels, we focused on investigating the role of PVA in the scaffold. Hence, in addition to two different concentrations of DAC crosslinker, PVA of different molecular weights (M_w =1 and 130 kDa) was used for the preparation of PVA/DAC hydrogels. The hydrogels were fabricated in the form of thin films, which are more suitable for coating by conducting polymers. The prepared samples were biocompatible, showed no observable cytotoxicity against fibroblasts, and had no negative impact on cell growth. The hydrogels prepared with a combination of a low amount of crosslinker and high-molecular weight PVA were found to be particularly suitable for topical applications, such as wound dressings or patches. They exhibited high porosity and a high content of water, good bioadhesivity (Fig. 15), and transdermal drug-delivery. This material is thus an ideal candidate for the development of conducting patches capable of further improving wound healing.

My research effort has also been directed towards preparing stimuli-responsive scaffolds with properties mimicking native tissues. The combination of PVA based matrices with conducting polymers was the subject of our research in **articles XIII.** and **XIV**. Both manuscripts are targeted at the synthesis of porous conducting PVA-based cryogels, one in combination with PANI, the other with PPy. Cryogels are gel matrices formed at sub-zero temperatures, and their preparation is carried out under freezing during

polymerization[138,139]. Usually, they exhibit a macroporous structure, good elasticity and good flexibility[140–142].

Article XIII describes the preparation of a novel macroporous material in the form of a PANI cryogel exhibiting good mechanical properties. This study reports the material characteristics of the gels, such as thermal conductivity, surface energy, pore-size distribution, and elasticity expressed by Young's modulus. The biocompatibility of these macroporous polyaniline cryogels was demonstrated by evaluating their cytotoxicity towards mouse embryonic fibroblasts and *via* the testing of embryotoxicity based on the formation of beating foci within spontaneously differentiating embryonic stem cells. In addition, the results of biological testing were related to impurities leached from the cryogel, which were characterized by liquid chromatography. The macroporous structure of the PANI cryogel is depicted in Fig. 16.

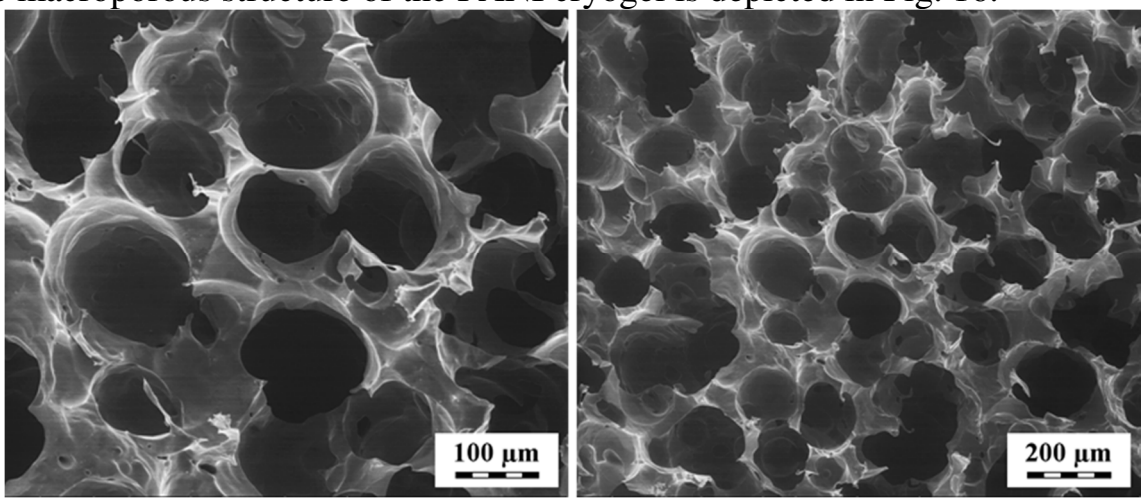

Fig. 16. *The SEM images of the cryogel structure. Adapted from article XIII.*[143].

The mean pore size was assessed to be 159 µm and the specific surface area to be 0.020 m^2 cm^{-3}. The mechanical properties were described by Young's modulus, which reached a mean value of 9.7 ± 0.5 kPa, meaning that the PANI cryogel was an elastic material, what can be seen in Fig. 17.

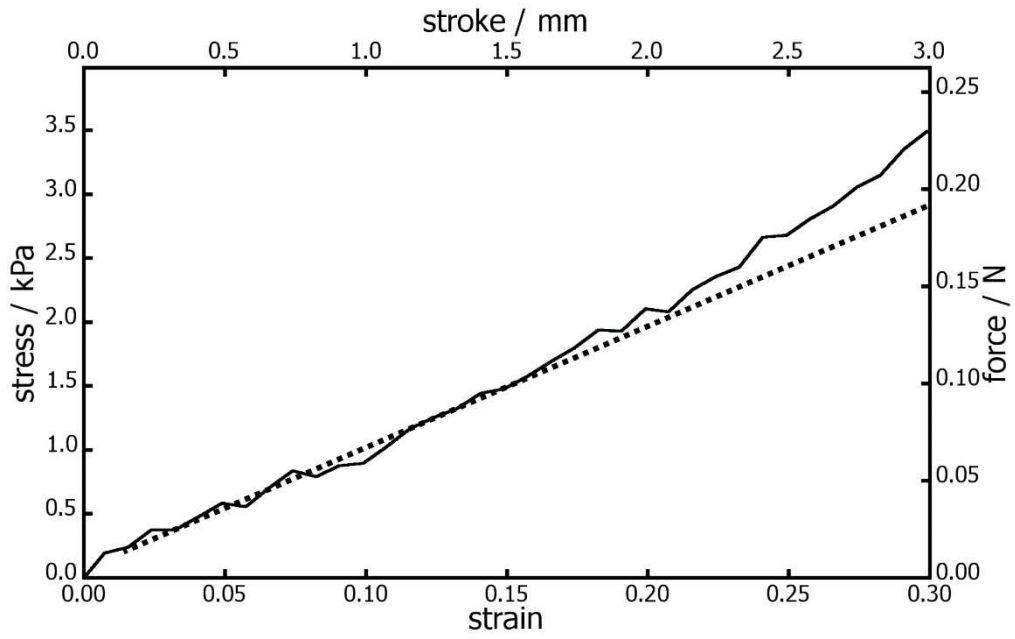

Fig. 17*. Stress-strain curve used for calculation of Young modulus of PVA-PANI cryogel measured under confined conditions. Adapted from article XIII.*[143].

The PANI cryogel also showed low levels of cytotoxicity and embryotoxicity. The embryonic stem cells and embryoid bodies were able both to adhere and grow well on its surfaces. This good biocompatibility can also be related to the low content of low-molecular-weight impurities in the cryogel. Unfortunately, a poor level of interaction of cardiomyocytes and neural progenitors with the PANI cryogel was detected. Cardiomyocytes were not able to attach to the cryogel and only a few neural progenitors, which failed to spread, were observed on its surface. However, the fact that the PANI cryogel mimicked the properties of native tissues and exhibited reasonable biocompatibility opens up possibilities for its utilization in regenerative medicine, given that suitable modifications or purifications can be developed.

Further research on conducting macroporous cryogel is presented in **article XIV.** Here, PPy was used as the conducting component and different concentrations of PVA (ranging from 5 to 8 wt.%) were used for sample preparation. The cryogels were characterized with respect to their morphology, mechanical properties, electrical conductivity, specific surface area, and cytotoxicity. According to SEM images, it can be concluded that cryogels with interconnected pores with macropore diameters ranging from 5 to 100 μm were successfully prepared. The mechanical properties of the PPy expressed by Young's moduli achieved a value of approximately 20 kPa. The stiffness as well as the pore diameters were independent of the concentration of PVA in the cryogel. The conductivity was enhanced compared to standard PPy and reached a value of 18 S cm^{-1}. This value remained unchanged after long-term treatment with water, i.e. close to physiological pH. These findings taken

together with comparatively good results from cytotoxicity testing suggest that these cryogels are potentially suitable for use in biomedical applications.

5 CONTRIBUTION TO SCIENCE AND PRACTICE

The main goal of my scientific career so far has been to prepare biocompatible stimuli-responsive scaffolds. These scaffolds should allow the modification of cell behaviour in desired ways through the application of external electrical fields. The conductivity of the scaffold can be achieved by using conducting polymers, such as polyaniline (PANI) or polypyrrole (PPY). However; crucial information about the biocompatibility of conducting polymers was lacking. Therefore, the first aim of my work was to increase our understanding of the factors which influence the impact of conducting polymers on cells. The importance of this research is evidenced by the publications summarized and described in this work. At the beginning, knowledge about thebiocompatibility of PANI was in the centre of attention, and this polymer was studied in the form of powders, colloidal dispersions and thin films. **New information about the influence of the PANI preparation procedure on various parameters of cytocompatibility was revealed.**

Before my work on conducting polymers began, it was generally accepted that pristine PANI powder exhibited a high level of cytotoxicity. Therefore, one of my works dealt with the detection of impurities leached from PANI and the methods of PANI purifications. It was shown that the cytotoxic potential of PANI is mainly induced by low-molecular-weight fractions of the polymer. As was shown by our team**, these cytotoxic fractions can be efficiently removed by purification – specifically, by extraction with organic solvents, a step which resulted in a significant decrease in PANI cytotoxicity.**

One important contribution of this dissertation thesis to science is related to the research of colloidal PANI dispersions, whose biological properties were hitherto unknown. One of my initial studies focused on this topic, and the biological activity of colloidal PANI was reported for the first time. This knowledge about colloidal PANI was further extended with respect to its cytotoxicity, the type of cell death, oxidative burst in neutrophils and whole blood, and its antibacterial activity. **This study significantly improved knowledge about the potential application of colloidal conducting dispersions in tissue engineering.** In addition, the new knowledge acquired through this study along with increased methodological experience and laboratory acumen with respect to the preparation and characterization of PANI led to **an innovative approach to the preparation of cytocompatible electro-conducting substrates, characterised as polymerization in colloidal dispersion mode.** Such prepared substrates have unique properties in terms of their cytocompatibility, as they combine the properties of both synthetic PANI and the biopolymers used as colloidal stabilizers.

Research on PANI continued with the aim of preparing conducting materials with even better cytocompatibility. As a result, various advanced modifications of this polymer were successfully developed. Here, the **incorporation of**

biomacromolecules into PANI films should be mentioned, a procedure which leads not only to the better biological response of these composite films but also to their improved pH stability in physiological environment. This improvement is especially important, as the decrease in the electrical conductivity of PANI at physiological pH is one of the crucial challenges.

When talking about the utilization of conducting polymer films as biomaterials, their surface properties should not be forgotten. Hence, some of the studies also dealt with this topic. One aspect of biocompatibility, important especially for scaffolds which can come in the contact with blood, is blood compatibility. In this resepct, important progress was achieved by the reprotonation of PANI film with polymeric acid, poly(2-acrylamido-2-methyl-1-propanesulfonic acid) PAMPSA. This modification led to a **significant reduction in platelet adhesion on the PANI/PAMPSA surface and significantly influenced blood coagulation.** Moreover, this modification also improved pH stability in comparison with pristine PANI film. One subsequent and exciting study concentrated on the preparation of PANI films in colloidal mode in the presence of surfactants used as stabilizers, e.g. sodium dodecylsulfate. The films thus prepared exhibited not only good cytocompatibility but were also shown to be non-irritant towards skin.

The biological response of PANI was also compared with that of another conducting polymer, PPy. In scientific literature, PPy was previously considered as a material with better biocompatibility than PANI. However, these findings were based on studies in which PPy was examined in the form of various composites and blends, not in its pristine form. These two polymers were therefore prepared in their pristine forms using standard procedures and studied using identical methods. It was shown that the **cytocompatibilities of PANI and PPy were very similar and depended mainly on the form of the polymer (salt or base).** As their differences in biological response were negligible, neither of them should be preferred for biomedical applications.

All the above investigated parameters relating to conducting polymers, such as their surface characteristics, the procedure for their preparation, and the cytocompatibility of their various forms and composites were summarised to collect knowledge crucial for the preparation of scaffolds. In particular, the focus of my research was stimuli-responsive scaffolds in which the responsivity is triggered by electrical conductivity. To determine optimal conditions for the preparation of such conducting scaffolds, several types of non-conducting PVA-based analogues were first prepared. These scaffolds exhibited good mechanical as well as biological properties. Therefore, the synthesis of conducting PVA-based scaffolds followed. As conducting components, both PANI and PPy were used. **These prepared scaffolds also showed good mechanical properties and were able to mimic the properties of native tissues. Even their cytocompatibility was good, which opens up the possibility to use such conducting scaffolds in biomedical applications.**

Besides the topics discussed above, my research also focused on investigating the influence of conducting polymers on the formation of bacterial biofilms. This is also a very important aspect of utilizing materials in the medical area, where bacterial contamination must be avoided. In addition to PANI and PPY, carbon quantum dots as antibacterial and antibiofouling coatings were also investigated and several studies dealing with this topic were conducted, these leading to the development of some promising materials. Another part of my research was also dedicated to drug delivery systems, especially related to cancer therapy and the controlled release of drugs.

6 FUTURE PERSPECTIVE

At present, also thanks to my work, knowledge about the biological properties of conducting polymers has expanded significantly and improved methods to enhance their biological properties have been developed. These two prerequisites open up new possibilities for the utilization of such polymers as conducting components in stimuli-responsive materials for medicine. Although various scaffolds with incorporated conducting polymers that exhibit good biocompatibility and mechanical properties have already been prepared by our team, they are still not perfect materials with the excellent properties required for targeted clinical use. For example, the level of biocompatibility is still not sufficient for general biomedical applications. Another parameter which needs additional improvement is the degree of porosity, which is also quite challenging, because we often encounter materials in which the interconnection of pores in the bulk material is missing or the pore size or shape are not adequate for cell ingrowth. Pore interconnection is an essential characteristic, as it supports cell migration and proliferation and also the penetration of the extracellular matrix into the scaffold. Besides this, it affects the diffusion and exchange of nutrients throughout the scaffold.

Therefore, the preparation of conducting scaffolds with interconnected pores, excellent biocompatibility, and mechanical properties mimicking those of native tissue is the goal of future research. In addition, the incorporation of various bioactive molecules into scaffolds will be undertaken. For example, growth factors which will influence cell differentiation will be used. Another aspect which must be taken into consideration is the real cell environment with its continuously changing mechanical, chemical, and biochemical gradients. Hence, respective gradients will be established to effectively mimic this real environment. All these aspects will be tested in bioreactors to resemble *in vivo* systems in the most consistent way.

LIST OF FIGURES

Fig. 1. Examples of conductive polymers. PAC – polyacetylene, PPy –polypyrrole, PANI – polyaniline, PTh – polythiophene, PEDOT –poly(3,4-ethylenedioxythiophene). 18
Fig. 2. Oxidation forms of PANI. 20
Fig. 3. PANI in the formo f A) powder, B) film, C) colloidal dispersion. 20
Fig. 4. The molecular structure of protonated and deprotonated PPy. 22
Figure 5. SEM images of A) P4APA/HCl, B) P4APA/HCl after the post-treatment, C) P4APA/SA, B) P4APA/SA after the post-treatment. Adapted from article II.[112] 25
Fig. 6. UV–vis spectra of PANI–PAMPSA films between pH 2–12. Adapted from article III.[113]. 26
Fig. 7. Dependence of biological properties on concentration of PANI in colloidal dispersion. Adapted from article V.[119]. 30
Fig. 8. Transmission electron micrographs of PANI colloids stabilized with A) sodium hyaluronate of lower molecular weight, B) sodium hyaluronate of higher molecular weight, and C) chitosan. Adapted from article VI.[120]. 30
Fig. 9. Cytotoxicity of colloidal PANI stabilized with sodium hyaluronate (molecular weights 1 800 – 2 100 kDa) for individual concentrations of PANI in colloid. Adapted from article VI.[120]. 31
Fig. 10. The molecular structure of heparin and PAMPSA. 32
Fig. 11. Cell growth on different PANI surfaces (after various times of proliferation). A) Reference (24 hrs), B) PANI salt (24 hrs), C) PANI modified with PAMPSA in the molar ratio of aniline hydrochloride to PAMPSA adjusted to 1:1 (144 hrs), D) PANI modified with PAMPSA in the molar ratio of aniline hydrochloride to PAMPSA adjusted to 2:1 (144 hrs). Adapted from article I.[111] 33
Fig 12. The cytoskeleton organization of NIH/3T3 cells cultivated for 24 hours on the PANI films prepared in the presence of A) SDS, B) HCl. Adapted from article VII.[123]. 34
Fig. 13. Cytotoxicity of extracts of PANI and PPy on ESc determined by the relative level of ATP compared to the reference. The different superscripts correspond to significant differences ($P \leq 0.05$) compared to the reference. The dashed lines highlight the limits of viability according to EN ISO 10993-5: viability > 0.8 corresponds to no cytotoxicity, > 0.6 – 0.8 mild cytotoxicity, > 0.4 – 0.6 moderate cytotoxicity and < 0.4 severe cytotoxicity. Adapted from article VIII.[129]. 36
Fig. 14. The conductivity of PANI doped with organic phosphonates under various pH and the comparison with pristine PANI-S. Adapted from article IX.[131]. 37
Fig. 15. Bioadhesivity of PVA/DAC hydrogels. Adapted from article XII.[137]. 39
Fig. 16. The SEM images of the cryogel structure. Adapted from article XIII.[143]. 40
Fig. 17. Stress-strain curve used for calculation of Young modulus of PVA-PANI cryogel measured under confined conditions. Adapted from article XIII.[143]. 41

LIST OF TABLES

Table 1. Surface energy evaluation of different surfaces..... 25
Table 2. The impurities removed from PANI after treatment with different solvents in a Soxhlet extractor (given in normalized peak area) determined by SEC and the extracted matter..... 29

LIST OF SYMBOLS AND ABBREVIATIONS

A549	Human cells from lung carcinoma
AH	Aniline hydrochloride
APS	Ammonium peroxydisulfate
CH	Chitosan
CSA	Camphorsulfonic acid
CP	Conducting polymer
DAC	Dialdehyde cellulose
DBPH	Dibutyl phosphonate
DEPH	Diethyl phosphonate
DMPH	Dimethyl phosphonate
DPPH	Diphenyl phosphonate
DBSA	Dodecylbenzenesulfonic acid
HA	Sodium hyaluronate
HaCaT	Human immortalized keratinocytes
HepG2	Hepatocellular carcinoma cell line
NIH/3T3	Mouse embryonic fibroblast
PAC	Polyacetylene
PAMPSA	Poly(2-acrylamido-2-methyl-1-propanesulfonic acid)
PANI	Polyaniline
PANI-B	Polyaniline base
PANI-S	Polyaniline salt
PBS	Phosphate buffered saline

PEDOT	Poly(3,4-ethylenedioxythiophene)
P4APA	Poly(4-aminodiphenylaniline)
PPy	Polypyrrole
PTh	Polythiophene (PTh)
PVA	Poly(vinyl alcohol)
PVP	N-poly(vinylpyrrolidone)
SA	Salycilic acid
SEM	Scanning electron microscopy
SDS	Sodium dodecyl sulfate
γ_{AB}	Acid-base (polar) part of surface energy
γ_{LW}	Disperse part of surface energy
γ_{tot}	Total surface energy

REFERENCES

(1) Leali, P. T.; Merolli, A. Fundamentals of Biomaterials. In *Biomaterials in Hand Surgery*; Merolli, A., Joyce, T. J., Eds.; Springer Milan: Milano, 2009; pp 1–11. https://doi.org/10.1007/978-88-470-1195-3_1.

(2) Bergmann, C. P.; Stumpf, A. Biomaterials. In *Dental Ceramics: Microstructure, Properties and Degradation*; Bergmann, C., Stumpf, A., Eds.; Topics in Mining, Metallurgy and Materials Engineering; Springer: Berlin, Heidelberg, 2013; pp 9–13. https://doi.org/10.1007/978-3-642-38224-6_2.

(3) Boateng, J. *Therapeutic Dressings and Wound Healing Applications*; John Wiley & Sons, 2020.

(4) Shi, D. *Introduction to Biomaterials*; Tsinghua University Press, 2006.

(5) Patel, N. R.; Gohil, P. P. A Review on Biomaterials : Scope , Applications & Human Anatomy Significance; 2012.

(6) Eliaz, N. Corrosion of Metallic Biomaterials: A Review. *Materials (Basel)* 2019, *12* (3). https://doi.org/10.3390/ma12030407.

(7) Ebnesajjad, S.; Landrock, A. H. Chapter 6 - Adhesives for Special Adherends. In *Adhesives Technology Handbook (Third Edition)*; Ebnesajjad, S., Landrock, A. H., Eds.; William Andrew Publishing: Boston, 2015; pp 160–182. https://doi.org/10.1016/B978-0-323-35595-7.00006-1.

(8) Huang, J.; Best, S. M. 1 - Ceramic Biomaterials. In *Tissue Engineering Using Ceramics and Polymers*; Boccaccini, A. R., Gough, J. E., Eds.; Woodhead Publishing Series in Biomaterials; Woodhead Publishing, 2007; pp 3–31. https://doi.org/10.1533/9781845693817.1.3.

(9) Stroganova, E. E.; Mikhailenko, N. Yu.; Moroz, O. A. Glass-Based Biomaterials: Present and Future (A Review). *Glass and Ceramics* 2003, *60* (9/10), 315–319. https://doi.org/10.1023/B:GLAC.0000008235.49161.32.

(10) Kohane, D. S.; Langer, R. Polymeric Biomaterials in Tissue Engineering. 5.

(11) Feldman, D. Polymer History. *Designed Monomers and Polymers* 2008, *11* (1), 1–15. https://doi.org/10.1163/156855508X292383.

(12) Jensen, W. B. The Origin of the Polymer Concept. *J. Chem. Educ.* 2008, *85* (5), 624. https://doi.org/10.1021/ed085p624.

(13) Mülhaupt, R. Hermann Staudinger and the Origin of Macromolecular Chemistry. *Angewandte Chemie International Edition* 2004, *43* (9), 1054–1063. https://doi.org/10.1002/anie.200330070.

(14) *Hierarchical Macromolecular Structures: 60 Years after the Staudinger Nobel Prize II*; Percec, V., Ed.; Advances in Polymer Science; Springer International Publishing: Cham, 2013; Vol. 262. https://doi.org/10.1007/978-3-319-03719-6.

(15) Jr, C. E. C. *Carraher's Polymer Chemistry, Ninth Edition*; CRC Press, 2016.

(16) Ignatyev, I. A.; Thielemans, W.; Vander Beke, B. Recycling of Polymers: A Review. *ChemSusChem* 2014, *7* (6), 1579–1593. https://doi.org/10.1002/cssc.201300898.

(17) Stuart, B. H. *Polymer Analysis*; John Wiley & Sons, 2008.

(18) Torres, T.; Bottari, G. *Organic Nanomaterials: Synthesis, Characterization, and Device Applications*; John Wiley & Sons, 2013.

(19) Ouellette, R. J.; Rawn, J. D. 15 - Synthetic Polymers. In *Principles of Organic Chemistry*; Ouellette, R. J., Rawn, J. D., Eds.; Elsevier: Boston, 2015; pp 397–419. https://doi.org/10.1016/B978-0-12-802444-7.00015-X.

(20) Rezaie, H. R.; Bakhtiari, L.; Öchsner, A. *Biomaterials and Their Applications*; SpringerBriefs in Materials; Springer International Publishing, 2015. https://doi.org/10.1007/978-3-319-17846-2.

(21) Mishra, M. *Encyclopedia of Polymer Applications, 3 Volume Set*; CRC Press, 2018.

(22) Dasmohapatra, G. *Engineering Chemistry I (WBUT), 3rd Edition*; Vikas Publishing House.

(23) Jr, C. E. C. *Introduction to Polymer Chemistry*; CRC Press, 2017.

(24) Olatunji, O. *Natural Polymers: Industry Techniques and Applications*; Springer, 2015.
(25) Goddard, E. D.; Gruber, J. V. *Principles of Polymer Science and Technology in Cosmetics and Personal Care*; CRC Press, 1999.
(26) Rotello, V.; Thayumanavan, S. *Molecular Recognition and Polymers: Control of Polymer Structure and Self-Assembly*; John Wiley & Sons, 2008.
(27) Dumitriu, S.; Popa, V. I. *Polymeric Biomaterials: Structure and Function*; CRC Press, 2013.
(28) Cao, S.; Zhu, H. *The Design, Synthetic Strategies and Biocompatibility of Polymer Scaffolds for Biomedical Application*; Bentham Science Publishers, 2014.
(29) Murphy, W.; Black, J.; Hastings, G. *Handbook of Biomaterial Properties*; Springer, 2016.
(30) Taubert, A.; Mano, J. F.; Rodr¿guez-Cabello, J. C. *Biomaterials Surface Science*; John Wiley & Sons, 2013.
(31) Hirsh, S. L.; McKenzie, D. R.; Nosworthy, N. J.; Denman, J. A.; Sezerman, O. U.; Bilek, M. M. M. The Vroman Effect: Competitive Protein Exchange with Dynamic Multilayer Protein Aggregates. *Colloids and Surfaces B: Biointerfaces* 2013, *103*, 395–404. https://doi.org/10.1016/j.colsurfb.2012.10.039.
(32) Hasirci, V.; Hasirci, N. *Fundamentals of Biomaterials*; Springer, 2018.
(33) Bobbert, F. S. L.; Zadpoor, A. A. Effects of Bone Substitute Architecture and Surface Properties on Cell Response, Angiogenesis, and Structure of New Bone. *J. Mater. Chem. B* 2017, *5* (31), 6175–6192. https://doi.org/10.1039/C7TB00741H.
(34) Anderson, J. M. 9.19 - Biocompatibility. In *Polymer Science: A Comprehensive Reference*; Matyjaszewski, K., Möller, M., Eds.; Elsevier: Amsterdam, 2012; pp 363–383. https://doi.org/10.1016/B978-0-444-53349-4.00229-6.
(35) *Definitions in Biomaterials: Proceedings of a Consensus Conference of the European Society for Biomaterials, Chester, England, March 3-5, 1986*; Williams, D. F., European Society for Biomaterials, Eds.; Elsevier: Amsterdam; New York, 1987.
(36) Williams, D. Chapter 9 - Biocompatibility. In *Tissue Engineering*; Blitterswijk, C. van, Thomsen, P., Lindahl, A., Hubbell, J., Williams, D. F., Cancedda, R., Bruijn, J. D. de, Sohier, J., Eds.; Academic Press: Burlington, 2008; pp 255–278. https://doi.org/10.1016/B978-0-12-370869-4.00009-4.
(37) Gad, S. C.; Gad-McDonald, S.; Gad-McDonald, S. *Biomaterials, Medical Devices, and Combination Products : Biocompatibility Testing and Safety Assessment*; CRC Press, 2015. https://doi.org/10.1201/b19086.
(38) ISO 10993-1:2018(en), Biological evaluation of medical devices — Part 1: Evaluation and testing within a risk management process https://www.iso.org/obp/ui/#iso:std:iso:10993:-1:ed-5:v2:en (accessed Oct 30, 2020).
(39) Hollinger, J. O. *An Introduction to Biomaterials*; CRC Press, 2005.
(40) ISO 10993-5:2009(en), Biological evaluation of medical devices — Part 5: Tests for in vitro cytotoxicity https://www.iso.org/obp/ui/#iso:std:iso:10993:-5:ed-3:v1:en (accessed Dec 3, 2020).
(41) Liu, X.; Rodeheaver, D. P.; White, J. C.; Wright, A. M.; Walker, L. M.; Zhang, F.; Shannon, S. A Comparison of in Vitro Cytotoxicity Assays in Medical Device Regulatory Studies. *Regulatory Toxicology and Pharmacology* 2018, *97*, 24–32. https://doi.org/10.1016/j.yrtph.2018.06.003.
(42) McKinnon, K. M. Flow Cytometry: An Overview. *Curr Protoc Immunol* 2018, *120*, 5.1.1-5.1.11. https://doi.org/10.1002/cpim.40.
(43) Salehi-Nik, N.; Amoabediny, G.; Pouran, B.; Tabesh, H.; Shokrgozar, M. A.; Haghighipour, N.; Khatibi, N.; Anisi, F.; Mottaghy, K.; Zandieh-Doulabi, B. Engineering Parameters in Bioreactor's Design: A Critical Aspect in Tissue Engineering https://www.hindawi.com/journals/bmri/2013/762132/ (accessed Jan 10, 2020). https://doi.org/10.1155/2013/762132.
(44) Wakatsuki, T.; Kolodney, M. S.; Zahalak, G. I.; Elson, E. L. Cell Mechanics Studied by a Reconstituted Model Tissue. *Biophysical Journal* 2000, *79* (5), 2353–2368. https://doi.org/10.1016/S0006-3495(00)76481-2.

(45) Kandárová, H.; Letašiová, S. Alternative Methods in Toxicology: Pre-Validated and Validated Methods. *Interdiscip Toxicol* 2011, *4* (3), 107–113. https://doi.org/10.2478/v10102-011-0018-6.
(46) Boateng, J. S.; Mitchell, J. C.; Pawar, H.; Ayensu, I. Functional Characterisation and Permeation Studies of Lyophilised Thiolated Chitosan Xerogels for Buccal Delivery of Insulin. *Protein Pept. Lett.* 2014, *21* (11), 1163–1175. https://doi.org/10.2174/0929866521666140805124403.
(47) Cui, Y.; Claus, S.; Schnell, D.; Runge, F.; MacLean, C. In-Depth Characterization of EpiIntestinal Microtissue as a Model for Intestinal Drug Absorption and Metabolism in Human. *Pharmaceutics* 2020, *12* (5). https://doi.org/10.3390/pharmaceutics12050405.
(48) Barosova, H.; Maione, A. G.; Septiadi, D.; Sharma, M.; Haeni, L.; Balog, S.; O'Connell, O.; Jackson, G. R.; Brown, D.; Clippinger, A. J.; Hayden, P.; Petri-Fink, A.; Stone, V.; Rothen-Rutishauser, B. Use of EpiAlveolar Lung Model to Predict Fibrotic Potential of Multiwalled Carbon Nanotubes. *ACS Nano* 2020, *14* (4), 3941–3956. https://doi.org/10.1021/acsnano.9b06860.
(49) Ayehunie, S.; Cannon, C.; Lamore, S.; Klausner, M.; Kubilus, J. EpiVaginal™ Human Vaginal-Ectocervical Tissue Models for Irritation and HIV-1 Studies. *Fertility and Sterility 84*, S60.
(50) Chen, C.; Bai, X.; Ding, Y.; Lee, I.-S. Electrical Stimulation as a Novel Tool for Regulating Cell Behavior in Tissue Engineering. *Biomater Res* 2019, *23* (1), 25. https://doi.org/10.1186/s40824-019-0176-8.
(51) Funk, R. H. W.; Monsees, T.; Ozkucur, N. Electromagnetic Effects - From Cell Biology to Medicine. *Prog Histochem Cytochem* 2009, *43* (4), 177–264. https://doi.org/10.1016/j.proghi.2008.07.001.
(52) Franzini-Armstrong, C. The Relationship between Form and Function throughout the History of Excitation–Contraction Coupling. *J Gen Physiol* 2018, *150* (2), 189–210. https://doi.org/10.1085/jgp.201711889.
(53) Tai, G.; Tai, M.; Zhao, M. Electrically Stimulated Cell Migration and Its Contribution to Wound Healing. *BURNS TRAUMA* 2018, *6* (1). https://doi.org/10.1186/s41038-018-0123-2.
(54) Taghian, T.; Narmoneva, D. A.; Kogan, A. B. Modulation of Cell Function by Electric Field: A High-Resolution Analysis. *J R Soc Interface* 2015, *12* (107). https://doi.org/10.1098/rsif.2015.0153.
(55) Otero, T. F.; Martinez, J. G.; Arias-Pardilla, J. Biomimetic Electrochemistry from Conducting Polymers. A Review: Artificial Muscles, Smart Membranes, Smart Drug Delivery and Computer/Neuron Interfaces. *Electrochimica Acta* 2012, *84*, 112–128. https://doi.org/10.1016/j.electacta.2012.03.097.
(56) Guo, B.; Ma, P. X. Conducting Polymers for Tissue Engineering. *Biomacromolecules* 2018, *19* (6), 1764–1782. https://doi.org/10.1021/acs.biomac.8b00276.
(57) Levin, M. Molecular Bioelectricity: How Endogenous Voltage Potentials Control Cell Behavior and Instruct Pattern Regulation in Vivo. *Mol Biol Cell* 2014, *25* (24), 3835–3850. https://doi.org/10.1091/mbc.E13-12-0708.
(58) Hammond, C. *Cellular and Molecular Neurophysiology*; Academic Press, 2014.
(59) Wardhan, R.; Mudgal, P. *Textbook of Membrane Biology*; Springer Singapore: Singapore, 2017. https://doi.org/10.1007/978-981-10-7101-0.
(60) Nuccitelli, R. A Role for Endogenous Electric Fields in Wound Healing. *Curr. Top. Dev. Biol.* 2003, *58*, 1–26. https://doi.org/10.1016/s0070-2153(03)58001-2.
(61) Fang, K. S.; Farboud, B.; Nuccitelli, R.; Isseroff, R. R. Migration of Human Keratinocytes in Electric Fields Requires Growth Factors and Extracellular Calcium. *J. Invest. Dermatol.* 1998, *111* (5), 751–756. https://doi.org/10.1046/j.1523-1747.1998.00366.x.
(62) Guo, A.; Song, B.; Reid, B.; Gu, Y.; Forrester, J. V.; Jahoda, C. A. B.; Zhao, M. Effects of Physiological Electric Fields on Migration of Human Dermal Fibroblasts. *J Invest Dermatol* 2010, *130* (9), 2320–2327. https://doi.org/10.1038/jid.2010.96.

(63) Chen, Y.; Ye, L.; Guan, L.; Fan, P.; Liu, R.; Liu, H.; Chen, J.; Zhu, Y.; Wei, X.; Liu, Y.; Bai, H. Physiological Electric Field Works via the VEGF Receptor to Stimulate Neovessel Formation of Vascular Endothelial Cells in a 3D Environment. *Biol Open* 2018, *7* (9). https://doi.org/10.1242/bio.035204.

(64) Arnold, C. E.; Rajnicek, A. M.; Hoare, J. I.; Pokharel, S. M.; Mccaig, C. D.; Barker, R. N.; Wilson, H. M. Physiological Strength Electric Fields Modulate Human T Cell Activation and Polarisation. *Scientific Reports* 2019, *9* (1), 17604. https://doi.org/10.1038/s41598-019-53898-5.

(65) Hoare, J. I.; Rajnicek, A. M.; McCaig, C. D.; Barker, R. N.; Wilson, H. M. Electric Fields Are Novel Determinants of Human Macrophage Functions. *J. Leukoc. Biol.* 2016, *99* (6), 1141–1151. https://doi.org/10.1189/jlb.3A0815-390R.

(66) PARK, E.-H.; BARRETO, E.; GLUCKMAN, B. J.; SCHIFF, S. J.; SO, P. A Model of the Effects of Applied Electric Fields on Neuronal Synchronization. *J Comput Neurosci* 2005, *19* (1), 53–70. https://doi.org/10.1007/s10827-005-0214-5.

(67) Xu, Y.; Jia, Y.; Ma, J.; Hayat, T.; Alsaedi, A. Collective Responses in Electrical Activities of Neurons under Field Coupling. *Scientific Reports* 2018, *8* (1), 1349. https://doi.org/10.1038/s41598-018-19858-1.

(68) Kowalski, P. S.; Bhattacharya, C.; Afewerki, S.; Langer, R. Smart Biomaterials: Recent Advances and Future Directions. *ACS Biomater. Sci. Eng.* 2018, *4* (11), 3809–3817. https://doi.org/10.1021/acsbiomaterials.8b00889.

(69) Moseley, P. T.; Crocker, J. *Sensor Materials*; CRC Press, 2020.

(70) Szuwarzyński, M.; Wolski, K.; Zapotoczny, S. Enhanced Stability of Conductive Polyacetylene in Ladder-like Surface-Grafted Brushes. *Polym. Chem.* 2016, *7* (36), 5664–5670. https://doi.org/10.1039/C6PY00977H.

(71) Bendrea, A.-D.; Cianga, L.; Cianga, I. Review Paper: Progress in the Field of Conducting Polymers for Tissue Engineering Applications. *J Biomater Appl* 2011, *26* (1), 3–84. https://doi.org/10.1177/0885328211402704.

(72) Filimon, A. Perspectives of Conductive Polymers Toward Smart Biomaterials for Tissue Engineering. *Conducting Polymers* 2016. https://doi.org/10.5772/63555.

(73) Inzelt, G. *Conducting Polymers: A New Era in Electrochemistry*; Springer Science & Business Media, 2012.

(74) Balint, R.; Cassidy, N. J.; Cartmell, S. H. Conductive Polymers: Towards a Smart Biomaterial for Tissue Engineering. *Acta Biomaterialia* 2014, *10* (6), 2341–2353. https://doi.org/10.1016/j.actbio.2014.02.015.

(75) Kumar, R.; Singh, S.; Yadav, B. C. Conducting Polymers: Synthesis, Properties and Applications. 2015, *2* (11), 15.

(76) de Albuquerque, J. E.; Mattoso, L. H. C.; Faria, R. M.; Masters, J. G.; MacDiarmid, A. G. Study of the Interconversion of Polyaniline Oxidation States by Optical Absorption Spectroscopy. *Synthetic Metals* 2004, *146* (1), 1–10. https://doi.org/10.1016/j.synthmet.2004.05.019.

(77) Stejskal, J.; Gilbert, R. G. Polyaniline. Preparation of a Conducting Polymer(IUPAC Technical Report). *Pure and Applied Chemistry* 2002, *74* (5), 857–867. https://doi.org/10.1351/pac200274050857.

(78) Stejskal, J.; Sapurina, I. Polyaniline: Thin Films and Colloidal Dispersions (IUPAC Technical Report). *Pure and Applied Chemistry* 2005, *77* (5), 815–826. https://doi.org/10.1351/pac200577050815.

(79) Wang, L.-X.; Li, X.-G.; Yang, Y.-L. Preparation, Properties and Applications of Polypyrroles. *Reactive and Functional Polymers* 2001, *47* (2), 125–139. https://doi.org/10.1016/S1381-5148(00)00079-1.

(80) Sanches, E. A.; Alves, S. F.; Soares, J. C.; da Silva, A. M.; da Silva, C. G.; de Souza, S. M.; da Frota, H. O. Nanostructured Polypyrrole Powder: A Structural and Morphological Characterization https://www.hindawi.com/journals/jnm/2015/129678/ (accessed Oct 30, 2020). https://doi.org/10.1155/2015/129678.

(81) Qi, G.; Huang, L.; Wang, H. Highly Conductive Free Standing Polypyrrole Films Prepared by Freezing Interfacial Polymerization. *Chem. Commun.* 2012, *48* (66), 8246–8248. https://doi.org/10.1039/C2CC33889K.
(82) Li, Y.; Bober, P.; Apaydin, D. H.; Syrový, T.; Sariciftci, N. S.; Hromádková, J.; Sapurina, I.; Trchová, M.; Stejskal, J. Colloids of Polypyrrole Nanotubes/Nanorods: A Promising Conducting Ink. *Synthetic Metals* 2016, *221*, 67–74. https://doi.org/10.1016/j.synthmet.2016.10.007.
(83) Ouyang, J.; Li, Y. Great Improvement of Polypyrrole Films Prepared Electrochemically from Aqueous Solutions by Adding Nonaphenol Polyethyleneoxy (10) Ether. *Polymer* 1997, *38* (15), 3997–3999. https://doi.org/10.1016/S0032-3861(97)00087-6.
(84) Duchet, J.; Legras, R.; Demoustier-Champagne, S. Chemical Synthesis of Polypyrrole: Structure–Properties Relationship. *Synthetic Metals* 1998, *98* (2), 113–122. https://doi.org/10.1016/S0379-6779(98)00180-5.
(85) Vernitskaya, T. V.; Efimov, O. N. Polypyrrole: A Conducting Polymer; Its Synthesis, Properties and Applications. *Russ. Chem. Rev.* 1997, *66* (5), 443. https://doi.org/10.1070/RC1997v066n05ABEH000261.
(86) Stejskal, J.; Trchová, M.; Bober, P.; Morávková, Z.; Kopecký, D.; Vrňata, M.; Prokeš, J.; Varga, M.; Watzlová, E. Polypyrrole Salts and Bases: Superior Conductivity of Nanotubes and Their Stability towards the Loss of Conductivity by Deprotonation. *RSC Advances* 2016, *6* (91), 88382–88391. https://doi.org/10.1039/C6RA19461C.
(87) Ateh, D. d; Navsaria, H. a; Vadgama, P. Polypyrrole-Based Conducting Polymers and Interactions with Biological Tissues. *Journal of The Royal Society Interface* 2006, *3* (11), 741–752. https://doi.org/10.1098/rsif.2006.0141.
(88) Armes, S. P. Optimum Reaction Conditions for the Polymerization of Pyrrole by Iron(III) Chloride in Aqueous Solution. *Synthetic Metals* 1987, *20* (3), 365–371. https://doi.org/10.1016/0379-6779(87)90833-2.
(89) Omastová, M.; Trchová, M.; Kovářová, J.; Stejskal, J. Synthesis and Structural Study of Polypyrroles Prepared in the Presence of Surfactants. *Synthetic Metals* 2003, *138* (3), 447–455. https://doi.org/10.1016/S0379-6779(02)00498-8.
(90) Stejskal, J.; Omastová, M.; Fedorova, S.; Prokeš, J.; Trchová, M. Polyaniline and Polypyrrole Prepared in the Presence of Surfactants: A Comparative Conductivity Study. *Polymer* 2003, *44* (5), 1353–1358. https://doi.org/10.1016/S0032-3861(02)00906-0.
(91) Lu, Y.; Shi, G.; Li, C.; Liang, Y. Thin Polypyrrole Films Prepared by Chemical Oxidative Polymerization. *Journal of Applied Polymer Science* 1998, *70* (11), 2169–2172. https://doi.org/10.1002/(SICI)1097-4628(19981212)70:11<2169::AID-APP10>3.0.CO;2-I.
(92) Torres-Gómez, G.; Gómez-Romero, P. Conducting Organic Polymers with Electroactive Dopants. Synthesis and Electrochemical Properties of Hexacyanoferrate-Doped Polypyrrole. *Synthetic Metals* 1998, *98* (2), 95–102. https://doi.org/10.1016/S0379-6779(98)00150-7.
(93) Nishio, K.; Fujimoto, M.; Ando, O.; Ono, H.; Murayama, T. Characteristics of Polypyrrole Chemically Synthesized by Various Oxidizing Reagents. *J Appl Electrochem* 1996, *26* (4), 425–429. https://doi.org/10.1007/BF00251328.
(94) Mazumder, M. A. J.; Sheardown, H.; Al-Ahmed, A. *Functional Polymers*; Springer International Publishing, 2019.
(95) Blasco, E.; Sims, M. B.; Goldmann, A. S.; Sumerlin, B. S.; Barner-Kowollik, C. 50th Anniversary Perspective: Polymer Functionalization https://pubs.acs.org/doi/pdf/10.1021/acs.macromol.7b00465 (accessed Dec 3, 2020). https://doi.org/10.1021/acs.macromol.7b00465.
(96) Günay, K. A.; Theato, P.; Klok, H.-A. History of Post-Polymerization Modification. In *Functional Polymers by Post-Polymerization Modification*; Theato, P., Klok, H.-A., Eds.; Wiley-VCH Verlag GmbH & Co. KGaA: Weinheim, Germany, 2013; pp 1–44. https://doi.org/10.1002/9783527655427.ch1.

(97) Pinson, J.; Thiry, D. *Surface Modification of Polymers: Methods and Applications*; John Wiley & Sons, 2019.
(98) Stejskal, J.; Prokeš, J.; Trchová, M. Reprotonation of Polyaniline: A Route to Various Conducting Polymer Materials. *Reactive and Functional Polymers* 2008, *68* (9), 1355–1361. https://doi.org/10.1016/j.reactfunctpolym.2008.06.012.
(99) Shishkanova, T. V.; Sapurina, I.; Stejskal, J.; Kral, V.; Volf, R. Ion-Selective Electrodes: Polyaniline Modification and Anion Recognition. *Anal. Chim. Acta* 2005, *553* (1–2), 160–168. https://doi.org/10.1016/j.aca.2005.08.018.
(100) Stejskal, J.; Trchová, M.; Bober, P.; Humpolíček, P.; Kašpárková, V.; Sapurina, I.; Shishov, M. A.; Varga, M. Conducting Polymers: Polyaniline. In *Encyclopedia of Polymer Science and Technology*; American Cancer Society, 2015; pp 1–44. https://doi.org/10.1002/0471440264.pst640.
(101) Konyushenko, E. N.; Stejskal, J.; Šeděnková, I.; Trchová, M.; Sapurina, I.; Cieslar, M.; Prokeš, J. Polyaniline Nanotubes: Conditions of Formation. *Polymer International* 2006, *55* (1), 31–39. https://doi.org/10.1002/pi.1899.
(102) Hu, X.; Lu, Y.; Liu, J. Synthesis of Polypyrrole Microtubes with Actinomorphic Morphology in the Presence of a β-Cyclodextrin Derivative-Methyl Orange Inclusion Complex. *Macromolecular Rapid Communications* 2004, *25* (11), 1117–1120. https://doi.org/10.1002/marc.200400067.
(103) Yang, X.; Zhu, Z.; Dai, T.; Lu, Y. Facile Fabrication of Functional Polypyrrole Nanotubes via a Reactive Self-Degraded Template. *Macromolecular Rapid Communications* 2005, *26* (21), 1736–1740. https://doi.org/10.1002/marc.200500514.
(104) Li, Y.; Bober, P.; Trchová, M.; Stejskal, J. Polypyrrole Prepared in the Presence of Methyl Orange and Ethyl Orange: Nanotubes versus Globules in Conductivity Enhancement. *J. Mater. Chem. C* 2017, *5* (17), 4236–4245. https://doi.org/10.1039/C7TC00206H.
(105) Yan, W.; Han, J. Synthesis and Formation Mechanism Study of Rectangular-Sectioned Polypyrrole Micro/Nanotubules. *Polymer* 2007, *48* (23), 6782–6790. https://doi.org/10.1016/j.polymer.2007.09.026.
(106) Stejskal, J.; Hlavatá, D.; Holler, P.; Trchová, M.; Prokeš, J.; Sapurina, I. Polyaniline Prepared in the Presence of Various Acids: A Conductivity Study. *Polymer International* 2004, *53* (3), 294–300. https://doi.org/10.1002/pi.1406.
(107) Bláha, M.; Varga, M.; Prokeš, J.; Zhigunov, A.; Vohlídal, J. Effects of the Polymerization Temperature on the Structure, Morphology and Conductivity of Polyaniline Prepared with Ammonium Peroxodisulfate. *European Polymer Journal* 2013, *49* (12), 3904–3911. https://doi.org/10.1016/j.eurpolymj.2013.08.018.
(108) Le, T.-H.; Kim, Y.; Yoon, H. Electrical and Electrochemical Properties of Conducting Polymers. *Polymers* 2017, *9* (4), 150. https://doi.org/10.3390/polym9040150.
(109) Ansari, R. Polypyrrole Conducting Electroactive Polymers: Synthesis and Stability Studies https://www.hindawi.com/journals/jchem/2006/860413/ (accessed Sep 2, 2020). https://doi.org/10.1155/2006/860413.
(110) Kang, H. C.; Geckeler, K. E. Enhanced Electrical Conductivity of Polypyrrole Prepared by Chemical Oxidative Polymerization: Effect of the Preparation Technique and Polymer Additive. *Polymer* 2000, *41* (18), 6931–6934. https://doi.org/10.1016/S0032-3861(00)00116-6.
(111) Rejmontova, P.; Capakova, Z.; Mikusova, N.; Marakova, N.; Kasparkova, V.; Lehocky, M.; Humpolicek, P. Adhesion, Proliferation and Migration of NIH/3T3 Cells on Modified Polyaniline Surfaces. *Int. J. Mol. Sci.* 2016, *17* (9), 1439. https://doi.org/10.3390/ijms17091439.
(112) Della Pina, C.; Capakova, Z.; Sironi, A.; Humpolicek, P.; Saha, P.; Falletta, E. On the Cytotoxicity of Poly(4-Aminodiphenylaniline) Powders: Effect of Acid Dopant Type and Sample Posttreatment. *Int. J. Polym. Mater. Polym. Biomat.* 2017, *66* (3), 132–138. https://doi.org/10.1080/00914037.2016.1190928.

(113) Humpolicek, P.; Kucekova, Z.; Kasparkova, V.; Pelkova, J.; Modic, M.; Junkar, I.; Trchova, M.; Bober, P.; Stejskal, J.; Lehocky, M. Blood Coagulation and Platelet Adhesion on Polyaniline Films. *Colloid Surf. B-Biointerfaces* 2015, *133*, 278–285. https://doi.org/10.1016/j.colsurfb.2015.06.008.

(114) Bober, P.; Lindfors, T.; Pesonen, M.; Stejskal, J. Enhanced PH Stability of Conducting Polyaniline by Reprotonation with Perfluorooctanesulfonic Acid. *Synthetic Metals* 2013, *178*, 52–55. https://doi.org/10.1016/j.synthmet.2013.07.002.

(115) Humpolicek, P.; Kasparkova, V.; Saha, P.; Stejskal, J. Biocompatibility of Polyaniline. *Synthetic Metals* 2012, *162* (7), 722–727. https://doi.org/10.1016/j.synthmet.2012.02.024.

(116) Jeong, S. I.; Jun, I. D.; Choi, M. J.; Nho, Y. C.; Lee, Y. M.; Shin, H. Development of Electroactive and Elastic Nanofibers That Contain Polyaniline and Poly(L-Lactide-Co-ε-Caprolactone) for the Control of Cell Adhesion. *Macromolecular Bioscience* 2008, *8* (7), 627–637. https://doi.org/10.1002/mabi.200800005.

(117) Bayer, C. L.; Trenchard, I. J.; Peppas, N. A. Analyzing Polyaniline-Poly(2-Acrylamido-2-Methylpropane Sulfonic Acid) Biocompatibility with 3T3 Fibroblasts. *J Biomater Sci Polym Ed* 2010, *21* (5), 623–634. https://doi.org/10.1163/156856209X434647.

(118) Kasparkova, V.; Humpolicek, P.; Stejskal, J.; Kopecka, J.; Kucekova, Z.; Moucka, R. Conductivity, Impurity Profile, and Cytotoxicity of Solvent-Extracted Polyaniline. *Polym. Adv. Technol.* 2016, *27* (2), 156–161. https://doi.org/10.1002/pat.3611.

(119) Kucekova, Z.; Humpolicek, P.; Kasparkova, V.; Perecko, T.; Lehocky, M.; Hauerlandova, I.; Saha, P.; Stejskal, J. Colloidal Polyaniline Dispersions: Antibacterial Activity, Cytotoxicity and Neutrophil Oxidative Burst. *Colloid Surf. B-Biointerfaces* 2014, *116*, 411–417. https://doi.org/10.1016/j.colsurfb.2014.01.027.

(120) Kasparkova, V.; Jasenska, D.; Capakova, Z.; Marakova, N.; Stejskal, J.; Bober, P.; Lehocky, M.; Humpolicek, P. Polyaniline Colloids Stabilized with Bioactive Polysaccharides: Non-Cytotoxic Antibacterial Materials. *Carbohydr. Polym.* 2019, *219*, 423–430. https://doi.org/10.1016/j.carbpol.2019.05.038.

(121) Liu, J.; Pedersen, L. C. Anticoagulant Heparan Sulfate: Structural Specificity and Biosynthesis. *Appl Microbiol Biotechnol* 2007, *74* (2), 263–272. https://doi.org/10.1007/s00253-006-0722-x.

(122) Tengvall, P. 4.406 - Protein Interactions with Biomaterials. In *Comprehensive Biomaterials*; Ducheyne, P., Ed.; Elsevier: Oxford, 2011; pp 63–73. https://doi.org/10.1016/B978-0-08-055294-1.00006-4.

(123) Kasparkova, V.; Humpolicek, P.; Capakova, Z.; Bober, P.; Stejskal, J.; Trchova, M.; Rejmontova, P.; Junkar, I.; Lehocky, M.; Mozetic, M. Cell-Compatible Conducting Polyaniline Films Prepared in Colloidal Dispersion Mode. *Colloid Surf. B-Biointerfaces* 2017, *157*, 309–316. https://doi.org/10.1016/j.colsurfb.2017.05.066.

(124) Alikacem, N.; Marois, Y.; Zhang, Z.; Jakubiec, B.; Roy, R.; King, M. W.; Guidoin, R. Tissue Reactions to Polypyrrole-Coated Polyesters: A Magnetic Resonance Relaxometry Study. *Artificial Organs* 1999, *23* (10), 910–919. https://doi.org/10.1046/j.1525-1594.1999.06231.x.

(125) Cui, X.; Lee, V. A.; Raphael, Y.; Wiler, J. A.; Hetke, J. F.; Anderson, D. J.; Martin, D. C. Surface Modification of Neural Recording Electrodes with Conducting Polymer/Biomolecule Blends. *Journal of Biomedical Materials Research* 2001, *56* (2), 261–272. https://doi.org/10.1002/1097-4636(200108)56:2<261::AID-JBM1094>3.0.CO;2-I.

(126) George, P. M.; Lyckman, A. W.; LaVan, D. A.; Hegde, A.; Leung, Y.; Avasare, R.; Testa, C.; Alexander, P. M.; Langer, R.; Sur, M. Fabrication and Biocompatibility of Polypyrrole Implants Suitable for Neural Prosthetics. *Biomaterials* 2005, *26* (17), 3511–3519. https://doi.org/10.1016/j.biomaterials.2004.09.037.

(127) Geetha, S.; Rao, C. R. K.; Vijayan, M.; Trivedi, D. C. Biosensing and Drug Delivery by Polypyrrole. *Analytica Chimica Acta* 2006, *568* (1), 119–125. https://doi.org/10.1016/j.aca.2005.10.011.

(128) Upadhyay, J.; Kumar, A.; Gogoi, B.; Buragohain, A. K. Biocompatibility and Antioxidant Activity of Polypyrrole Nanotubes. *Synthetic Metals* 2014, *189*, 119–125. https://doi.org/10.1016/j.synthmet.2014.01.004.
(129) Humpolicek, P.; Kasparkova, V.; Pachernik, J.; Stejskal, J.; Bober, P.; Capakova, Z.; Radaszkiewicz, K. A.; Junkar, I.; Lehocky, M. The Biocompatibility of Polyaniline and Polypyrrole: A Comparative Study of Their Cytotoxicity, Embryotoxicity and Impurity Profile. *Mater. Sci. Eng. C-Mater. Biol. Appl.* 2018, *91*, 303–310. https://doi.org/10.1016/j.msec.2018.05.037.
(130) Molina, J.; Fernández, J.; del Río, A. I.; Lapuente, R.; Bonastre, J.; Cases, F. Stability of Conducting Polyester/Polypyrrole Fabrics in Different PH Solutions. Chemical and Electrochemical Characterization. *Polymer Degradation and Stability* 2010, *95* (12), 2574–2583. https://doi.org/10.1016/j.polymdegradstab.2010.07.028.
(131) Capakova, Z.; Radaszkiewicz, K. A.; Acharya, U.; Truong, T. H.; Pachernik, J.; Bober, P.; Kasparkova, V.; Stejskal, J.; Pfleger, J.; Lehocky, M.; Humpolicek, P. The Biocompatibility of Polyaniline and Polypyrrole 2(1): Doping with Organic Phosphonates. *Mater. Sci. Eng. C-Mater. Biol. Appl.* 2020, *113*, 110986. https://doi.org/10.1016/j.msec.2020.110986.
(132) Paradossi, G.; Cavalieri, F.; Chiessi, E.; Spagnoli, C.; Cowman, M. K. Poly(Vinyl Alcohol) as Versatile Biomaterial for Potential Biomedical Applications. *Journal of Materials Science: Materials in Medicine* 2003, *14* (8), 687–691. https://doi.org/10.1023/A:1024907615244.
(133) Hassan, C. M.; Trakampan, P.; Peppas, N. A. Water Solubility Characteristics of Poly(Vinyl Alcohol) and Gels Prepared by Freezing/Thawing Processes. In *Water Soluble Polymers: Solutions Properties and Applications*; Amjad, Z., Ed.; Springer US: Boston, MA, 2002; pp 31–40. https://doi.org/10.1007/0-306-46915-4_3.
(134) Ta, V. D.; Nguyen, T. V.; Pham, Q. V.; Nguyen, T. V. Biocompatible Microlasers Based on Polyvinyl Alcohol Microspheres. *Optics Communications* 2020, *459*, 124925. https://doi.org/10.1016/j.optcom.2019.124925.
(135) Morandim-Giannetti, A. de A.; Rubio, S. R.; Nogueira, R. F.; Ortega, F. D. S.; Magalhães Junior, O.; Schor, P.; Bersanetti, P. A. Characterization of PVA/Glutaraldehyde Hydrogels Obtained Using Central Composite Rotatable Design (CCRD). *J. Biomed. Mater. Res. Part B Appl. Biomater.* 2018, *106* (4), 1558–1566. https://doi.org/10.1002/jbm.b.33958.
(136) Agudelo, J. I. D.; Ramirez, M. R.; Henquin, E. R.; Rintoul, I. Modelling of Swelling of PVA Hydrogels Considering Non-Ideal Mixing Behaviour of PVA and Water. *J. Mater. Chem. B* 2019, *7* (25), 4049–4054. https://doi.org/10.1039/C9TB00243J.
(137) Muchová, M.; Münster, L.; Capáková, Z.; Mikulcová, V.; Kuřitka, I.; Vícha, J. Design of Dialdehyde Cellulose Crosslinked Poly(Vinyl Alcohol) Hydrogels for Transdermal Drug Delivery and Wound Dressings. *Materials Science and Engineering: C* 2020, *116*, 111242. https://doi.org/10.1016/j.msec.2020.111242.
(138) Memic, A.; Colombani, T.; Eggermont, L. J.; Rezaeeyazdi, M.; Steingold, J.; Rogers, Z. J.; Navare, K. J.; Mohammed, H. S.; Bencherif, S. A. Latest Advances in Cryogel Technology for Biomedical Applications. *Advanced Therapeutics* 2019, *2* (4), 1800114. https://doi.org/10.1002/adtp.201800114.
(139) Bakhshpour, M.; Idil, N.; Perçin, I.; Denizli, A. Biomedical Applications of Polymeric Cryogels. *Applied Sciences* 2019, *9* (3), 553. https://doi.org/10.3390/app9030553.
(140) Sudhakar, C. K.; Upadhyay, N.; Jain, A.; Verma, A.; Narayana Charyulu, R.; Jain, S. Chapter 5 - Hydrogels—Promising Candidates for Tissue Engineering. In *Nanotechnology Applications for Tissue Engineering*; Thomas, S., Grohens, Y., Ninan, N., Eds.; William Andrew Publishing: Oxford, 2015; pp 77–94. https://doi.org/10.1016/B978-0-323-32889-0.00005-4.
(141) Nayak, A. K.; Das, B. 1 - Introduction to Polymeric Gels. In *Polymeric Gels*; Pal, K., Banerjee, I., Eds.; Woodhead Publishing Series in Biomaterials; Woodhead Publishing, 2018; pp 3–27. https://doi.org/10.1016/B978-0-08-102179-8.00001-6.

(142) Henderson, T. M. A.; Ladewig, K.; Haylock, D. N.; McLean, K. M.; O'Connor, A. J. Cryogels for Biomedical Applications. *J. Mater. Chem. B* 2013, *1* (21), 2682–2695. https://doi.org/10.1039/C3TB20280A.
(143) Humpolicek, P.; Radaszkiewicz, K. A.; Capakova, Z.; Pachernik, J.; Bober, P.; Kasparkova, V.; Rejmontova, P.; Lehocky, M.; Ponizil, P.; Stejskal, J. Polyaniline Cryogels: Biocompatibility of Novel Conducting Macroporous Material. *Sci Rep* 2018, *8*, 135. https://doi.org/10.1038/s41598-017-18290-1.

CURRICULUM VITAE

Personal information	
Surname/ First name	Capáková Zdenka (born Kuceková)
Adress	Lužné 268, 763 26 Luhačovice
Telephone	+420 576 038 047
E-mail	capakova@utb.cz
Nationality	Slovak
Date of birth	1.8.1985
Work experiences	
Dates	04/2018 – now
Occupation or position held	Senior researcher
Name of employer	Tomas Bata University in Zlin, Centre of Polymer Systems
Dates	08/2014 – 04/2018
Occupation or position held	Junior researcher
Name of employer	Tomas Bata University in Zlin, Centre of Polymer Systems
Dates	02/2012 – 08/2014
Occupation or position held	Project researcher
Name of employer	Tomas Bata University in Zlin, Centre of Polymer Systems
Education and training	
Dates	2010 – 2014
Title of qualification awarded	Ph.D.
Principal branch	Technology of macromolecular substances
Name and type of organisation providing education and training	Tomas Bata University in Zlin, Faculty of Technology
Dates	2007 – 2009
Title of qualification awarded	Ing.
Principal branch	Food technology, hygiene and chemistry
Name and type of organisation providing education and training	Tomas Bata University in Zlin, Faculty of Technology
Dates	2004 – 2007
Title of qualification awarded	Bc.
Principal branch	Food chemistry and technology
Name and type of organisation providing education and training	Tomas Bata University in Zlin, Faculty of Technology
Dates	2000 – 2004
Title of qualification awarded	Absolvent
Name and type of organisation providing education and training	Milana Rastislav Štefánik Grammar School, Nové Mesto nad Váhom, SK
Professional orientation	
Area of Scientific Interest	Biomaterials, Cell biology, Biological testing of materials

Team member in projects	GAČR 13-08944S (2013-2015) – Grant agency of Czech republic GAČR 17-05095S (2017-2019) – Grant agency of Czech republic GAČR 19-16861S (2019-2021) – Grant agency of Czech republic GAČR 20-28731S (2020-2023) – Grant agency of Czech republic CZ.02.2.69/0.0/0.0/16_018/0002720 Developing Research-oriented Degree Programmes at UNI CZ.02.2.69/0.0/0.0/16_015/0002204 Strategic Project of TBU in Zlín DS-2016-021 Multilateral Acientific and Technological Cooperation in the Danube Region
Principle investigator of projects	IGA/20/FT/11/D - Internal grant agency FT UTB IGA/FT/2012/029 - Internal grant agency FT UTB IGA/FT/2013/019 - Internal grant agency FT UTB
International cooperation	Jozef Stefan Institute, Department of surface engineering and optoelectronics, Slovenia Polymer institute SAV, Slovakia Univesity of Belgrade, Vinca institute of nuclear sciences, Serbia Abo Akademi University, Faculty of science and engineering, Finland Universita degli studi di Milano, Department of chemistry, Italy
Memberships	
Dates	2019 – now
Position held	Member of The European Society for Biomaterials

Publication summary and citations according to Web of Science Core Collection:

Number of articles in last 5 years: 38 (during 2016 – 2020)
Number of articles in total: 48 (during 2011 – 2020)
Number of citations without self-citations: 473
h-Index: 14

Article I.

Rejmontova, P.; **Capakova, Z**.; Mikusova, N.; Marakova, N.; Kasparkova, V.; Lehocky, M.; Humpolicek, P. Adhesion, Proliferation and Migration of NIH/3T3 Cells on Modified Polyaniline Surfaces. Int. J. Mol. Sci. 2016, 17 (9), 1439. https://doi.org/10.3390/ijms17091439.

International Journal of
Molecular Sciences

MDPI

Article

Adhesion, Proliferation and Migration of NIH/3T3 Cells on Modified Polyaniline Surfaces

Petra Rejmontová, Zdenka Capáková, Nikola Mikušová, Nela Maráková, Věra Kašpárková, Marián Lehocký and Petr Humpolíček *

Centre of Polymer Systems, Tomas Bata University in Zlín, třída Tomáše Bati 5678, 760 01 Zlín, Czech Republic; rejmontova@cps.utb.cz (P.R.); kucekova@cps.utb.cz (Z.C.); mikusova@ft.utb.cz (N.M.); marakova@ft.utb.cz (N.M.); vkasparkova@ft.utb.cz (V.K.); lehocky@ft.utb.cz (M.L.)
* Correspondence: humpolicek@ft.utb.cz; Tel.: +420-576-038-035

Academic Editor: Iolanda Francolini
Received: 28 July 2016; Accepted: 26 August 2016; Published: 15 September 2016

Abstract: Polyaniline shows great potential and promises wide application in the biomedical field thanks to its intrinsic conductivity and material properties, which closely resemble natural tissues. Surface properties are crucial, as these predetermine any interaction with biological fluids, proteins and cells. An advantage of polyaniline is the simple modification of its surface, e.g., by using various dopant acids. An investigation was made into the adhesion, proliferation and migration of mouse embryonic fibroblasts on pristine polyaniline films and films doped with sulfamic and phosphotungstic acids. In addition, polyaniline films supplemented with poly (2-acrylamido-2-methyl-1-propanesulfonic) acid at various ratios were tested. Results showed that the NIH/3T3 cell line was able to adhere, proliferate and migrate on the pristine polyaniline films as well as those films doped with sulfamic and phosphotungstic acids; thus, utilization of said forms in biomedicine appears promising. Nevertheless, incorporating poly (2-acrylamido-2-methyl-1-propanesulfonic) acid altered the surface properties of the polyaniline films and significantly affected cell behavior. In order to reveal the crucial factor influencing the surface/cell interaction, cell behavior is discussed in the context of the surface energy of individual samples. It was clearly demonstrated that the lesser the difference between the surface energy of the sample and cell, the more cyto-compatible the surface is.

Keywords: polyaniline; fibroblast; cyto-compatibility; sulfamic acid; phosphotungstic acid; poly (2-acrylamido-2-methyl-1-propanesulfonic) acid

1. Introduction

Recently, a rise in interest has been shown in research on polyaniline (PANI), which represents a highly attractive material due to its intrinsic conductivity, simple and inexpensive synthesis, versatile surface properties and favorable biological properties. As a direct consequence of such unique properties, PANI exhibits potential for diverse applications—ranging from microelectronics [1] on through biosensors [2] to tissue engineering [3]. Moreover, PANI, as representative of conducting polymers, has the application potentials as micro-electrodes for cell stimulation embedded in the bio-hybrid actuators [4] or material mimicking neuronal activity and neuromorphic functionalities [5]. In terms of biomedicine, a promising PANI electroactive scaffold could be utilized specifically in cardiac or neuronal tissue engineering [6]. However, utilizing PANI in biosensing and tissue engineering assumes that substantial knowledge exists on its bio-interface properties. In this context, a number of studies have already been published, e.g., PANI films doped with perchloride, hydrochloride, malic and citric acid are suitable for adhesion and proliferation of PC-12 [7], PANI films deposited with poly (2-acrylamido-2-methyl-1-propanesulfonic) acid (PAMPSA) allow an embryonic stem cell to adhere and

grow [8]. Therefore, polyaniline coating has been used in the past to improve the physical and biological properties of materials such as polyurethane [9] or graphene and graphene oxide [10]. Moreover, not only the modification of the cell/PANI surface interaction is possible, but also the interaction with blood can be influenced. The anticoagulation effect of PANI reprotonated with PAMPSA via the interaction of film with coagulation factors X, V and II has previously been described [11]. Apart from PAMPSA, other acids may be utilized, e.g., sulfamic and phosphotungstic acid.

Thus, the aim herein is to reveal the biological properties of PANI films synthesized by chemical oxidation in pristine forms as well as modified with poly (2-acrylamido-2-methyl-1-propanesulfonic), sulfamic and phosphotungstic acid. The mouse embryonic fibroblast cell line NIH/3T3 was utilized for this purpose. This cell line is generally considered as a suitable cell model for studying material biocompatibility and was already used for the determination of biological properties of conducting polymers [12,13].

2. Results and Discussion

2.1. Surface Energy

In the case of the evaluation of surface properties and related interactions of NIH/3T3 cells with the studied surfaces, the surface energy of the tested samples as well as the cell monolayer was determined. The total surface energy (γ^{tot}) was obtained and the absolute value of the difference between the surface energy of the cells and the sample (γ^{dif}) was calculated (Table 1).

Table 1. Surface energy evaluation of different polyaniline surfaces.

Sample	Surface Energy Components (mN·m^{-1})			
	γ^{tot}	γ^{LW}	γ^{AB}	γ^{dif}
PANI-S	52.54 *	46.05 *	6.49 *	3.33
PANI-B	50.88 *	46.54 *	4.35 *	1.67
PANI-SULF	52.13	44.97	7.17	2.92
PANI-PT	51.89	47.39	4.50	2.68
PANI-PAMPSA-1:1	41.85	40.98	0.87	7.36
PANI-PAMPSA-2:1	56.35	43.91	12.45	7.14
Cells	49.21	23.21	26.00	-

* The values presented in [14].

An interesting phenomena was observed for polyaniline samples that contained PAMPSA in the reaction mixture. As previously published, a significant decrease in γ^{tot} occurred when pristine polyaniline substrate was doped with PAMPSA [14]. In the present study, in the case of PANI-PAMPSA-1:1, the values obtained for the surface energy corresponded to PANI doped with PAMPSA. This may indicate that the characteristics of PAMPSA predominated and significantly impacted the surface properties of PANI-PAMPSA-1:1. Surface energy changed dramatically when a reduced amount of PAMPSA was used during polyaniline synthesis (the ratio of aniline hydrochloride to PAMPSA for synthesis was 2:1). In this case, the results approximated values for γ^{tot} as observed for pristine PANI-S and PANI-B. Thus, the surface properties of PANI-PAMPSA-2:1 are primarily governed by polyaniline, and only to a lesser extent by PAMPSA. Moreover, as can be seen, doping PANI with sulfamic acid and phosphotungstic acid did not influence surface properties in terms of γ^{tot} in comparison with PANI-S and PANI-B. Furthermore, the obtained γ^{tot} resembled that for the cell monolayer and so should indicate that suitable biological properties exist.

2.2. Cyto-Compatibility

To reveal the cyto-compatibility of tested samples, the adhesion, proliferation and migration of the mouse embryonic fibroblast NIH/3T3 cell line was investigated. The NIH/3T3 cell line is one of the most frequently used lines in material/cell interaction research and has been previously used for

cytotoxicity testing of PANI [15–17]. Thus, the results provided by these tests can easily be compared with data published in the literature. The micrographs clearly show that although the NIH/3T3 cells were able to adhere to all the tested surfaces in a similar way as the reference (Figure 1, only PANI-S is presented), remarkable differences in the subsequent cell proliferation and morphology existed (see Figure 2).

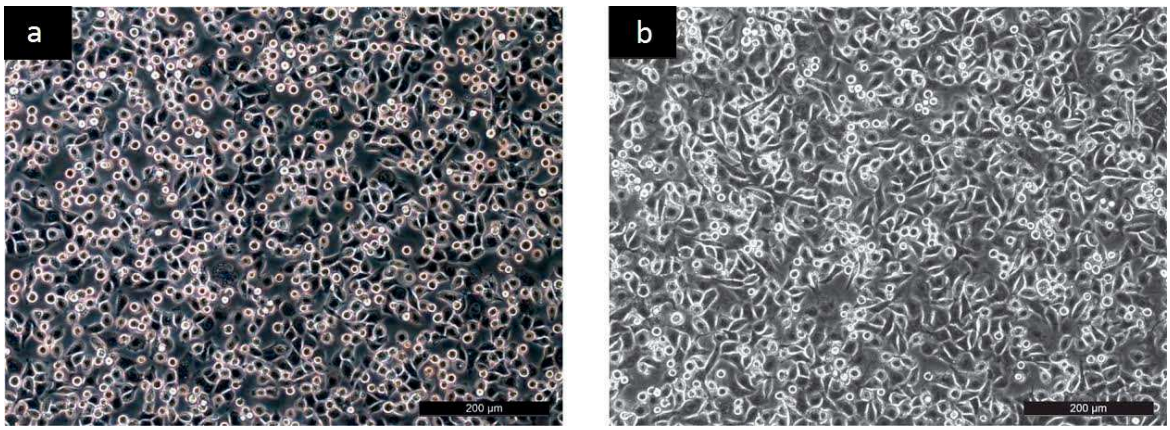

Figure 1. Adhesion: (**a**) Reference; (**b**) PANI-B.

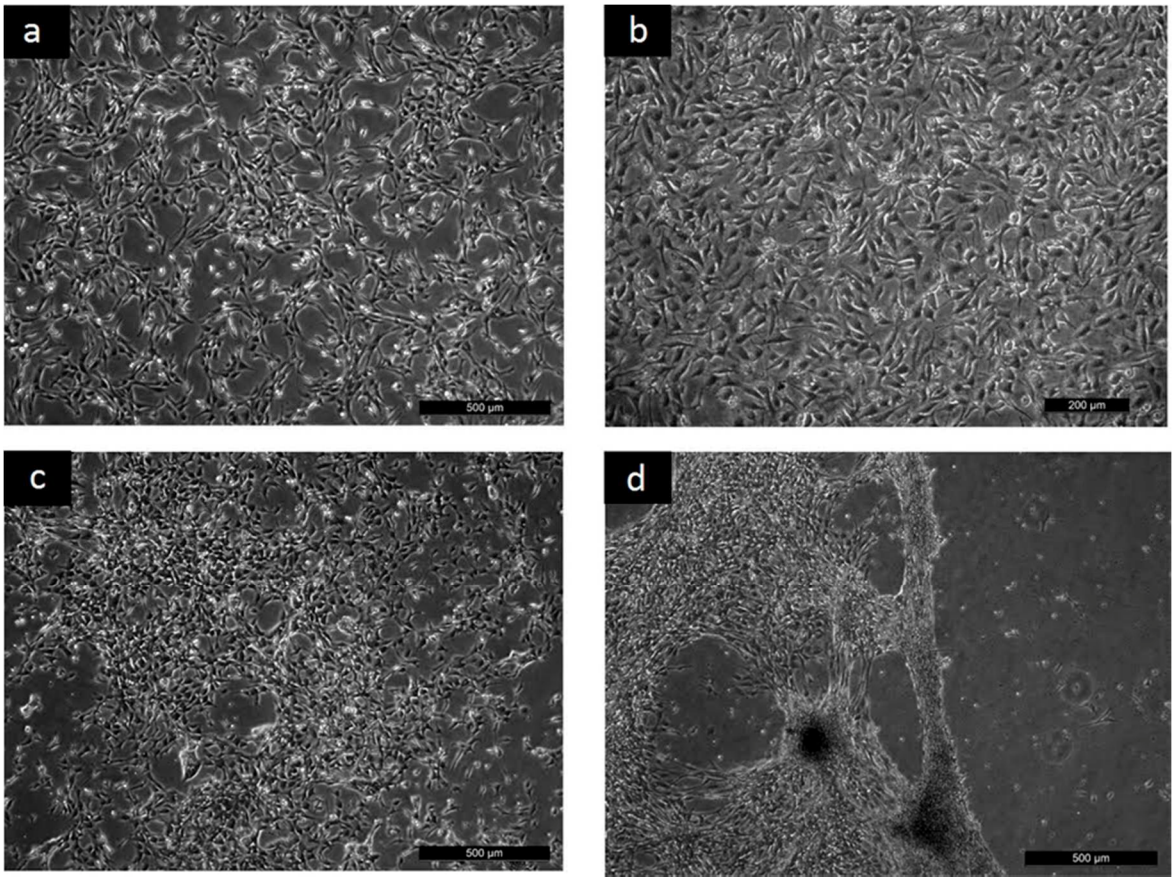

Figure 2. Proliferation: (**a**) Reference 24 h; (**b**) PANI-S 24 h; (**c**) PANI-PAMPSA-1:1 144 h; (**d**) PANI-PAMPSA-2:1 144 h.

It was clearly demonstrated that after 24 h, the cells reached semi-confluence on the reference sample (Figure 2a). Behavior comparable to that for the reference was observed on the surfaces of

PANI-S, PANI-B, PANI-SULF, and PANI-PT (see Figure 2b, where PANI-S is presented as an example). In contrast, on the PANI-PAMPSA-1:1 sample, proliferation was significantly decreased and the cells initially reached a semi-confluent state after 144 h (see Figure 2c). Cell proliferation then improved on PANI-PAMPSA-2:1, which contained a lower amount of PAMSPA compared to PANI-PAMPSA-1:1. This also corresponded to the better cell proliferation observed on pristine PANI-S and PANI-B surfaces, where PAMPSA was absent. Nevertheless, attachment was weak and any cells adhered on PANI-PAMPSA-2:1 easily detached from its surface; even gentle handling during media exchange caused cell detachment (Figure 2d). Consequently, it can be concluded that introducing PAMPSA into the polymer bulk during synthesis notably affected NIH/3T3 cell proliferation in comparison with reference and pristine polyaniline. These results correspond to observing the preferable behavior of mouse embryonic stem cells on pristine PANI forms, in comparison with PANI deposited with PAMPSA [14].

The results of cell migration on the tested surfaces are presented in Figure 3.

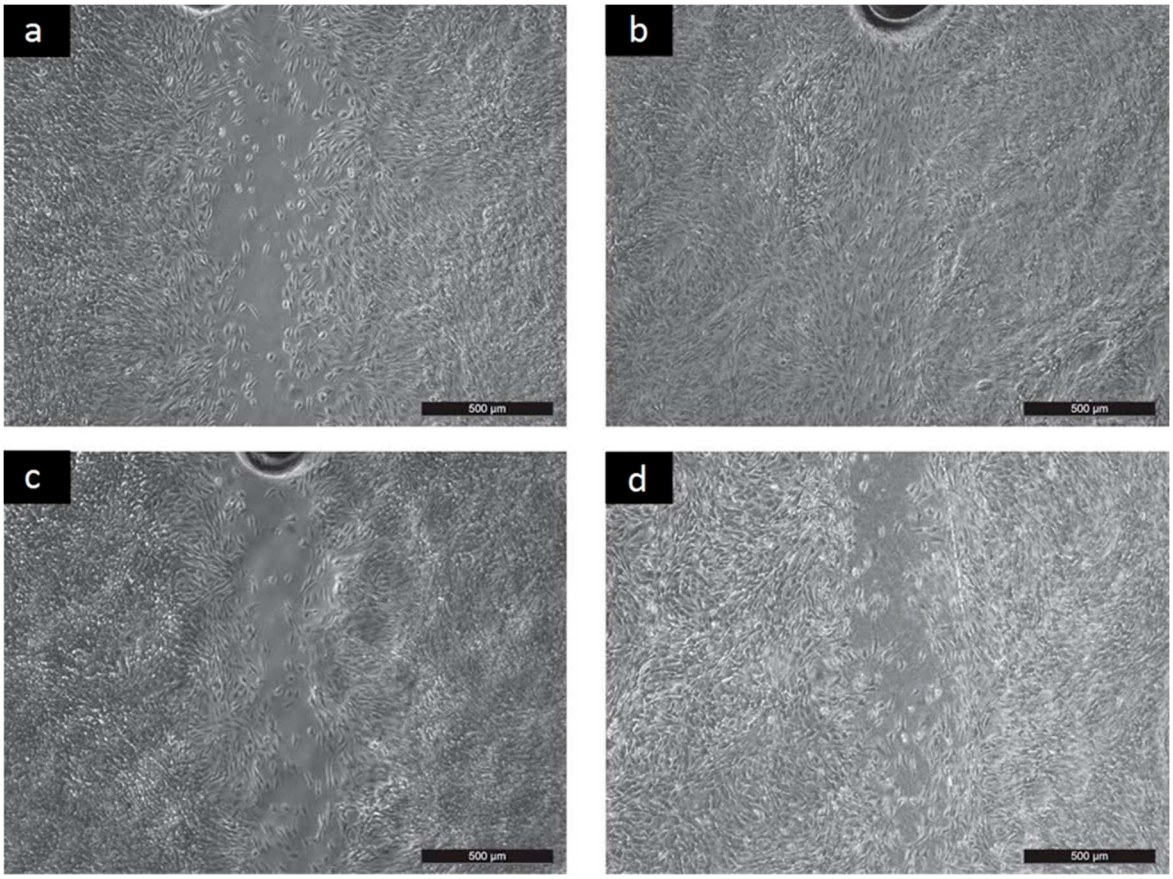

Figure 3. Migration 48 h: (**a**) Reference; (**b**) PANI-B; (**c**) PANI-PAMPSA-1:1; (**d**) PANI-SULF.

As can be seen, migration on PANI-PAMPSA surfaces was significantly less than for the reference (Figure 3c, only PANI-PAMPSA-1:1 is given as an example). This finding fully corresponds with the limited cell proliferation observed on these surfaces, and correlates with the results obtained for the surface energy. Obtained results indicate utilization of this modification in the field of biosensors rather than biomaterials. Nevertheless, the migration of cells on PANI-S, PANI-B, PANI-SULF and PANI-PT was comparable to cell behavior on the reference sample (see PANI-B in Figure 3b and PANI-SULF in Figure 3d). In summary, cell behavior corresponds to the surface energy of individual samples. It can be concluded that the less variation there is in the surface energy of a tested sample, the more compatible the surface is. Overall, these findings supported cell behavior in terms of adhesion

and proliferation, suggesting the potential of applying such PANI forms in biomedicine, e.g., tissue engineering of electrically responsive tissues.

3. Materials and Methods

3.1. Preparation of Polyaniline Films

The PANI films were formed in situ directly on the tissue culture plates (TPP, Trasadingen, Switzerland). The polyaniline salt (PANI-S) was prepared by chemical oxidation of aniline hydrochloride with ammonium peroxydisulfate in aqueous solution according to IUPAC technical report [18]. An appropriate amount of aniline hydrochloride (2.59 g, Neratovice, Czech Republic) and ammonium peroxydisulfate (5.71 g, Sigma-Aldrich, St. Louis, MO, USA) was separately dissolved in 50 mL of water. Both solutions were mixed, briefly stirred and poured into culture plates. The polymerization reaction lasted 1 h at room temperature. Then, the solution was poured out and deposited green film of PANI-S was rinsed with 0.2 M hydrochloric acid followed by methanol. The films were left to dry in air overnight.

To prepare polyaniline base (PANI-B), the films were immersed in 1 M ammonium hydroxide for 12 h.

In order to prepare films doped with sulfamic acid (PANI-SULF) and phosphotungstic acid (PANI-PT), the PANI-B films were re-protonated with either 1 M sulfamic acid (Sigma-Aldrich, St. Louis, MO, USA) or 50 wt % aqueous solution of phosphotungstic acid (Sigma-Aldrich, St. Louis, MO, USA). The solutions of acids were poured onto the surface of the PANI-B film and the reaction was left to proceed for 24 h. Afterwards, the residual solutions were poured out and the films were rinsed with methanol and left to dry in air.

The second type of modified film was prepared using direct polymerization with PAMPSA present in the reaction mixture of aniline hydrochloride and ammonium peroxydisulfate. To this end, modified procedures published by Bayer et al. [19], Stejskal et al. [20], and Yoo et al. [21] were employed. Firstly, an aqueous solution of PAMPSA was prepared, its target concentration corresponding to 0.028 mol of its monomer, acrylamido-2-methyl-propanesulfonic acid. Aniline hydrochloride (0.028 mol) was then added to the PAMPSA solution and stirred at room temperature for 1 h. The mole ratio of aniline hydrochloride to PAMPSA was adjusted to 1:1 (PANI-PAMPSA-1:1) or 2:1 (PANI-PAMPSA-2:1). The oxidant, ammonium peroxydisulfate (0.025 mol), was dissolved separately in ultrapure water and added to the reaction mixture at the mole ratio for aniline hydrochloride to oxidizing agent of 1:0.9. Polymerization was completed within 60 min. The films were rinsed with water and methanol to remove any adherent PAMPSA, and left to dry in air.

3.2. Surface Energy

The surface energy evaluation system ("SEE System", Advex Instruments, Brno, Czech Republic) was used to measure contact angle and determine surface energy of tested samples. Deionized water, ethylene glycol and diiodomethane (Sigma-Aldrich, St. Louis, MO, USA) in volume of 2 μL was utilized as testing liquids for PANI films. To obtain the value of contact angle, ten separate readings were performed for each testing liquid. The surface energy was determined by the "acid-base" method.

In order to evaluate the interaction of NIH/3T3 cells with the studied surfaces, the surface energy of the cells was determined. The cell suspension was thoroughly filtered through a filtration paper to obtain a homogeneous cell layer on the paper and this sample was immediately subjected to contact angle measurement. For the cells, glycerol (Sigma-Aldrich, St. Louis, MO, USA) and diiodomethane were used as the testing liquids, and the droplet volume of these liquids was also set to 2 μL for all experiments. In a corresponding manner to the aforementioned polyaniline samples, ten separate readings were taken to obtain one representative average value for the contact angle. Using these data, the surface energy of the cells was calculated by the "OWRK" (Owens-Wendt-Rabel-Kaelble) method, in addition to obtaining total surface energy (γ^{tot}) including its components, disperse part (γ^{LW}) and

polar part (γ^{AB}). Finally, calculation was made of γ^{dif}, denoting the absolute value of the difference between the surface energy of the cells and sample, according to equation $\gamma^{dif} = |\gamma^{tot,cell} - \gamma^{tot,sample}|$.

3.3. Cyto-Compatibility

Prior to in vitro testing, the samples were disinfected by 30 min of exposure to a UV-radiation source operating at a wavelength of 258 nm, emitted by a low-pressure mercury lamp. Investigation was conducted into the compatibility of the polyaniline films with the mouse embryonic fibroblast NIH/3T3 cell line (ATCC CRL-1658 NIH/3T3, Marlboro, MA, USA). NIH/3T3 cell line is abundantly used in material biocompatibility testing, thus obtained results are readily comparable to published data in literature. Definitively, study was made of cell adhesion, proliferation and migration. ATCC-formulated, Dulbecco's Modified Eagle's Medium (PAA, Trasadingen, Switzerland) containing 10% calf serum (PAA, Trasadingen, Switzerland) and 100 U·mL^{-1} Penicillin/Streptomycin (PAA, Trasadingen, Switzerland) was used as the culture medium.

Tests were conducted as follows:

1. To reveal the ability of cells to adhere to the surfaces, the cells were seeded on reference culture dishes (TPP, Trasadingen, Switzerland) and the studied polymer films at a concentration of 1×10^7 cells·mL^{-1}. After one hour, the cells were gently rinsed and micrographs were taken.
2. Cell proliferation and morphology were evaluated on cells that had been seeded at an initial concentration of 1×10^5 cells·mL^{-1} and cultivated.
3. Cell migration was determined by the scratch assay according to Liang et al. [22] with modification. The scratch assay was created in a confluent cell monolayer. After 48 h had passed, micrographs were captured with an Olympus inverted fluorescent microscope (Olympus, IX51, Tokyo, Japan) equipped with a digital color camera (Leica DFC480, Wetzlar, Germany).

4. Conclusions

The cell/surface interaction of pristine polyaniline films, films doped with sulfamic and phosphotungstic acid and films incorporating poly (2-acrylamido-2-methyl-1-propanesulfonic) were studied. The mouse embryonic fibroblasts were able to adhere, proliferate and migrate on pristine polyaniline films and those doped with sulfamic or phosphotungstic acids. Therefore, these polyaniline forms should be suitable for utilization in biomedicine, e.g., tissue engineering of electrically responsive tissues. Contrarily, incorporating poly (2-acrylamido-2-methyl-1-propanesulfonic) acid actually affected the surface properties of the polyaniline films, significantly influencing cell proliferation and migration; hence, the potential for application in the biomedical sector is limited, but opens the door for utilization as a biosensor. The surface energy constitutes the crucial factor that influences cell/surface interaction and the determination of surface energy is essential to attaining appropriate surface modifications.

Acknowledgments: This work was supported by the Ministry of Education, Youth and Sports of the Czech Republic, Program NPU I (LO1504).

Author Contributions: Věra Kašpárková and Petr Humpolíček conceived the study, designed the experiments and drafted the manuscript. Petra Rejmontová, Zdenka Capáková, Nikola Mikušová, Nela Maráková and Marián Lehocký performed the experiments and analyzed the data. Every author has approved the final version of the manuscript.

Conflicts of Interest: The authors declare no conflict in financial interests.

References

1. Cate, A.T.; Gaspar, C.H.; Virtanen, H.L.K.; Stevens, R.S.A.; Koldeweij, R.B.J.; Olkkonen, J.T.; Rentrop, C.H.A.; Smolander, M.H. Printed electronic switch on flexible substrates using printed microcapsules. *J. Mater. Sci.* **2014**, *49*, 5831–5837. [CrossRef]

2. Zhybak, M.; Beni, V.; Vagin, M.Y.; Dempsey, E.; Turner, A.P.F.; Korpan, Y. Creatinine and urea biosensors based on a novel ammonium ion-selective copper-polyaniline nano-composite. *Biosens. Bioelectron.* **2016**, *77*, 505–511. [CrossRef] [PubMed]
3. Qazi, T.H.; Rai, R.; Boccaccini, A.R. Tissue engineering of electrically responsive tissues using polyaniline based polymers: A review. *Biomaterials* **2014**, *35*, 9068–9086. [CrossRef] [PubMed]
4. Ricotti, L.; Menciassi, A. Bio-hybrid muscle cell-based actuators. *Biomed. Microdevices* **2012**, *14*, 987–998. [CrossRef] [PubMed]
5. Juarez-Hernandez, L.J.; Comella, N.; Pasquardini, L.; Battistoni, S.; Vidalino, L.; Vanzetti, L.; Caponi, S.; Dalla Serra, M.; Iannotta, S.; Pederzolli, C.; et al. Bio-hybrid interfaces to study neuromorphic functionalities: New multidisciplinary evidences of cell viability on poly(anyline) (PANI), a semiconductor polymer with memristive properties. *Biophys. Chem.* **2016**, *208*, 40–47. [CrossRef] [PubMed]
6. Bidez, P.R.; Li, S.X.; MacDiarmid, A.G.; Venancio, E.C.; Wei, Y.; Lelkes, P.I. Polyaniline, an electroactive polymer, supports adhesion and proliferation of cardiac myoblasts. *J. Biomater. Sci. Polym. Ed.* **2006**, *17*, 199–212. [CrossRef] [PubMed]
7. Wang, H.; Ji, L.; Li, D.; Wang, J. Characterization of nanostructure and cell compatibility of polyaniline films with different dopant acids. *J. Phys. Chem. B* **2008**, *112*, 2671–2677. [CrossRef] [PubMed]
8. Bober, P.; Humpolicek, P.; Pachernik, J.; Stejskal, J.; Lindfors, T. Conducting polyaniline based cell culture substrate for embryonic stem cells and embryoid bodies. *RSC Adv.* **2015**, *5*, 50328–50335. [CrossRef]
9. Prabhakar, P.K.; Raj, S.; Anuradha, P.R.; Sawant, S.N.; Doble, M. Biocompatibility studies on polyaniline and polyaniline-silver nanoparticle coated polyurethane composite. *Colloids Surf. B Biointerfaces* **2011**, *86*, 146–153. [CrossRef] [PubMed]
10. Yan, X.; Chen, J.; Yang, J.; Xue, Q.; Miele, P. Fabrication of free-standing, electrochemically active, and biocompatible graphene oxide-polyaniline and graphene-polyaniline hybrid papers. *ACS Appl. Mater. Interfaces* **2010**, *2*, 2521–2529. [CrossRef] [PubMed]
11. Humpolicek, P.; Kucekova, Z.; Kasparkova, V.; Pelkova, J.; Modic, M.; Junkar, I.; Trchova, M.; Bober, P.; Stejskal, J.; Lehocky, M. Blood coagulation and platelet adhesion on polyaniline films. *Colloids Surf. B Biointerfaces* **2015**, *133*, 278–285. [CrossRef] [PubMed]
12. Sivaraman, K.M.; Oezkale, B.; Ergeneman, O.; Luhmann, T.; Fortunato, G.; Zeeshan, M.A.; Nelson, B.J.; Pane, S. Redox cycling for passive modification of polypyrrole surface properties: Effects on cell adhesion and proliferation. *Adv. Healthc. Mater.* **2013**, *2*, 591–598. [CrossRef] [PubMed]
13. Zhang, X.; Qi, H.; Wang, S.; Feng, L.; Ji, Y.; Tao, L.; Li, S.; Wei, Y. Cellular responses of aniline oligomers: A preliminary study. *Toxicol. Res.* **2012**, *1*, 201–205. [CrossRef]
14. Humpolicek, P.; Radaszkiewicz, K.A.; Kasparkova, V.; Stejskal, J.; Trchova, M.; Kucekova, Z.; Vicarova, H.; Pachernik, J.; Lehocky, M.; Minarik, A. Stem cell differentiation on conducting polyaniline. *RSC Adv.* **2015**, *5*, 68796–68805. [CrossRef]
15. Kasparkova, V.; Humpolicek, P.; Stejskal, J.; Kopecka, J.; Kucekova, Z.; Moucka, R. Conductivity, impurity profile, and cytotoxicity of solvent-extracted polyaniline. *Polym. Adv. Technol.* **2016**, *27*, 156–161. [CrossRef]
16. Kucekova, Z.; Humpolicek, P.; Kasparkova, V.; Perecko, T.; Lehocky, M.; Hauerlandova, I.; Saha, P.; Stejskal, J. Colloidal polyaniline dispersions: Antibacterial activity, cytotoxicity and neutrophil oxidative burst. *Colloids Surf. B: Biointerfaces* **2014**, *116*, 411–417. [CrossRef] [PubMed]
17. Stejskal, J.; Hajna, M.; Kasparkova, V.; Humpolicek, P.; Zhigunov, A.; Trchova, M. Purification of a conducting polymer, polyaniline, for biomedical applications. *Synth. Met.* **2014**, *195*, 286–293. [CrossRef]
18. Stejskal, J.; Sapurina, I. Polyaniline: Thin films and colloidal dispersions—(IUPAC Technical Report). *Pure Appl. Chem.* **2005**, *77*, 815–826. [CrossRef]
19. Bayer, C.L.; Trenchard, I.J.; Peppas, N.A. Analyzing polyaniline-poly (2-acrylamido-2-methylpropane sulfonic acid) biocompatibility with 3T3 fibroblasts. *J. Biomater. Sci. Polym. Ed.* **2010**, *21*, 623–634. [CrossRef] [PubMed]
20. Stejskal, J.; Sapurina, I.; Prokes, J.; Zemek, J. In-situ polymerized polyaniline films. *Synth. Met.* **1999**, *105*, 195–202. [CrossRef]

21. Yoo, J.E.; Cross, J.L.; Bucholz, T.L.; Lee, K.S.; Espe, M.P.; Loo, Y. Improving the electrical conductivity of polymer acid-doped polyaniline by controlling the template molecular weight. *J. Mater. Chem.* **2007**, *17*, 1268–1275. [CrossRef]
22. Liang, C.; Park, A.Y.; Guan, J. In vitro scratch assay: A convenient and inexpensive method for analysis of cell migration in vitro. *Nat. Protoc.* **2007**, *2*, 329–333. [CrossRef] [PubMed]

Article II.

Della Pina, C.; **Capakova, Z**.; Sironi, A.; Humpolicek, P.; Saha, P.; Falletta, E. On the Cytotoxicity of Poly(4-Aminodiphenylaniline) Powders: Effect of Acid Dopant Type and Sample Posttreatment. Int. J. Polym. Mater. Polym. Biomat. 2017, 66 (3), 132–138. https://doi.org/10.1080/00914037.2016.1190928.

INTERNATIONAL JOURNAL OF POLYMERIC MATERIALS AND POLYMERIC BIOMATERIALS
2017, VOL. 66, NO. 3, 132–138
http://dx.doi.org/10.1080/00914037.2016.1190928

Taylor & Francis
Taylor & Francis Group

On the cytotoxicity of poly(4-aminodiphenylaniline) powders: Effect of acid dopant type and sample posttreatment

C. Della Pina[a], Z. Capáková[b], A. Sironi[a], P. Humpolíček[b,c], P. Sáha[b] and E. Falletta[a]

[a]Dipartimento di Chimica, Università degli Studi di Milano, CNR-ISTM, Milano, Italy; [b]Centre of Polymer Systems, Tomas Bata University in Zlin, Zlin, Czech Republic; [c]Polymer Centre, Faculty of Technology, Tomas Bata University in Zlin, Zlin, Czech Republic

ABSTRACT

Thanks to their unique properties, as intrinsic conductivity and simple preparation, conducting polymers are highly applicable in tissue engineering, regenerative medicine, and biosensors. Pristine polymers often include residual precursors or other low molecular impurities, which have a negative impact on their biocompatibility. Concerning poly(4-aminodiphenylaniline), its cytotoxicity and biocompatibility have not yet been investigated. Herein, the cytotoxicity of poly(4-aminodiphenylaniline), prepared by an innovative green approach, as well as the effect of samples' posttreatment and kind of dopant acid used, are reported for the first time. The results show that not only the type of used dopant but also polymers' washing in phosphate saline buffer and material's morphology has a significant impact on materials' cytotoxicity. After a proper posttreatment or when salicylic acid is used as the doping agent the cytotoxicity of poly(4-aminodiphenylaniline) seem to be lower than those obtained for traditional PANI.

GRAPHICAL ABSTRACT

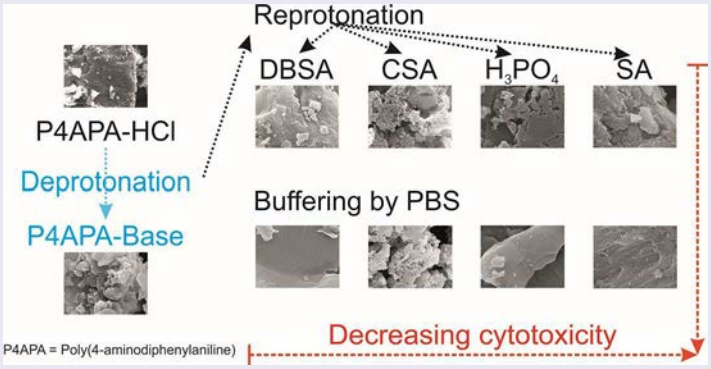

ARTICLE HISTORY
Received 24 February 2016
Accepted 14 May 2016

KEYWORDS
Poly(4-aminodiphenylaniline); biocompatibility; cytotoxicity; dopant acid

1. Introduction

Although intrinsically conducting polymers (ICPs) were discovered over 150 years ago, their popularity is still growing thanks to their versatile properties. Among them polyaniline (PANI) is unique owing to its extraordinary features, such as ease of synthesis [1], environmental stability [2], and simple doping/dedoping process [3,4]. Furthermore, easy modifications of the polymer allow to give new properties (e.g., heamocompatibility, [5] etc.). The high interest in ICPs and in particular in PANI is, however, related to their ability to respond to external stimuli (e.g., force, pressure, pH) by conductivity changes. This latter ability makes them promising candidates for many applications in numerous technological fields: electrochromic devices [6,7], stress/strain sensors [8–10], electromagnetic shields [11,12], and anticorrosion paints [13,14]. The recent open scenarios for ICPs applications in medical and biomedical fields [15–18] have boosted the scientific interest in their biocompatibility.

In this regard, many efforts have been recently addressed to enhance PANI biocompatibility by different approaches, such as purification after synthesis [19,20], presoaking in medium before cell culturing, or grafting adhesive peptides [21].

The cytotoxicity of PANI prepared by traditional way [22] has been deeply explored by Humpolíček et al. [19], demonstrating that thanks to its high insolubility PANI itself is not cytotoxic. However, the presence of low molecular impurities and other byproducts [23] may cause cytotoxicity [19,20]. To improve the cytocompatibility of PANI prepared according to the IUPAC procedure, some purification steps have been introduced [23]. Another general way to improve biocompatibility is using other oxidation [24] or doping agents [25].

Starting from the pioneering investigations of Geniès et al. [26] and Kitani et al. [27], another approach, consisting of ICPs production by innovative environmentally friendly protocols, has been recently developed [28–31]. More in

CONTACT P. Humpolíček humpolicek.petr@ft.utb.cz Centre of Polymer Systems, Tomas Bata University in Zlin, 760 01 Zlin, Czech Republic; E. Falletta ermelinda.falletta@unimi.it Dipartimento di Chimica, Università degli Studi di Milano, CNR-ISTM, via C. Golgi, 19-20133-Milan, Italy.
Color versions of one or more of the figures in the article can be found online at www.tandfonline.com/gpom.

detail, the possibility to synthesize polyaniline, more correctly poly(4-aminodiphenylaniline) (P4APA), by oxidative polymerization of *N*-(4-aminophenyl)aniline, a commercially available chemical, using hydrogen peroxide or molecular oxygen as the oxidants in the presence of proper catalysts, allows for water to be obtained as the unique coproduct, simplifying posttreatment steps, and avoiding the formation of toxic/mutagen pollutants (i.e., benzidine).

The conductivity of P4APA was found to be lower (typically 10^{-3} S cm^{-1}) [30] than that of PANI prepared from aniline monomer (typically 4.4 S cm^{-1}) [31]. Geniès et al. [26] and Kitani et al. [27] attributed such behavior to different length of the polymeric chains, shorter in P4APA than in traditional PANI, even though our recent results belie them (data not published). Further investigations are in progress to clarify this aspect. Moreover, the high solubility of P4APA has recently led to promising results in many sectors, such as nanofibers preparation by electrospinning technique [32,33]. However, if on the one hand results on biocompatibility of PANI prepared by traditional methods are available [19,20,34], on the other hand the impact of P4APA-based materials in human and environmental health is not well studied. In this work, we present our recent achievements in the *in vitro* cytotoxicity of poly(4-aminophenylaniline) powders detected on mouse embryonic fibroblast cell line. Moreover, the effect of acid dopant type and proper posttreatments are also discussed.

2. Experimental

All chemicals were used as received (Sigma Aldrich) without further purification unless stated otherwise.

2.1. Samples preparation

Poly(4-aminodiphenylaniline) was prepared following a synthetic procedure similar to that reported elsewhere [30,34]. Briefly, 8 g of *N*-(4-aminophenyl)aniline (43.5 mmol) were dissolved in 800 mL of 0.8 M HCl. Then, 22 mL of H_2O_2 30% (213.5 mmol) were quickly added under stirring followed by 32.4 mg of $FeCl_3 \cdot 6H_2O$ (0.12 mmol). The mixture was stirred for 24 h at room temperature. Finally, a dark green product was collected on a filter, abundantly washed with deionized water and acetone, until the washings became colorless, and dried in an oven at 65°C overnight. The spectroscopic characterizations of this product confirmed that it was P4APA/HCl, according to the literature [30,34]. The present synthesis was repeated three times to obtain enough product for all the investigations reported. 1 g of P4APA/HCl was put aside for further investigations.

To test the influence of different doping agents on P4APA biocompatibility, the remaining part of the previously prepared sample (P4APA/HCl) was deprotonated to obtain the corresponding base and divided into different portions. Each lot was then subjected to a protonation process by the use of proper acids.

More in detail, P4APA/HCl was dispersed in a large excess of 1 M ammonium hydroxide for 24 h. The resulting base (P4APA_B) was collected on a filter and washed several timed with water until neutral washings and dried in an oven at 65°C overnight. 1 g of this product was put aside for further investigations.

Different portions (1 g each) of P4APA_B were separately suspended in 150 mL of deionized water treated with proper amounts of water soluble acids (H_3PO_4 and salycilic acid, SA) maintaining an *N*-(4-aminophenyl)aniline/acid molar ratio of 1. The resulting P4APA/H_3PO_4 and P4APA/SA samples were filtered, washed several times with water, and dried in an oven at 65°C overnight.

Other portions of P4APA_B were separately dispersed in 150 mL of chloroform and treated with proper amounts of dodecylbenzenesulfonic acid (DBSA) and camphorsulfonic acid (CSA). The resulting products (P4APA/DBSA and P4APA/CSA) were filtered and dried in an oven at 65°C overnight.

2.2. Samples posttreatment

500mg of each sample (P4APA/HCl, P4APA_B, P4APA/H_3PO_4, P4APA/SA, P4APA/DBSA, and P4APA/CSA) was separately soaked in 10 mL of a phosphate-buffered saline (PBS; pH = 7.3) at room temperature for three days. Finally, each solid was recovered by centrifugation, washed with a small volume of deionized water and dried in an oven at 65°C overnight. From now on, these materials will be indicated as P4APA/HCl_B, P4APA/H_3PO_4_B, P4APA/SA_B, P4APA/DBSA_B, and P4APA/CSA_B.

2.3. Characterization

All samples were characterized by diverse techniques.

FT-IR spectra of KBr dispersed samples were recorded on a JASCO FT/IR-410 spectrophotometer in the 500–4000 cm^{-1} range. UV–Vis spectra were recorded on a Hewlett Packard 8453 spectrophotometer using *N,N*-dimethylformamide (DMF) as the solvent.

Molecular weights distribution of the P4APA samples' fractions soluble in DMF were determined by size exclusion chromatography (SEC) using a Shimadzu LC10ADVP HPLC equipped with a refractive index (RI) as the detector. A Phenomenex Phenogel 5 u 55 A (300 × 4.6 mm) was used as the column. All the measurements were carried out at room temperature using ultra-pure DMF as the eluent. The flow rate was set at 0.3 mL min^{-1} and the injection volume was 20 µL. Polystyrene standards were used for calibration. Samples for SEC analysis were prepared using the following procedure. 5 mL of DMF were added at approximately 20 mg of each material. The mixtures were sonicated for 20 minutes at room temperature. Then, the insoluble parts were removed by filtration on 0.2 µm Teflon syringe filters and only the soluble fractions were analyzed.

For conductivity measurement, 200 mg of three samples (P4APA/HCl, P4APA/SA, and P4APA/DBSA) were pressed between 13 mm anvils with force 10 ton for 30 min. The resulting disks were next pressed with force 2 kg for 30 min. Resistance R was measured by an AMEL 338 multimeter and conductivity σ was obtained as

$$\sigma = (1/R)(l/A)$$

where l is the thickness of the disks, R is the resistance, and A is the area of the disks' base.

2.4. Cytotoxicity test

Prior to *in vitro* cytotoxicity testing, the samples were homogenized and disinfected by dry heat at 120°C for 40 min. The extracts from powders were prepared according to ISO standard 10993-12 in the ratio of 0.2 g per 1 mL of culture medium. Dulbecco's modified Eagle medium high glucose, 10% calf serum, and penicillin/streptomycin, 100 U mL^{-1} (PAA Laboratories GmbH, Austria) were used as the medium. Extractions were performed in chemically inert closed containers using aseptic techniques at 37 ± 1°C under stirring for 24 ± 1 h. After extraction, the parent extracts (100%) were diluted in culture medium to obtain a series of dilutions with concentrations of 75%, 50%, 25%, 10%, and 1% have been used further for cell viability tests. All the extracts were used within 24 h. The ability of cells to respond to cytotoxic substances was verified by the application of sodium dodecyl sulfate solution (SDS; Sigma, Czech Republic).

Cytotoxicity testing was conducted in accordance with EN ISO 10993-5, using mouse embryonic fibroblast cell line (ATCC CRL-1658 NIH/3T3, USA). Cells were seeded in the suspension of 1×10^5 cells mL^{-1} and precultivated for 24 h. After a preincubation period, the cultivation medium was replaced with the extracts. As a reference giving 100% cell proliferation, cells cultivated in the pure medium were used. The cells were observed by an inverted Olympus phase contrast microscope (Olympus IX81, Japan). To assess cytotoxic effects, the MTT assay was performed after 24 hours of cell cultivation in the presence of extracts at 37 ± 0.1°C and 5% CO_2. The absorbance was measured at 570 nm by an Infinite M200 PRO (Tecan, Switzerland). All the tests were performed in quadruplicates. Cell viability was expressed as the percentage of viable cells present in the corresponding extract relative to cells cultivated in pure growth medium (100% viability).

3. Results and discussion

3.1. Spectroscopic characterization

All samples were spectroscopically characterized by FT-IR and UV-Vis techniques to evaluate the oxidation level of the polymeric chains. It is known, in fact, that only the half-oxidized and half-protonated form of polyaniline (emeraldine) and its derivatives are stable and interesting for their conductive properties. This form can be easily confirmed by the FT-IR (Figures 1A and 1B) and UV-Vis spectra (Figures 1B and 1D), as discussed subsequently.

In particular, in the FT-IR spectra the two bands at 1569 cm^{-1} and 1499 cm^{-1}, having an intensity ratio of about 1, can be attributed to the stretching vibration modes of quinoid (N=Q=N) and benzenoid rings (N-B-B) C=C respectively, whereas that one at about 1150 cm^{-1}, also called an electronic-like band, is associated to the conjugation level [35].

Similarly, the UV-vis spectra exhibit the typical bands of emeraldine base. The first band at around 300 nm is related to the π–π* transition of the benzenoid rings and the second one at around 600 nm is due to the transition from a localized benzenoid highest occupied molecular orbital to a quinoid lowest unoccupied molecular orbital, that is a benzenoid to quinoid excitonic transition [36].

On the base of these results it is possible to conclude that considering the molecular structure all the materials resulted similar in terms of backbone's oxidation level also after the buffer treatment.

3.2. Size exclusion chromatography

To measure the molecular weight distribution of P4APA-based materials, all samples were analyzed by SEC using polystyrene standards. As polystyrene and P4APA have different hydrodynamic volumes, these measurements must be considered as apparent molecular weights and not absolute ones. The results are reported in Table 1.

As reported in section 2, only the P4APA fractions soluble in DMF were analyzed by this technique. The data show that all the samples consist of polymers characterized by different molecular weight. Before the buffer treatment all the materials contain short oligomers attributable to aniline dimer (214 uma), hexamer (598 and 630 uma), and octamer (757 and 718 uma) derivatives. Except for P4APA/HCl, in all the other cases the buffer treatment allows to remove these potential toxic species, as confirmed by the percentage areas reported in Table 1. This suggests that the buffer-treated materials do not contain short oligomers that could be responsible of samples' cytotoxicity.

3.3. Morphological characterization

The morphology of all the P4APA-based samples was analyzed by scanning electron microscopy and the results are reported in the Figure 2.

Even though methods and conditions (e.g., stirrer speed, temperature, type and amount of acid) used for the preparation of PANI and its derivatives mainly affect their morphology [37,38], also the dedoping/redoping process can have a role [39], strictly related to penetration depth of dopant in the polymer structures, kind of dopant-polymer interactions, and so on.

In the present work, if on the one hand before the buffered treatment all the P4APA-based samples showed an irregular morphology (Figures 2A, 2B, 2D, 2F, 2H, and 2L), however, after stirring in PBS some of them, in particular P4APA/HCl and P4APA/SA, exhibited SEM images characterized by layer-by-layer oriented rod-like structures, suggesting that the $H_2PO_4^-/HPO_4^{2-}$ couple in some cases or in the presence of proper dopants could play a role in the P4APA orientation.

3.4. Conductivity measurements

Table 2 reports the conductivity values of measured for three samples: P4APA/HCl, P4APA/SA, and P4APA/DBSA. It is possible to observe that the electroconductivity of these materials decreases in the following order: P4APA/HCl > P4APA/SA > P4APA/DBSA.

According to the scientific literature [40], the amount and type of acid used as the dopant strictly affects polymers'

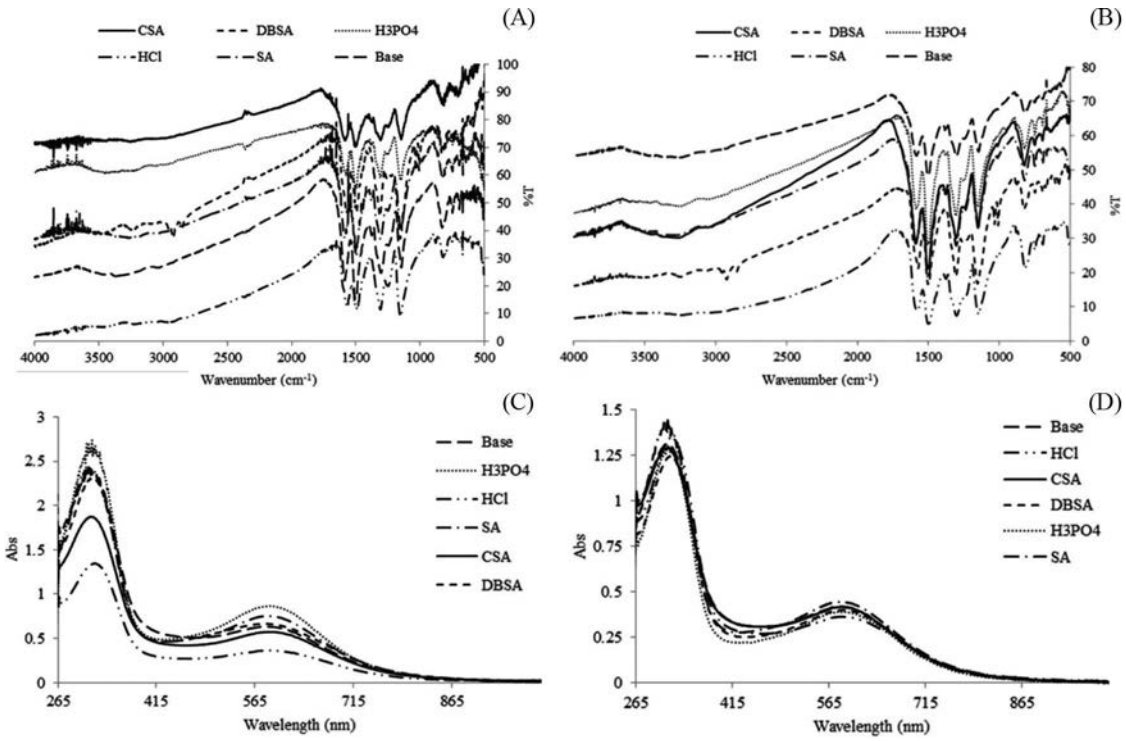

Figure 1. FT-IR and UV-Vis spectra of P4APA-based materials before (A and C) and after (B and D) buffer treatment.

electroconductivity. In fact, as well as for polyaniline also for poly(4-aminodiphenylaniline) electroconductivity is higher for polymers doped with inorganic acids than for those protonated with organic acids. This because the small dimensions of inorganic dopant counterions allow a highly efficient penetration of the latter through the polymeric chains guaranteeing a high protonation level and, as a consequence, good conductivity. On the contrary, organic dopants counter ions are big. Therefore, their diffusion through the chains is restricted and there are localized. This reduces the mobility of doped centers inside the polymeric matrix, making these materials less conductive than those doped with inorganic acids.

Even though SA and DBSA are acids characterized by different acidic functions (SA is a carboxylic acid and DBSA is a sulfonic acid), the difference in conductivity observed for SA- and DBSA-doped polymers can be reasonably attributed to the different sizes of the acids.

3.5. Cytotoxicity test

The cytotoxicity tests were performed according to the ISO standard to be comparable with previously published results about polyaniline cytotoxicity. The complete results of cytotoxicity testing are presented in Table 3, the micrographs representing the impact of P4APA on the cell morphology are shown in Figure 3. It can be assumed that cytotoxicity of individual samples can be assigned to the following factors: (a) pH of extracts and (b) correlated impact of used dopant acid, (c) effect of buffer treatment, and (d) presence of short oligomers.

The micrographs reported in the Figure 3 clearly demonstrate the significant impact of extracts on the cells. The micrograph 3A represents the reference and similar cell morphology and quantity were observed in the case of micrograph 3B, when the cells were exposed to the 25% extract in the P4APA/CSA_B cultivation medium. If compared to the Figure 3A, a

Table 1. Molecular weights of P4APA-based materials before and after buffer treatment by SEC technique.

Sample	M_w	Area (%)
P4APA_B	(Peak1#) 311331; (Peak2#) 74677	(Peak1#) 75.06; (Peak2#) 24.14
P4APA/HCl	(Peak1#) 217330; (Peak2#) 757	(Peak1#) 48.16; (Peak2#) 51.03
P4APA/HCl_B	(Peak1#) 369096; (Peak2#) 757	(Peak1#) 77.11; (Peak2#) 22.10
P4APA/H_3PO_4	(Peak1#) 356504; (Peak2#) 253647; (Peak3#) 1567; (Peak4#) 718; (Peak5#) 209	(Peak1#) 21.56; (Peak2#) 49.13; (Peak3#) 7.19; (Peak4#) 12.24; (Peak5#) 12.45
P4APA/H_3PO_4_B	(Peak1#) 276177; (Peak2#) 110509; (Peak3#) 1549; (Peak4#) 214	(Peak1#) 33.12; (Peak2#) 60.35; (Peak3#) 5.01; (Peak4#) 0.52
P4APA/SA	(Peak1#) 256216; (Peak2#) 598	(Peak1#) 81.55; (Peak2#) 16.24
P4APA/SA_B	(Peak1#) 287538	(Peak1#) 99.93
P4APA/DBSA	(Peak1#) 557936; (Peak2#) 85035; (Peak3#) 64057; (Peak4#) 2688; (Peak5#) 1668; (Peak6#) 630	(Peak1#) 40.07; (Peak2#) 13.22; (Peak3#) 18.05; (Peak4#) 6.11; (Peak5#) 12.04; (Peak6#) 8.91
P4APA/DBSA_B	(Peak1#) 416543; (Peak2#) 279600; (Peak3#) 110508; (Peak4#) 1584	(Peak1#) 38.36; (Peak2#) 36.77; (Peak3#) 21.16; (Peak4#) 2.01
P4APA/CSA	(Peak1#) 396074	(Peak1#) 99.74
P4APA/CSA_B	(Peak1#) 4233678	(Peak1#) 99.85

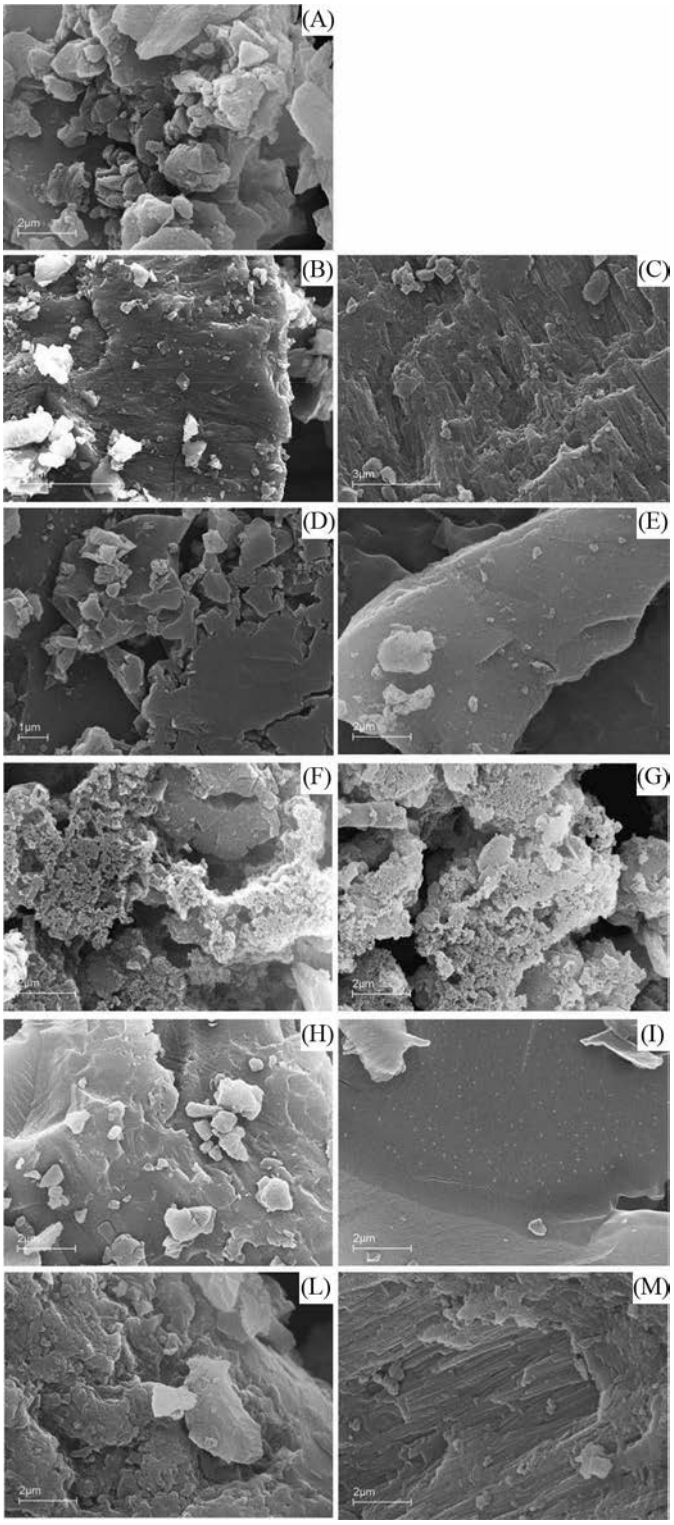

Figure 2. SEM images of P4APA_B (A), P4APA/HCl (B), P4APA/HCl_B (C), P4APA/H3PO4 (D), P4APA/H3PO4_B (E), P4APA/CSA (F), P4APA/CSA_B (G), P4APA/DBSA (H), P4APA/DBSA_B (I), P4APA/SA (L), and P4APA/SA_B (M).

Table 2. Conductivity data of P4APA/HCl, P4APA/SA, and P4APA/DBSA.

Sample	Conductivity (S/cm)
P4APA/HCl	5.04×10^{-4}
P4APA/SA	3.50×10^{-6}
P4APA/DBSA	1.92×10^{-6}

significantly lower cells' amount of cells and presence of debris can be consider responsible to the mild cytotoxicity of sample P4APA/SA_B (Figure 3C). The severe cytotoxicity of sample P4APA/DBSA is presented on micrograph 3D, where almost no cell can be found.

The pH has a negative impact only in case of sample HCl protonated and surprisingly this effect persists even after the buffer treatment. In fact, after the material is stirred in the buffering solution, the pH of extract does not change significantly. The negative impact of acidity can be observed until 25% of extracts in cultivation medium when the buffering capacity of medium neutralizes it. Under this concentration P4APA/HCl and P4APA/HCl_B samples express moderate or no cytotoxicity, respectively. The pH of native extracts of all the other samples was within the range, which is easily buffered by cultivation medium. Therefore, an acidity impact is not expected.

Conversely to the pH impact, the effect of dopant acid can be assigned as significant. In general, except of P4APA_B, all samples in concentrations higher than 50% show moderate or severe cytotoxicity. Considering P4APA-based materials before the buffer treatment, the lowest cytotoxicity was observed when HCl or SA is used as the dopant acid. Surprisingly, using H_3PO_4, DBSA or CSA as the dopants, the samples induce significant toxicity even in low extract concentration in the medium. This effect is probably connected to the presence of oligomers in these samples (see Table 1).

Remarkably, the stirring in PBS decreases the cytotoxicity. This step is similar to the redeprotonation, which was previously described as possible way for improvement of cytotoxicity of polyaniline [19]. The observed impact of PBS is exciting as this effect was not correlated to the change of acidity. As the stirring in PBS was performed by the same way in all samples, its effect must be connected either to (a) the removal of oligomers from polymeric species (see Table 1) or to (b) the different samples' morphology related to the ability of buffer solution to penetrate into the materials. Based on the results from SEC and SEM it is possible to conclude that both the mentioned effects related to the stirring in PBS contribute to the decreased toxicity of samples. In fact, as it is clearly reported in the Table 1, the oligomeric fractions are missing in the buffered samples if compared to the parent samples (e.g., missing octamers at P4APA/H_3PO_4_B or hexamers at P4APA/DBSA_B). After the buffering treatment the different morphology of individual samples (see Figure 2) significantly influences their cytotoxicity. The impact of different morphology on cytotoxic effect is also known, mainly on nanostructures [41,42].

Finally, it can be assumed that the lowest cytotoxicity was expressed by P4APA/H_3PO_4_B, P4APA/CSA_B, and P4APA/SA, where 1%, 10%, and 25% of extracts were without cytotoxic effect. Good results were also achieved for extract of P4APA/SA_B, concentrations 1% and 10% were noncytotoxic. Compared to the PANI prepared according to the IUPAC [22] presented in the work of Humpolíček et al. [19] the cytotoxicity of P4APA are slightly better in case of P4APA/SA, P4APA/H_3PO_4_B, and P4APA/CSA_B. The nanotubular PANI [20] or PANI purified by Soxhlet extraction [23] express slightly higher cytotoxicity than those samples. Therefore, it can be

Table 3. Cytotoxicity of PANI samples determined for various extract concentrations presented as relative value compared to reference (RV) according to ISO 10 993-5 standard.

Sample (pH of native extract)	100%	75%	50%	25%	10%	1%
P4APA_B (8.13)	0.39 ± 0.07 **D**	0.42 ± 0.04 **C**	0.66 ± 0.08 **B**	0.91 ± 0.16 **A**	0.92 ± 0.14 **A**	0.91 ± 0.13 **A**
P4APA/HCl (1.65)	0.33 ± 0.05 **D**	0.40 ± 0.07**C**	0.42 ± 0.06 **C**	0.41 ± 0.08 **C**	0.40 ± 0.07 **C**	0.58 ± 0.10 **C**
P4APA/HCl_B (2.18)	0.39 ± 0.03 **D**	0.42 ± 0.03 **C**	0.40 ± 0.03 **C**	0.39 ± 0.06 **D**	0.92 ± 0.08 **A**	0.88 ± 0.08 **A**
P4APA/H_3PO_4 (8.12)	0.37 ± 0.03 **D**	0.37 ± 0.03 **D**	0.35 ± 0.04 **D**	0.79 ± 0.06 **B**	0.78 ± 0.06 **B**	0.79 ± 0.04 **B**
P4APA/H_3PO_4_ buffer (8.54)	0.43 ± 0.03 **C**	0.43 ± 0.03 **C**	0.47 ± 0.04 **C**	0.84 ± 0.06 **A**	1.05 ± 0.12 **A**	0.99 ± 0.26 **A**
P4APA/ SA (7.63)	0.43 ± 0.04 **C**	0.43 ± 0.05 **C**	0.47 ± 0.06 **C**	0.81 ± 0.08 **A**	1.03 ± 0.12 **A**	1.02 ± 0.10 **A**
P4APA/ SA_B (7.22)	0.42 ± 0.06 **C**	0.40 ± 0.05 **C**	0.47 ± 0.14 **C**	0.67 ± 0.27 **B**	0.94 ± 0.23 **A**	1.00 ± 0.22 **A**
P4APA/DBSA (5.34)	0.38 ± 0.01 **D**	0.35 ± 0.03 **D**	0.36 ± 0.03 **D**	0.36 ± 0.03 **D**	0.37 ± 0.02 **D**	0.67 ± 0.15 **B**
P4APA/DBSA _B (7.41)	0.41 ± 0.07 **C**	0.38 ± 0.05 **D**	0.38 ± 0.05 **D**	0.42 ± 0.03 **C**	0.42 ± 0.02 **C**	0.60 ± 0.04 **B**
P4APA/CSA (5.95)	0.38 ± 0.03 **D**	0.34 ± 0.02 **D**	0.37 ± 0.04 **D**	0.36 ± 0.02 **D**	0.35 ± 0.02 **D**	1.03 ± 0.08 **A**
P4APA/CSA_B (7.32)	0.40 ± 0.04 **C**	0.39 ± 0.04 **D**	0.39 ± 0.04 **D**	0.80 ± 0.11 **A**	0.94 ± 0.12 **A**	0.85 ± 0.17 **A**

Note. Cytotoxicity in relative values equal to 1 corresponds to 100% cell survival compared to reference. Values >0.8 are assigned to no cytotoxicity (A), 0.6–0.8 to mild cytotoxicity (B), 0.4–0.6 to moderate cytotoxicity (C), and <0.4 to severe cytotoxicity (D).

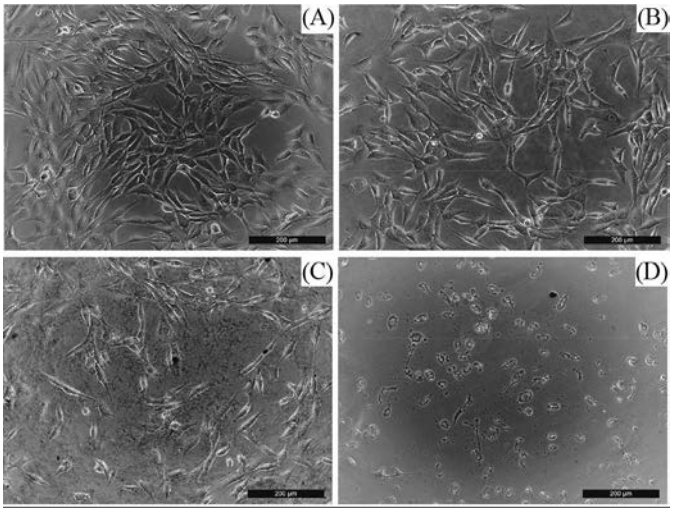

Figure 3. The cell morphology after the 24-h cultivation in the presence of 25% extracts in cultivation medium. (A) Reference, (B) P4APA/CSA_B, (C) P4APA/SA_B, (D) P4APA/DBSA.

concluded that cytotoxicity of the P4APA is comparable to that of PANI prepared by the IUPAC procedure when SA is used as the dopant acid or when buffering treatment is applied.

4. Conclusion

The biological properties of poly(4-aminodiphenylaniline) are presented for the first time. The significant impact of presence of oligomers on cytotoxicity was proved. Based on the size exclusion chromatography it is clear that those oligomers can be easily removed by a proper posttreatment, consisting in the polymer washing by a phosphate buffered solution. This procedure positively affects materials' cytotoxicity. Remarkably, the acid used for protonation has also significant impact on the polymer's cytotoxicity. However, the proper posttreatment seems to have higher impact on cytotoxicity than choice of dopant acid.

Salicylic acid seems to lead to a polymer with the highest cytocompability. It can be concluded that this polymer is simply modifiable in terms of its final cytotoxicity working on the type of acid used as the doping agent and on an easy posttreatment process.

Acknowledgments

E. Falletta and P. Humpolíček contributed equally to the manuscript. The manuscript was written through contributions of all authors. Sample preparation and characterization was carried out by E. Falletta, C. Della Pina, and A. Sironi. The cell studies were carried out by P. Humpolíček, Z. Kuceková, and P. Sáha. All authors have given approval to the final version of the manuscript.

Funding

This work was supported by the Ministry of Education, Youth and Sports of the Czech Republic–Program NPU I (LO1504). The authors gratefully acknowledge financial support by Fondazione Cariplo (Milano, Italy) under grant no. 2012-0872 (Magnetic-nanoparticle-filled conductive polymer composites for EMI reduction).

References

[1] Della Pina, C.; Falletta, E.; Rossi, M. *Catal. Today* **2011**, *160*, 11–27.
[2] Ansari, R.; Keivani, M. *J. Chem.* **2006**, *3*, 202–217.
[3] Li, M.; Guo, Y.; Wei, Y.; MacDiarmid, A. G.; Lelkes, P. I. *Biomaterials* **2006**, *27*, 2705–2715.
[4] Ghasemi-Mobarakeh, L.; Prabhakaran, M. P.; Morshed, M.; Nasr-Esfahani, M. H.; Ramakrishna, S. *Tissue Eng. Part A* **2009**, *15*, 3605–3619.
[5] Humpolíček, P.; Kuceková, Z.; Kašpárková, V.; Pelková, J.; Modic, M.; Junkar, I.; Trchová, M.; Bober, P.; Stejskal, J.; Lehocký, M. *Colloids Surf. B* **2015**, *133*, 278–285.
[6] Ma, L.; Li, Y.; Yu, X.; Yang, Q.; Noh, C. *Sol. Energy Mat. Sol. C.* **2009**, *93*, 564–570.
[7] Sheng, K.; Bai, H.; Sun, Y.; Li, C.; Shi, G. *Polymer* **2011**, *52*, 5567–5572.
[8] Falletta, E.; Costa, P.; Della Pina, C.; Lanceros-Mendez, S. *Sens. Actuators A: Phys.* **2014**, *220*, 13–21.
[9] Della Pina, C.; Zappa, E.; Busca, G.; Sironi, A.; Falletta, E. *Sens. Actuators A: Chem.* **2014**, *201*, 395–401.
[10] Singh, U.; Prakash, V.; Abramson, A. R.; Chen, W.; Qu, L.; Dai, L. *Appl. Phys. Lett.* **2006**, *89*, 073103.
[11] Dhawan, S.; Singh, N.; Rodrigues, D. Sci. *Technol. Adv. Mat.* **2003**, *4*, 105–113.
[12] Tantawy, H. R.; Aston, D. E.; Smith, J. R.; Young, J. L. *ACS Appl. Mater. Interfaces* **2013**, *5*, 4648–4658.
[13] Armelin, E.; Oliver, R.; Liesa, F.; Iribarren, J. I.; Estrany, F.; Alemán, C. *Prog. Org. Coat.* **2007**, *59*, 46–52.
[14] Yang, X.; Li, Y.; Wang, X. *Semiconducting Polymer Composites: Principles, Morphologies, Properties and Applications, Intrinsically Conducting Polymers and Their Composites for Anticorrosion and Antistatic Applications*; Wiley-VCH Verlag, Weinheim, Germany, 2012.
[15] Fernandes, E. G.; Zucolotto, V.; De Queiroz, A. A. *J. Macromol. Sci. A* **2010**, *47*, 1203–1207.

[16] McKeon, K.; Lewis, A.; Freeman, J. *J. Appl. Polym. Sci.* **2010**, *115*, 1566–1572.
[17] Svirskis, D.; Travas-Sejdic, J.; Rodgers, A.; Garg, S. *J. Control. Release* **2010**, *146*, 6–15.
[18] Humpolicek, P.; Radaszkiewicz, K. A.; Kasparkova, V.; Stejskal, J.; Trchova, M.; Kucekova, Z.; Vicarova, H.; Pachernik, J.; Lehocky, M.; Minarik, A. *RSC Adv.* **2015**, *5*, 68796–68805.
[19] Humpolicek, P.; Kasparkova, V.; Saha, P.; Stejskal, J. *Synth. Met.* **2012**, *162*, 722–727.
[20] Stejskal, J.; Hajna, M.; Kasparkova, V.; Humpolicek, P.; Zhigunov, A.; Trchova, M. *Synth. Met.* **2014**, *195*, 286–293.
[21] Qazi, T. H.; Rai, R.; Boccaccini, A. R. *Biomaterials* **2014**, *35*, 9068–9086.
[22] Stejskal, J.; Gilbert, R. G. *Pure Appl. Chem.* **2002**, *74*, 857–867.
[23] Kašpárková, V.; Humpolíček, P.; Stejskal, J.; Kopecká, J.; Kuceková, Z.; Moučka, R. *Polym. Adv. Technol.* **2016**, *27*, 156–161.
[24] Sapurina, I. Y.; Stejskal, J. *Russ. J. Gen. Chem.* **2012**, *82*, 256–275.
[25] Jelmy, E. J.; Ramakrishnan, S.; Rangarajan, M.; Kothurkar, N. K. *Bull. Mater. Sci.* **2013**, *36*, 37–44.
[26] Genies, E.; Penneau, J.; Lapkowski, M.; Boyle, A. *J. Electroanal. Chem. Interfacial Electrochem.* **1989**, *269*, 63–75.
[27] Kitani, A.; Yano, J.; Kunai, A.; Sasaki, K. *J. Electroanal. Chem. Interfacial Electrochem.* **1987**, *221*, 69–82.
[28] Chen, Z.; Della Pina, C.; Falletta, E.; Faro, M. L.; Pasta, M.; Rossi, M.; Santo, N. *J. Catal.* **2008**, *259*, 1–4.
[29] Della Pina, C.; Rossi, M.; Ferretti, A. M.; Ponti, A.; Faro, M. L.; Falletta, E. *Synth. Met.* **2012**, *162*, 2250–2258.
[30] Chen, Z.; Della Pina, C.; Falletta, E.; Rossi, M. *J. Catal.* **2009**, *267*, 93–96.
[31] Della Pina, C.; Ferretti, A. M.; Ponti, A.; Falletta, E. *Compos. Sci. Technol.* **2015**, *110*, 138–144.
[32] Frontera, P.; Busacca, C.; Trocino, S.; Antonucci, P.; Faro, M. L.; Falletta, E.; Pina, C. D.; Rossi, M. *J. Nanosci. Nanotechnol.* **2013**, *13*, 4744–4751.
[33] Della Pina, C.; Busacca, C.; Frontera, P.; Antonucci, P. L.; Scarpino, L. A.; Sironi, A.; Falletta, E. *J. Nanosci. Nanotechnol.* **2016**, *15*, 1–9.
[34] Kucekova, Z.; Humpolicek, P.; Kasparkova, V.; Perecko, T.; Lehocky, M.; Hauerlandova, I.; Saha, P.; Stejskal, J. *Colloids Surf. B* **2014**, *116*, 411–417.
[35] Li, Y.; Fang, Y.; Liu, H.; Wu, X.; Lu, Y. *Nanoscale* **2012**, *4*, 2867–2869.
[36] Mallick, K.; Witcomb, M. J.; Dinsmore, A.; Scurrell, M. S. J. *Polym. Res.* **2006**, *13*, 397–401.
[37] Gospodinova, N.; Terlemezyan, L.; Mokreva, P.; Stejskal, J.; Kratochvil, P. *Eur. Polym. J.* **1993**, *29*, 1305–1309.
[38] Stejskal, J.; Kratochvil, P.; Spírková, M. *Polymer* **1995**, *36*, 4135–4140.
[39] Titelman, G. I.; Siegmann, A.; Narkis, M.; Wei, Y. *J. Appl. Polym. Sci.* **1998**, *69*, 2205–2212.
[40] Kar, P. *Doping in Conjugated Polymers*; Wiley, New York, 2013.
[41] Wang, L.; Ai, W.; Zhai, Y.; Li, H.; Zhou, K.; Chen, H. *Int. J. Environ. Res. Public Health* **2015**, *12*, 10806–10819.
[42] Chao, C.; Chang, Y.; Hsu, Y.; Liu, F.; Chang, F.; Lin, P.; Ko, F. *Int. J. Electrochem. Sci.* **2013**, *8*, 9082–9092.

Article III.

Humpolicek, P.; **Kucekova, Z**.; Kasparkova, V.; Pelkova, J.; Modic, M.; Junkar, I.; Trchova, M.; Bober, P.; Stejskal, J.; Lehocky, M. Blood Coagulation and Platelet Adhesion on Polyaniline Films. Colloid Surf. B-Biointerfaces 2015, 133, 278–285. https://doi.org/10.1016/j.colsurfb.2015.06.008.

Colloids and Surfaces B: Biointerfaces 133 (2015) 278–285

Contents lists available at ScienceDirect

Colloids and Surfaces B: Biointerfaces

journal homepage: www.elsevier.com/locate/colsurfb

Blood coagulation and platelet adhesion on polyaniline films

Petr Humpolíček[a,b,*], Zdenka Kuceková[a], Věra Kašpárková[a,c], Jana Pelková[d,e], Martina Modic[f], Ita Junkar[f], Miroslava Trchová[g], Patrycja Bober[g], Jaroslav Stejskal[g], Marián Lehocký[a]

[a] Centre of Polymer Systems, Tomas Bata University in Zlin, 760 01 Zlin, Czech Republic
[b] Polymer Centre, Faculty of Technology, Tomas Bata University in Zlin, T.G.M. Sq. 5555, 760 01 Zlin, Czech Republic
[c] Department of Fat, Surfactant and Cosmetics Technology, Faculty of Technology, Tomas Bata University in Zlin, Zlin, Czech Republic
[d] Department of Hematology, Tomas Bata Regional Hospital in Zlin, 762 75 Zlin, Czech Republic
[e] Department of Health Care Sciences, Faculty of Humanities, Tomas Bata University in Zlin, 760 05 Zlin, Czech Republic
[f] Department of Surface Engineering, Plasma Laboratory, Josef Stefan Institute, 1000 Ljubljana, Slovenia
[g] Institute of Macromolecular Chemistry, Academy of Sciences of the Czech Republic, 162 06 Prague 6, Czech Republic

ARTICLE INFO

Article history:
Received 12 January 2015
Received in revised form 1 June 2015
Accepted 3 June 2015
Available online 11 June 2015

Keywords:
Polyaniline
Poly(2-acrylamido-2-methyl-1-propanesulfonic acid)
Hemocompatibility
Blood coagulation
Platelet adhesion

ABSTRACT

Polyaniline is a promising conducting polymer with still increasing application potential in biomedicine. Its surface modification can be an efficient way how to introduce desired functional groups and to control its properties while keeping the bulk characteristics of the material unchanged. The purpose of the study was to synthetize thin films of pristine conducting polyaniline hydrochloride, non-conducting polyaniline base and polyaniline modified with poly(2-acrylamido-2-methyl-1-propanesulfonic acid) (PAMPSA) and investigate chosen parameters of their hemocompatibility. The modification was performed either by introduction of PAMPSA during the synthesis or by reprotonation of polyaniline base. The polyaniline hydrochloride and polyaniline base had no impact on blood coagulation and platelet adhesion. By contrast, the polyaniline reprotonated with PAMPSA completely hindered coagulation thanks to its interaction with coagulation factors Xa, Va and IIa. The significantly lower platelets adhesion was also found on this surface. Moreover, this film maintains its conductivity at pH of 6, which is an improvement in comparison with standard polyaniline hydrochloride losing most of its conductivity at pH of 4. Polyaniline film with PAMPSA introduced during synthesis had an impact on platelet adhesion but not on coagulation. The combined conductivity, anticoagulation activity, low platelet adhesion and improved conductivity at pH closer to physiological, open up new possibilities for application of polyaniline reprotonated by PAMPSA in blood-contacting devices, such as catheters or blood vessel grafts.

1. Introduction

Despite remarkable progress in understanding the blood coagulation system, as well as in the development of blood-compatible biomaterials and blood-contacting devices, the problem of foreign-surface-induced thrombosis still remains unsolved [1]. In fact, the contact of any material with blood induces multiple defensive mechanisms, such as the activation of coagulation cascade, platelet adhesion, the triggering of complementary systems, and others [2]. The most common compound with known anticoagulant activity is heparin, and its efficacy is mainly ascribed to the simultaneous presence of sulfate, sulfamic, and carboxylic groups and their arrangement along the polysaccharide backbone of this polymer (Fig. 1a). It has already been reported that synthetic polymers and copolymers with heparin-like activity might be applicable to medical devices or surfaces coming into contact with blood.

Polyaniline (PANI), as a conducting polymer, has immense potential with regard to practical applications in the biomedical field. In particular, cardiomyocyte synchronization [3], myoblast differentiation [4], neuronal lineage differentiation, and cardiac tissue engineering [5] have been highlighted with respect to the use of conducting polymers. Commonly, the standard PANI, emeraldine salt is prepared *via* oxidative polymerization of aniline hydrochloride with ammonium peroxydisulfate [6]. Considering the biological properties of PANI, the number of papers is surprisingly limited. Humpolicek et al. [7] studied pristine PANI powders

* Corresponding author at: Polymer Centre, Faculty of Technology, Tomas Bata University in Zlin, T.G.M. Sq. 5555, 760 01 Zlin, Czech Republic. Tel.: +420 734 792 298; fax: +420 57 603 1444.
E-mail address: humpolicek@ft.utb.cz (P. Humpolíček).

http://dx.doi.org/10.1016/j.colsurfb.2015.06.008

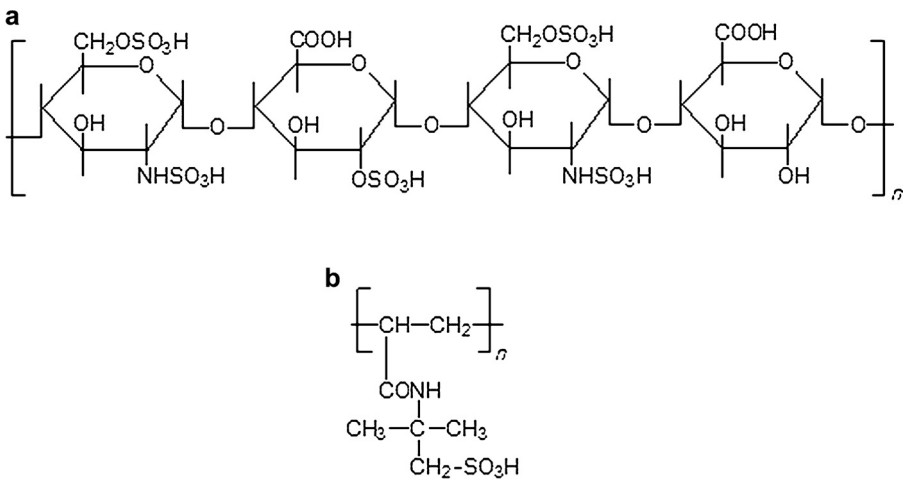

Fig. 1. Formulae of (a) heparin and (b) poly(2-acrylamido-2-methyl-1-propanesulfonic acid).

for their cytotoxicity, skin irritation and sensitization. Also cell proliferation on PANI films [8] and implantability in tissues was investigated by Kamalesh et al. [9] and Mattioli-Belmonte et al. [10]. To the best of authors' knowledge, no information about PANI hemocompatibility has previously been published.

Considerable advantage of PANI consists also in its ability to easily form thin films on substrates immersed in the reaction mixture used for PANI preparation [11]. The films can be further modified by using various dopant acids with the aim to change their surface properties [12]. This opens new possibilities for targeted surface modification of PANI by acids, or generally substances showing desired properties. Polyacids are good candidates for protonation of PANI, and some of them alone have been observed to exhibit notable anticoagulant effects. Methacrylic copolymers containing, similarly to heparin, the above-mentioned functional groups, can be listed as examples [13]. Poly(2-acrylamido-2-methyl-1-propanesulfonic acid) (PAMPSA; Fig. 1b) was shown to act against blood clotting in a similar way to heparin, either alone [14] or incorporated in copolymers [15]. Setoyama et al. [16] also reported that PAMPSA is capable of inhibiting the activation of serum complement activity, which is another important factor with respect to the applicability of materials in biomedical engineering.

In the present study, PANI has a dual role. The first is represented by easy modification of surfaces by deposition of thin PANI films of sub-micrometre thickness. This is done *in situ* on substrates immersed in the reaction mixture used for the oxidation of aniline [11]. The second role then consists in the subsequent immobilization of PAMPSA onto PANI films by the formation of a salt (Fig. 2). The feasibility of a polyanion–polycation complex formation between PANI and PAMPSA has been demonstrated [17,18] and the resulting material was used in the electrodes of energy-storage devices [19,20]. PANI films with PAMPSA have also been tested for their biocompatibility [21], and normal cell adhesion, proliferation, and low cytotoxicity was observed. Polymer combining hemocompatibility and conductivity can be with advantage used for example in biosensors. These types of sensing materials can be safely placed *in vivo* while monitoring the desired parameters *via* conductivity. Moreover, inherently conducting PANI can easily be combined with other biocompatible materials and applied for example for artificial blood vessels where electrical performance can be used to monitor a range of medically important parameters, such as triacylglycerol/cholesterol concentration in blood or velocity of blood flow. A growing interest has been also in electrochemical sensors capable of *in vivo* monitoring of metabolites, for example glucose, hormones, neurotransmitters, antibodies and antigens [22,23].

The present paper is focused on the changes in blood coagulation and platelet adhesion induced by the surfaces of different PANI films, namely PANI hydrochloride, PANI base and PANI salts with PAMPSA. The films with PAMPSA were prepared using two procedures. In the first, reprotonation of PANI base using PAMPSA solution was performed giving rise to films with acid deposited onto the PANI surface. In the second procedure, a standard oxidative polymerization of aniline was conducted, with PAMPSA added directly into the reaction mixture of aniline hydrochloride and ammonium peroxydisulfate. While the PANI film reprotonated with PAMPSA contains exclusively polymeric counter-ions, the second PANI is protonated in part with sulfuric acid produced in the course of aniline oxidation from peroxydisulfate.

2. Materials and methods

2.1. Deposition of polyaniline films

The surfaces of blood collection tubes (Vacuette, Austria) were coated with conducting films of PANI hydrochloride. Aniline

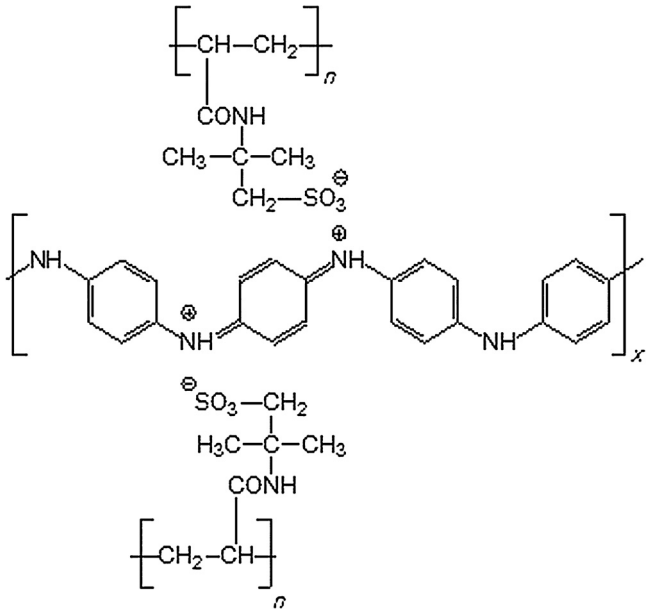

Fig. 2. Polyaniline salt with poly(2-acrylamido-2-methyl-1-propanesulfonic acid).

hydrochloride (2.59 g; Sigma-Aldrich) was dissolved in water to yield 50 mL of solution; ammonium peroxydisulfate (5.71 g; Sigma-Aldrich) was similarly dissolved to 50 mL of solution. Subsequently, both solutions were mixed at room temperature and immediately poured into tubes [11]. The concentrations of reactants were thus 0.2 M aniline hydrochloride and 0.25 M ammonium peroxydisulfate [6]. After 1 h, the tubes were emptied and the films of green conducting PANI hydrochloride deposited on the walls were rinsed with 0.2 M hydrochloric acid, followed by methanol, and left to dry in air for 5 days.

Some films were deprotonated by immersion in 1 M ammonium hydroxide for 12 h and thus converted to blue, non-conducting films of PANI base.

In order to prepare first type of PANI film with poly(2-acrylamido-2-methyl-1-propanesulfonic acid) (PANI–PAMPSA), the reprotonation of PANI base with a 7.5% (v/v) aqueous solution of PAMPSA (molecular weight $M = 2 \times 10^6$ g mol^{-1}, Sigma-Aldrich) was performed by exposing the film to the PAMPSA solution. The neutralization reaction was left to proceed for 24 h; then the residual PAMPSA solution was poured out, the film was rinsed with methanol and left to dry in air.

The second type of film combining PANI and PAMPSA was prepared with PAMPSA present in the reaction mixture of aniline hydrochloride and ammonium peroxydisulfate. For this purpose, modified procedures published by Stejskal et al. [24], Yoo et al. [25], and Bayer et al. [21] were employed. First, an aqueous solution of PAMPSA was prepared with a target concentration corresponding to 0.028 mol (5.8 g) of its constitutional unit, (2-acrylamido-2-methyl-1-propanesulfonic acid). In practice, 38.5 mL of 15% PAMPSA solution was diluted by water to 375 mL. Aniline hydrochloride (0.028 mol, 3.6 g) was then added to the PAMPSA solution and stirred at room temperature for 1 h. The mole ratio of aniline hydrochloride to PAMPSA units was adjusted to 1:1 (PANI-1:1). Then the oxidant, ammonium peroxydisulfate (0.025 mol, 5.8 g), at a 1:0.9 aniline hydrochloride to oxidant mole ratio, was dissolved separately in 25 mL water and added to this solution. The polymerization was completed within 60 min. The films were rinsed with water to remove the adhering precipitate and left to dry in air. In the contrast to PANI–PAMPSA, the PANI-1:1 film contains also sulfate or hydrogen sulfate counter-ions produced by the decomposition of peroxydisulfate in addition to PAMPSA. For that reason, the molecular structure of PANI-1:1 may be structurally closer to PANI hydrochloride films than to PANI–PAMPSA.

2.2. Spectroscopic characterization

The UV–Vis spectra of films were recorded in the presence of buffer solutions with pH ranging from 2 to 12 using the UV/VIS Spectrometer (Lambda 25, Perkin Elmer, UK). The inner surfaces of standard polystyrene cuvettes were coated by PANI–PAMPSA films according to procedure described above. The buffer solutions consisted of 0.0225 M solutions of citric acid (monohydrate) (≥99.5%), Tris (p.a. ≥ 99.8%), KCl (p.a. ≥ 99.5%), obtained from Fluka, KH_2PO_4 and $Na_2B_4O_7{\cdot}10H_2O$ (Merck), and the pH was adjusted in the individual buffer solutions by adding either HCl or NaOH solutions. In the UV–Vis measurements, a syringe was used to manually fill the sample cuvettes with buffer solution and to remove the previous solution. UV–Vis spectra were recorded within the wavelength range 360–1100 nm after 1 h at each pH.

Fourier-transform infrared (FTIR) spectra of the films deposited on silicon windows were recorded with a Thermo Nicolet NEXUS 870 FTIR Spectrometer with a DTGS TEC detector in the 400–4000 cm^{-1} wavenumber region.

2.3. Contact angle measurements

Contact angle measurements were conducted with the aid of the "SEE system" (surface energy evaluation system) (Advex Instruments, Czech Republic) with deionized water as a testing liquid. The droplet volume was set to 2 μL in all experiments.

2.4. Anticoagulation test

In all tests, venous blood was collected from healthy donors by venipuncture using the vacuum blood collection system into the 5 mL collecting tubes (VACUETTE, Greiner Bio-One) after obtaining informed consent. All tests were conducted in accordance with the Helsinki Declaration. Plasma was prepared by centrifugation (15 min, 3000 × *g*). The following coagulation parameters in human blood plasma treated with citric acid (0.109 mol/L) have been studied: (1) thrombin clotting time (TCT), (2) activated partial thromboplastin time (aPTT), and (3) prothrombin time (PT). The tests were performed using a SYSMEX CA-1500 (Siemens, Germany). Each of the samples was assessed three times. To determine the interaction of PANI films on the surface with blood plasma, the coagulation factors Xa (Stuart-Prower factor), Va (proaccelerin), IIa (prothrombin), factor I (fibrinogen), antithrombin III (AT) and D-dimer were selected and the following methods were employed for their determination. The Clauss assay was used to detect the impact on factor I using a SYSMEX CA-1500 (Siemens, Germany). The same equipment with INNOVANCE® Antithrombin and INNOVANCE D-Dimer reagents was used to determine the AT and D-dimer. The activities of factors Xa, Va and IIa in the plasma have been determined by a modified prothrombin time test using an ACL ELITE Pro (IL-Instruments, Italy). Tested plasma was diluted and added to commercial plasma which was deficient always in one of the individual factors (HemosIL™, Instrumentation Laboratory, USA). The clotting time of the deficient plasma is proportional to the concentration (% activity) of a factor in the tested plasma, interpolated from a calibration curve.

2.5. Platelet adhesion

Additional information about the interaction of films with human blood was obtained by the modified TOX 6 assay (Sigma-Aldrich, USA). For this type of experiment, the PANI films were deposited on discs of 10 mm diameter. The discs were subsequently incubated in the presence of 1 mL of human blood. Sample incubation was performed in a 24-well microtiter plate at 37 °C under shaking at 200 rpm for 15 min. After incubation, the samples were rinsed with phosphate buffered saline in order to remove all unattached blood constituents and fixed with 1 mL 50% trichloroacetic acid (Sigma-Aldrich) at 4 °C. After 1 h the platelets adhered on the surface were stained with the Sulforhodamine B. The incorporated dye was liberated from the platelets using Tris base solution. Difference in the number of platelets on different surfaces results in the amount of dye incorporated by the platelets. The incubation of all samples without blood was performed to reveal if used dye did not interact with tested surfaces. The intensity of released colour by the means of absorbance was measured with a Lambda 1050 UV/VIS/NIR spectrophotometer (Perkin Elmer, USA) at a wavelength of 565 nm. The assay was performed on three discs in triplicates.

3. Results and discussion

3.1. Blood plasma coagulation

Standard films of PANI hydrochloride, PANI base and PANI-1:1 did not have any significant impact on the coagulation parameters

Table 1
Impact of PANI surfaces on selected coagulation parameters expressed as times (s) to the coagulation start.

	Reference[a]	PANI base	PANI hydrochloride	PANI–PAMPSA	PANI-1:1
PT	12.1 ± 0.1	11.9 ± 0.2	12.2 ± 0.1	NC[b]	12.0 ± 0.1
aPPT	26.4 ± 0.1	25.6 ± 1.1	26.4 ± 0.0	NC[b]	29.9 ± 0.2
TCT	18.6 ± 0.1	16.7 ± 0.1	17.56 ± 0.2	NC[b]	18.8 ± 0.1

[a] The surface of blood collection tube.
[b] No coagulation. Normal ranges for a healthy person are: PT 11.0–13.5, aPTT 25–32, TCT > 20. The values are expressed as mean value ± standard deviation, $n = 3$.

(Table 1). The coagulation on the PANI–PAMPSA surface, however, was prevented. The fact that neither standard PANI hydrochloride nor PANI base induce any changes in blood clotting suggests that the anticoagulant activity of PANI–PAMPSA is a surface effect of the used polymeric acid and is not inherently caused by PANI as such. The role of PANI thus consists in the immobilization of PAMPSA. This conclusion can be supported by the fact that PANI-1:1, in which the PAMPSA is incorporated directly under polymerization into the PANI film and not attached on its surface, does not show the above-described anticoagulation effect. In this case, however, also the fraction of PAMPSA on the surface may be lower due to the presence of sulfate counter-ions that compete with PAMPSA for the interaction with PANI.

In principle, three important variables influencing coagulation of blood in the contact with foreign matter can be identified: (1) the acidity (pH), (2) the surface charge, and (3) the interaction with coagulation factors. As acidity is one of the above mentioned factors, the pH was measured on freshly taken blood and after blood addition to Vacuette tubes coated with the PANI films. The pH of blood was not notably influenced by any of the tested samples and remained within the range of values for which no effect on blood clotting is expected (PANI hydrochloride: pH = 7.02 ± 0.01; PANI base: pH = 7.06 ± 0.02; PANI–PAMPSA: pH = 6.95 ± 0.01). This is understandable because the specific mass of thin PANI films coated on the tubes is low, of the order of 10 $\mu g\,cm^{-2}$. Such small quantities cannot significantly affect the bulk acidity of the blood in the tube. There are several studies about the impact of pH on the blood coagulation [26], but it is generally accepted that a reduction in thrombus formation starts at a pH below 6.8 and thus coagulation is reduced [27]. Moreover, the pH values of all tested samples were almost equal and impact on coagulation was observed only in case of PANI–PAMPSA. Based on this we can conclude, that reported effect of PANI–PAMPSA on blood plasma coagulation is not related to change of pH value.

As to the second factor, blood coagulation on foreign materials is activated by negative charge present on the hydrophilic surfaces [28,29]. Considering the surface properties of all the tested samples, it can be concluded that their behaviour with respect to coagulation is not influenced by surface charge, because negative charges on PAMPSA are balanced by the positively charged PANI backbone.

The fact that the PANI–PAMPSA film is conducting, and thus antistatic, may also play some role. The conductivity alone, however, cannot be the reason for anticoagulation effect. Typical conductivities of PANI hydrochloride and PANI base are of the orders 10^{0} and $10^{-11}\,S\,cm^{-1}$, respectively [6]. Irrespective of these significantly different values, the coagulation properties of both films are comparable. A conductivity of $\approx 10^{-2}\,S\,cm^{-1}$ was reported for PANI–PAMPSA [17], which is a value within the above interval. Also the conductivity of PANI-1:1 with anticoagulation activity absent does not deviate from the values typically reported for conducting PANI and is of $1.7\,S\,cm^{-1}$ [21].

Although it is known that both extrinsic (tissue factor) and intrinsic (contact activation) coagulation pathways are interconnected *in vivo* [30], the plasma-coagulation cascade is usually divided into the two pathways for the convenience of discussion and coagulopathy testing. It is beyond the scope of this article to provide a comprehensive explanation of coagulation cascade and platelet adhesion in its complexity; this can be found, for example, in the paper by Vogler and Siedlecki [31]. Generally, PT detects the defects or deficits in extrinsic and common coagulation pathways, aPTT similarly in intrinsic and common coagulation pathways, and TCT is used for discriminating between problems in thrombin generation (normal TCT) and the inhibition of thrombin activity (abnormal TCT). Considering the fact that PANI–PAMPSA influences all studied coagulation variables (Table 2), it can be concluded that it affects the common pathway as a consequence of interference with coagulation factors. Thus, the effect of films on the main factors of the common pathway, factor Xa, factor Va, factor IIa, and factor I, was studied in more detail (Table 2). The results clearly show that, in the contrast to all other tested films, PANI–PAMPSA interacts with factor Xa, factor Va and factor IIa. To verify that the surfaces do not induce fibrin production, its amount was measured. The results confirm that none of tested surfaces increase the concentration of fibrin (Table 2). Such effect might be regarded as parallel to that of heparin sulfate, which binds to the enzyme inhibitor antithrombin III (AT), thus causing its activation. The activated AT then inactivates thrombin and other proteases involved in blood clotting, most notably factor Xa formation found in the common pathway. PANI–PAMPSA, therefore, might follow a similar pathway, as it further influences factors in a common way, with the exception of factor I. To test this theory, the activity of AT after contact with tested surfaces was performed. The results clearly show (Table 2), that the activity of AT is physiological after contact with all tested surfaces. The above given conclusion indicates that although PAMPSA acts against blood clotting in a similar way to heparin, which confirms the results of previous studies [14,15], the mechanism must be different. The similarity relies on the fact that heparin and PAMPSA exhibit some common features, which probably play a role in their anticoagulation activity. The fact, that both substances are polymers, although the molecular weight

Table 2
Impact of PANI surfaces on selected coagulation factors.

Factor	Reference[a]	PANI base	PANI hydrochloride	PANI–PAMPSA	PANI-1:1
Xa (%)	100	100	98.4	25.8	94.5
Va (%)	100	89.8	70.5	0.7	86.2
IIa (%)	100	92.7	86.7	0.4	83.6
I (g/L)	3.6[b]	3.7	3.5	2.3	3.3
AT (%)	101.4[b]	107.2	110.0	101.6	104.5
D-dimer (ng/mL FEU)	430[b]	470	450	480	460

[a] Uncoated surfaces of blood collection tube. The factors Xa, Va and IIa are expressed as percentage of values determined for reference.
[b] Normal range for a healthy person are I = 2–4 g/L; AT = 80–120% and D-dimer = 0–500 ng/mL FEU.

Table 3
Platelets adhesion on PANI surfaces determined as absorbance at 565 nm.

	Reference[a]	PANI base	PANI hydrochloride	PANI–PAMPSA	PANI-1:1
Platelet adhesion	2.5 ± 0.2	2.0 ± 0.3	2.5 ± 0.5	0.4 ± 0.0	1.0 ± 0.0

[a] Polystyrene was used as a reference. The values are expressed as mean value ± standard deviation, $n = 3$.

of heparin is much lower compared to PAMPSA, and the polysaccharide backbone of heparin is rigid in contrast to the flexible chain observed in PAMPSA [18], must also be taken into account. Moreover, both polymers are polyanions and both contain nitrogen- and sulfur-containing ionizable groups. This is illustrated by the covalent bond –NH–SO_3^- H^+ in heparin (Fig. 1a) and the ionic bond –NH^+ SO_3^- in PANI–PAMPSA (Fig. 2). On the other hand, the heparin effect is complex and depends not only on mentioned factors but also on certain pentasaccharide sequence in the polymer. The above results again indicate that the role of PANI is limited to the immobilization of PAMPSA at its surface.

Formation of thrombus can be also initiated by protein adsorption on polymer surfaces, which can be minimized when surface energy is on the minimum [32]. This situation occurs on highly hydrophilic surfaces. On the other hand, surfaces of higher hydrophobicity are able to more absorb the protein from plasma, as well as to induce more conformation changes of the adsorbed proteins [33,34]. More comments on this topic is provided in Section 3.5.

3.2. Platelet adhesion on polyaniline surfaces

Using sulforhodamine B colorimetric assay, the total mass of platelets adhered to the surfaces was determined, after the staining of their intracellular proteins. The platelet adhesion significantly decreased on both PANI films modified with PAMPSA irrespective of whether the PAMPSA was deposited on PANI film or added to the polymerization mixture. Of all the tested samples PANI–PAMPSA exhibited the lowest platelet adhesion compared to PANI hydrochloride, and PANI base (Table 3). The behaviour of samples with PAMSA anchored to the surface or incorporated directly into the polymer is hence similar with respect to platelet adhesion, but dissimilar with respect to the behaviour during the blood plasma coagulation.

Surface properties can be considered as an important factor in PANI/platelet interactions and therefore the water contact angle, as a measure of surface hydrophilicity/hydrophobicity was determined. The PANI hydrochloride and PANI–PAMPSA surfaces (Table 4) were the most hydrophilic of all surfaces tested and showed similar behaviour in contact with water. The lowest value (34.24 ± 1.46°) was, however observed for film composed of PANI–PAMPSA. Significant change was then observed for PANI base and PANI 1:1, both showing increase in contact angle to 66.33 ± 2.45° and 69.95 ± 3.42°, respectively. It is generally accepted that hydrophobic surfaces adsorb more plasma proteins than those with hydrophilic character. This corresponds to the lowest platelet adhesion observed on the most hydrophilic surface of PANI–PAMPSA. Nevertheless, the differences in surface hydrophilicity alone, measured on the tested surfaces, cannot unambiguously explain the observed changes in either platelet adhesion or blood coagulation.

Table 4
Contact angle (°) of individual surfaces.

	PANI base	PANI hydrochloride	PANI–PAMPSA	PANI-1:1
Water	63.33 ± 2.47	44.97 ± 3.53	34.21 ± 1.46	69.95 ± 3.42

3.3. pH stability of PANI–PAMPSA films

The UV–Vis spectra of the PANI–PAMPSA films under different pH were recorded with the aim to evaluate the pH of the transition between conducting PANI–PAMSA salt and its non-conducting, deprotonated base. From the spectra (Fig. 3) it is seen that, at pH 2, PANI–PAMPSA has two absorption maxima typical for the conducting PANI form, namely at 410 nm and at approximately 840 nm, which are assigned to the π–π* transition of the benzenoid rings and the polaron band transitions, respectively [35]. The figure also illustrates that at pH higher than 5 the conversion from the conducting salt to non-conducting base occurs. The evidence of this transition is a gradual shift of the spectrum maxima from 840 nm towards lower values. At the same time the shift of the maximum is not abrupt but gradual and, at pH > 8, the maxima are located at 605–650 nm, which corresponds to the n–π* transition of quinonoid rings. Under these conditions the film is fully deprotonated and non-conducting PANI base is formed. The results obtained thus indicate that surface deposition of PANI with PAMPSA improved the pH stability of the film, which was able to retain at least part of its conductivity at pH 6. In the comparison with standard PANI, emeraldine hydrochloride, with transition from salt to base occurring at pH ≈ 4 [36], this is clear improvement. The enhanced stability under physiological conditions might be of importance for PANI applications in biomedicine.

3.4. Spectroscopic investigation

The FTIR spectroscopic analysis has been performed (Fig. 4) to prove the presence of PAMPSA in the films and its interaction with PANI. The infrared spectrum of PANI–PAMPSA strongly differs from the spectrum of the original PANI base, and it is very close to the spectrum of PANI hydrochloride, which exhibits the typical bands of the emeraldine salt [37,38]. This confirms the protonation of the PANI base with PAMPSA.

Absorption bands of the secondary amine –NH– and protonated imine –NH^+= are detected in the region 3400–2800 cm^{-1} (Fig. 4b).

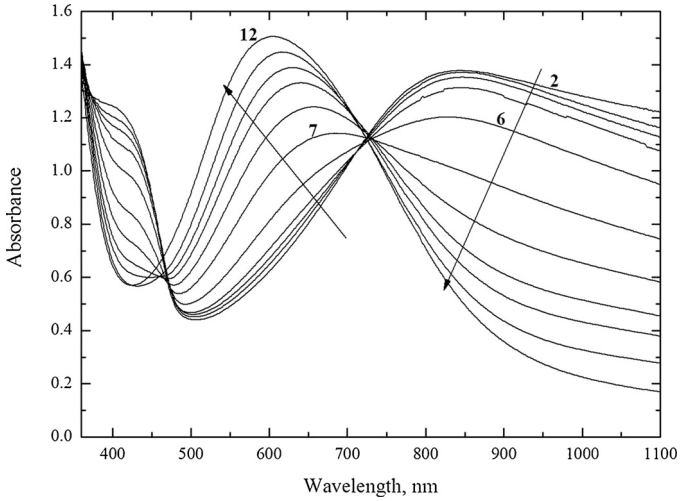

Fig. 3. UV–Vis spectra of the PANI–PAMPSA films measured in buffer solutions between pH 2 and 12.

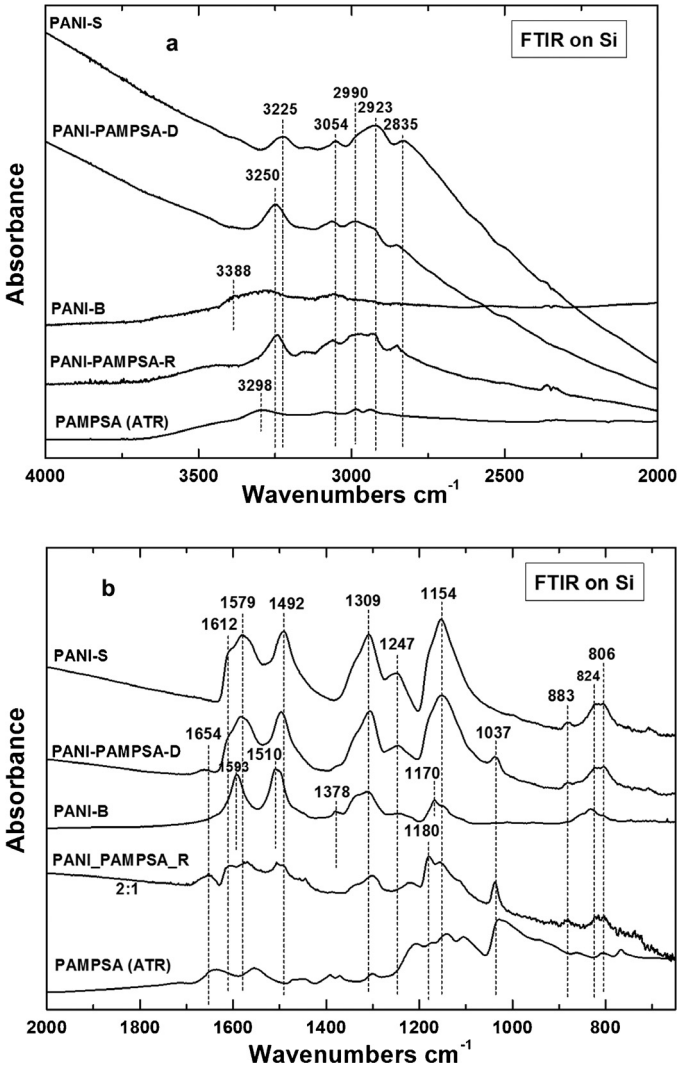

Fig. 4. FTIR spectra of the *in situ* deposited standard PANI hydrochloride (S), PANI base (B), PANI–PAMPSA (D) and PANI-1:1(R) on silicon window in (a) high and (b) low wavenumber regions. Spectrum of neat PAMPSA is shown for comparison.

They reflect the organization of PANI chains within the film by hydrogen bonding involving these groups. A relatively sharp peak with a maximum at 3225 cm^{-1} is attributed to the secondary amine $N–H^+$ stretching vibrations hydrogen-bonded with hydrogen sulfate HSO_4^- and sulfate SO_4^{2-} counter-ions which are present due to the protonation of PANI with sulfuric acid which is a by-product of the aniline oxidation (spectrum PANI-1:1). In the case of reprotonation of PANI base with PAMPSA this peak is stronger and it is shifted to higher wavenumber 3250 cm^{-1} (spectrum PANI–PAMPSA). The maximum of the broad band observed at 2990 cm^{-1} corresponds to the stretching vibrations of $–NH^+=$ in protonated imine groups bonded by a hydrogen bond with hydrogen sulfate HSO_4^- or sulfate SO_4^{2-} counter-ions. This supports the interaction of PANI with PAMPSA by stronger hydrogen bonding [12] and explains the fact that PANI–PAMPSA has improved pH stability in the transition from conducting salt to non-conducting base.

The band typical of the conducting form of PANI is observed at wavenumbers higher than 2000 cm^{-1} (Fig. 4b). Two main bands with maxima situated at 1579 and 1492 cm^{-1}, assigned to quinonoid and benzenoid ring-stretching vibrations, respectively, dominate the spectrum of protonated film in the region bellow 2000 cm^{-1}. The absorption band corresponding to π-electron delocalization induced in the polymer by protonation is situated at 1309 cm^{-1}, the band of $C{\sim}N^{+\bullet}$ stretching vibrations is observed at 1247 cm^{-1}, and the prominent band situated at 1154 cm^{-1}, has been assigned to the vibrations of the $–NH^+=$ structure. The region 900–700 cm^{-1} corresponds to the aromatic ring out-of-plane deformation vibrations. The presence of PAMPSA on the surface of PANI film is reflected in the bands at 1654 and 1037 cm^{-1} observed also in the spectrum of PAMPSA (Fig. 4b).

The shift of the sharp peak present at 3225 cm^{-1} and the maximum of the broad band at 2990 cm^{-1} in the spectrum of PANI salt is lower than in the case of the film PANI–PAMPSA. This signifies that the hydrogen bonding of PAMPSA is weaker in the film of PANI-1:1. The broad polaron band above 2000 cm^{-1} disappeared, as it is observed after deprotonation of the PANI salt to PANI base (Fig. 4). The bands of quinonoid and benzenoid-ring vibrations shift to higher wavenumbers, 1593 cm^{-1} and 1510 cm^{-1}. The band of the C–N stretching vibrations in the neighbourhood of a quinonoid ring at 1378 cm^{-1} appeared in the spectrum of PANI-1:1 and of PANI base. The 1309 cm^{-1} band of the C–N stretching of a secondary aromatic amine and of the aromatic C–H in-plane bending modes are observed in the region at about 1170 cm^{-1} and they are not enhanced in the spectrum of PANI-1:1 and PANI base. Out-of-plane deformations of C–H on 1,4-disubstituted rings are located in the region of 800–880 cm^{-1}. The presence of PAMPSA in the film is also reflected by the bands present at 1654 and 1037 cm^{-1} observed also in the spectrum of PAMPSA (Fig. 4b).

3.5. General discussion

In blood-contacting devices, various polymers can be applied. Just briefly listed, catheters are made of poly(vinylchloride), poly(tetrafluorethylene), polyethylene, polyurethanes and polysiloxane; hemodialysis membranes of polyethersulfone and regenerated cellulose, and oxygenator membranes of polysiloxane or polypropylene [39]. These polymers, however, do not possess an electrical conductivity which can be important in some applications where both conductivity and contact with blood are expected, *e.g. in vivo* sensing materials.

Considering the complexity of material/blood interaction, some general rules have to be considered regarding hemocompatibility of the polymer materials. It is well known, that uncharged hydrophilic surfaces exhibit low interaction with proteins and blood. Nevertheless, this is not a general rule, as for example plasma oxidation of polyethylene substrate was reported to increase wettability with increased protein adsorption while the platelet adhesion was reduced [40]. With respect to hydrophilicity, hydrogels for application in blood contacting devices were shown to be efficient to cause steric repulsion of blood proteins and were prepared for example of poly(vinyl alcohol), poly(*N*-vinylpyrrolidone), poly(ethylene oxide) or cellulose [41]. The poor mechanical properties of hydrogels can be avoided by their grafting on the surfaces of standard polymers. However, highly hydrophobic polytetreafluorethylene or fluorinated surfaces also show high hemocompatibility [42,43]. Surface charge plays also an important role. Positive surface charges stimulate platelet adhesion and activation [44] and negative surface charges activate the plasmatic coagulation systems [29].

In general, there are several approaches to prepare modified materials with improved hemocompatibility. The first one, passivation of the surface can be performed with the aim to achieve minimal interaction with blood proteins and cells. The next approach relies in immobilization of active molecules interacting with blood proteins and cells; and finally, promotion of the growth of endothelial cells is also a possible way of modification. In this context, the surface fluorination [45,46], immobilization of heparin (*e.g.* [29]) as well PEGylation (immobilization of polyethylene glycol) [47] can serve as examples of modified surfaces. Also, the

prevention of non-specific adsorption while selective adsorption of proteins can lead to the desired bioactive function. In this context, the main advantages of PANI relies not only in its conductivity, but also in its ability to be modified by another biological active substances or to act as a surface modifier itself.

The mentioned protein adsorption can be also affected by surface topography of a substrate. Rough surfaces adsorb more proteins than relatively smooth ones [48]. Moreover, the nanoscale surface topography [49] can play an important role. As the polymer chain of PAMPSA modifies the surface topography of PANI, it can also contribute to a different anticoagulation activity on its surface.

4. Conclusions

The PANI film reprotonated with poly(2-acrylamido-2-methyl-1-propanesulfonic acid) had a significant impact on blood coagulation, which was hindered by the interaction with three coagulation factors, Xa, Va and IIa. Such modified polymer film also significantly reduced platelet adhesion, when compared with standard PANI films or uncoated reference surface, which exhibited neither of the mentioned effects. Anticoagulation activity and reduction of platelet adhesion was attributed to presence of PAMPSA polyanion immobilized on PANI polycationic surface. Reprotonation of PANI with poly(2-acrylamido-2-methyl-1-propanesulfonic acid) also yielded other interesting results, namely improved pH stability of the PANI–PAMPSA polymer. While the standard PANI shows transition from non-conducting to conducting form at pH below 4–6, PANI modified with PAMPSA exhibited this transition at increased pH of 6. This is a notable improvement, shifting the conductivity of this polymer closer to physiological pH. The combination of conductivity, anticoagulation activity, low platelet adhesion capacity as well as improved pH stability of PANI coated with poly(2-acrylamido-2-methyl-1-propanesulfonic acid) opens up new possibilities for application of this polymer as a biomaterial, for example in blood-contacting or collecting devices or for *in vivo* sensing materials requiring mentioned properties.

Acknowledgments

Financial support of the Czech Science Foundation (13-08944S) and the Ministry of Education, Youth and Sport of the Czech Republic (CZ.1.05/2.1.00/03.0111) is gratefully acknowledged. One of us (Zdenka Kucekova) also appreciates support from an internal grant of TBU in Zlin IGA/FT/2014/004 financed from funds of specific academic research. Authors thank Ms. H. Hanáková for technical assistance.

References

[1] L. Xu, J.W. Bauer, C.A. Siedlecki, Proteins, platelets, and blood coagulation at biomaterial interfaces, Colloids Surf. B: Biointerf. 124 (2014) 49–68.
[2] F. Jung, S. Braune, A. Lendlein, Haemocompatibility testing of biomaterials using human platelets, Clin. Hemorheol. Microcirc. 53 (2013) 97–115.
[3] C. Hsiao, M. Bai, Y. Chang, M. Chung, T. Lee, C. Wu, B. Maiti, Z. Liao, R. Li, H. Sung, Electrical coupling of isolated cardiomyocyte clusters grown on aligned conductive nanofibrous meshes for their synchronized beating, Biomaterials 34 (2013) 1063–1072.
[4] S.H. Ku, S.H. Lee, C.B. Park, Synergic effects of nanofiber alignment and electroactivity on myoblast differentiation, Biomaterials 33 (2012) 6098–6104.
[5] R.M. Moura, A.A. Alencar de Queiroz, Dendronized polyaniline nanotubes for cardiac tissue engineering, Artif. Organs 35 (2011) 471–477.
[6] J. Stejskal, R.G. Gilbert, Polyaniline preparation of a conducting polymer (IUPAC technical report), Pure Appl. Chem. 74 (2002) 857–867.
[7] P. Humpolicek, V. Kasparkova, P. Saha, J. Stejskal, Biocompatibility of polyaniline, Synth. Met. 162 (2012) 722–727.
[8] P. Humpolicek, V. Kasparkova, J. Stejskal, Z. Kucekova, P. Sevcikova, Cell proliferation on a conducting polymer (polyaniline), Chem. Listy. 106 (2012) 380–383.
[9] S. Kamalesh, P.C. Tan, J.J. Wang, T. Lee, E.T. Kang, C.H. Wang, Biocompatibility of electroactive polymers in tissues, J. Biomed. Mater. Res. 52 (2000) 467–478.
[10] M. Mattioli-Belmonte, G. Giavaresi, G. Biagini, L. Virgili, M. Giacomini, M. Fini, F. Giantomassi, D. Natali, P. Torricelli, R. Giardino, Tailoring biomaterial compatibility: in vivo tissue response versus in vitro cell behavior, Int. J. Artif. Organs 26 (2003) 1077–1085.
[11] J. Stejskal, I. Sapurina, Polyaniline thin films and colloidal dispersions (IUPAC technical report), Pure Appl. Chem. 77 (2005) 815–826.
[12] J. Stejskal, J. Prokeš, M. Trchová, Reprotonated polyanilines: the stability of conductivity at elevated temperature, Polym. Degrad. Stab. 102 (2014) 67–73.
[13] M. Sorm, S. Nespurek, L. Mrkvickova, J. Kalal, Z. Vorlova, Anticoagulation activity of some sulfate-containing polymers of the methacrylate type, J. Polymer Sci. Part C-Polymer Symp. (1979) 349–356.
[14] D. Paneva, O. Stoilova, N. Manolova, D. Danchev, Z. Lazarov, I. Rashkov, Copolymers of 2-acryloylamido-2-methylpropanesulfonic acid and acrylic acid with anticoagulant activity, E-Polymers (2003) 52.
[15] E. Yancheva, D. Paneva, D. Danchev, L. Mespouille, P. Dubois, N. Manolova, I. Rashkov, Polyelectrolyte complexes based on (quaternized) poly[(2-dimethylamino)ethyl methacrylate]: behavior in contact with blood, Macromol. Biosci. 7 (2007) 940–954.
[16] H. Setoyama, Y. Murakami, K. Inoue, H. Iwata, H. Kitamura, T. Shimada, H. Kaji, Y. Ikada, M. Imamura, Extracorporeal circulation with an anticomplement synthetic polymer prolongs guinea pig-to-rat cardiac xenograft survival, Transpl. Proc. 31 (1999) 2818–2822.
[17] O.L. Gribkova, A.A. Nekrasov, V.F. Ivanov, O.A. Kozarenko, O.Yu. Posudievsky, A.V. Vannikov, V.G. Koshechko, V.D. Pokhodenko, Mechanochemical synthesis of polyaniline in the presence of polymeric sulfonic acids of different structure, Synth. Met. 180 (2013) 64–72.
[18] O.L. Gribkova, O.D. Omelchenko, M. Trchová, A.A. Nekrasov, V.F. Ivanov, V.A. Tverskoy, A.V. Vannikov, Preparation of polyaniline in the presence of polymeric sulfonic acids mixtures: the role of intermolecular interactions between polyacids, Chem. Papers 67 (2013) 952–960.
[19] J. Jeon, Y. Ma, J.F. Mike, L. Shao, P.B. Balbuena, J.L. Lutkenhaus, Oxidatively stable polyaniline:polyacid electrodes for electrochemical energy storage, Phys. Chem. Chem. Phys. 15 (2013) 9654–9662.
[20] J. Jeon, J. O'Neal, L. Shao, J.L. Lutkenhaus, Charge storage in polymer acid-doped polyaniline-based layer-by-layer electrodes, ACS Appl. Mater. Interf. 5 (2013) 10127–10136.
[21] C.L. Bayer, I.J. Trenchard, N.A. Peppas, Analyzing polyaniline-poly(2-acrylamido-2-methylpropane sulfonic acid) biocompatibility with 3T3 fibroblasts, J. Biomater. Sci.: Polymer Ed. 21 (2010) 623–634.
[22] C. Mao, A. Zhu, Q. Wu, X. Chen, J. Kim, J. Shen, New biocompatible polypyrrole-based films with good blood compatibility and high electrical conductivity, Colloids Surf. B: Biointerf. 67 (2008) 41–45.
[23] S. Singh, A. Chaubey, B.D. Malhotra, Amperometric cholesterol biosensor based on immobilized cholesterol esterase and cholesterol oxidase on conducting polypyrrole films, Anal. Chim. Acta 502 (2004) 229–234.
[24] J. Stejskal, I. Sapurina, J. Prokeš, J. Zemek, In-situ polymerized polyaniline films, Synth. Met. 105 (1999) 195–202.
[25] J.E. Yoo, J.L. Cross, T.L. Bucholz, K.S. Lee, M.P. Espe, Y. Loo, Improving the electrical conductivity of polymer acid-doped polyaniline by controlling the template molecular weight, J. Mater. Chem. 17 (2007) 1268–1275.
[26] M. Engstrom, U. Schott, B. Romner, P. Reinstrup, Acidosis impairs the coagulation: a thromhoelastographic study, J. Trauma-Injury Infect. Crit. Care 61 (2006) 624–628.
[27] G. Scharbert, G. Franta, L. Wetzel, S. Kozek-Langenecker, Effect of pH levels on platelet aggregation and coagulation: a whole blood in vitro study, Crit. Care 15 (2011) 1–190.
[28] Y. Marikovs, D. Danon, A. Katchals, Agglutination by polylysine of young and old red blood cells, Biochim. Biophys. Acta 124 (1966), 154.
[29] M.B. Gorbet, M.V. Sefton, Biomaterial-associated thrombosis: roles of coagulation factors, complement, platelets and leukocytes, Biomaterials 25 (2004) 5681–5703.
[30] I.M. Sainz, R.A. Pixley, R.W. Colman, Fifty years of research on the plasma kallikrein-kinin system: from protein structure and function to cell biology and in-vivo pathophysiology, Thromb. Haemost. 98 (2007) 77–83.
[31] E.A. Vogler, C.A. Siedlecki, Contact activation of blood–plasma coagulation, Biomaterials 30 (2009) 1857–1869.
[32] Y. Ikada, M. Suzuki, Y. Tamada, Polymer surfaces possessing minimal interaction with blood components, in: Polymers as Biomaterials, Springer, Heidelberg, 1984, pp. 135–147.
[33] T. Klose, P.B. Welzel, C. Werner, Protein adsorption from flowing solutions on pure and maleic acid copolymer modified glass particles, Colloid Surf. B: Biointerf. 51 (2006) 1–9.
[34] M. Okubo, H. Hattori, Competitive adsorption of fibrinogen and albumin onto polymer microspheres having hydrophilic/hydrophobic heterogeneous surface structures, Colloid Polym. Sci. 271 (1993) 1157–1164.
[35] A.P. Monkman, P. Adams, Structural characterization of polyaniline free standing films, Synth. Met. 41 (1991) 891–896.
[36] T. Lindfors, L. Harju, Determination of the protonation constants of electrochemically polymerized poly(aniline) and poly(*o*-methylaniline) films, Synth. Met. 158 (2008) 233–241.
[37] I. Šeděnková, J. Prokeš, M. Trchová, J. Stejskal, Conformational transition in polyaniline films – spectroscopic conductivity studies of ageing, Polym. Degrad. Stab. 93 (2008) 428–435.
[38] M. Trchová, Z. Morávková, I. Šeděnková, J. Stejskal, Spectroscopy of thin polyaniline films deposited during chemical oxidation of aniline, Chem. Papers 66 (2012) 415–445.

[39] C. Werner, M.F. Maitz, C. Sperling, Current strategies towards hemocompatible coatings, J. Mater. Chem. 17 (2007) 3376–3384.
[40] J.H. Lee, H.B. Lee, Platelet adhesion onto wettability gradient surfaces in the absence and presence of plasma proteins, J. Biomed. Mater. Res. 41 (1998) 304–311.
[41] N.A. Peppas, Y. Huang, M. Torres-Lugo, J.H. Ward, J. Zhang, Physicochemical, foundations and structural design of hydrogels in medicine and biology, Ann. Rev. Biomed. Eng. 2 (2000) 9–29.
[42] A.R. Jahangir, W.G. McClung, R.M. Cornelius, C.B. McCloskey, J.L. Brash, J.P. Santerre, Fluorinated surface-modifying macromolecules: modulating adhesive protein and platelet interactions on a polyether-urethane, J. Biomed. Mater. Res. 60 (2002) 135–147.
[43] J.Y. Ho, T. Matsuura, J.P. Santerre, The effect of fluorinated surface modifying macromolecules on the surface morphology of polyethersulfone membranes, J. Biomater. Sci. Polym. Ed. 11 (2000) 1085–1104.
[44] S. Sagnella, K. Mai-Ngam, Chitosan based surfactant polymers designed to improve blood compatibility on biomaterials, Colloid Surf. B: Biointerf. 42 (2005) 147–155.
[45] K. Tokuda, T. Ogino, M. Kotera, T. Nishino, Simple method for lowering poly(methyl methacrylate) surface energy with fluorination, Polym. J. 47 (2015) 66–70.
[46] T. Hasebe, A. Shimada, T. Suzuki, Y. Matsuoka, T. Saito, S. Yohena, A. Kamijo, N. Shiraga, M. Higuchi, K. Kimura, H. Yoshimura, S. Kuribayashi, Fluorinated diamond-like carbon as antithrombogenic coating for blood-contacting devices, J. Biomed. Mater. Res. Part A 76A (2006) 86–94.
[47] B. Balakrishnan, D. Kumar, Y. Yoshida, A. Jayakrishnan, Chemical modification of poly (vinyl chloride) resin using poly (ethylene glycol) to improve blood compatibility, Biomaterials 26 (2005) 3495–3502.
[48] B. Walivaara, B.O. Aronsson, M. Rodahl, J. Lausmaa, P. Tengvall, Titanium with different oxides – in-vitro studies of protein adsorption and contact activation, Biomaterials 15 (1994) 827–835.
[49] C.C. Mohan, K.P. Chennazhi, D. Menon, In vitro hemocompatibility and vascular endothelial cell functionality on titania nanostructures under static and dynamic conditions for improved coronary stenting applications, Acta Biomater. 9 (2013) 9568–9577.

Article IV.

Kasparkova, V.; Humpolicek, P.; Stejskal, J.; Kopecka, J.; **Kucekova, Z**.; Moucka, R. Conductivity, Impurity Profile, and Cytotoxicity of Solvent-Extracted Polyaniline. Polym. Adv. Technol. 2016, 27 (2), 156–161. https://doi.org/10.1002/pat.3611.

Research article

polymers for advanced technologies

Received: 22 May 2014, Revised: 26 June 2015, Accepted: 26 June 2015, Published online in Wiley Online Library: 27 July 2015

(wileyonlinelibrary.com) DOI: 10.1002/pat.3611

Conductivity, impurity profile, and cytotoxicity of solvent-extracted polyaniline

Věra Kašpárková[a,b], Petr Humpolíček[a,c]*, Jaroslav Stejskal[d], Jitka Kopecká[e], Zdenka Kuceková[a] and Robert Moučka[a]

Understanding the correlation between the preparation, purification, impurity leaching, and cytotoxicity of polyaniline is crucial for the application of this conducting polymer in biomedicine. Polyaniline hydrochloride was purified in a Soxhlet extractor by using six different solvents: methanol, 1,2-dichloroethane, acetone, ethyl acetate, hexane, or 0.2 M aqueous hydrochloric acid. The chromatographic analyses of impurities leached out of the polymer into the solvents confirmed differences in impurity profiles, which depended on the polarity of the extraction solvent. Compared with the original polymer, the conductivity of purified polyanilines increased in dependence on the amount and type of extracted impurities. The cytotoxicity of purified samples determined on the mouse embryonic fibroblast cell line NIH/3T3 using MTT assay improved as well. Methanol and 0.2 M hydrochloric acid were the most efficient solvents capable of extracting low-molecular-weight impurities, and thus reducing polyaniline cytotoxicity. The absence of cytotoxicity was observed at an extract concentration of 10%. Extraction with suitable solvents can, therefore, be a possible way of obtaining cyto-compatible polyaniline with sufficient conductivity.

Keywords: polyaniline; Soxhlet extraction; purification; biocompatibility

INTRODUCTION

Polyaniline (PANI) is one of the promising polymers for the applications in the life sciences.[1] Synthesis and processing of PANI are governed by several factors resting on its target utilization. A number of applications of polyaniline in biomedicine have recently appeared[2] requiring, in addition to conductivity, the special properties of this polymer, namely its biocompatibility. The biological properties of PANI, emeraldine salt in powdered form, prepared by chemical oxidation according to Stejskal and Gilbert,[3] were investigated by Humpolicek *et al.*,[4] who found that the polymer exhibited notable cytotoxicity towards HaCaT and HepG2 cells. The modification of PANI used for biomedical applications is therefore essential. In scientific literature, procedures for purifying PANI have already been published; however, they were mainly focused on the improvement of material properties, such as conductivity investigated by Zhang and Jing.[5] In their work, PANI emeraldine base was treated in Soxhlet extractor with tetrahydrofuran, and the purified polymer was reprotonated with hydrochloric, sulfuric, *p*-toluenesulfonic, and methanesulfonic acids to obtain emeraldine salt with increased conductivity compared to the original sample. The purification of PANI with the aim of improving its compatibility with cells was, to the best of the authors' knowledge, performed only in the study of Humpolicek *et al.*,[4] who used re-protonation for this purpose; and in the work of Stejskal *et al.*,[6] who investigated PANI purified by precipitation from *N*-methyl-2-pyrrolidone or sulfuric acid in acidified methanol.

It is assumed, but not unambiguously confirmed, that the observed cytotoxicity of PANI is connected with occurrence of low-molecular-weight impurities present in the polymer. Both precursors used for PANI synthesis, ammonium peroxydisulfate (APS) and aniline hydrochloride (AH), are water soluble, and their residues might be easily released from otherwise insoluble PANI, when subjected to physiological conditions in the body. Briefly, their acute toxicity,[7,8] carcinogenicity[9,10] teratogenity,[11] genotoxicity,[12] mutagenicity,[13,14] Ames assay,[15] and influence on chromosomal aberrations[16,17] have been tested and reported. The cytotoxicity and cellular response of aniline oligomers have also been the subject of a study published by Zhang *et al.*,[18] who reported that, of the tested oligomers, aniline trimer was the most cytotoxic to mouse embryo fibroblast and adenocarcinoma human alveolar basal epithelial cells.

* *Correspondence to: Petr Humpolíček, Centre of Polymer Systems, Tomas Bata University in Zlin, T.G.M. Sq. 5555, 760 01 Zlin, Czech Republic. E-mail: humpolicek@ft.utb.cz*

a *V. Kašpárková, P. Humpolíček, Z. Kuceková, R. Moučka*
Centre of Polymer Systems, Tomas Bata University in Zlin, 760 01 Zlin, Czech Republic

b *V. Kašpárková*
Department of Fat, Surfactant, and Cosmetics Technology, Faculty of Technology, Tomas Bata University in Zlin, 762 72 Zlin, Czech Republic

c *P. Humpolíček*
Polymer Centre, Faculty of Technology, Tomas Bata University in Zlin, 760 01 Zlin, Czech Republic

d *J. Stejskal*
Institute of Macromolecular Chemistry, Academy of Sciences of the Czech Republic, 162 06 Prague 6, Czech Republic

e *J. Kopecká*
University of Chemistry and Technology, Prague 166 28 Prague 6, Czech Republic

polymers for advanced technologies

Soxhlet extraction is a well-established method for the purification of solids. In the present study, the extraction of PANI in the Soxhlet extractor with organic solvents including methanol, 1,2-dichloroethane, acetone, ethyl acetate, and hexane, as well as 0.2 M aqueous hydrochloric acid was followed, and the efficacy of the solvents to remove impurities from the polymer was investigated. The cytotoxicity and conductivity of the purified polymer were then evaluated and are discussed.

EXPERIMENTAL

Polyaniline preparation

Aniline hydrochloride (Fluka, Switzerland) and ammonium peroxydisulfate (Lach-Ner, Czech Republic) were used as delivered. Polyaniline salt hydrochloride was prepared by oxidation of 0.2 M aniline hydrochloride with 0.25 M ammonium peroxydisulfate in water at room temperature.[3] Aniline hydrochloride (0.2 mol) was dissolved in water to 500 ml of solution; ammonium peroxydisulfate (0.25 mol) was separately dissolved to the same solution volume. Both solutions were mixed in a beaker, stirred briefly, and aniline left to polymerize. The next day, a green polyaniline powder was collected on a filter, rinsed with 0.2 M hydrochloric acid, and similarly with acetone, dried in air, and then in a desiccator over silica gel.

Extraction

Polyaniline hydrochloride (5 g) was weighed, transferred to an extraction thimble, and loaded in the chamber of the Soxhlet extractor. Five hundred milliliters of solvent was taken in a distillation flask; the extractor was assembled and heated to reflux. The extraction continued until the solvent became colorless (Table 1). After the extraction, the polyaniline powder was collected, dried in air, measured for conductivity, and used for the testing of cytotoxicity. Samples were designated PANI-S. The solvent extract was evaporated in a rotary evaporator, and solids were dried to constant weight. The procedure was repeated with each of the solvents used: methanol, 1,2-dichloroethane, acetone, ethyl acetate, hexane, and 0.2 M aqueous hydrochloric acid (Table 1).

Conductivity

The conductivity of the purified samples was measured by the four-point van der Pauw method on polymers compressed into pellets with a diameter of 13 mm and a thickness of around 1 mm. A programmable high-voltage sourcemeter Keithley 2410 and electrometer/high resistance meter Keithley 6517B with a switch Keithley 7002 were employed. Measurements were carried out at ambient temperature.

Table 1. Extraction solvents used for purification of PANI salt and their parameters[29]: Boiling point, T, relative permittivity (25°C), ε_r, Hildebrandt parameter, δ, and time required for solvent decoloration τ

Solvent	T [°C]	ε_r	δ	τ [hr]
0.2 M HCl (water)	100.0	78.4	23.50	5.5
Methanol	64.5	32.7	14.28	3.0
Acetone	56.1	20.7	9.77	2.0
1,2-Dichloroethane	83.5	10.4	9.76	4.5
Ethyl acetate	77.2	6.2	9.10	3.5
Hexane	68.7	1.9	7.24	2.0

Size exclusion chromatography

The analyses were performed on solids collected from extracts using a PLGPC-200 chromatograph (Polymer Laboratories, United Kingdom) equipped with a PL differential refractometer and a set of two PL MIXED D columns (Agilent) at 150 °C with *N*-methyl-2-pyrrolidone as the mobile phase. Flow rate of 0.8 ml min^{-1} and a 100-μl injection loop was used. Data processing was performed with a Cirrus GPC, Multi Detector Software (Polymer Laboratories Ltd). Dry extracts were accurately weighed and dissolved for approximately 10 hr at 160 °C under continuous shaking in the mobile phase and filtered through a 0.45-μm syringe filter. The filter was weighed before and after filtering in order to take in account possible mass loss caused by the residual, non-dissolved polymer. The contents of impurities were expressed as the peak areas of low-molecular-weight impurities (monomer, oligomers, and by-products) and any high-molecular-weight impurities (polymer) recorded for each of the samples, normalized with its mass used for analysis.

Cytotoxicity

Prior to *in-vitro* cytotoxicity testing, the samples were disinfected by dry heat at 120 °C for 40 min. Purified polymer powders (PANI-S) were homogenized in a mortar and extracted according to ISO 10993-12 in the ratio of 0.2 g per 1 ml of cultivation medium. Dulbecco's Modified Eagle Medium high glucose, 10% fetal calf serum, and penicillin/streptomycin, 100 U ml^{-1} (PAA Laboratories GmbH, Austria) was used as the medium. Extraction was performed in chemically inert closed containers using aseptic techniques at 37 ± 1°C under stirring for 24 ± 1 hr. The parent extracts (100%) were then diluted in a culture medium to obtain a series of dilutions with concentrations of 50, 25, 10, 5, and 1%. All extracts were used within 24 hr. The ability of cells to respond to cytotoxic substances was verified by the application of sodium dodecyl sulfate solution (SDS; Sigma, Czech Republic).

Cytotoxicity testing was conducted in accordance with EN ISO 10993-5, using the mouse embryonic fibroblast cell line NIH/3T3 (American Type Culture Collection, HB-8065), cultivated according to the protocol recommended by the supplier. Cells were pre-cultivated for 24 hr, and the culture medium was subsequently replaced with PANI extracts. As a reference giving 100% cell proliferation, cells cultivated in the pure medium were used. To assess cytotoxic effects, the MTT assay (Invitrogen Corporation, USA) was performed after one-day cell cultivation at 37 ± 0.1°C. The absorbance was measured at 570 nm by an Infinite M200 PRO (Tecan, Switzerland). All the tests were performed in quadruplicates. Dixon's Q test was used to remove outlying values, and means were calculated. Cell viability was expressed (i) as mean values and standard deviations of individual absorbances measured with statistical differences compared to the reference, determined by a *t*-test; and (ii) as the percentage of viable cells present in the corresponding extract relative to cells cultivated in pure growth medium (100% viability). Values >0.8 were assigned to no cytotoxicity, 0.6–0.8 to mild cytotoxicity, 0.4–0.6 to moderate cytotoxicity, and <0.4 to severe cytotoxicity. The morphology of the cells was observed using an inverted Olympus phase contrast microscope (Olympus IX81, Japan).

RESULTS

In previously published papers dealing with the preparation of PANI for applications in biomedicine, different purification procedures, such as deprotonation or reprecipitation were introduced, providing polymers varying in cytotoxicity and hence in anticipated performance *in vivo*.[4,6] In none of these studies, however, the changes in cytotoxicity after purification have been related to changes in the conductivity of the purified polymer or to the impurity profile of the extracts. In the present study, PANI was treated by another alternative method, a solvent extraction, and the conductivity and cytotoxicity of the extracted samples were assessed.

Conductivity

The conductivity of the PANI-S samples after treatment in a Soxhlet extractor was of the order of S cm^{-1}, ranging from 2.6 S cm^{-1} to 6.7 S cm^{-1} (Table 2). Untreated pristine sample exhibited conductivity of 1.5 S cm^{-1}, which was slightly lower in comparison with the typical value of approximately 4 S cm^{-1} reported by Stejskal and Gilbert[3] for non-purified polyaniline, emeraldine salt. The differences in conductivity determined among purified samples depended on the extraction medium used, with hexane and ethylacetate providing the most notable increases in conductivity. In the contrast, 0.2 M hydrochloric acid and methanol yielded less conducting product compared to the product treated with all other solvents employed.

It is well known that the conductivity of PANI decreases during long-term exposure to the elevated temperature and the decrease depends on temperature, time of treatment, and counter-ion present in PANI.[19] One would expect that the use of solvents with higher boiling point (Table 1) would lead to the larger decrease in the conductivity. Such trends, however, have not been confirmed.

The increase in the conductivity reflects the changes caused in the PANI by purification. Pristine, standard PANI contains low-molecular weight fractions and sections of chains with molecular defects, which both limit the charge transfer along the polymer backbone, as well as intermolecular transport, and thus decrease the electrical conductivity of the polymer. Using the purification procedure, low-molecular weight fractions are removed, and, in consequence, the conductivity of the polymer can increase. This situation is evident also in the case of the samples studied. Compared to untreated samples with a conductivity of 1.5 S cm^{-1}, all purified PANI-S samples exhibited higher conductivity relative to the original polymer. It seems that the impurities, whose removal most notably contributed to increase of conductivity are of hydrophobic nature, and are more efficiently extracted out with non-polar organic solvents. Contrary to this observation, removal of low-molecular weight, polar impurities by using methanol, and aqueous hydrochloride acid caused only minor increase in polymer conductivity.

Impurity content

The primary insight into the efficiency of each of the solvents to remove impurities from PANI-S is provided by the evaluation of the weight of dry matter obtained after evaporation of the extract. The results, in terms of sample weight in mg contained in 100 ml of extract, are summarized in Table 3. It is worth noting that this simple test already divides the solvents used into two distinct groups, the first including 0.2 M HCl and methanol, i.e. polar solvents, and the second, comprising the other four, less polar or non-polar solvents.

The content of impurities presented in Table 3 clearly demonstrates that only methanol and 0.2 M aqueous HCl have been able to extract the low-molecular-weight impurities from PANI powder, such as a monomer or oligomer salts. On the other hand, ethyl acetate, acetone, and partially also 1,2-dichloroethane predominantly extract the impurities of higher molecular weight and non-polar nature.

The solvents listed in Table 3 are all considered incapable of dissolving PANI of sufficiently high molecular weight. Polyaniline is generally characterized by very poor solubility and the only solvent commonly used for its dissolution in base form is *N*-methylpyrrolidone. Some papers report that the polymer does not completely dissolve in this solvent, either,[20,21] and the insoluble fraction in "standard" polyaniline base can be even higher than 80 wt%.[6]

The data (Table 3) also illustrate the fact that the amounts of impurities, either of low-molecular-weight or higher molecular

Table 2. Conductivity (S cm^{-1}) of PANI-S samples purified in a Soxhlet extractor with various solvents

Untreated	0.2 M HCl	Methanol	Acetone	Dichloroethane	Ethyl acetate	Hexane
1.5	2.6	2.7	5.4	6.5	6.7	6.1

Table 3. The content of impurities removed from PANI-S treated with different solvents in a Soxhlet extractor (given in normalized peak area) determined by SEC and weighing of matter after evaporation of extract to dryness (mg/100 ml)

Extraction solvent	Monomers and oligomers	Dissolved polymer	Total impurities	Extracted matter [mg/100 ml]
0.2 M HCl	1445	15	1460	113
Methanol	840	80	920	87
Acetone	50	410	460	14
Dichloroethane	125	195	320	17
Ethyl acetate	80	480	560	9
Hexane	12	43	55	8

polymers for advanced technologies

weight, roughly correlate with the Hildebrand solubility parameter δ_H and solvent relative permittivity, which can be considered as a measure of its polarity (Table 1). The Hildebrand parameter is a quantity used to provide an estimate of the interaction between polymers and solvents and can serve as an indication of the solubility of polymers. The highest solubility of the materials may be expected when the values of its Hildebrant parameter and that of the solvent are close to each other. Theoretically, δ_H is the square root of the cohesive energy density, which was suggested in numerical values as a criterion of solvency behavior. Strongly polar solvents, such as methanol or aqueous solution of hydrochloric acid are capable of extracting polar, low-molecular impurities, namely PANI precursors. By contrast, non-polar hexane removes only a very limited amount of impurities, as it is incapable of dissolving low-molecular-weight precursors and does not dissolve fractions of PANI of higher molecular weight, either. The relation between the conductivity and total impurity content is visualized in Fig. 1. It can be seen that the purification influences conductivity of PANI only in a minor extent (the order of magnitude is of 10^0). Most notable difference can be observed between performance of polar and non-polar solvents.

Cytotoxicity

The cytotoxicity of PANI powders after purification in Soxhlet extractor depended on the solvent used for its purification (Table 4). The cytotoxic values of polymer purified with 1,2-dichloroethane, acetone, ethyl acetate, and hexane, extracted into cell-growth medium, were rather similar. For example, only the 1% polymer extract in cultivation medium was non-cytotoxic, with a cell viability higher than 80%. Already 10% polymer extracts showed severe cytotoxicity, similarly to all remaining extracts with higher concentrations. On the other hand, PANI purification by methanol and 0.2 M HCl was beneficial, as the 10% extracts were still non-cytotoxic with a cell viability higher than 80%. Moreover, even 25% extracts were slightly under the threshold "non-cytotoxic", providing more than 70% viable cells, relative to reference.

DISCUSSION

The cytotoxicity of PANI powder prepared by the oxidative polymerization of aniline hydrochloride according to Stejskal and Gilbert[3] has previously been published by Humpolicek *et al.*,[4] who observed that extracts of PANI, emeraldine salt and base, possess a significant cytotoxicity. Extracts of PANI salt with concentrations higher than 25% applied on HaCaT cells exhibited severe cytotoxicity, decreasing cell viability below 40%. As regards HepG2 cells, concentrations of extract higher than 10% were moderately cytotoxic, and only the 1% extract was non-cytotoxic when applied on both used cell lines. The cytotoxicity of PANI base was lower compared with that observed for the salt. Here, the cytotoxic effect on both cell lines was absent at a concentration of about 25%.

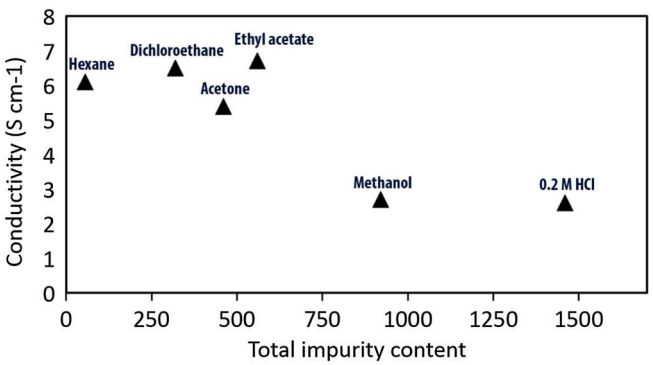

Figure 1. The relation between the total impurity content (normalized peak area) and conductivity (S cm^{-1}) determined for samples purified with studied solvents. This figure is available in colour online at wileyonlinelibrary.com/journal/pat

Two purification procedures have already been reported to decrease cytotoxicity of PANI extracts. Purification by deprotonation of the emeraldine salt to the base, and its subsequent reprotonation with acids[4] revealed a significant reduction in cytotoxicity. Its threshold increased from 1% extract concentrations observed for non-purified PANI to 5% (HaCaT) and 10% (HepG2) for purified samples, respectively. The second purification method, a re-precipitation, has also recently been published.[6] Here, a reduction in cytotoxicity was achieved by PANI dissolution in *N*-methyl-2-pyrrolidone or concentrated sulfuric acid followed by the precipitation in acidified methanol. The limited solubility of PANI is a serious drawback of this method. The cytotoxicity was absent at extract concentration of 5% in the cultivation medium. In the present study utilizing Soxhlet extraction with solvents, methanol and 0.2 M HCl were the most effective to purify PANI; their application significantly decreased the cytotoxicity of PANI, with a threshold cytotoxic concentration of extract being 25%. This suggests that the cytotoxicity is caused mainly by polar compounds, such as salts of primary aromatic amines that are the intermediates or by-products of aniline oxidation.[22]

It is worth mentioning, that the nanotubular PANI salt exhibited the lowest cytotoxicity of all ever investigated polyanilines (72% cell survival even in 100% extract).[6] Such PANI is prepared by oxidative polymerization of aniline in weakly acidic medium, e.g. 0.4 M acetic acid.[23] The nanotubular form can be therefore considered as the most promising PANI for biomedical applications, despite its somewhat lower conductivity.

Interesting and comprehensive research related to PANI purification was published by Laska and Widlarz,[24] who studied low-molecular-weight compounds formed during aniline polymerization. They were mainly interested in changes in the material properties of PANI caused by purification and concluded that low-molecular weight fractions influenced physico-chemical properties of the polymer, such as density and solubility. These low-molecular-weight products were removed from the PANI by means of Soxhlet extraction using methanol, chloroform, tetrahydrofuran (THF), benzyl alcohol, and *N*-methylpyrrolidinone as the individual solvents, and it was found that the solubility of PANI depended on the solvent used in the order methanol < chloroform < THF < benzyl alcohol. This corresponds with results from the current study also showing methanol as the least powerful organic solvent for the dissolution of PANI, capable of removing only low-molecular-weight, polar impurities. Another study employing Soxhlet extraction for purification of PANI was reported by Bari *et al.*[20] and was conducted with the aim to separate low- and high-molecular-weight fractions from the crude polymer. Here, different approach was applied, and one polymer sample was successively extracted with all solvents (methanol, chloroform,

Table 4. Cytotoxicity of PANI-S samples determined for various extract concentrations presented as average absorbance ± standard deviation (Abs) and as relative value compared to reference (RV) according to ISO 10 993-5 standard [a]

Sample		100%	75%	50%	25%	10%	1%
PANI salt[b]	RV	0.40 C	/	0.40 C	0.40 C	0.54 C	0.90 A
Nanotubular PANI salt[c]	RV	0.72 B	/	0.76 B	0.79 B	0.67 B	0.85 A
0.2 M aqueous HCl	Abs	0.343 ± 0.028	0.347 ± 0.023	0.349 ± 0.007	0.789 ± 0.095	0.871 ± 0.056	0.884 ± 0.104
	RV	0.32 D	0.32 D	0.32 D	0.73 B	0.81 A	0.82 A
Methanol	Abs	0.401 ± 0.030	0.383 ± 0.014	0.381 ± 0.017	0.821 ± 0.145	0.916 ± 0.129	0.957 ± 0.055
	RV	0.37 D	0.36 D	0.35 D	0.76 B	0.85 A	0.89 A
Acetone	Abs	0.378 ± 0.013	0.381 ± 0.031	0.460 ± 0.033	0.394 ± 0.011	0.365 ± 0.012	1.165 ± 0.061
	RV	0.35 D	0.35 D	0.43 C	0.37 D	0.34 D	1.08 A
1,2-Dichlorethane	Abs	0.393 ± 0.018	0.400 ± 0.018	0.621 ± 0.068	0.403 ± 0.027	0.365 ± 0.004	0.916 ± 0.137
	RV	0.36 D	0.37 D	0.58 C	0.37 D	0.34 D	0.85 A
Ethyl acetate	Abs	0.376 ± 0.035	0.423 ± 0.022	0.516 ± 0.113	0.414 ± 0.015	0.378 ± 0.017	1.213 ± 0.063
	RV	0.35 D	0.39 D	0.48 C	0.38 D	0.35 D	1.12 A
Hexane	Abs	0.395 ± 0.048	0.448 ± 0.016	0.569 ± 0.063	0.413 ± 0.028	0.379 ± 0.029	1.180 ± 0.107
	RV	0.37 D	0.42 C	0.53 C	0.38 D	0.35 D	1.09 A

[a]Cytotoxicity in relative values equal to 1 corresponds to 100% cell survival compared to reference. Values >0.8 are assigned to no cytotoxicity (A), 0.6–0.8 to mild cytotoxicity (B), 0.4–0.6 to moderate cytotoxicity (C), and <0.4 to severe cytotoxicity (D). Reference absorbance was 1.0784 ± 0.0951 = 100%.
[b]Results published in (Humpolicek *et al.*[4]).
[c]Results published in (Stejskal *et al.*[6]).

THF, and benzyl alcohol), the same as in the previous work. The order in which the solvents were employed was based on the solubility of different polymer weight fractions in each of the solvents, reported by Laska and Widlarz.[24] As a result of purification, PANI with narrow molecular weight was obtained.

Taking into account the correlation between cytotoxicity and the profile of impurities in the samples tested in the current work, it can be seen that cytotoxicity is mainly caused by low-molecular-weight fractions, as demonstrated by behavior of polymers treated with methanol and 0.2 M aqueous HCl (Table 2), which both decreased in their cytotoxicity. Simultaneously, only a slight growth in conductivity was observed in PANI purified in such way. Zhang and Jing,[5] similarly to earlier study of Stejskal *et al.*[25] reported that PANI with a higher molecular weight and greater crystallinity also exhibits a slightly higher conductivity. This was connected with a more integrated π-conjugation system and a better mobility of charge carriers along the polymer chain. In this context it is worth mentioning that PANI hydrochloride is completely insoluble in any of the solvents used for the purification.[26] For that reason, no changes in the molecular-weight-distribution could reasonably be expected after treatment with chosen solvents. Regarding crystallinity, which is another important characteristic with impact on conductivity, it can be noted that the used PANI is virtually amorphous. Based on previously reported work, the degree of crystallinity is below 10%[27] and no measurable changes in the degree of crystallinity are anticipated as a result of purification process.

The increase in conductivity can hardly be related to the change in content of low-molecular-weight components. Naturally, absence of conductivity is expected in case of both precursors, aniline hydrochloride and ammonium peroxydisulfate. As regards oligomers, their conductivity was determined to be of 1.2×10^{-8} S cm^{-1},[28] which is notably lower compared to conducting PANI salt, however one order of magnitude higher than that of non-conducting PANI base. The increase in conductivity after extensive purification with solvents can therefore be, in general, related to combination of two effects: (i) a decrease in defects within the chain-space of the purified polymer and (ii) the removal of low-molecular-weight compounds with low conductivity. In the present study, the removal of impurities of higher molar mass, using for example 1,2-dichloroethane, also caused increase in the conductivity of purified samples. It can therefore be speculated that, through the extraction, poorly organized polymer chains with defects are removed and chain organization is improved.

CONCLUSIONS

The cytotoxicity of polyaniline purified using six different solvents in a Soxhlet extractor was determined and correlated with the content of low- and high-molecular-weight impurities extracted from pristine polymer. The purification procedure reduced the cytotoxicity of standard polyaniline and increased the cytotoxicity threshold from 1% (pristine PANI) to 10% (methanol and 0.2 M HCl purified PANI), showing in both cases a viability of cells higher than 80% relative to the reference. The contents of respective impurities in the extracts provided information about the reason for the cytotoxicity of pristine PANI, which is closely connected to the presence of low-molecular-weight fractions in the polymer. Simultaneously, the purification led to a moderate increase in polymer conductivity, though, unfortunately, this increase was the smallest for samples with the lowest cytotoxicity. The obtained results contribute to the understanding of the impact of polyaniline on eukaryotic cells and should be considered when designing biocompatible forms of polyaniline.

Acknowledgements

Authors thank to Dr. Jan Prokeš for kind measurements of conductivity and Dr. Pavel Kucharczyk for technical assistance.

Financial support of the Czech Science Foundation (13-08944S) is gratefully acknowledged. This work was supported by the Ministry of Education, Youth and Sports of the Czech Republic – Program NPU I (LO1504). This research is sponsored by NATO's Public Diplomacy Division in the framework of Science for Peace (984597).

REFERENCES

[1] N. K. Guimard, N. Gomez, C. E. Schmidt, *Prog. Polym. Sci.* **2007**, *32*, 876-921.
[2] T. H. Qazi, R. Rai, A. R. Boccaccini, *Biomaterials* **2014**, *35*, 9068-9086.
[3] J. Stejskal, R. G. Gilbert, *Pure Appl. Chem.* **2002**, *74*, 857-867.
[4] P. Humpolicek, V. Kasparkova, P. Saha, J. Stejskal, *Synthetic Met.* **2012**, *162*, 722-727.
[5] K. Zhang, X. Jing, *Polym. Adv. Technol.* **2009**, *20*, 689-695.
[6] J. Stejskal, M. Hajna, V. Kasparkova, P. Humpolicek, A. Zhigunov, M. Trchova, *Synthetic Met.* **2014**, *195*, 286-293.
[7] F. P. Jenkins, J. B. Gellatly, G. W. A. Salmond, J. A. Robinson, *Food Cosmet. Toxicol.* **1972**, *10*, 671.
[8] J. Signorin, C. E. Ulrich, M. T. Butt, E. A. D'Amato, *Inhal. Toxicol.* **2001**, *13*, 1033-1045.
[9] H. Ma, J. Wang, S. Z. Abdel-Rahman, P. J. Boor, M. F. Khan, *Toxicol. Appl. Pharm.* **2008**, *233*, 247-253.
[10] Y. Kurokawa, N. Takamura, Y. Matsushima, T. Imazawa, Y. Hayashi, *Cancer Lett.* **1984**, *24*, 299-304.
[11] K. Matsumoto, N. Seki, K. Fukuta, Y. Congenit. *Anom.* **2001**, *41*, 112-117.
[12] K. Sekihashi, A. Yamamoto, Y. Matsumura, S. Ueno, M. Watanabe-Akanuma, F. Kassie, S. Knasmuller, S. Tsuda, Y. F. Sasaki, *Mutat. Res.-Gen. Tox. En.* **2002**, *517*, 53-75.
[13] A. Martinez, A. Urios, V. Felipo, M. Blanco, *Muta. Res.-Gen. Tox. En.* **2001**, *497*, 159-167.
[14] M. Ishidate, T. Sofuni, K. Yoshikawa, M. Hayashi, T. Nohmi, M. Sawada, A. Matsuoka, *Food Chem. Toxicol.* **1984**, *22*, 623-636.
[15] R. J. Brennan, R. H. Schiestl, *Mutagenesis*, **1997**, *12*, 215-220.
[16] K. T. Chung, C. A. Murdock, S. E. Stevens, Y. S. Li, C. I. Wei, T. S. Huang, M. W. Chou, *Toxicol. Lett.* **1995**, *81*, 23-32.
[17] M. Ishidate, *Data book of chromosomal aberration test in vitro*. Elsevier Publishing Company, Amsterdam, **1988**.
[18] X. Zhang, H. Qi, S. Wang, L. Feng, Y. Ji, L. Tao, S. X. Li, Y. Wei, *Toxicol. Res.-UK*, **2012**, *1*, 201-205.
[19] J. Prokes, J. Stejskal, *Polym. Degrad. Stabil.* **2004**, *86*, 187-195.
[20] V. G. Bairi, S. E. Bourdo, J. A. Moore, L. K. Schnackenberg, B. C. Berry, A. S. Biris, T. Viswanathan, *J. Polym. Res.* **2013**, *20*, 193.
[21] Y. Li, X. Ren, W. He, X. Jing, *Colloid Polym. Sci.* **2014**, *292*, 1099-1110.
[22] I. Sapurina, A. V. Tenkovtsev, J. Stejskal, *Polym. Int.* **2015**, *64*, 453-465.
[23] J. Stejskal, I. Sapurina, M. Trchova, E. N. Konyushenko, *Macromolecules* **2008**, *41*, 3530-3536.
[24] J. Laska, J. Widlarz, *Polymer* **2005**, *46*, 1485-1495.
[25] J. Stejskal, A. Riede, D. Hlavata, J. Prokes, M. Helmstedt, P. Holler, *Synthetic Met.* **1998**, *96*, 55-61.
[26] I. Sapurina, A.Y. Osadchev, B.Z. Volchek, M. Trchova, A. Riede, J. Stejskal, *Synthetic Met.* **2002**, *129*, 29-37.
[27] J. Stejskal, A. Riede, D. Hlavata, J. Prokes, M. Helmstedt, P. Holler, *Synthetic Met.* **1998**, *96*, 55-61.
[28] J. Stejskal, M. Trchova, *Polym. Int.* **2012**, *61*, 240-251.
[29] C. Reichardt, T. Welton, *Solvents and solvent effects in organic chemistry*. Wiley-VCH Verlag GmbH & Co. KGaA, Weinheim, Germany, **2010**.

Article V.

Kucekova, Z.; Humpolicek, P.; Kasparkova, V.; Perecko, T.; Lehocky, M.; Hauerlandova, I.; Saha, P.; Stejskal, J. Colloidal Polyaniline Dispersions: Antibacterial Activity, Cytotoxicity and Neutrophil Oxidative Burst. Colloid Surf. B-Biointerfaces 2014, 116, 411–417. https://doi.org/10.1016/j.colsurfb.2014.01.027.

Colloids and Surfaces B: Biointerfaces 116 (2014) 411–417

Contents lists available at ScienceDirect

Colloids and Surfaces B: Biointerfaces

journal homepage: www.elsevier.com/locate/colsurfb

Colloidal polyaniline dispersions: Antibacterial activity, cytotoxicity and neutrophil oxidative burst

Zdenka Kucekova[a,b], Petr Humpolicek[a,b,*], Vera Kasparkova[b,c], Tomas Perecko[d], Marián Lehocký[b], Iva Hauerlandová[c], Petr Sáha[b], Jaroslav Stejskal[e]

[a] Polymer Centre, Faculty of Technology, Tomas Bata University in Zlin, T.G.M. Sq. 5555, 760 01 Zlin, Czech Republic
[b] Centre of Polymer Systems, Tomas Bata University in Zlin, T.G.M. Sq. 5555, 760 01 Zlin, Czech Republic
[c] Department of Fat, Surfactant and Cosmetics Technology, Faculty of Technology, Tomas Bata University in Zlin, T.G.M. Sq. 5555, 760 01 Zlin, Czech Republic
[d] Institute of Biophysics, Academy of Sciences of the Czech Republic, 612 65 Brno, Czech Republic
[e] Institute of Macromolecular Chemistry, Academy of Sciences of the Czech Republic, 162 06 Prague 6, Czech Republic

ARTICLE INFO

Article history:
Received 6 November 2013
Received in revised form 14 January 2014
Accepted 19 January 2014
Available online 25 January 2014

Keywords:
Cytotoxicity
Apoptosis
Necrosis
Antibacterial activity
Oxidative burst
Colloidal polyaniline

ABSTRACT

Polyaniline colloids rank among promising application forms of this conducting polymer. Cytotoxicity, antibacterial activity, and neutrophil oxidative burst tests were performed on cells treated with colloidal polyaniline dispersions. The antibacterial effect of colloidal polyaniline against gram-positive and gram-negative bacteria was most pronounced for *Bacillus cereus* and *Escherichia coli*, with a minimum inhibitory concentration of 3500 $\mu g\,mL^{-1}$. The data recorded on human keratinocyte (HaCaT) and a mouse embryonic fibroblast (NIH/3T3) cell lines using an MTT assay and flow cytometry indicated a concentration-dependent cytotoxicity of colloid, with the absence of cytotoxic effect at around 150 $\mu g\,mL^{-1}$. The neutrophil oxidative burst test then showed that colloidal polyaniline, in concentrations <150 $\mu g\,mL^{-1}$, was not able to stimulate the production of reactive oxygen species in neutrophils and whole human blood. However, it worked efficiently as a scavenger of those already formed.

1. Introduction

Ever increasing numbers of papers dealing with the biocompatibility of conducting polymers are evidence of the growing interest in these materials. Whereas polypyrrole is better described and more intensively studied in the context of biological properties, information about polyaniline uses in biosciences is less frequent. So far, conductivity and electrochemical behavior were the main focuses of attention. The interesting properties of polyaniline have recently led to an investigation of its possible uses in biomedical applications. This concerns especially the objects that are associated with electrical properties, such as brain, cardiac or neural tissues and cells. Namely, applications in cardiomyocyte synchronization [1], myoblast differentiation [2], neuronal lineage differentiation [3], skeletal muscle [4] or cardiac tissue engineering [5] have been reported. Also, the cytotoxicity, irritation and sensitization potential [6], cell proliferation [7] and antibacterial properties [8–10] of polyaniline powder prepared according to a procedure provided by IUPAC [11] have already been described. Other studies, dealing with biological properties, such as the *in-vivo* tissue response of polyaniline, are mostly based on the testing of polyaniline films cast on various carrier surfaces [12], polyaniline composites [13] or electrospun blends [14].

Although the biological applications of polyaniline are on the rise, they are limited to a certain extent by its insolubility in aqueous media. It is commonly known that conducting polyaniline is poorly soluble even in organic solvents, which strongly influences its processability. Hence, a considerable effort has been devoted to the preparation of processable forms of this polymer. Possible solutions to this challenge can be found in copolymerization [15] or protonation with acids containing relatively long alkyl side chains, which may enhance the solubility in solvents [16]. The preparation of conducting polymer colloids is another approach how to cope with this problem.

Colloidal polyaniline dispersions are prepared when aniline is oxidized in an aqueous medium containing a suitable water-soluble polymer acting as a steric stabilizer. Various polymers have been tested as stabilizers, including poly(vinyl alcohol-*co*-vinyl acetate) [17], poly(vinyl alcohol) [18], poly(methyl vinyl ether) [19], poly(ethylene oxide) [20] or cellulose ethers [21–23]. Also poly(*N*-vinylpyrrolidone) turned out to be an efficient stabilizer of polyaniline colloidal particles and has been successfully employed [24–26]. In light of the numerous applications of colloidal

* Corresponding author at: Polymer Centre, Faculty of Technology, Tomas Bata University in Zlin, T.G.M. Sq. 5555, 760 01 Zlin, Czech Republic. Tel.: +420 777673396.
E-mail address: humpolicek@ft.utb.cz (P. Humpolicek).

0927-7765/$ – see front matter © 2014 Elsevier B.V. All rights reserved.
http://dx.doi.org/10.1016/j.colsurfb.2014.01.027

polyaniline that have been proposed [27–29], it seems worthwhile to examine the basic biological properties of this promising material.

In the present study, a colloidal polyaniline dispersion, employing poly(*N*-vinylpyrrolidone) as the stabilizer, was prepared and characterized. The main target of the study was to determine the influence of the colloid on prokaryotic and eukaryotic cells via assessing the cytotoxicity on two cell lines and determining the antibacterial properties on representatives of gram-positive and gram-negative bacteria. In addition, the generation of human reactive oxygen species by neutrophils has also been studied. The biological properties of colloidal polyaniline are being reported here for the first time.

2. Materials and methods

2.1. Preparation of colloidal polyaniline dispersion

Aniline hydrochloride (0.2 M) was oxidized with ammonium peroxydisulfate (0.25 M) [30] in the presence of a stabilizer, 2 wt% poly (*N*-vinylpyrrolidone) (PVP; Fluka, type K90, molecular weight 360,000). Aniline hydrochloride (259 mg) was dissolved in an aqueous solution of PVP (4 wt%) to 5 mL of solution. The polymerization of aniline was started at room temperature, close to 20 °C, by adding 5 mL of aqueous solution containing 571 mg ammonium peroxydisulfate. The mixture was briefly stirred and left at rest for 2 h. The resulting dark green dispersion of polyaniline hydrochloride was transferred into a membrane tubing (Spectra/Por 1, Spectrum Medical Instruments, USA; molecular weight cut-off 7,000) and exhaustively dialyzed against 0.2 M hydrochloric acid to remove residual monomers and by-products, such as ammonium sulfate.

2.2. Particle size

The size and distribution of the colloidal particles were determined by dynamic light scattering using a Zetasizer Nano ZS instrument (Malvern Instruments, UK). Measurements of the hydrodynamic radii of colloidal particles, expressed as z-average particle diameters, were performed at 25 °C. The intensity of scattered light ($\lambda = 633$ nm) was observed at a scattering angle of 173°. The polydispersity index (PDI) was evaluated by assuming log-normal distribution of particle sizes. Prior to measurements, the performance of the instrument was verified by using polystyrene latex nanoparticles with the nominal size of 92 ± 3 nm (Thermo Scientific, Germany).

2.3. Polyaniline concentration

Optical spectra of polyaniline colloids were recorded in the wavelength range of 200–800 nm with a Photo Lab 6600 UV-vis spectrometer (WTW, Germany) after defined dilution with 1 M hydrochloric acid. The concentration of polyaniline in colloidal dispersion was calculated from the absorbance at wavelength of 395 nm by using the Lambert–Beer law, $A = \varepsilon cl$, where $\varepsilon = 31{,}500 \pm 1{,}700\ \mathrm{cm^2\ g^{-1}\ cm^{-1}}$ is absorption coefficient [18], c is the concentration of polyaniline and $l = 1$ cm is the optical path.

2.4. Antibacterial testing

The testing of antibacterial properties of polyaniline was conducted with representatives of gram-negative and gram-positive bacterial strains. *Bacillus cereus* (CCM 2010), *Staphylococcus aureus* (CCM 3953), *Escherichia coli* (CCM 3954) and *Pseudomonas aeruginosa* (CCCM 3955) were employed in the test. All strains were obtained from the Czech Collection of Microorganisms (CCM, Czech Republic). Bacteria were grown on nutrient agar ($5\ \mathrm{g\ L^{-1}}$ peptone, $3\ \mathrm{g\ L^{-1}}$ beef extract, $15\ \mathrm{g\ L^{-1}}$ agar; Hi-Media Laboratories, India) and $5\ \mathrm{g\ L^{-1}}$ sodium chloride (Lach-Ner, Czech Republic) at 37 °C. Initial inocula of the microorganisms were prepared from the 24 h cultures, and bacterial suspensions were adjusted to contain 10^6 CFU $\mathrm{mL^{-1}}$ by diluting them with a nutrient broth containing $5\ \mathrm{g\ L^{-1}}$ peptone, $3\ \mathrm{g\ L^{-1}}$ beef extract and $5\ \mathrm{g\ L^{-1}}$ sodium chloride.

For antibacterial testing, the colloidal polyaniline dispersion was diluted with a nutrient broth to obtain polyaniline concentrations ranging from 2,000 to 8,500 $\mu\mathrm{g\ mL^{-1}}$ and inoculated with 200 μL of bacterial suspension. After a 24 h incubation, 100 μL of decimal dilutions were spread over agar plate surfaces and incubated for 24 h at 37 °C. Colonies were counted and minimum inhibitory concentration (MIC) was calculated. Each experiment was repeated four times.

The pH determination of the bacterial suspension in the absence and the presence of a polyaniline colloid was carried out by using a Spear pH meter tester (Eutech) before and after cultivation in order to monitor the pH changes occurring in the suspension during bacterial growth.

2.5. Test of cytotoxicity

Prior to *in-vitro* cytotoxicity testing, the samples were disinfected by dry heat at 120 °C for 40 min. Cytotoxicity testing was performed with a human immortalized keratinocyte cell line (HaCaT, Cell Lines Service, Catalog No. 300493, Germany) [31] and a mouse embryonic fibroblast cell line (ATCC CRL-1658 NIH/3T3, USA). The HaCaT cells were cultivated using Dulbecco's Modified Eagle Medium – high glucose, with added 10% fetal bovine serum and penicillin/streptomycin, $100\ \mathrm{U\ mL^{-1}}$ (PAA Laboratories GmbH, Austria). The ATCC-formulated Dulbecco's Modified Eagle's Medium (catalog No. 30-2002), with added bovine calf serum to a final concentration of 10% and penicillin/streptomycin, $100\ \mathrm{U\ mL^{-1}}$, was used as the culture medium in case of NIH/3T3 cells.

The tested samples were diluted to concentrations of 520, 345, 171, 155, 130, 105, 70, 35, and 20 $\mu\mathrm{g\ mL^{-1}}$ in the culture medium. Cytotoxicity testing was conducted according to the EN ISO 10993-5 standard procedure, with modification. Cells were pre-cultivated for 24 h, and the culture medium was subsequently replaced with dilutions of polyaniline colloid. As a reference, cultivation in a pure medium without colloid was used. To assess cytotoxic effect, a MTT assay (Invitrogen Corporation, USA) was performed after one-day cell cultivation in the presence of colloidal polyaniline. All the tests were performed in quadruplicates. The absorption was measured at 570 nm with an Infinite M200 Pro NanoQuant (Tecan, Switzerland). Dixon's Q test was used to remove outlying values, and mean values were calculated. The cell viability is presented in two ways in order to provide a comprehensive view of the results: (1) as a percentage of cells present in the respective extract relative to cells cultivated in a pure extraction medium without colloidal polyaniline (100% viability), and (2) by using the *t*-test expressing the statistical differences between the averages of individual dilutions compared to the reference.

The morphology of the cells was assessed after 24 h of cultivation in the presence of a colloid. The changes in the cell morphology were observed with an Olympus inverted fluorescent microscope (Olympus, CKX 41, Japan). The fluorescent staining of DNA was performed using the Hoechst 33258 dye (Invitrogen Corporation, USA).

2.6. Apoptosis versus necrosis rate

To distinguish healthy, apoptotic and necrotic cells after the contact of the cell cultures with colloidal polyaniline, staining with annexin V/propidium iodide (BD Biosciences, Canada) was

used. The method of cell cultivation, sample preparation and precultivation was the same as in the cytotoxicity test. After that, the colloidal dispersion was removed, and the remaining adherent cells were rinsed with a phosphate buffered saline (PBS), treated with trypsin and added to a previously removed, non-adherent cell population from the same treatment. Cells were re-suspended in a buffer and stained by annexin V–FITC in a concentration of 2.5 $\mu g\,mL^{-1}$ and by propidium iodide in a concentration of 5 $\mu g\,mL^{-1}$. After 15 min in the dark, cells were analyzed by a BD FACSCanto flow cytometer (BD Biosciences, Canada).

2.7. Oxidative burst in human neutrophils and whole blood

The effect of polyaniline on (1) the activation of neutrophils, determined by a generation of reactive oxygen species (ROS) and (2) the scavenging of already formed ROS, where neutrophil ROS production was initiated by the addition of phorbol 12-myristate 13-acetate (PMA), was tested. The following tests were, therefore, performed: (a) measurements of chemiluminescence in whole human blood; (b) measurements of chemiluminescence in isolated neutrophils with discrimination of the effects on extra- and intracellular ROS production; and (c) cell-free assay as a reference.

The neutrophils were isolated from the human blood of healthy donors with written informed consent. Blood was collected by venous puncture. The study was performed in accordance with the Declaration of Helsinki. The blood was gently mixed with dextran from *Leuconostoc mesenteroides*, M_r 425,000–575,000 (Sigma Aldrich, D1037, USA) (2:1) and left at room temperature for 20 min. A buffy coat was collected and centrifuged at 190 g for 10 min at 4 °C. Red blood cells were lysed with hypotonic cold hemolysis and overlaid on Ficoll (GE Healthcare, Sweden). After centrifugation at 390 *g* for 30 min at 4 °C, the neutrophils were washed in cold PBS and used for the experiment. The neutrophil viability was over 95%, as verified with a CASY cytometer (Roche, Switzerland). The statistical differences between reference and individual studied samples were evaluated using a *t*-test.

2.8. Chemiluminescence

The chemiluminescence of human neutrophils in the whole blood was measured in a 96-well microplate luminometer (Luminometer LM-01T, Immunotech, Czech Republic) at 37 °C. Aliquots of polyaniline and luminol (250 $\mu mol\,L^{-1}$) were mixed. To ensure a sufficient concentration of extracellular peroxidase in PMA-stimulated cells, the mixture was supplemented with horseradish peroxidase (HRP; Sigma Aldrich, USA) with the final concentration of 8 $U\,L^{-1}$. Finally, 50-times diluted blood was added and the reaction started via the addition of PMA (0.05 $\mu mol\,L^{-1}$, Sigma Aldrich, USA). The chemiluminescence of the samples was recorded for 1 h, and a quantitative determination of the signals was performed by integrating the chemiluminescence signal over the entire measuring period [32]. Activated samples without polyaniline served as a positive reference. Spontaneous chemiluminescence (without activators) was also measured. The colloidal polyaniline dispersions with concentrations of 171, 17, 1.7, 0.17, 0.017, and 0.0017 $\mu g\,mL^{-1}$ were tested.

The extracellular chemiluminescence in isolated neutrophils was determined by using isoluminol (Sigma Aldrich) and HRP; in the case of intracellular chemiluminescence, luminol was applied. For elimination of extracellular ROS, catalase (2000 $U\,L^{-1}$) (Sigma Aldrich, USA) and superoxide dismutase (100 $U\,L^{-1}$) (Worthington Biochemical Corporation, USA) were added. The samples were measured for 30 min in a 96-well microplate luminometer (Luminometer LM-01T, Immunotech, Czech Republic) at 37 °C [32].

In a cell-free assay, the chemiluminescence was initiated in a culture medium containing polyaniline with the addition of hydrogen peroxide (100 $\mu g\,mL^{-1}$) in the presence of horse radish peroxidase (2 $U\,mL^{-1}$) and luminol (10 $\mu g\,mL^{-1}$). The experiment was conducted in triplicates and each of the samples was measured for 30 min [33]. Correspondingly, as in the previous test dealing with ROS formation, the statistical differences between the reference and individual samples were determined using a *t*-test.

3. Results and discussion

3.1. Characterization of colloidal dispersion

The size of the dispersion particles is one of the crucial parameters influencing the performance of colloids in biological applications. As reported earlier [30], polyaniline particles in dispersion have a typical average size of hundreds of nanometers and are therefore rated as colloids. Dynamic light scattering measurements showed that the particle size of the tested dispersion, expressed as a z-average diameter, was of 226.5 ± 0.5 nm, with an average polydispersity index of 0.145 ± 0.004. These data indicate that colloidal polyaniline is a homogeneous dispersion with a nearly uniform, single population of particles in the expected size range. However, it must be remembered that the size of particles, determined by dynamic light scattering, is z-averaged according to the scattering intensity of each particle fraction. In practice relevant to biological applications, volume and even number averages are more appropriate, and they are smaller than *z*-averages.

The UV–vis spectra of the dispersion diluted with 1 M hydrochloric acid showed a pattern slightly different from that reported by Stejskal and Sapurina [30], with a broad absorption maxima at about 310–395 nm and increasing absorbance toward the measuring limit of the instrument, 800 nm. Stejskal and Sapurina reported an additional local maximum at the wavelength of 854 nm [30]. The above characteristics confirm that the tested sample can be considered as a representative of the standard colloid prepared using procedure recommended by IUPAC, with a poly-(*N*-vinylpyrrolidone) as a stabilizer.

3.2. Antibacterial properties

The susceptibility of bacteria against colloidal polyaniline seems to be species dependent (Table 1). The results showed that the growth of gram-negative *E. coli* was insignificantly reduced from 8.6 to 8.4 log CFU mL^{-1} by 2,000 $\mu g\,mL^{-1}$ of colloidal polyaniline, and full inhibition was observed at a concentration of 3,500 $\mu g\,mL^{-1}$. *P. aeruginosa* was the most resistant bacteria, and colloidal polyaniline with a concentration of 3,500 $\mu g\,mL^{-1}$ only caused a decrease by two orders of magnitude (from 8.9 to 6.9 log CFU mL^{-1}). An antibacterial effect was first observed at the highest tested concentration of 8,500 $\mu g\,mL^{-1}$. The behavior of gram-positive *S. aureus* was analogous to *P. aeruginosa*, with MIC detected at 8,500 $\mu g\,mL^{-1}$. However, a lower colloid concentration of 3,500 $\mu g\,mL^{-1}$ inhibited the growth of *S. aureus* slightly better compared to *P. aeruginosa*, with a reduction of three orders of magnitude (from 8.6 to 5.7 log CFU mL^{-1}) (Table 1). The second tested gram-positive bacteria, *B. cereus*, was completely eliminated after a colloidal polyaniline concentration of 3,500 $\mu g\,mL^{-1}$ was applied, as similarly observed for *E. coli*.

The antibacterial activity observed in the current study can be compared with that determined on polyaniline powder published by Gizdavic-Nikolaidis et al. [34]. Although their paper is primarily devoted to antibacterial properties of functionalized polyanilines and polyaniline copolymers with aminobenzoic acids, standard polyaniline (emeraldine) salt was used as a reference. This comparison can be also performed, thanks to the similarity of the methods used for antibacterial testing. Correspondingly to current

Table 1
Values of minimum inhibitory concentration (MIC) and log CFU for tested bacteria.

Polyaniline [μg mL^{-1}]	*Staphylococcus aureus*	*Bacillus cereus*	*Escherichia coli*	*Pseudomonas aeruginosa*
0	8.6	7.2	8.6	8.9
2000	7.6	7.2	8.4	8.7
3500	5.7	MIC	MIC	6.9
8500	MIC	N/A	N/A	MIC

N/A, not applicable.

work employing a polyaniline colloid, Gizdavic-Nikolaidis et al. [34] prepared suspensions of standard polyaniline powder in a nutrient broth. A comparison of results on polyaniline colloid with those recovered from re-suspended polyaniline powder revealed that colloid seems to possess higher antibacterial activity. Tests performed on powdered polyaniline showed that concentrations higher than 10,000 μg mL^{-1} are efficient against *P. aeruginosa* and *S. aureus*. *E. coli* was inhibited exactly by 10,000 μg mL^{-1}. Hence, all the concentrations here were higher compared with those determined for a colloidal form.

An interesting observation was made on bacterial suspension-added polyaniline at low concentrations, where bacterial growth was observed. Here, the suspension changed its color from originally being green to gray/colorless, except for the suspension containing *P. aeruginosa*, which turned out to be red due to naturally red color of these bacteria. The reason for the bleaching was found in the change of the pH which, thanks to the bacterial growth, increased, thus causing a gradual de-protonation of the polyaniline and resulting in the change of color. As an example, for *E. coli* and *S. aureus*, the pH increased from 6.9 to 8.3 and from 6.6 to 7.5, respectively.

3.3. Cytotoxicity

The results of *in-vitro* cytotoxicity testing are reported in two ways: (1) as mean values and standard deviations of individual measurements with the statistical differences compared to the reference, determined by a *t*-test; and (2) according to the procedure given in the international standard ISO 10993-5, where a cytotoxicity equal to 1 corresponds to 100% cell survival, values of >0.8 are assigned to the absence of cytotoxicity, 0.6–0.8 to mild, 0.4–0.6 to moderate and <0.4 to severe cytotoxicity (Table 2). The results show that with an increasing concentration of colloidal polyaniline in the cultivation media, the viability of cells decreased. The threshold polyaniline concentration for cytotoxicity is about 345 and 105 μg mL^{-1} in the case of HaCaT and NIH/3T3 cells, respectively. Below these concentrations, the colloidal polyaniline does not negatively influence the cells viability. Analogous results were published in the work of Oh et al. [35], who tested the cytotoxicity of polyaniline in the form of nanoparticles with poly(*N*-vinylpyrrolidone) as a stabilizer, and a non-spherical shape differing in aspect ratio. The authors did not observe any notable impact on cell viability below the polyaniline concentration of 25 μg mL^{-1}, and significant decreasing in cell viability was first detected above the concentration of 100 μg mL^{-1}. From the current results recorded on both cell lines, it can be concluded that the HaCaT cell line is more resistant toward the cytotoxic action of colloidal polyaniline and even above the threshold concentration, the cytotoxic effect is only mild in regard to the ISO standard scale. More sensitive NIH/3T3 cells, which are widely used for cytotoxicity evaluation, were damaged to a greater extent at higher concentrations of colloidal polyaniline in the cultivation medium, and the cytotoxic effect, at the two highest concentrations of 345 and 520 μg mL^{-1} upon this cell line, can be described as severe.

Microscopic observations of HaCaT cells (Fig. 1) support the previously discussed results demonstrating the changes in cell quantity and morphology induced by polyaniline dispersion. At the concentration of 70 μg mL^{-1}, only rare and negligible cell damage can be observed, which is visualized in red circles. An increase of polyaniline concentration to 345 μg mL^{-1} undoubtedly influenced cell viability via decreasing cell numbers and simultaneous changes to their morphology. This is especially notable after DNA staining.

Interesting conclusions can be drawn from a comparison of the current results with the report of Vaitkuviene et al. [36], who studied the effect of polypyrrole nanoparticles on cell viability. Primarily mouse embryonic fibroblasts (MEF), mouse hepatoma (MH-22A) cells, and human Jurkat T lymphocytes were used in their work. Although polypyrrole is generally considered to be a biocompatible polymer, the level of cytotoxicity was of 77.6 μg mL^{-1}, and in the case of one of the studied cell lines, Jurkat cells, even of 19.4 μg mL^{-1}. The authors also described the dose- and cell line-dependent cytotoxic effects. The average diameter of polypyrrole particles was of 28 nm. This might explain these surprising differences because the size of the particles, considered as one of the most important factors influencing the biological properties of materials, lies well below the limit of 100 nm, which is

Table 2
Cytotoxicity and apoptotic/necrotic rates of various concentrations of colloidal polyaniline reported as means ± standard deviations (SD) ($n = 4$) according to requirements of ISO 10993-5.

Polyaniline [μg mL^{-1}]	HaCaT		NIH/3T3		Apoptotic/necrotic rate on NIH/3T3		
	Mean ± SD	ISO	Mean ± SD	ISO	Necrotic (%)	Apoptotic (%)	Healthy (%)
520	0.409 ± 0.032**	0.61	0.227 ± 0.008*	0.36	24	54	22
345	0.446 ± 0.045**	0.67	0.220 ± 0.005*	0.34	19	57	24
170	0.579 ± 0.056	0.86	0.428 ± 0.012*	0.67	12	36	52
155	0.632 ± 0.043	0.94	0.374 ± 0.022*	0.58	11	16	73
130	0.651 ± 0.037	0.97	0.413 ± 0.012*	0.65	13	19	68
105	0.663 ± 0.029	0.99	0.499 ± 0.006*	0.78	12	8	80
35	0.660 ± 0.049	0.99	0.529 ± 0.008*	0.83	12	21	67
20	0.672 ± 0.015	1.00	0.528 ± 0.006*	0.83	16	14	70
Reference	0.666 ± 0.061	1.00	0.639 ± 0.025	1.00	9	16	75

According to requirements of ISO 10993-5: cytotoxicity equal to 1 corresponds to 100% cell survival, values of >0.8 are assigned to no cytotoxicity, 0.6–0.8 mild cytotoxicity, 0.4–0.6 moderate toxicity, and <0.4 severe cytotoxicity.

* $P < 0.05$, statistical difference between the reference and individual concentration of polyaniline.

** $P \leq 0.01$, statistical difference between the reference and individual concentration of polyaniline.

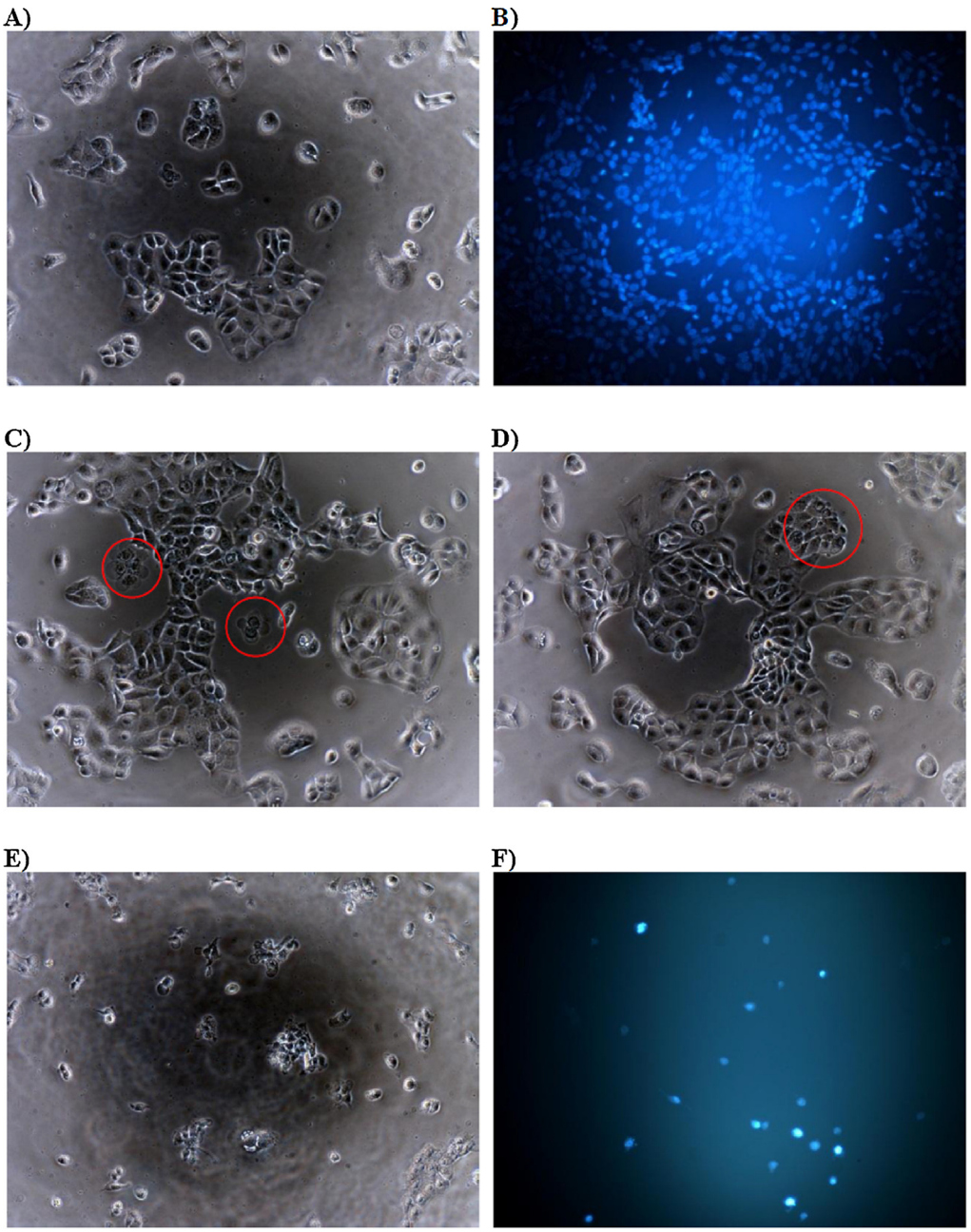

Fig. 1. Microphotographs of HaCaT cell line after the cytotoxicity test: (A) reference; (B) reference – DNA stained by Hoechst; cells treated with (C) 70 μg mL^{-1} colloidal polyaniline; (D) 130 μg mL^{-1} colloidal polyaniline; (E) 345 μg mL^{-1} colloidal polyaniline; (F) 345 μg mL^{-1} colloidal polyaniline – DNA stained by Hoechst. Magnification – 100×.

considered critical for entering the particular material into the cells.

Unfortunately, the cytotoxicity data recorded on colloidal polyaniline are incomparable to the cytotoxicity of standard polyaniline powder, as the testing methodologies are completely different. The cytotoxicity testing of polyaniline in powder form was performed only by Humpolicek et al. [6], who tested an extract (0.2 g of polyaniline in 1 mL of cultivation medium) according to ISO 10993-5. Here, the polyaniline polymer was absent, and the cytotoxicity was mainly assigned to the presence of residual monomers and low-molar mass oligomers present in the extract. Thanks to purification through dialysis, the colloidal dispersion should be free of these impurities, and its cytotoxicity should likely be a result of the polyaniline polymer as such, and not the low-molecular-weight substances.

3.4. Apoptosis versus necrosis rate

The cytotoxicity determined by MTT assay represents the total number of viable cells surviving contact with the cytotoxic substance. It does not reveal, however, the reason why the viability is decreasing. Moreover, as the MTT assay is based on the mitochondrial metabolism, which is also expressed by early apoptotic cells, the test does not distinguish between early apoptotic and healthy cells. Thus, the combination of MTT assay with the annexin/propidium iodide assay can provide a more informative view on the impact of tested materials on the cells. In the case of colloidal polyaniline, the number of healthy, necrotic and apoptotic cells was observed to be dose dependent, and the impact of colloidal polyaniline on each of the groups can be clearly seen (Table 2). According to the annexin/propidium iodide assay, the

Table 3
Neutrophils activation measured as ROS production.

Polyaniline [μg mL^{-1}]	0.00171	0.0171	0.171	1.71	17.1	171
Blood	99.97 ± 3.16	100.71 ± 0.01	98.93 ± 0.94	98.17 ± 1.04	96.10 ± 0.27	98.05 ± 3.58
Neutrophils extracellular	89.14 ± 6.12	89.38 ± 8.52	82.29 ± 11.56	65.02 ± 9.06*	62.22 ± 10.50*	61.07 ± 9.09*
Neutrophils intracellular	101.84 ± 1.10	101.90 ± 0.49	100.37 ± 3.22	97.13 ± 0.44	95.99 ± 4.46	95.66 ± 2.23

The results are shown as % of spontaneously formed ROS = 100% (reference). The values are expressed as mean value ± standard deviation, $n = 3$.
* $P < 0.05$.

Table 4
Polyaniline scavenging of ROS (where neutrophils ROS production was initiated by PMA).

Polyaniline [μg mL^{-1}]	0.00171	0.0171	0.171	1.71	17.1	171
Cell-free assay	96.0 ± 3.4	94.1 ± 5.4	95.6 ± 2.5	75.9 ± 1.5*	6.4 ± 1.6*	0.0 ± 0.00*
Blood	104.4 ± 4.1	105.5 ± 1.3	95.6 ± 6.2	66.7 ± 4.2*	2.8 ± 1.0*	0.0 ± 0.0*
Neutrophils extracellular	108.2 ± 5.1	107.8 ± 4.5	99.4 ± 6.3	52.1 ± 4.2*	0.0 ± 0.0*	0.0 ± 0.0*
Neutrophils intracellular	114.3 ± 12.7	117.7 ± 10.3	113.0 ± 13.1	96.6 ± 3.8	23.2 ± 5.3*	0.0 ± 0.0*

The effects of colloid on ROS production in a cell-free assay as well as in blood and isolated neutrophils. The results are shown as a % of stimulated control where H_2O_2 and PMA stimulated samples = 100% (reference). The values are expressed as mean value ± standard deviation, $n = 3$.
* $P < 0.01$.

cytotoxicity threshold is of around 150 μg mL^{-1} and is higher than the limit of 105 μg mL^{-1} determined according to MTT. Below this concentration, the number of healthy cells increases and the number of apoptotic cells dramatically decreases. Due to the aforementioned differences between the MTT and annexin/propidium assays, the concentration of 150 μg mL^{-1} seems to be more relevant for potential applications of colloidal polyaniline in biomedicine.

3.5. Suppression of oxidative burst in human neutrophils

Neutrophil leucocytes represent professional phagocytic cells. When appropriately stimulated, they undergo dramatic physiological and biochemical changes resulting in phagocytosis, chemotaxis and degranulation with the activation of ROS production, known as the respiratory burst [37]. Neutrophils work as professional killers and instructors of the immune system in the context of infection and inflammatory diseases. Thus, the investigation of their reactions is an important part of biocompatibility studies.

At first, the effect of colloidal polyaniline on the activation of neutrophils was measured by monitoring ROS generation. The amount of formed ROS was then compared with the spontaneous (not induced) chemiluminescence of neutrophils. The results revealed that ROS were absent, and therefore colloidal polyaniline alone did not cause the neutrophil activation (Table 3). However, the measurements of extracellular chemiluminescence indicated that colloidal polyaniline, at concentrations of 171, 17 and 1.71 μg mL^{-1}, was able to work as an ROS scavenger. The cell-free assay also showed that the scavenging effect of polyaniline colloid toward ROS, generated in a cell-free system of luminol–hydrogen peroxide–peroxidase, is concentration dependent. Namely, the concentrations of 171, 17 and 1.7 μg mL^{-1} significantly decreased the ROS content, while the lower tested concentrations were inefficient. Based on these results, a second test was performed on whole blood and isolated neutrophils, in which ROS formation was stimulated with PMA prior to colloidal polyaniline addition (Table 4). Correspondingly to the cell-free assay, the significant scavenging effect of polyaniline colloid toward ROS generated by PMA-stimulated neutrophils was observed in concentrations of 171 and 17 μg mL^{-1}.

To disclose whether the polyaniline colloid can influence intra or extracellular ROS production, an additional experiment was conducted resulting in the conclusion that in isolated neutrophils stimulated with PMA, colloidal polyaniline inhibited both extracellular and intracellular ROS production. Polyaniline was, however, more efficient in the inhibition of extracellular ROS. The inhibition of both extra- and intracellular ROS production initiated with polyaniline correlated with its effects on ROS, determined in the cell-free assay. It can be therefore suggested that the influence of colloidal polyaniline on ROS occurrence in whole blood or isolated neutrophils arise due to the ROS scavenging properties. In the context of the cytotoxicity results recorded on an annexin/propidium assay, the critical concentration of colloidal polyaniline for biologically safe application is 150 μg mL^{-1}, which is also an un-provoking concentration for the neutrophil activity.

4. Conclusions

Aqueous dispersions of colloidal polyaniline can be included among the promising conducting and electroactive systems, possessing advantageous properties for biomedical applications. The information on its fundamental biological characteristics is presented here for the first time. The summary results from the study show that polyaniline colloid demonstrates a low antibacterial activity with the most susceptible bacterial species being *B. cereus* and *E. coli*, which were both inhibited with a colloid concentration of 3500 μg mL^{-1}. In the context of the cytotoxicity results recorded on an MTT assay, the toxic effect of this system was found to be dose- and cell-line dependent; more sensitive NIH/3T3 cells were damaged to a higher extent compared with HaCaT cells. Flow-cytometry data recorded on an annexin/propidium assay, capable of distinguishing healthy, apoptotic and necrotic cells after polyaniline treatment, indicated that the critical colloid concentration for biologically safe applications is of 150 μg mL^{-1}. This is also an un-provoking concentration limit for neutrophil activity, measured through the detection of reactive oxygen species. The combination and mutual assessment of obtained results suggests that the conducting polyaniline colloid possesses low cytotoxicity and the absence of an oxidative burst, however a weak antibacterial performance should be considered a known limitation.

Acknowledgements

Financial support of the Czech Science Foundation (13-08944S) is gratefully acknowledged. One of us (Tomas Perecko) also appreciates the support of the grant OPVK CZ.1.07/2.3.00/30.0030.

References

[1] C.W. Hsiao, M.Y. Bai, Y. Chang, M.F. Chung, T.Y. Lee, C.T. Wu, B. Maiti, Z.X. Liao, R.K. Li, H.W. Sung, Biomaterials 34 (2013) 1063–1072.
[2] S.H. Ku, S.H. Lee, C.B. Park, Biomaterials 33 (2012) 6098–6104.

[3] E.A. Ostrakhovitch, J.C. Byers, K.D. O'Neil, O.A. Semenikhin, Arch. Biochem. Biophys. 528 (2012) 21–31.
[4] M.C. Chen, Y.C. Sun, Y.H. Chen, Acta Biomater. 9 (2013) 5562–5572.
[5] R.M. Moura, A.A. de Queiroz, Artif. Organs 35 (2011) 471–477.
[6] P. Humpolicek, V. Kasparkova, P. Sáha, J. Stejskal, Synth. Met. 162 (2012) 722–727.
[7] P. Humpolicek, V. Kasparkova, J. Stejskal, Z. Kucekova, P. Sevcikova, Chem. Listy 106 (2012) 380–383.
[8] D.T. Seshadri, N.V. Bhat, Indian J. Fibre Text. 30 (2005) 204–206.
[9] N. Shi, X. Guo, H. Jing, J. Gong, C. Sun, K. Yang, J. Mater. Sci. Technol. 22 (2006) 289–290.
[10] Z. Kucekova, V. Kasparkova, P. Humpolicek, P. Sevcikova, J. Stejskal, Chem. Pap. 67 (2013) 1103–1108.
[11] J. Stejskal, R.G. Gilbert, Pure Appl. Chem. 75 (2002) 857–867.
[12] S. Liu, J.Q. Wang, D. Zhang, P. Zhang, J. Ou, B. Liu, S. Yang, Appl. Surf. Sci. 256 (2010) 3427–3431.
[13] E.G.R. Fernandes, V. Zucolotto, A.A. De Queiroz, J. Macromol. Sci. A: Pure Appl. Chem. 47 (2010) 1203–1207.
[14] K.D. McKeon, A. Lewis, J.W. Freeman, J. Appl. Polym. Sci. 115 (2010) 1566–1572.
[15] J.Y. Bergeron, L.H. Dao, Macromolecules 25 (1992) 3332–3337.
[16] J. Guay, R. Paynter, L.H. Dao, Macromolecules 23 (1990) 3598–3605.
[17] J. Stejskal, P. Kratochvíl, N. Gospodinova, L. Terlemezyan, P. Mokreva, Polymer 33 (1992) 4857–4858.
[18] J. Stejskal, P. Kratochvíl, N. Radhakrishnan, Synth. Met. 61 (1993) 225–231.
[19] P. Banerjee, S.N. Bhattacharyya, B.M. Mandal, Langmuir 11 (1995) 2414–2418.
[20] P.C. Innis, I.D. Norris, L.A.P. Kane-Maguire, G.G. Wallace, Macromolecules 31 (1998) 6521–6528.
[21] D. Chattopadhyay, B.M. Mandal, Langmuir 12 (1996) 1585–1588.
[22] D. Chattopadhyay, S. Banerjee, I. Chakravorty, B.M. Mandal, Langmuir 14 (1998) 1544–1547.
[23] D. Chattopadhyay, M. Chakravorty, B.M. Mandal, Polym. Int. 50 (2001) 538–544.
[24] J. Stejskal, P. Kratochvíl, M. Helmstedt, Langmuir 12 (1996) 3389–3392.
[25] A. Riede, M. Helmstedt, V. Riede, J. Stejskal, Langmuir 14 (1998) 6767–6771.
[26] H. Eisazadeh, G. Spinks, G.G. Wallace, Polym. Int. 37 (1995) 87–91.
[27] J. Stejskal, J. Polym. Mater. 18 (2001) 225–258.
[28] S.P. Armes, in: T.A. Skotheim, R.L. Elsenbaumer, J.R. Reynolds (Eds.), Handbook of Conducting Polymers, 2nd ed., Marcel Dekker, Inc., New York, 1998 (Chapter 17).
[29] B. Wessling, Synth. Met. 93 (1998) 143–154.
[30] J. Stejskal, I. Sapurina, Pure Appl. Chem. 77 (2005) 815–826.
[31] P. Boukamp, R. Petrussevska, D. Breitkreutz, J. Hornung, A. Markham, J. Cell Biol. 106 (1988) 761–771.
[32] V. Jančinová, T. Perečko, R. Nosál', J. Harmatha, J. Smidrkal, K. Drábiková, Acta Pharmacol. Sin. 33 (2012) 1285–1292.
[33] M. Banasova, V. Sasinkova, R. Mendichi, T. Perecko, K. Valachova, I. Juranek, L. Soltes, Neuroendocrinol. Lett. 33 (2012) 151–154.
[34] M.R. Gizdavic-Nikolaidis, J.R. Bennett, S. Swift, A.J. Easteal, M. Ambrose, Acta Biomater. 7 (2011) 4204–4209.
[35] W.K. Oh, S. Kim, O. Kwon, J. Jang, J. Nanosci. Nanotechnol. 11 (2011) 4254–4260.
[36] A. Vaitkuviene, V. Kaseta, J. Voronovic, G. Ramanauskaite, G. Biziuleviciene, A. Ramanaviciene, A. Ramanavicius, J. Hazard. Mater. 250–251 (2013) 167–174.
[37] V. Witko-Sarsat, P. Rieu, B. Descamps-Latscha, P. Lesavre, L. Halbwachs-Mecarelli, Lab. Invest. 80 (2000) 617–653.

Article VI.

Kasparkova, V.; Jasenska, D.; **Capakova, Z**.; Marakova, N.; Stejskal, J.; Bober, P.; Lehocky, M.; Humpolicek, P. Polyaniline Colloids Stabilized with Bioactive Polysaccharides: Non-Cytotoxic Antibacterial Materials. Carbohydr. Polym. 2019, 219, 423–430. https://doi.org/10.1016/j.carbpol.2019.05.038.

Carbohydrate Polymers 219 (2019) 423–430

Contents lists available at ScienceDirect

Carbohydrate Polymers

journal homepage: www.elsevier.com/locate/carbpol

Polyaniline colloids stabilized with bioactive polysaccharides: Non-cytotoxic antibacterial materials

Věra Kašpárková[a,b], Daniela Jasenská[a], Zdenka Capáková[a], Nela Maráková[a], Jaroslav Stejskal[c], Patrycja Bober[c], Marián Lehocký[a,b], Petr Humpolíček[a,b,*]

[a] Centre of Polymer Systems, Tomas Bata University in Zlin, 760 01 Zlin, Czech Republic
[b] Tomas Bata University in Zlin, Faculty of Technology, 760 01 Zlin, Czech Republic
[c] Institute of Macromolecular Chemistry, Academy of Sciences of the Czech Republic, 162 06 Prague 6, Czech Republic

ARTICLE INFO

Keywords:
Sodium hyaluronate
Chitosan
Colloid
Polyaniline
Antibacterial effect
Cytotoxicity

ABSTRACT

Colloidal polyaniline dispersions stabilized with biocompatible polysaccharides, sodium hyaluronate and chitosan (both with two different molecular weights), were successfully formulated. The colloids were characterized by UV–vis spectra, particle-size distributions and morphology, as well as by their biological properties in terms of cytotoxicity and antibacterial activity. Colloids containing both chitosan and hyaluronate showed only mild cytotoxicities, which were mainly governed by the concentration of conducting polyaniline in the colloid. Antibacterial activity of the samples, however, depended both on the type of polysaccharide and the ratio between the stabilizer and polyaniline mass. The colloid synthetized using 0.2 M aniline hydrochloride, 0.1 M ammonium persulfate, and 1 wt.% sodium hyaluronate of molecular weight of 1.8–2.1 × 10^6 exhibited the highest antibacterial activity against both gram positive and gram negative bacteria. This formulation, therefore, allowed for the formation of potentially stimuli-responsive antibacterial colloidal particles with low cytotoxicity.

1. Introduction

Polyaniline (PANI) belongs to the family of conducting polymers advantageously combining the properties of classical polymer materials with those of organic semiconductors. This polymer is well known for its attractive properties, including simple straightforward synthesis, mixed electron and ionic conductivity, environmental stability, and the ability to undergo salt–base transition resulting to redox switching (Stejskal et al., 2015). These properties make PANI advantageous for various biological applications, mainly for tissue engineering directed towards cells and tissues responding to electric stimuli, and for biosensors (Jiang et al., 2015; Jun et al., 2015; Mazrad et al., 2017; Park et al., 2016; Zhang & Choi, 2014). Standard PANI is prepared by the oxidation of aniline with ammonium persulfate in acidic aqueous medium. With no stabilizer added to the reaction mixture used for the polymerization, PANI precipitates as an insoluble powder, which is difficult to process (Stejskal & Gilbert, 2002). To avoid this shortcoming, aniline polymerization can be carried out in the presence of a suitable stabilizer, such as water-soluble polymer, which produces colloidal PANI particles in the form of aqueous dispersion (Stejskal & Sapurina, 2005). Several synthetic water-soluble polymers, such as poly(vinyl alcohol) (PVAL) (Chakraborty et al., 2000; Stejskal et al., 1996), poly(*N*-vinylpyrrolidone) (PVP) (Ghosh et al., 1999), and poly(ethylene oxide) (Eisazadeh et al., 1995), have been used as steric stabilizers. So far, however, only a few biomacromolecules, such as cellulose derivatives (Chattopadhyay et al., 1998; Stejskal et al., 1999), proteins (Eisazadeh et al., 1995), or gelatin (Bober et al., 2017), have been exploited for the synthesis of colloidal PANI. With respect to biological applications, polysaccharides, particularly sodium hyaluronate and chitosan, are promising candidates as colloid stabilizers, as they are both biodegradable and exhibit certain types of biological activity.

Sodium hyaluronate (HA) is one of the most remarkable biomacromolecules. It is formed by linear polysaccharide chains consisting of repeating units of *N*-acetyl-*D*-glucosamine and *D*-glucuronic acid linked by β-(1,4) and β-(1,3) glycosidic bonds. As an endogeneous substance, it is present in different tissues of living organism and plays a key role in numerous biochemical and cellular processes involving, among others, the attachment, migration, and proliferation of cells. HA has therefore became an attractive component of biocompatible and biodegradable systems with potential applications in tissue engineering (Collins & Birkinshaw, 2013; Prestwich, 2011). Recently, the following interesting formulation involving nanoparticles composed of hyaluronic acid and PANI have emerged. Jiang et al. (2015) prepared water-soluble hyaluronic acid-hybridized nanoparticles for phototherapy, these showing targeted specificity against CD44 mediated cancer cells. The prepared

* Corresponding author.
E-mail address: humpolicek@utb.cz (P. Humpolíček).

https://doi.org/10.1016/j.carbpol.2019.05.038
Received 29 November 2018; Received in revised form 27 February 2019; Accepted 10 May 2019
Available online 11 May 2019
0144-8617/

nanoparticles exhibited low cytotoxicity *in vitro*, and were able to selectively kill cancer cells of HeLa and HCT-116 cells rather than normal HFF cells upon exposure to a NIR 808 nm laser.

A second polysaccharide with a broad potential for application in biomedicine is chitosan, a copolymer of *D*-glucosamine and *N*-acetyl-*D*-glucosamine (Foster et al., 2015; Wang et al., 2016). Chitosan is a cationic polyelectrolyte with a number of advantageous properties, including antibacterial activity (Ozkan & Sasmazel, 2018), haemostatic properties (Jayakumar et al. 2011; Muzzarelli, 2009), and the ability to stimulate wound healing in tissues (Berce et al., 2018; Lu et al., 2017). Currently, a broad range of devices and products based on chitosan are available, including those based on particles and nanoparticles (Chaudhury & Das, 2011; Ali & Ahmed, 2018; Hussein-Al-Ali et al., 2018). Previously, Cruz-Silva et al. (2007) reported the use of chitosan as a steric stabilizer for the synthesis of PANI colloids. In that work, the authors prepared PANI colloids using the enzymatic polymerization of aniline with soybean peroxidase and *p*-toluenesulfonic or camphorsulfonic acids as dopants. Interestingly, the prepared colloidal particles had strong pH-dependent colloidal stability and underwent rapid flocculation in near-neutral or alkaline media.

Though certain applications of PANI/polysaccharide colloids can be found in the literature, their fundamental properties have yet to be fully clarified. Therefore, the objective of this study was to contribute to a more detailed investigation of these promising systems and to formulate colloidal PANI dispersions with enhanced bioavailability based on each of the two above-mentioned polysaccharides. This approach offers the possibility to advantageously combine biodegradable and biocompatible polymers with PANI, the latter possessing both ionic and electronic conductivity, which is advantageous in biomedical applications. In present study, the colloids were prepared by means of the oxidative polymerization of aniline hydrochloride with ammonium persulfate in the presence of each stabilizer, with various ratios of reactants in the reaction mixture. The resulting colloidal dispersions were characterized with respect to their physico-chemical properties (UV–vis spectra, size distribution, and the stability of colloidal particles) and biocompatibility. The biological properties in terms of cytotoxicity to mouse embryonic fibroblast cells were determined together with the antimicrobial efficacy of the formulated colloids against the most common spoilage pathogens *S. aureus* and *E. coli*.

2. Materials and methods

2.1. Materials

Reagent-grade aniline hydrochloride (≥98%) and ammonium persulfate (98%) were purchased from Sigma Aldrich (Germany). Sodium hyaluronate (HA-A; molecular weight 1.8–2.1 × 10^6 and HA-B; molecular weight 50,000) was purchased from Contipro a.s. (Czech Republic). Chitosan, labelled by the supplier as "average molecular weight" (CH-A; molecular weight ˜ 400,000, deacetylation degree of 75–85%) or "low molecular weight" (CH-B; molecular weigh 50–190,000, deacetylation degree ≥75%) was purchased from Sigma Aldrich (Germany).

2.2. Preparation of colloidal polyaniline dispersions

Colloidal PANI was prepared *via* the oxidation of aniline hydrochloride with ammonium persulfate (APS) in the presence of each of the above-mentioned polymer stabilizers (Scheme 1). The solution of the stabilizing sodium hyaluronate was prepared by the dissolution of polymer in demineralized water; corresponding chitosan was dissolved in 1 M aqueous hydrochloric acid. In both cases, the dissolution was carried out under stirring at 55 °C overnight. Chitosan solutions were then filtered to remove any non-dissolved polymer residue.

For dispersion polymerization, aniline hydrochloride was dissolved in 5 mL of the respective polymer solution. Polymerization was started at temperature of 23 ± 2 °C by adding 5 mL of aqueous solution APS to the reaction mixture (Table 1). The mixture was stirred for 10 min and then left at rest to polymerize. Polymerization was completed within 24 h. In order to remove residual monomers and low-molecular-weight impurities, colloidal dispersions were purified through exhaustive dialysis using Spectra Por 2 dialysis tubing (molecular weight cut-off 12,000–14,000; Spectrum Laboratories Inc., USA). Prior to dialysis, the membrane was soaked in demineralized water for 30 min to remove membrane preservatives and then thoroughly rinsed in water. PANI colloid (10 mL) was pipetted into the tubing and transferred into beaker containing 800 mL of 0.2 M hydrochloric acid solution, which was daily exchanged for period of 14 days.

2.3. Physico-chemical characterization

The course of aniline polymerization was monitored by absorption spectra recorded on the respective reaction mixture in the wavelength range 200–800 nm using a Photo Lab 6600 UV–vis spectrometer (WTW, Germany). Initially, spectra were taken at ten minute intervals; later, the intervals were prolonged, and spectra were recorded after 1, 2, 4, 8, and 24 h from the start of the reaction. For the analysis, 60 µL aliquots were sampled from the reaction mixture and added to 3 mL of 1 M hydrochloric acid in a quartz cuvette.

After dialysis, UV–vis spectra of PANI dispersions were also

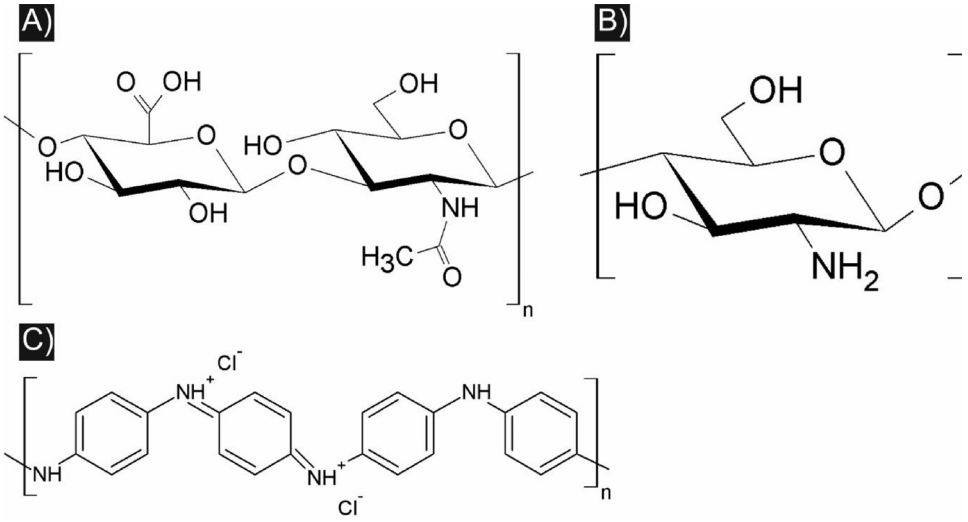

Scheme 1. Structural formulae of A) sodium hyaluronate, B) chitosan, and C) polyaniline.

Table 1
Compositions of the reaction mixtures used for the preparation of colloids stabilized with sodium hyaluronate and chitosan *via* the oxidation of aniline hydrochloride with ammonium persulfate[a].

Sample	Stabilizer [wt.%]	Aniline hydrochloride [M]	APS [M]
HA-A1*	1.0	0.2	0.1
HA-A2*	1.0	0.2	0.05
HA-A3	1.0	0.2	0.01
HA-B1	2.0	0.2	0.1
HA-B2*	2.0	0.2	0.05
HA-B3	2.0	0.2	0.01
CH-A1	2.0	0.2	0.05
CH-A2*	2.0	0.2	0.01
CH-A3	2.0	0.1	0.05
CH-A4*	2.0	0.1	0.01
CH-B1	2.0	0.2	0.05
CH-B2	2.0	0.2	0.01
CH-B3	2.0	0.1	0.05
CH-B4	2.0	0.1	0.01

[a] Only the colloids marked with an asterisk have been subsequently physicochemically characterized.

recorded with the aim of determining the concentration of PANI in the colloidal dispersion. This data was required for testing the biological properties of samples. The concentration of PANI in each of the dispersions was calculated from the local maximum of absorbance at wavelength of 395 nm using the Lambert-Beer law, $A = \varepsilon cl$, where $\varepsilon = 31{,}500 \pm 1700\ \mathrm{cm^2\,g^{-1}}$ is the absorption coefficient (Stejskal et al., 1993), c is the concentration of PANI, and $l = 1$ cm is the optical path.

The particle sizes were determined on freshly prepared samples by dynamic light scattering (DLS) using a Zetasizer Nano ZS instrument (Malvern Instrument, UK). Measurements of the hydrodynamic radii of colloidal particles, expressed as *z*-average particle diameters (D_z), were performed at 25 °C. The intensity of scattered light was observed at a scattering angle of 173°. The polydispersity index (PDI) describing the width of the particle-size distribution was also determined. Samples were prepared for measurement by diluting 10 µL of freshly prepared dispersion in 1 mL of 0.1 M hydrochloric acid. The particle size and distribution were verified on dialysed samples using the same procedure.

The morphology of colloidal particles was assessed with a transmission electron microscope (TEM) JEOL JEM 2000 FX (Japan).

2.4. Antibacterial properties

The antibacterial properties of colloidal PANI with biopolymers were determined using the gram-positive and gram-negative bacterial strains, *Staphylococcus aureus* CCM 4516 and *Escherichia coli* CCM 4517 (Czech Collection of Microorganisms). Bacterial suspensions were prepared by diluting bacterial strains with Mueller-Hinton broth (MHB). The density of bacterial suspensions was adjusted to 0.5 ° of McFarland standard ($1–2 \times 10^8$ CFU $\mathrm{mL^{-1}}$). Bacteria were grown on Trypton Soya Agar (HiMedia, India) at 37 °C for 24 h. The assessment of antibacterial activity was based on the determination of the minimum inhibitory concentration (MIC). The colloidal PANI dispersion was diluted with distilled water to the required concentrations and inoculated with 2 mL of bacterial suspension. The samples were incubated at 37 °C for 24 h and then 100 µL of sample was spread over agar plate surfaces and incubated at 37 °C. After 24 h of incubation, the MIC was determined. Each experiment was conducted twice.

2.5. Cytotoxicity

Cytotoxicity testing was performed with a mouse embryonic fibroblast cell line (ATCC CRL-1658 NIH/3T3, USA). The NIH/3T3 cells were cultivated using ATCC-formulated Dulbecco's Modified Eagle's Medium (catalog No. 30-2002) with added bovine calf serum to a final concentration of 10% and penicillin/streptomycin with a concentration of 100 U $\mathrm{mL^{-1}}$. Cells were pre-cultivated for 24 h at 37 °C under a 5% CO_2 atmosphere in a HERAcell 150i incubator (Thermo Scientific, USA), and the culture medium was subsequently replaced with dilutions of PANI colloid. Cells cultivated in pure medium without colloid were used as a reference. The effect of the tested colloidal dispersion on the growth and viability of NIH/3T3 cells was examined after one day of cell cultivation in the presence of colloid. The assessment of cytotoxic effects was performed using the MTT assay (Invitrogen Corporation, USA). All tests were performed in quadruplicates. Absorption was measured at 570 nm with an Infinite M200 Pro NanoQuant (Tecan, Switzerland). Dixon's Q test was used to remove outlying values, and mean values were calculated. The cytotoxic effect was evaluated according to the procedure provided by international standard EN ISO 10993-5 *via* the scaling of cell viability after the application of test substances for 24 h. Assuming that the cell viability of the reference sample was 100%, a viability higher than 80% was rated as the absence of cytotoxicity, a viability of between 80% and 60% to mild cytotoxicity, a viability of between 60 and 40% to moderate cytotoxicity, and a viability of below 40% to severe cytotoxicity.

3. Results and discussion

3.1. Particle sizes

The preparation of polysaccharide-based PANI colloids was carried out using a modified protocol for the synthesis of colloidal PANI stabilized with PVP (Stejskal & Sapurina, 2005). Commonly, a 2 wt.% concentration of stabilizing polymer was used during synthesis; however, in the case of HA with a molecular weight of between 1.8 and 2.1×10^6, only a 1% solution was employed, as HA is known to form highly viscous gel-like solutions at concentrations above 1 wt.%. Concentrations of chitosan in the reaction mixture were kept at the usual level of 2 wt.% during synthesis. Two different concentrations of HA and three different concentrations of APS were employed (Table 1).

DLS analyses as well as visual inspection revealed that HA-based samples synthetized with 0.1 and 0.05 M APS were of colloidal character, irrespective of the molecular weight of polymer used. The colloidal particles, however, had different sizes (Table 2) and, not surprisingly, the lower-molecular-weight HA afforded colloidal particles with smaller diameters. In samples stabilized with lower-molecular-weight polymer (HA-B3) polymerized with 0.01 M APS, typical colloidal particles did not arise, and PANI precipitated. The sample HA-A3 then formed a thick gel structure, which can be explained by the combination of the high molecular weight of the polymer and the low concentration of the oxidant.

Depending on the composition of the reaction mixture, PANI colloids prepared in the presence of chitosan of "average" molecular weight (CH-A) contained particles with sizes ranging from 376 to

Table 2
Size (*z*-average particle diameter $D_z \pm$ SD) and polydispersity index (PDI ± SD) of colloidal particles prepared by the oxidation of aniline hydrochloride (AH) with ammonium persulfate (APS) in the presence of HA.

	After preparation		After six months	
Sample	D_z [nm]	PDI	D_z [nm]	PDI
HA-A1	1,100 ± 15	0.45 ± 0.011	1,393 ± 14	0.47 ± 0.008
HA-A2	655 ± 2	0.35 ± 0.014	741 ± 5	0.30 ± 0.007
HA-A3	The highly viscous gel-like product was formed			
HA-B1	485 ± 1	0.20 ± 0.003	638 ± 2	0.25 ± 0.003
HA-B2	574 ± 5	0.28 ± 0.001	489 ± 2	0.16 ± 0.006
HA-B3	PANI powder was formed		4,300 ± 81	0.35 ± 0.034

Table 3
Size (z-average particle diameter $D_z \pm$ SD) and polydispersity index (PDI ± SD) of colloidal particles prepared by the oxidation of aniline hydrochloride (AH) with ammonium persulfate (APS) in the presence of chitosan (CH-A average molecular weight, CH-B low molecular weight).

	After preparation		After six months	
Sample	D_z [nm]	PDI	D_z [nm]	PDI
CH-A1	1,332 ± 2	0.44 ± 0.020	920 ± 2	0.55 ± 0.011
CH-A2	512 ± 2	0.39 ± 0.001	356 ± 2	0.22 ± 0.004
CH-A3	753 ± 9	0.36 ± 0.004	530 ± 4	0.33 ± 0.008
CH-A4	376 ± 0	0.26 ± 0.004	481 ± 2	0.36 ± 0.013
CH-B1	*N/M*		1,102 ± 8	0.36 ± 0.011
CH-B2			662 ± 1	0.45 ± 0.007
CH-B3			*N/M*	
CH-B4			819 ± 13	0.47 ± 0.005

N/M: Not-measurable. The size of particles was out of measuring range of instrument (≈5 μm).

1330 nm and PDI ranging from 0.20 to 0.45 (Table 3). Colloids with the smallest particles were prepared with 0.01 M APS with both 0.2 and 0.1 M AH. Under these reaction conditions, the particles were of 376 ± 1 and 512 ± 2 nm in diameter for samples CH-A2 (0.2 M AH) and CH-A4 (0.1 M AH), respectively. Particle sizing analyses therefore lead to the conclusion that the size of colloidal particles is directly influenced by the ratio of AH to APS in the reaction mixture. In the contrast to these colloids, freshly prepared samples stabilized with low-molecular-weight chitosan (CH-B) were not of colloidal character and reactions resulted in the formation of unstable coarse particle dispersions with sedimentation occurring almost immediately after preparation.

The inability of polymers with low molecular weights to perform as stabilizers for the growth of colloidal PANI was previously observed by Cooper & Vincent (1989), who prepared and studied PANI colloid stabilized with poly(ethylene oxide). By using this polymer with a molecular weight above 10^6 g mol^{-1}, the polymerization reaction afforded colloidal particles; however, when the molecular weight was below 10^6 g mol^{-1}, the polymer lost its stabilizing function and PANI powder was prepared instead.

In the comparison with PVP-stabilized PANI colloid (average particle size 240 ± 50 nm, PDI 0.264 ± 0.116), which is the most studied and described conducting colloid (Stejskal and Sapurina, 2005), particles stabilized with both polysaccharides were bigger and also their size distributions were broader. However, for all prepared samples, the recorded distribution curves were monomodal, thus illustrating the formation of only one main population of particles in the sample.

The long-term stability of the prepared colloids was determined after 6 months storage at room temperature *via* the measurement of their particle sizes (Tables 2 and 3) and the obtained data evidenced that changes in particle sizes clearly depended on the composition of the reaction mixture and the used stabilizing polymer. However, a noteworthy variation in the colloidal behavior of samples was observed mainly for samples stabilized with chitosan of lower molecular weight (CH-B). Whilst immediately after preparation the sizes of colloidal particles were outside the measuring range of the Zeta sizer, the six months of storage at room temperature reduced these particle sizes, the measurement was possible and colloids with particles ranging from 660 to 1100 nm in size were obtained. Similar effect was also observed by Li et al. (2016) for polypyrrole colloid stabilized with PVP. In that case, colloidal particles decreased their sizes after 3 months of storage, and the effect was attributed to the disentanglement of some colloidal aggregates formed immediately after polymerization. This expectation could be supported by our own observations concerning chitosan-stabilized colloidal particles, whose sizes obviously decreased during the storage.

3.2. UV–vis spectroscopy

The course of colloid formation was monitored by UV–vis spectroscopy; corresponding spectra are compared in Fig. 1A and B (stabilization with HA) and Fig. 1C and D (stabilization with CH). From the spectra, it is obvious that the course of the reaction and the formation of

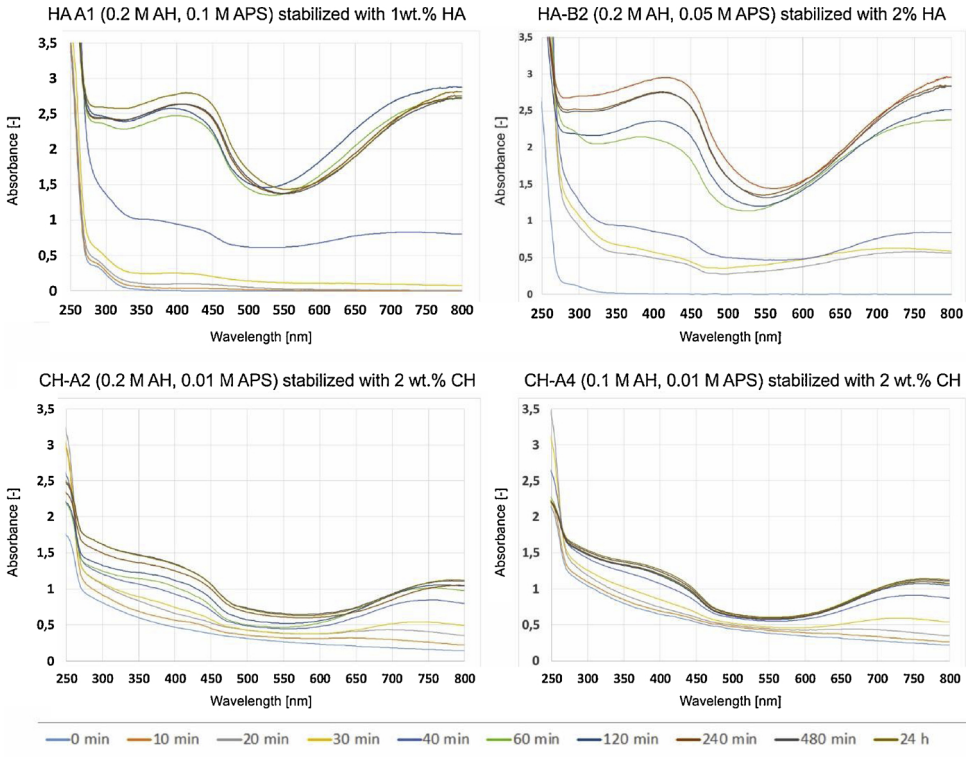

Fig. 1. The course of formation of colloidal PANI followed by the changes in UV–vis spectra.

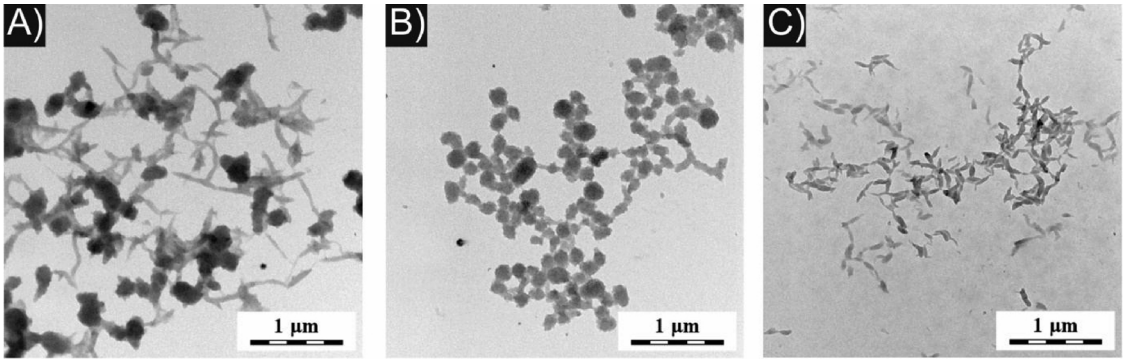

Fig. 2. Transmission electron micrographs of PANI colloids stabilized with sodium hyaluronate of A) lower molecular weight (HA-B), B) higher molecular weight (HA-A), and C) chitosan (CH-A).

the final product are controlled both by the type of stabilizing polymer and by the composition of the reaction mixture. The formation of a colloid stabilized with chitosan containing the higher concentration of aniline hydrochloride (0.2 M) proceeded uniformly with a gradual increase in absorbance over time. The lower concentration of AH in the reaction mixture (0.1 M) led to lower absorbance at the reaction end when compared with the previously described sample; however, almost identical spectra were recorded for reaction times of 240 min, 480 min, and 24 h. This may indicate the termination of the reaction occurring after 240 min, due to the depletion of reactants in the reaction mixture as lower than stechiometric amount of APS was used. In the case of HA stabilized colloids, in addition to the concentrations of AH and APS, the reaction course could also be influenced by the molecular weight of the polymer; however, the resulting colloids were, as for UV–vis spectra, identical.

In this context, the comparison of recorded spectra with spectra published for the most studied colloids stabilized with PVP and PVAL can be useful. The spectra of PVP-containing colloid are characterized by two maxima located at λ = 356 and 852 nm, when determined in 1 M HCl (Stejskal and Sapurina, 2005). Whilst the first absorption band arises from the π–π^* electron transition within the aromatic ring, the second is typical for presence of polaron states (charged cation radicals) and is assigned to $\pi-$polaron and polaron$-\pi^*$ transitions (Stejskal et al., 2015). With respect to the absorption spectra of colloidal PANI stabilized with PVAL, Stejskal et al. (1993) also reported on an absorption band at 430 nm which is often merged with the above-mentioned peak located at around 356 nm into a flat or distorted single peak and represents π–π^* transition. In comparison with these data, the recorded spectra from HA colloids (Fig. 1A and B) are more similar to those recorded for the mentioned PVAL-based colloid, exhibiting maxima at 430 and 800 nm. The maximum at about 356 nm is absent and a plateau is observed in the wavelength region from about 300–400 nm. Also, the maximum in the red region is less notable in comparison with PVP based samples. On the other hand, the spectrum recorded for CH colloids includes distinct maxima at 390 nm and 800 nm and is, therefore, more similar to spectra from samples containing PVP.

3.3. Morphology

The visualization of colloidal particles by transmission electron microscopy revealed their different morphologies (Fig. 2), and undoubtedly confirmed the influence of the polysaccharides on the shape and size of colloidal particles.

A typical image of colloids stabilized with low-molecular-weight HA shows particles with average sizes ranging from ≈ 100–400 nm in diameter, which roughly correspond to the results obtained by DLS. The fact that sizes of particles determined by DLS are expressed as intensity-weighted *z*-average diameters and that TEM provides number-averaged particle sizes has to be considered in this respect. By visual assessment, the particles are regular and globular in shape. The morphology of samples stabilized with high-molecular-weight HA is more complicated and the figure depicts round particles (darker) connected by oblong rods/tubes (brighter part), which are distributed around them. The appearance of chitosan stabilized colloids is even more different, showing rod-like structures with a higher aspect ratio (Fig. 2). Interestingly, the morphology of colloids stabilized with two synthetic polymers, PVAL (Stejskal et al., 1996; Stejskal & Sapurina, 2005) and poly(*N*-vinylpyrrolidone) (Stejskal et al., 1996) was different. These samples formed irregular rice-grain particles and were noticeably polydisperse in their sizes. On the other side, the PANI colloids prepared in the presence of biodegradable and biocompatible gelatin yielded particles with spindle-like morphology and the authors reported on their non-uniformity in size, which decreased with increasing concentration of gelatin (Bober et al., 2017). Influence of the type and molecular weight of stabilizing polymer on the shape, size and size distribution of colloidal particles is, therefore, obvious.

3.4. Biological properties

Cytotoxicity and antibacterial activity were studied using samples with the best physico-chemical properties and stability; all prepared sample types were tested, except for CH-B. The testing of CH-B samples was omitted, as polymerization in the presence of this polymer did not provide colloidal particles. Prior to the determination of biological properties, PANI dispersions were thoroughly dialyzed against 0.1 M hydrochloric acid to remove residual monomer and other low-molecular-weight impurities or by-products. According to DLS measurements, the sizes of colloidal particles were shown to be unchanged in

Table 4
Concentration of PANI in colloids (μg mL^{-1}) related to dilution (%) of the parent colloidal dispersion.

% of parent colloidal dispersion	Concentration of PANI in colloid (μg mL^{-1})		
	HA-A1	HA-B2	CH-A2
100.0	6,200	8,400	1,200
50.0	3,100	4,200	600
25.0	1,550	2,100	300
12.5	775	1,050	150
10.0	620	840	120
7.5	465	630	90
6.25	387	525	75
5.0	310	420	60
2.5	155	210	30
1.0	62	84	12
0.5	31	42	6
Ref	0	0	0

Table 5
Antibacterial activity of PANI colloidal dispersions stabilized with HA-A1, HA-B2, and CH-A2 recorded for different dilutions (%) of parent colloidal dispersions.

%	HA-A1		HA-B2		CH-A2	
	S. aureus	*E. coli*	*S. aureus*	*E. coli*	*S. aureus*	*E. coli*
50	0	0	10	MIC	177	MIC
25	MIC	MIC	69	3	#	2
12.5	#	#	#	2	#	5
6.25	#	#	#	#	#	#
Ref	#	#	#	#	#	#

#: Number of colonies was uncountable as the bacteria covered entire surface of the agar.

comparison with non-dialyzed samples.

Because of the variation in starting reaction mixtures used for the synthesis of colloids, and in order to compare their biological properties, concentrations of PANI in each of the colloids were determined by UV–vis spectrophotometry (Table 4). Descending concentrations of tested colloidal dispersions, obtained after dilution in cultivation media, were used for biological testing.

As already mentioned above, the ratios between the contents of PANI and the contents of stabilizer were different in the prepared colloids and were notably lower for CH used as a stabilizer in comparison with colloids stabilized with HA. As both PANI alone and the stabilizing polysaccharides are biologically active, their ratio can be crucial for understanding the biological properties of colloids described below.

3.4.1. Antibacterial properties

The antibacterial activity of colloids was tested using the two most common representatives of bacterial species, gram negative *E. coli* and gram positive *S. aureus*. The studied colloidal dispersions comprise particles of small sizes, stable in aqueous environment, and are therefore advantageous for a number applications where antibacterial activity is required. Moreover, chitosan is known for its inherent antibacterial activity, and the efficacy of PANI against bacteria has also been proven (Kuceková et al., 2014; Maráková et al., 2017; Mikušová et al., 2017). Therefore, the combination of these two components in colloidal particles might be of particular advantage with respect to their antibacterial activity.

On the basis of the determined MIC (Table 5), it can be concluded that the antibacterial activity of colloids depends both on the type of stabilizer used and on the ratio between the stabilizer and PANI. If the concentrations of colloidal particles in a medium are considered, sample HA-A1 demonstrated the highest antibacterial activity against *S. aureus* and *E. coli*, showing an MIC at about 25% dilution of the parent dispersion. This effect might be because of the presence of PANI, whose concentration is notably higher in comparison with colloids stabilized with chitosan. Remarkably, the HA-B2 sample, containing an even higher concentration of PANI, first showed an MIC at 50% and only with respect to the growth suppression of *E. coli*. This suggests that the molecular weight of HA and the size of colloidal particles might have influenced the antibacterial activity of the samples. Chitosan-stabilized colloids showed the lowest antibacterial activity, which, moreover, can be mainly assigned to the antibacterial effect of chitosan itself. As the concentration of PANI in this sample was low, its contribution to the overall efficacy of the sample was only minor.

3.4.2. Cytotoxicity

Correspondingly to antibacterial tests, cytotoxicity was also investigated using samples with the best properties and stability. The testing was conducted according to the protocol of ISO standard 10993-5.

The relative viabilities of cells in the presence of the tested colloids are depicted in Fig. 3. The absence of cytotoxicity (viability of cells

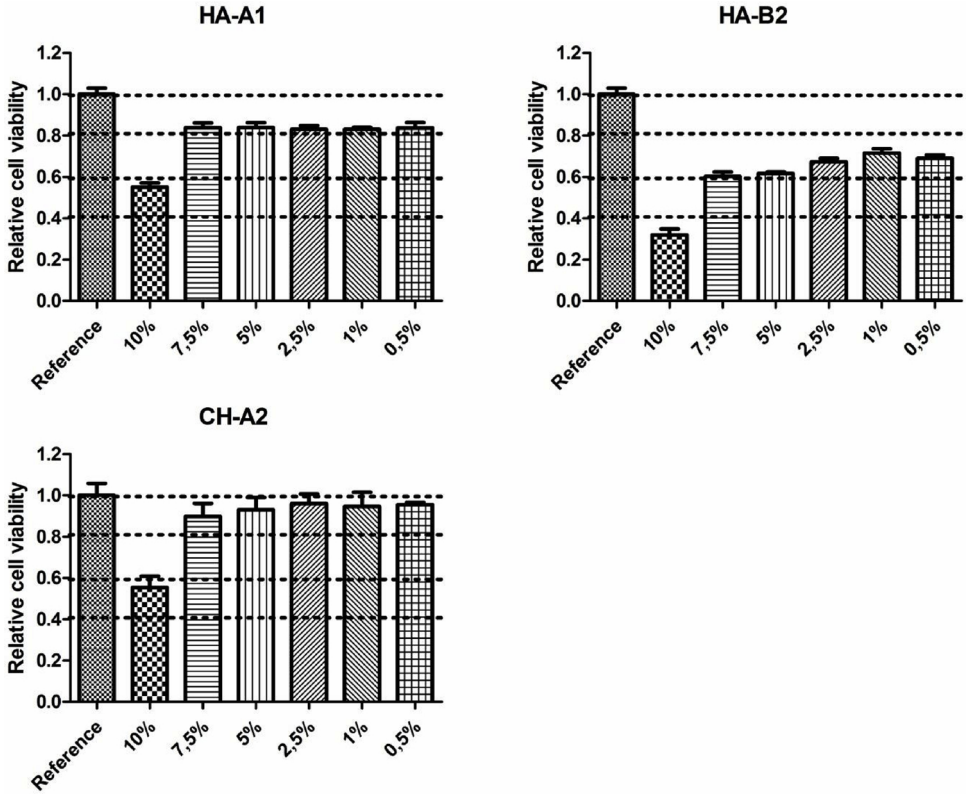

Fig. 3. Cytotoxicityof PANI colloids. The dashed lines highlight the limits of cell viability according to EN ISO 10993-5: viability > 0.8 corresponds to absence of cytotoxicity, > 0.6 – 0.8 mild cytotoxicity, > 0.4–0.6 moderate cytotoxicity, and < 0.4 severe cytotoxicity.

higher than 80%) was observed for sample HA-A1, prepared with the higher molecular weight of stabilizing polymer at colloid dilutions lower than 10% (less than 620 μg mL^{-1} PANI). Corresponding behavior was observed for the colloid stabilized with CH. In this case, the concentration of PANI at 10% dilution of the colloidal dispersion was notably lower at 120 μg mL^{-1}. In both cases, however, the cell viabilities were still lower than those determined for reference cells. Higher cytotoxicity was then determined for colloid stabilized with HA-B2 of lower molecular weight, which contained, at the corresponding dilution of 10%, the highest amount of PANI, or 840 μg mL^{-1}. Within dilutions ranging from 7.5 to 0.5%, HA-B2 then showed mild cytotoxicity corresponding to a cell viability ranging from 60 to 80%. The testing of HA-stabilized colloids at dilutions higher than 10% was impossible, as they formed a gel when added to the cultivation medium.

In the corresponding dilution range, CH-stabilized samples exhibited the lowest cytotoxicity, which undoubtedly resulted from the low amount of PANI present in this sample. On the basis of these observations, it can be concluded that cytotoxicity is more likely connected with the presence of PANI, the concentration of which was highest in the HA-B2 sample, than with the presence of polymeric stabilizer. It can also be speculated that different molecular weights of HA can play a certain role.

A pioneering study exploring the biological properties of colloidal PANI was published by Kuceková et al. (2014). In that study, the properties of PANI stabilized with PVP were investigated and cytotoxicity, antibacterial activity, and the impact of colloid on neutrophile oxidative burst were studied. The results of this research are therefore worth comparing with the current work, mainly with respect to the influence of PANI concentration and type of stabilizer on the studied biological properties. In this context, it can be concluded that the use of both types of HA as colloid stabilizers afforded dispersions with lower cytotoxicity.

As regards the comparison of antibacterial properties, PANI colloids stabilized with HA of higher molecular weight demonstrated higher antibacterial activity against *S. aureus*, similarly to colloids stabilized with PVAL containing a comparable amount of PANI. Thus, the effect of stabilizer must also be taken into consideration. Interestingly, gram negative *E. coli* was more sensitive to colloidal PANI no matter whether it was stabilized with HA, CH or PVP.

4. Conclusions

Aqueous colloidal polyaniline dispersions stabilized with bioactive polysaccharides, sodium hyaluronate and chitosan have been successfully synthesized. They can be considered as promising materials applicable in their original colloidal form as well as precursors for preparation of conducting layers mediating contact with cells and tissues capable to respond to electrical stimuli (*e.g.*, cardiac or nervous cells). Physico-chemical characteristics of prepared colloids, namely their UV–vis spectra, morphology, and particle sizes, proved that all these parameters depend upon composition of reaction mixture in terms of concentrations of reactants and molecular weight and type of the stabilizer. The tests on cytotoxicity performed on mouse embryonic fibroblasts (NIH/3T3) demonstrated that both hyaluronate- and chitosanstabilized colloids have low toxicity, which mainly depends on the concentration of polyaniline in the respective sample. The threshold for the absence of cytotoxicity (cell viability higher than 80%) appeared at PANI concentration of 465 μg mL^{-1}. The antibacterial testing evidenced activity of colloids both against gram positive *S. aureus* and gram negative *E. coli* strains. Surprisingly, the best-performing sample was the polyaniline stabilized with sodium hyaluronate (molecular weight 1.8–2.1 × 10^6), which had minimum inhibitory concentration of 1550 μg mL^{-1}.

Acknowledgements

This work was supported by the Czech Science Foundation (17-05095S), and by the Ministry of Education, Youth and Sports of the Czech Republic (NPU I, LO1504). One of us (D.J.) also appreciates support of the internal grants of Tomas Bata University in ZlínIGA/CPS/2019/004 funded from the resources of specific academic research. Authors thank Ms. Daniela Veselá for technical support and Petr Ponížil for help with statistical evaluation.

References

Ali, A., & Ahmed, S. (2018). A review on chitosan and its nanocomposites in drug delivery. *International Journal of Biological Macromolecules, 109*, 273–286.
Berce, C., Muresan, M. S., Soritau, O., Petrushev, B., Tefas, L., Rigo, I., Ungureanu, G., Catoi, C., Irimie, A., & Tomuleasa, C. (2018). Cutaneous wound healing using polymeric surgical dressings based on chitosan, sodium hyaluronate and resveratrol. A preclinical experimental study. *Colloids and Surfaces B, Biointerfaces, 163*, 155–166.
Bober, P., Humpolíček, P., Syrový, T., Capáková, Z., Syrová, L., & Hromádková, J. and Stejskal J., (2017). Biological properties of printable polyaniline and polyaniline–silver colloidal dispersions stabilized by gelatin. *Synthetic Metals, 232*, 52–59.
Chakraborty, M., Mukherjee, D. C., & Mandal, B. M. (2000). Dispersion polymerization of aniline in different media: A UV-visible spectroscopic and kinetic study. *Langmuir, 16*, 2482–2488.
Chattopadhyay, D., Banerjee, S., Chakravorty, D., & Mandal, B. M. (1998). Ethyl(hydroxyethyl)cellulose stabilized polyaniline dispersions and destabilized nanoparticles therefrom. *Langmuir, 14*, 1544–1547.
Chaudhury, A., & Das, S. (2011). Recent advancement of chitosan-based nanoparticles for oral controlled delivery of insulin and other therapeutic agents. *AAPS Pharmaceutical Science & Technology, 12*, 10–20.
Collins, M. N., & Birkinshaw, C. (2013). Hyaluronic acid based scaffolds for tissue engineering – A review. *Carbohydrate Polymers, 92*, 1262–1279.
Cooper, E. C., & Vincent, B. (1989). Electrically conducting organic films and beads based on conducting latex particles. *Journal of Physics D: Applied Physics, 22*, 1580–1585.
Cruz-Silva, R., Escamilla, A., Nicho, M. E., Padron, G., Ledezma-Perez, A., Arias-Marin, E., Moggio, I., & Romero-Garcia, J. (2007). Enzymatic synthesis of pH-responsive polyaniline colloids by using chitosan as steric stabilizer. *European Polymer Journal, 43*, 3471–3479.
Eisazadeh, H., Gilmore, K. J., Hodgson, A. J., Spinks, G., & Wallace, G. G. (1995). Electrochemical production of conducting polymer colloids. *Colloids and Surfaces A, Physicochemical and Engineering Aspects, 103*, 281–288.
Foster, L. J. R., Ho, S., Hook, J., Basuki, M., & Marcal, H. (2015). Chitosan as a biomaterial: Influence of degree of deacetylation on its physiochemical, material and biological properties. *PloS One, 10*, e0135153.
Ghosh, P., Siddhanta, S. K., & Chakrabarti, A. (1999). Characterization of poly(vinyl pyrrolidone) modified polyaniline prepared in stable aqueous medium. *European Polymer Journal, 35*, 699–710.
Hussein-Al-Ali, S. H., Kura, A., Hussein, M. Z., & Fakurazi, S. (2018). Preparation of chitosan nanoparticles as a drug delivery system for perindopril erbumine. *Polymer Composites, 39*, 544–552.
Jayakumar, R., Chennazhi, K. P., Srinivasan, S., Nair, S. V., Furuike, T., & Tamura, H. (2011). Chitin scaffolds in tissue engineering. *International Journal of Molecular Sciences, 12*, 1876–1887.
Jiang, B. P., Zhang, L., Zhu, Y., Shen, X. C., Ji, S. C., Tan, X. Y., Cheng, L., & Liang, H. (2015). Water-soluble hyaluronic acid-hybridized polyaniline nanoparticles for effectively targeted photothermal therapy. *Journal of Materials Chemistry B, 3*, 3767–3776.
Jun, C. S., Sim, B., & Choi, H. J. (2015). Fabrication of electric-stimuli responsive polyaniline/laponite composite and its viscoelastic and dielectric characteristics. *Colloids and Surfaces A, Physicochemical and Engineering Aspects, 482*, 670–677.
Kuceková, Z., Humpolíček, P., Kašpárková, V., Perecko, T., Lehocký, M., Hauerlandová, I., Sáha, P., & Stejskal, J. (2014). Colloidal polyaniline dispersions: Antibacterial activity, cytotoxicity and neutrophil oxidative burst. *Colloids and Surfaces B, Biointerfaces, 116*, 411–417.
Li, Y., Bober, P., Apaydin, D. H., Syrový, T., Sariciftci, N. S., Hromádková, J., Sapurina, I., Trchová, M., & Stejskal, J. (2016). Colloids of polypyrrole nanotubes/nanorods: A promising conducting ink. *Synthetic Metals, 221*, 67–74.
Lu, Z., Gao, J. T., He, Q. F., Wu, J., Liang, D. H., & Yang, H. and Chen R. (2017). Enhanced antibacterial and wound healing activities of microporous chitosan-Ag/ZnO composite dressing. *Carbohydrate Polymers, 156*, 460–469.
Maráková, N., Humpolíček, P., Kašpárková, V., Capáková, Z., Martinková, L., Bober, P., Trchová, M., & Stejskal, J. (2017). Antimicrobial activity and cytotoxicity of cotton fabric coated with conducting polymers, polyaniline or polypyrrole, and with deposited silver nanoparticles. *Applied Surface Science, 396*, 169–176.
Mazrad, Z. A. I., Choi, C. A., Kim, S. H., Lee, G., Lee, S., In, I., Lee, K. D., & Park, S. Y. (2017). Target-specific induced hyaluronic acid decorated silica fluorescent nanoparticles@polyaniline for bio-imaging guided near-infrared photothermal therapy. *Journal of Materials Chemistry B, 5*, 7099–7108.
Mikušová, N., Humpolíček, P., Růžička, J., Capáková, Z., Janů, K., Kašpárková, V., Bober, P., Stejskal, J., Koutný, M., Filátová, K., Lehocký, M., & Ponížil, P. (2017). Formation of bacterial and fungal biofilm on conducting polyaniline. *Chemical Papers, 71*, 505–512.

Muzzarelli, R. A. A. (2009). Chitins and chitosans for the repair of wounded skin, nerve, cartilage and bone. *Carbohydrate Polymers, 76*, 167–182.
Ozkan, O., & Sasmazel, H. T. (2018). Antibacterial performance of PCL-chitosan core-shell scaffolds. *Journal of Nanoscience and Nanotechnology, 18*, 2415–2421.
Park, D. E., Choi, H. J., & Vu, C. M. (2016). Stimuli-responsive polyaniline coated silica microspheres and their electrorheology. *Smart Materials & Structures, 25*, 055020.
Prestwich, G. D. (2011). Hyaluronic acid-based clinical biomaterials derived for cell and molecule delivery in regenerative medicine. *Journal of Controlled Release, 155*, 193–199.
Stejskal, J., & Gilbert, R. G. (2002). Polyaniline. Preparation of a conducting polymer (IUPAC technical report). *Pure and Applied Chemistry, 74*, 857–867.
Stejskal, J., & Sapurina, I. (2005). Polyaniline: Thin films and colloidal dispersions (IUPAC technical report). *Pure and Applied Chemistry, 77*, 815–826.
Stejskal, J., Trchová, M., Bober, P., Humpolíček, P., Kašpárková, V., Sapurina, I., Shishov, M. A., & Varga, M. (2015). *Conducting polymers: Polyaniline. Encyclopedia of polymer science and technology*. Wiley Online Library1–44. https://doi.org/10.1002/0471440264.pst640.
Stejskal, J., Kratochvíl, P., & Helmstedt, M. (1996). Polyaniline dispersions. 5. Poly(vinyl alcohol) and poly(*N*-vinylpyrrolidone) as steric stabilizers. *Langmuir, 12*, 3389–3392.
Stejskal, J., Kratochvil, P., & Radhakrishnan, N. (1993). Polyaniline dispersions. 2. UV-vis absorption spectra. *Synthetic Metals, 61*, 225–231.
Stejskal, J., Špírková, M., Riede, A., Helmstedt, M., Mokreva, P., & Prokeš, J. (1999). Polyaniline dispersions 8. The control of particle morphology. *Polymer, 40*, 2487–2492.
Wang, X. Y., Wang, G., Liu, L., & Zhang, D. Y. (2016). The mechanism of a chitosan-collagen composite film used as biomaterial support for MC3T3-E1 cell differentiation. *Scientific Reports, 6*, 39322.
Zhang, W. L., & Choi, H. J. (2014). Stimuli-responsive polymers and colloids under electric and magnetic fields. *Polymers, 6*, 2803–2818.

Article VII.

Kasparkova, V.; Humpolicek, P.; **Capakova, Z.**; Bober, P.; Stejskal, J.; Trchova, M.; Rejmontova, P.; Junkar, I.; Lehocky, M.; Mozetic, M. Cell-Compatible Conducting Polyaniline Films Prepared in Colloidal Dispersion Mode. Colloid Surf. B-Biointerfaces 2017, 157, 309–316. https://doi.org/10.1016/j.colsurfb.2017.05.066.

Colloids and Surfaces B: Biointerfaces 157 (2017) 309–316

Contents lists available at ScienceDirect

Colloids and Surfaces B: Biointerfaces

journal homepage: www.elsevier.com/locate/colsurfb

Protocols

Cell-compatible conducting polyaniline films prepared in colloidal dispersion mode

Věra Kašpárková[a,b], Petr Humpolíček[a,c,*], Zdenka Capáková[a], Patrycja Bober[d], Jaroslav Stejskal[d], Miroslava Trchová[d], Petra Rejmontová[a,c], Ita Junkar[e], Marián Lehocký[a], Miran Mozetič[e]

[a] Centre of Polymer Systems, Tomas Bata University in Zlin, 76001 Zlin, Czech Republic
[b] Department of Fat, Surfactant, and Cosmetics Technology, Faculty of Technology, Tomas Bata University in Zlin, 760 01 Zlin, Czech Republic
[c] Polymer Centre, Faculty of Technology, Tomas Bata University in Zlin, 760 01 Zlin, Czech Republic
[d] Institute of Macromolecular Chemistry, Academy of Sciences of the Czech Republic, 162 06 Prague 6, Czech Republic
[e] Department of Surface Engineering, Plasma Laboratory, Josef Stefan Institute, 1000 Ljubljana, Slovenia

ARTICLE INFO

Article history:
Received 14 March 2017
Received in revised form 20 May 2017
Accepted 26 May 2017
Available online 31 May 2017

Keywords:
Polyaniline
Conducting films
Colloidal dispersions
Surface analysis
Cell compatibility
Skin irritation

ABSTRACT

Conducting polyaniline can be prepared and modified using several procedures, all of which can significantly influence its applicability in different fields of biomedicine or biotechnology. The modifications of surface properties are crucial with respect to the possible applications of this polymer in tissue engineering or as biosensors. Innovative technique for preparing polyaniline films *via in-situ* polymerization in colloidal dispersion mode using four stabilizers (poly-*N*-vinylpyrrolidone; sodium dodecylsulfate; Tween 20 and Pluronic F108) was developed. The surface energy, conductivity, spectroscopic features, and cell compatibility of thin polyaniline films were determined using contact-angle measurement, the van der Pauw method, Fourier-transform infrared spectroscopy, and assay conducted on mouse fibroblasts, respectively. The stabilizers significantly influenced not only the surface and electrical properties of the films but also their cell compatibility. Sodium dodecylsulfate seems preferentially to combine both the high conductivity and good cell compatibility. Moreover, the films with sodium dodecylsulfate were non-irritant for skin, which was confirmed by their *in-vitro* exposure to the 3D-reconstructed human tissue model.

1. Introduction

The combination of intrinsic electrical conductivity with easy preparation and modification procedures opens the door for the promising application of conducting polymers in engineering of excitable tissues. Among conducting polymers, polyaniline (PANI) receives particular and still increasing attention, mainly because it can be prepared by various methods [1–3] and it is subsequently easily modified in order to change its surface properties [4]. Therefore, this polymer seems to be well suited for application in tissue engineering and biosensors. PANI prepared in powder form, however, possesses notable cytotoxicity [5], which is believed to be mainly connected to the presence of low-molecular-weight impurities [6]. The purification of PANI powder after preparation [7], as well as methods of its green synthesis [8], are alternatives to the standard route of preparation [2]. Compared to powders, thin PANI films grown on the supporting surfaces seem to be purified more easily. Thanks to this fact, pristine PANI films [9,10] as well as films combined with other polymers [11] enable cell growth on their surfaces. PANI films coated with poly(2-acrylamido-2-methyl-1-propanesulfonic acid) were compatible with blood cells and allowed for platelet adhesion [12]. Another way how cell compatibility, or more generally the biocompatibility of PANI, can be controlled is the combination with various stabilizers, whether they are standard surfactants or water-soluble polymers. Some of these stabilizers have been used to prepare colloidal PANI [13]; some were even tested for their biological properties [14]. In comparison with standard PANI films, they have reduced surface roughness, as the stabilizer prevents the macroscopic precipitation of PANI from the reaction mixture. Moreover, films grown on surfaces immersed in mixtures containing stabilizers are thinner compared to those prepared from a reaction mixture without stabilizer [15]. The present study therefore focuses on PANI

* Corresponding author at: Centre of Polymer Systems, Tomas Bata University in Zlin, Trida Tomase Bati 5678, 76001 Zlin, Czech Republic.
E-mail address: humpolicek@utb.cz (P. Humpolíček).

http://dx.doi.org/10.1016/j.colsurfb.2017.05.066
0927-7765/

modification using various surfactants or colloidal stabilizers with the aim to control the surface and electrical properties and also the cell compatibility.

2. Materials and methods

2.1. Preparation of polyaniline films

PANI films were prepared *in situ* on a suitable substrate *via* the oxidation of aniline hydrochloride (0.2 mol L^{-1}, Lach-Ner) with ammonium peroxydisulfate (0.25 mol L^{-1}, Sigma-Aldrich) in the presence of a stabilizer (2 wt%). Four different substrates were used as supports: tissue polystyrene culture dishes (TPP; Switzerland) for the determination of cell compatibility, a glass support for conductivity measurements, polypropylene foil for the measurement of surface properties, and silicon wafer for spectroscopic analysis. To produce PANI films, aniline hydrochloride (2.59 g) was dissolved in 50 mL of an aqueous solution of the respective stabilizer (40 g L^{-1}), namely poly(*N*-vinylpyrrolidone) (PVP), sodium dodecylsulfate (SDS), Tween 20 (T20), or Pluronic F108 (F108) (all Sigma-Aldrich). An aqueous solution (50 mL) containing 5.71 g of ammonium peroxydisulfate was added, and the reaction mixture was stirred and poured over the substrate. The oxidation of aniline was left to proceed for 1 h. PANI films formed on supports were then rinsed with 0.2 mol L^{-1} HCl and left to dry in air. The samples were designated PANI-PVP-H_2O, PANI-SDS-H_2O, PANI-T20-H_2O, and PANI-F108-H_2O. Similar films were also prepared with aniline hydrochloride and stabilizer dissolved in 1 mol L^{-1} hydrochloric acid instead of water (samples PANI-PVP-HCl, PANI-SDS-HCl, PANI-T20-HCl, and PANI-F108-HCl), *i.e.* under higher acidity of the reaction medium. The films prepared in the absence of stabilizer are referred to as standard films.

2.2. Conductivity

The conductivity of the samples was measured by the four-point van der Pauw method. A programmable electrometer with an SMU Keithley 237 current source and a Multimeter Keithley 2010 voltmeter with a 2000 SCAN 10-channel scanner card were employed. Measurements were carried out at ambient temperature.

2.3. Surface energy

Contact angle measurements and the determination of surface energy were conducted with the aid of the "SEE system" (surface energy evaluation system) (Advex Instruments, Czech Republic). For polyaniline samples, deionized water, ethylene glycol, and diiodomethane (Sigma–Aldrich) have been used as test liquids. The droplet volume of the test liquids was set to 2 μL in all experiments. Ten separate readings were averaged to obtain one representative contact-angle value. By using these data, the substrate surface free energy was determined by the "acid–base" method.

In order to evaluate the interaction of fibroblasts cells with PANI films, the surface free energy of the cells was also determined. The cell suspension was thoroughly filtered through a filtration paper to obtain a homogeneous cell layer on the paper, and this sample was immediately subjected to contact-angle measurement. For cells, glycerol (Sigma–Aldrich) and diiodomethane were used as the test liquids, and the droplet volume of these liquids was also set to 2 μL for all experiments. Correspondingly to PANI films, ten separate readings were taken to obtain one representative average contact angle value. Using these data, the cell surface free energy was calculated by the Owens-Wendt-Rabel-Kaelble (OWRK) method, and the total surface energy (γ^{tot}), including its components, the disperse part (γ^{LW}) and the polar part (γ^{AB}), were obtained. Finally, the cell-film interaction was determined and γ^{dif}, denoting the absolute value of the difference between the surface energy of cells and that of the film, was calculated according to the equation $\gamma^{dif} = |\gamma^{tot,cell} - \gamma^{tot,sample}|$.

2.4. Spectroscopic analysis

Fourier-transform infrared (FTIR) spectra of the films deposited on silicon windows were recorded in the range of 650–4000 cm^{-1} at 256 scans per spectrum at a 4 cm^{-1} resolution by means of a fully computerized Thermo Nicolet NEXUS 870 FTIR Spectrometer using a DTGS detector. After measurements, spectra were corrected for moisture and carbon dioxide in the optical path. An absorption subtraction technique was used to remove the spectral features of silicon wafers. Golden GateTM Heated Diamond ATR Top-Plate (MKII Golden Gate single reaction ATR system) was applied for the supporting measurements of pure surfactants.

Raman spectra excited with an HeNe 633 nm laser were collected on a Renishaw inVia Reflex Raman microspectrometer. A research-grade Leica DM LM microscope with ×50 objective magnification was used to focus the laser beam on the sample placed on an X–Y motorized sample stage. The scattered light was analyzed by a spectroscope with holographic gratings with 1800 lines mm^{-1}. A Peltier-cooled CCD detector (576 × 384 pixels) was used to register the dispersed light.

2.5. Cell compatibility

Prior to *in-vitro* testing, the samples were disinfected by 30 min exposure to a UV-radiation source operating at a wavelength of 258 nm emitted from a low-pressure mercury lamp. The compatibility of polyaniline films with the mouse embryonic fibroblast NIH/3T3 cell line (ATCC; US) was investigated. Cell adhesion, proliferation, and migration were studied. The ATCC–formulated Dulbecco's Modified Eagle's Medium (PAA; Switzerland) containing 10% calf serum (PAA; Switzerland) and 100 U mL^{-1} Penicillin/Streptomycin (PAA; Switzerland) was used as the culture medium.

Tests were conducted as follows: (1) To reveal the ability of cells to adhere to surfaces, the cells were seeded on reference culture dishes (TPP; Switzerland) and the studied polymer films in a concentration of 1×10^7 cells mL^{-1}. After one or six hours, the cells were gently rinsed and micrographs were taken. (2) Cell proliferation was evaluated with cells seeded in an initial concentration of 1×10^5 cells mL^{-1} and cultivated for 72 h. Micrographs were also taken. (3) To show the changes in cytoskeleton, the actin filaments staining with ActinRed™ 555 (Thermo Fisher Scientific, USA) was used. Cells were seeded in an initial concentration of 1×10^5 cells mL^{-1} and cultivated for 24 h. Subsequently, cells were fixed and permeabilized using the following procedure. Cells were fixed using 4% formaldehyde (Penta, Czech Republic) for 15 min, rinsed with PBS and subsequently poured with 0.5% Triton X-100 (Sigma-Aldrich,USA) for 5 min for permeabilization. After this time, cells were rinsed 3 times with PBS (Invitrogen, USA). PBS (1 mL) containing 10 μL of ActinRed™ 555 was added and cells were left to incubate for 30 min in the dark. Morphology of cells was observed and micrographs were taken using an inverted fluorescence phase contrast microscope (Olympus IX 81, Japan). (4) Cell migration was determined by scratch assay according to Liang et al. [16] with modification. A scratch was created in a confluent cell monolayer and after 24 h micrographs were captured with an Olympus inverted fluorescent microscope (Olympus, IX 51; Japan) equipped with a digital colour camera (Leica DFC480; Germany).

Table 1
The conductivity (S cm^{-1} ± SD) and surface energy (mN m^{-1} ± SD) of polyaniline films prepared *in situ* in the presence of various stabilizers in water and in 1 M HCl.[a]

Stabilizer		PVP		SDS		Tween 20		Pluronic F-108	
Dispersion medium		H_2O	1 M HCl	H_2O	1 M HCl	H_2O	1 M HCl	H_2O	1 M HCl
Conductivity		1.96 ± 0.01	18.4 ± 0.02	3.60 ± 0.01	30.40 ± 0.08	6.07 ± 0.03	8.39 ± 0.04	1.74 ± 0.01	25.9 ± 0.01
Surface energy	γ^{TOT}	49 ± 5	55 ± 4	43 ± 3	46 ± 2	69 ± 2	61 ± 2	59 ± 4	56 ± 4
	γ^{LW}	46 ± 1	46 ± 1	41 ± 2	41 ± 1	50 ± 1	50 ± 1	51 ± 1	50 ± 1
	γ^{AB}	3 ± 4	9 ± 3	2 ± 3	5 ± 2	19 ± 1	11 ± 2	8 ± 4	6 ± 4
	γ^{dif}	0.21	5.79	6.21	3.21	19.79	11.79	9.79	6.79

[a] Surface energy of NIH/3T3 cells alone: γ^{TOT} = 49.21, γ^{LW} = 23.21, γ^{AB} = 26.00.

2.6. Skin irritation test

The skin irritation potential of PANI-SDS-HCl was tested *in vitro* after application onto a 3D reconstructed human tissue model (RHT) EpiDerm (MatTek, Slovakia). The exposure time was adjusted to 1 h. After exposure, RHT was carefully rinsed and incubated in fresh medium for 42 h. After the incubation period, skin irritation was evaluated using MTT assay. The test was performed according to OECD Guideline for the Testing of Chemicals, No. 439: *In Vitro* Skin Irritation: Reconstructed Human *Epidermis* Test Method [17].

3. Results and discussion

Virtually any substrate, which is immersed in the reaction mixture used for the oxidation of aniline hydrochloride becomes coated with a thin polyaniline film [3] of the typical thickness 100–150 nm and fused globular morphology. The films are thinner and more conducting if the polymerization is carried out in 1 M hydrochloric acid instead of water, *i.e.* under higher acidity of the reaction medium. Polyaniline is obtained in both cases as an accompanying precipitate and collected as a powder.

If the synthesis takes place in the presence of a stabilizer, such as water-soluble polymer, poly(*N*-vinylpyrrolidone), the colloidal dispersions with the particle size is of 200–400 nm are produced instead of the precipitate. Also in this case the thin films are also produced on immersed interfaces during the oxidation [15] and we refer to them as being *in-situ* prepared in colloidal dispersion mode. They are thinner and smoother compared with the films prepared in the absence of stabilizer [18]. Please note that such films qualitatively differ in morphology from the films cast from colloidal dispersions that are produced by printing techniques [19,20].

Surfactants may play a similar role in the stabilization of polyaniline colloids like PVP and they similarly affect the growth of polyaniline films. In this case, the incorporation of surfactants into or onto the films is likely due to hydrophobic or ionic interactions with polyaniline. Anionic surfactant SDS, and non-ionic surfactants T20 and F108 were employed for obtaining films with different surface properties. SDS [21,22] and T20 [23] have previously been used as stabilizers for the synthesis of colloidal polyaniline, however, the properties of thin films obtained simultaneously have not been addressed.

3.1. Conductivity

Higher conductivity is achieved for PANI films formed during the synthesis in 1 M hydrochloric acid in comparison with samples prepared *via* reaction using water as a reaction medium (Table 1). These results correspond to the findings presented in the IUPAC technical report [3], in which the conductivity of the standard PANI film prepared in aqueous medium and in 1 mol L^{-1} HCl reached 2.6 ± 0.7 S cm^{-1} and 18.8 ± 7.1 S cm^{-1}, respectively. In the present study, the conductivities ranged from 1.74 ± 0.01 (PANI-F108-H_2O) to 30.40 ± 0.08 S cm^{-1} (PANI-SDS-HCl). The films prepared from stabilizer-containing reaction mixtures had generally higher conductivities (Table 1) than commonly prepared PANI films as reported in the literature [18]. The explanation of this

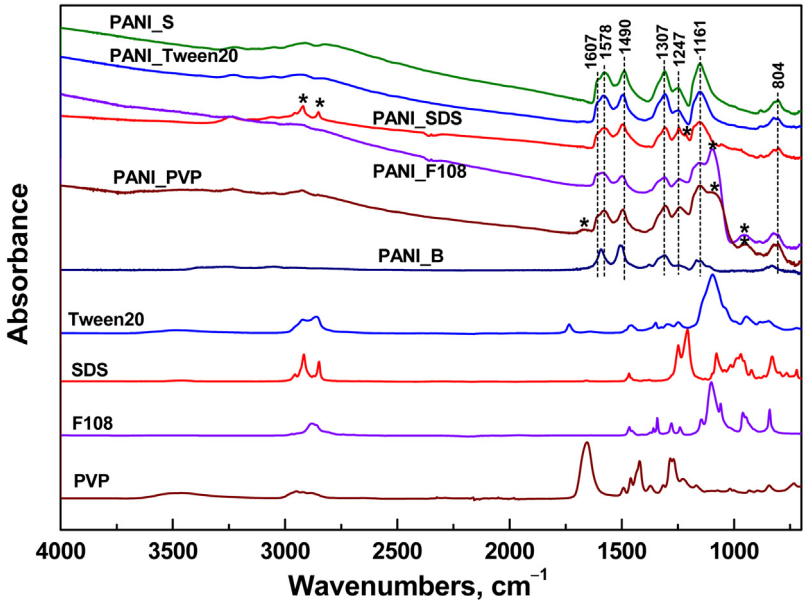

Fig. 1. FTIR spectra of standard PANI film (PANI-S), corresponding film of PANI base (PANI-B), and the films prepared in water in the presence surfactants (PANI-T20, PANI-SDS, PANI-F108, and PANI-PVP) deposited *in-situ* on Si wafer, and the spectra of corresponding stabilizers alone. The peaks of surfactants are marked with asterisks.

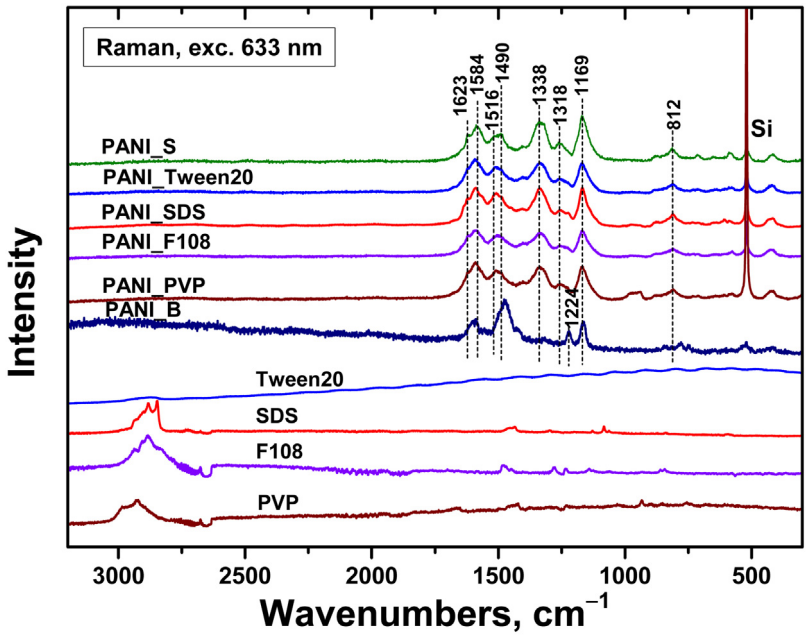

Fig. 2. Raman spectra of standard PANI film (PANI-S), corresponding film of PANI base (PANI-B), and the films prepared in water in the presence surfactants (PANI-T20, PANI-SDS, PANI-F108, and PANI-PVP) deposited *in-situ* on Si wafer, and the spectra of corresponding stabilizers alone. The excitation wavelength was 633 nm.

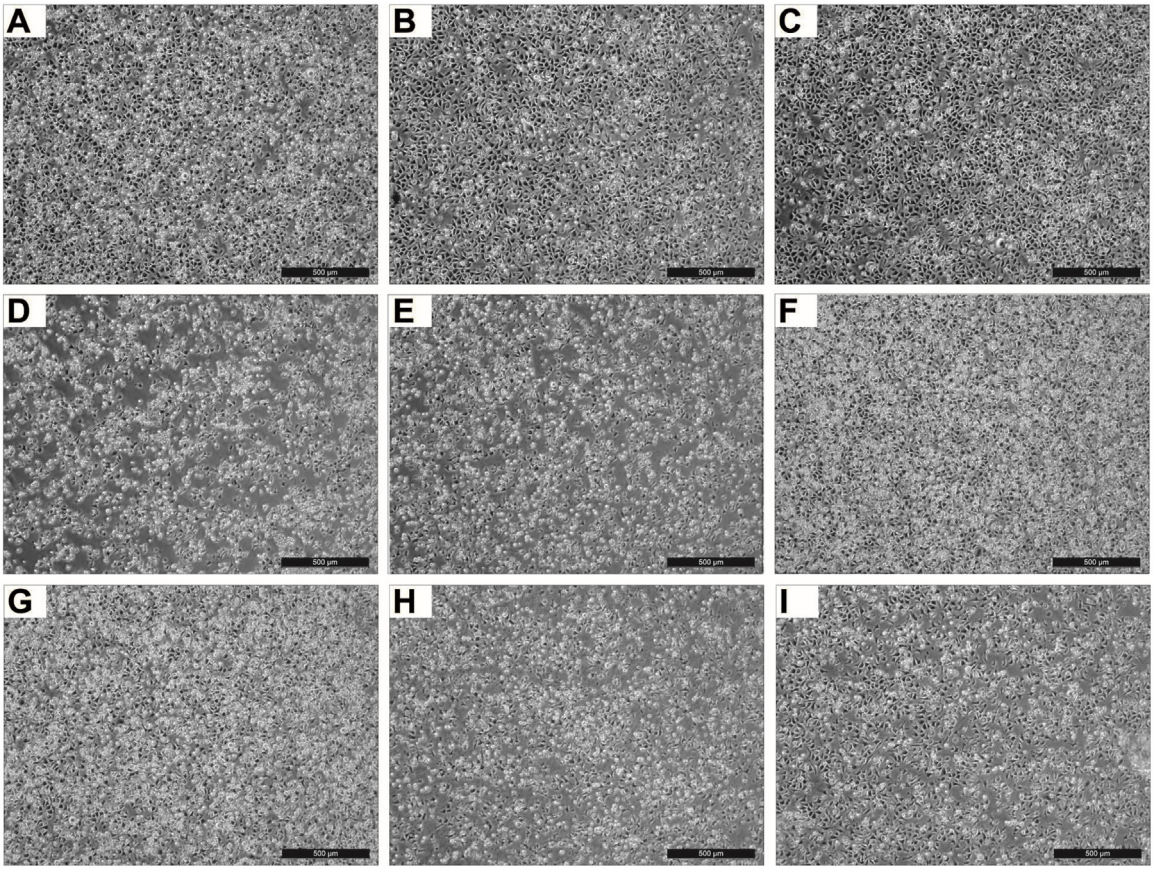

Fig. 3. Adhesion of NIH/3T3 cells on the surfaces of PANI films prepared in the presence of different stabilizers evaluated after 1 h incubation. A) reference; B) PANI-SDS-H_2O; C) PANI-SDS-HCl; D) PANI-PVP-H_2O; E) PANI-PVP-HCl; F) PANI-F108-H_2O; G) PANI-F108-HCl; H) PANI-T20-H_2O; I) PANI-T20-HCl. Scale bars correspond to 500 μm.

difference is based on the brush-like chain morphology of the film prepared in the presence of a stabilizer and its gradual disorganization during the polymer chain growth in its absence.

3.2. Surface energy

The surface energies of pristine PANI films prepared in the absence of stabilizers were determined earlier [9]: $\gamma^{TOT} = 52.54$,

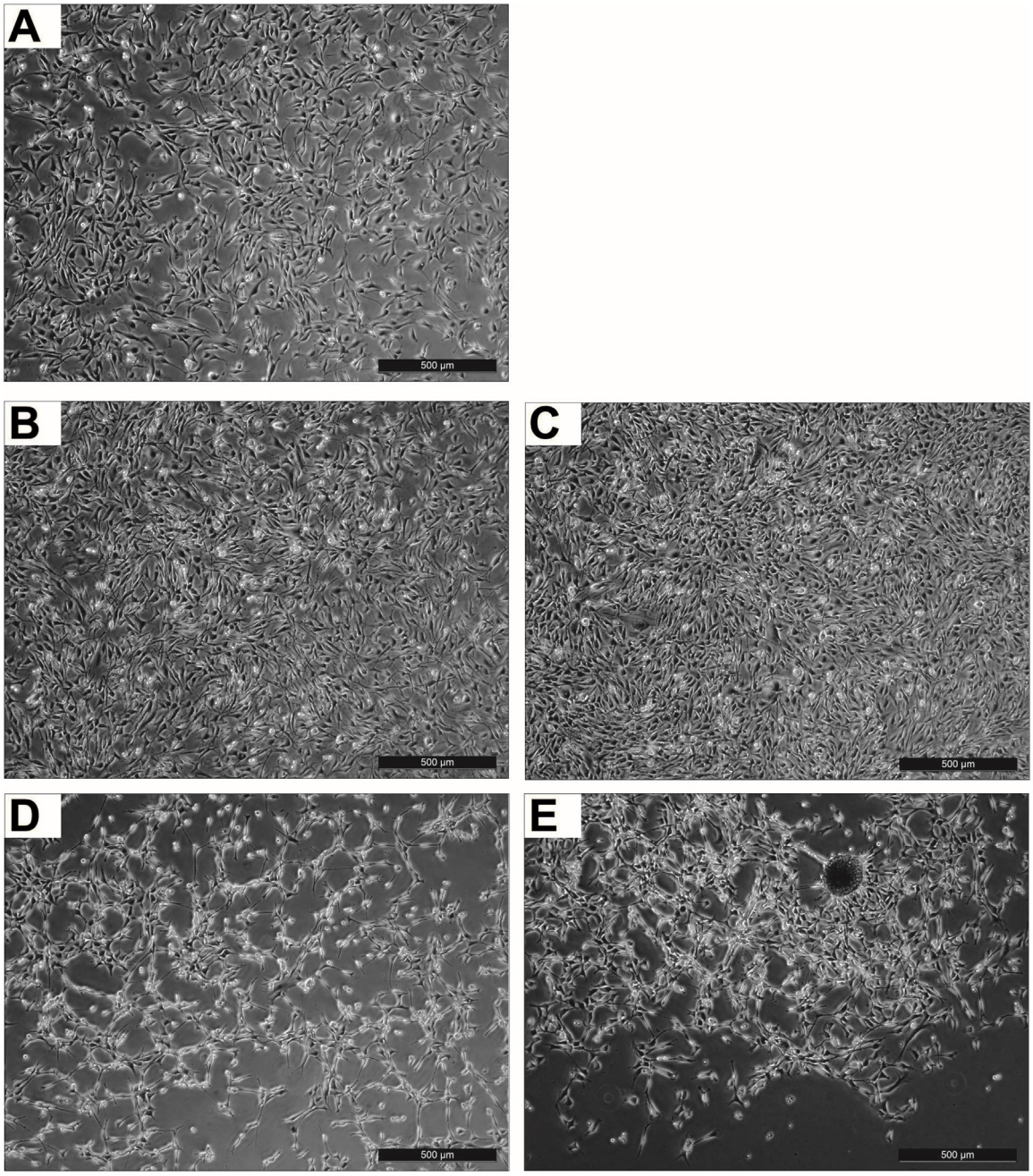

Fig. 4. Proliferation of NIH/3T3 cells on surfaces of PANI films prepared in the presence of different stabilizers evaluated after 72 h incubation. A) reference; B) PANI-SDS-H_2O; C) PANI-SDS-HCl; D) PANI-PVP-H_2O; E) PANI-PVP-HCl. Scale bars correspond to 500 µm.

$\gamma^{LW} = 46.05$ and $\gamma^{AB} = 6.49\,mN\,m^{-1}$. The values of γ^{TOT} from the current study show that the films prepared in the presence of both non-ionic surfactants Tween 20 and Pluronic F108 were the most different in comparison with the pristine films (Table 1). This difference was not so notable for remaining samples. The surface energy mainly depended on the type of stabilizer and it was not significantly influenced by the particular reaction medium. Interestingly, the disperse part γ^{LW} of the surface energy was equal for all films prepared in water and in 1 M HCl. The surface energies γ^{TOT} of the samples containing the stabilizers increased in the following order: PANI-SDS < PANI-PVP < PANI-F-108 < PANI-T20.

3.3. Spectroscopic analysis

Infrared spectra of standard PANI, PANI prepared in the presence of Tween, SDS, Pluronic F108, and PVP deposited *in-situ* on silicon wafer, and the corresponding stabilizers are shown in Fig. 1. The spectra of PANI prepared in the presence of stabilizers exhibit main bands of standard PANI salt [24]. The broad band observed above 2000 cm^{-1} in the spectra corresponds to the polaron band of protonated PANI. The presence of SDS, Pluronic F108, and PVP manifests itself by the peaks of surfactants in corresponding spectra of the oxidation products (marked with asterisk in Fig. 1). In the case of PANI-T20-H_2O, the spectrum is practically identical with the spectrum of standard PANI salt and the bands of the surfactant are not identified.

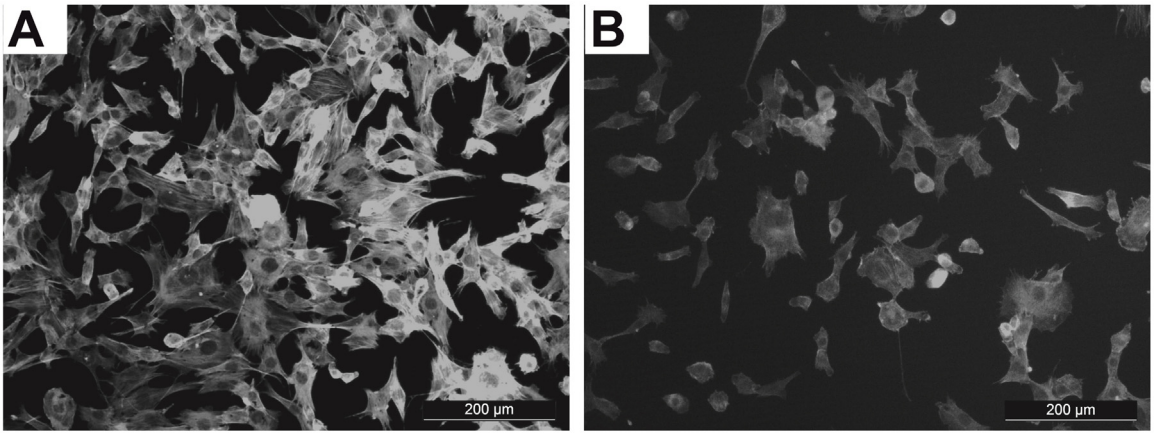

Fig. 5. The differences in cytoskeleton organization of NIH/3T3 cells on surfaces of PANI films prepared in the presence of different stabilizers evaluated after 24 h. A) PANI-SDS-H_2O; B) PANI-PVP-HCl. Scale bars correspond to 200 µm.

Raman spectra (Fig. 2) strongly support the results of the infrared analysis, *i.e.* that the oxidation in the presence of stabilizers leads to the protonated form of PANI [25]. In the case of Raman spectra, the peaks of stabilizers have not been detected. Some small changes in the spectra correspond to the fact that the degree of protonation is lower than in standard PANI salt.

3.4. Cell compatibility

Cell compatibility is a complex of various cell characteristics covering, for example, cell adhesion, growth, and proliferation. The compatibility of cells with a given substrate is mainly connected with its surface chemistry and topography and the presence of functional groups, which can interact with cell receptors and membrane proteins.

Cell adhesion to the tested PANI films after 1 h is visualised in Fig. 3. Though significant differences were detected in the values of γ^{dif}, which expresses the ability of a cell to adhere to a given surface, cell behaviour was similar and unaffected by small differences in the numbers of cells or their morphology. After 6 h after seeding, cells quantity was still unaltered. The differences was observable no soon than after 24 h. It can be concluded that the cells were able to adhere equally to all tested surfaces.

Significant differences were observed, however, in the subsequent behaviour of cells. These were able to grow and proliferate only on PANI-SDS-H_2O and PANI-SDS-HCl films (Fig. 4), but not on the remaining surfaces. On PANI-PVP-H_2O and PANI-PVP-HCl films, the cell growth was rare and only a few cell enclaves were present (Fig. 4D, E). The situation was even worse on PANI films containing F108 or T20 surfactants, where the cells were not able to proliferate at all. Proliferation was, however, slightly improved after serum albumin solution was poured onto the films; however, even after 7 days, the cells did not create a semi-confluence layer (data not presented). The positive effect of serum albumin on proliferation is not surprising, as this protein is well known to improve the compatibility of surfaces with cells.

As previously described, the cells were able to adhere on PANI-PVP films but they did not behave in physiological manner after 72 h. To reveal the differences in cell behaviour on films with SDS or PVP, the cytoskeleton of cells was visualised using ActinRed (see Fig. 5). It is clearly seen that there are differences not only in the amount of the cells but also in the cytoskeleton organization. In Fig. 5A, the cells cultivated on SDS displayed normal cytoskeleton organization while on PVP (Fig. 5B) the cytoskeleton does not form much filopodia and cells do not spread out.

As cells proliferated well only on PANI-SDS-H_2O and PANI-SDS-HCl, scratch assays were performed only on these surfaces. The respective micrographs (Fig. 6) demonstrate that cells were able to migrate into the scratches on these films in a comparable manner to cells on the reference. It can therefore be concluded that both PANI films containing SDS offer good cell compatibility.

Considering the above-described behaviour of cells, it can be summarized that cells were able to adhere on all surfaces but, except in the case of PANI-SDS-H_2O and PANI-SDS-HCl, were incapable of proliferation. This is likely due to a non-receptor mediated cell/surface binding, which allows cells to adhere but is not sufficient for the survival of anchorage-dependent cells (NIH/3T3), which therefore undergo apoptosis. This is also supported by the fact that the pouring of serum albumin over film surfaces improved the adhesion and proliferation of cells on these surfaces. This effect was, however, expectable thanks to the ability of albumin to mimic the extracellular matrix. The growth of cells in enclaves, which was observed on the PANI-PVP-H_2O and PANI-PVP-HCl films, can be explained by the fact that some of the adhered cells can start to synthesize their own extracellular matrix and deposit it on the film surface. On the other hand, the surfaces of PANI-SDS-H_2O and PANI-SDS-HCl must also allow for receptor-mediated adhesion which facilitates not only the adhesion of cells on these films, but also their growth and proliferation. Explanation of the exceptional behaviour of PANI films incorporating SDS can be connected to the fact that SDS contains sulfate groups, which were reported to stimulate cell adhesion, activate the spread of cells, and influence cytoskeleton reorganization [26]. In this respect, it is interesting that PANI films in their native form, *i.e.* without stabilizes, allow not only for cell adhesion and proliferation [5] but also for cardiomyogenesis and neurogenesis [9].

3.5. Skin irritation test

Interesting results were also gathered from the skin irritation test conducted on the RHT model. The best performing film with respect to cell compatibility, PANI-SDS-HCl, was tested for the production of reversible damage to skin. After skin irritation testing was performed, this film was classified as a non-irritating material, as the viability of cells in the RHT model treated with the tested sample reached $112 \pm 6\%$, which indicated even less irritating potential than that of the reference. The skin irritation potential of standard PANI films without stabilizers was determined *in vivo* on a number of volunteers in study by Humpolíček et al. [5], who reported that this material also induced significantly less irritation than the positive control. Comparison of both studies demonstrates

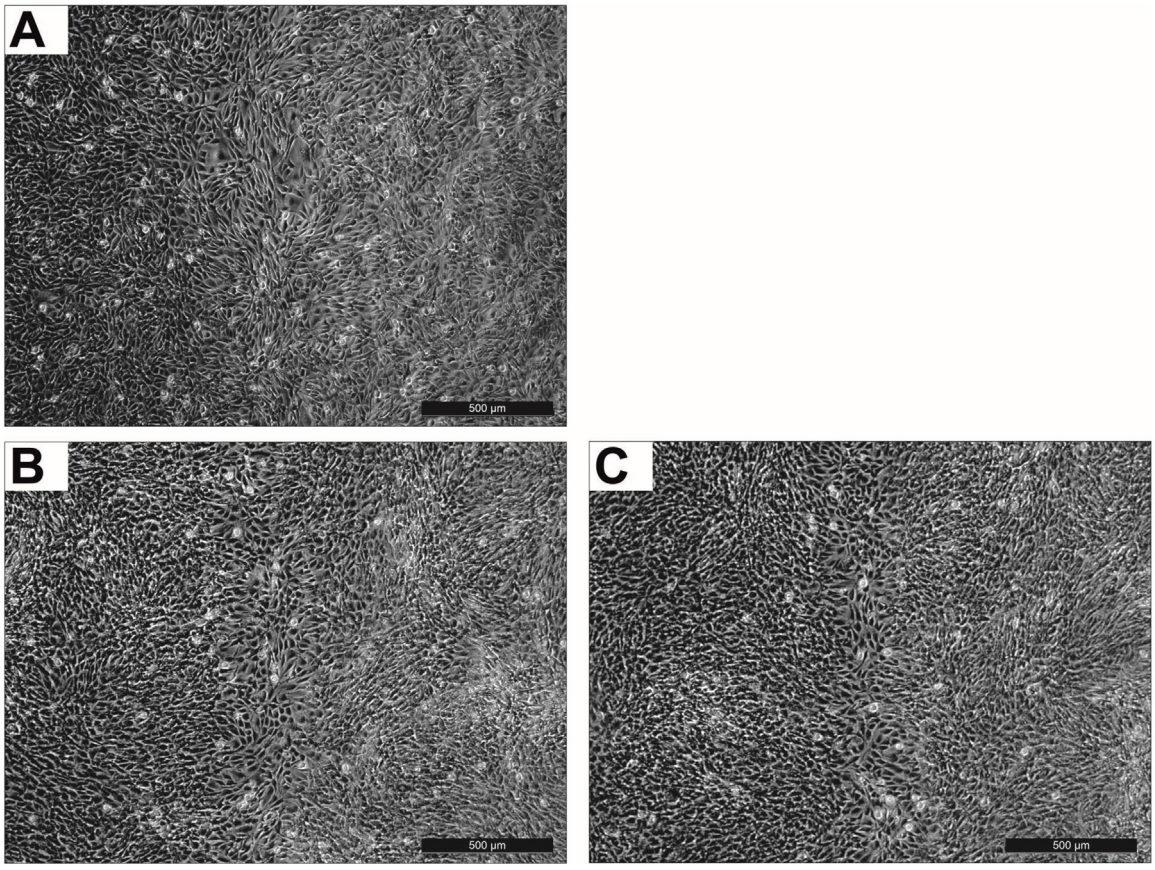

Fig. 6. Scratch assay – cell migration of NIH/3T3 cells on surfaces of PANI films prepared in the presence of different stabilizers evaluated after 24 h incubation. A) reference; B) PANI-SDS-H_2O; C) PANI-SDS-HCl. PANI-PVP, PANI-F108 and PANI-T20 were not tested. Scale bars correspond to 500 µm.

that the incorporation of SDS into PANI films didn't influence their irritation potential.

4. Conclusions

PANI films with advanced biological properties can be efficiently prepared using colloidal dispersion mode, *i.e.* during the synthesis of conducting polymer in the presence of different stabilizers. The type and character of stabilizer incorporated into the PANI film significantly influenced not only conductivity and surface properties, but also primarily the cell compatibility. Among the stabilizers used, SDS had the most positive impact as the best properties in terms of conductivity and cell compatibility were recorded for films incorporating this surfactant. Moreover, these films were non-irritating and displayed no harmful effects on human skin. It can be concluded, therefore, that the preparation of PANI films using a colloidal dispersion mode can lead to a significant improvement in the biological properties of PANI. This significantly enhances the applicability of PANI in tissue engineering and, more generally, in biomedicine. In particular, its use in biosensors capable of conductometric monitoring of ongoing changes on the skin surface should be of particular interest.

Acknowledgments

This work was supported by the Ministry of Education, Youth and Sports of the Czech Republic (Program NPU I, LO1504) and Czech Science Foundation (17-05095S). Authors thank Karel Netík for technical support. One of us (P.R.) also appreciates support from an internal grant of TBU in Zlin IGA/CPS/2017/001 financed from funds of specific academic research. The authors M.M. and I.J. would like to acknowledge Slovenian Research Agency (ARRS) for the financial support (project L7-7566).

References

[1] S. Bhadra, D. Khastgir, N.K. Singha, J.H. Lee, Progress in preparation, processing and applications of polyaniline, Prog. Polym. Sci. 34 (2009) 783–810.
[2] J. Stejskal, R.G. Gilbert Polyaniline, Preparation of a conducting polymer (IUPAC technical report), Pure Appl. Chem. 74 (2002) 857–867.
[3] J. Stejskal, I. Sapurina, Polyaniline: thin films and colloidal dispersions (IUPAC technical report), Pure Appl. Chem. 77 (2005) 815–826.
[4] Z.F. Li, E. Ruckenstein, Improved surface properties of polyaniline films by blending with Pluronic polymers without the modification of the other characteristics, J. Colloid Interface Sci. 264 (2003) 362–369.
[5] P. Humpolicek, V. Kasparkova, P. Saha, J. Stejskal, Biocompatibility of polyaniline, Synth. Met. 162 (2012) 722–727.
[6] V. Kašpárková, P. Humpolíček, J. Stejskal, J. Kopecká, Z. Kuceková, R. Moučka, Conductivity impurity profile, and cytotoxicity of solvent-extracted polyaniline, Polym. Adv. Technol. 27 (2016) 156–161.
[7] J. Stejskal, M. Hajná, V. Kašpárková, P. Humpolíček, A. Zhigunov, M. Trchová, Purification of a conducting polymer polyaniline, for biomedical applications, Synth. Met. 195 (2014) 286–293.
[8] S. Tanwar, J.A. Ho, Green synthesis of novel polyaniline nanofibers: application in pH sensing, Molecules 20 (2015) 18585–18596.
[9] P. Humpolíček, K.A. Radaszkiewicz, V. Kašpárková, J. Stejskal, M. Trchová, Z. Kuceková, H. Vičarová, J. Pacherník, M. Lehocký, A. Minařík, Stem cell differentiation on conducting polyaniline, RSC Adv. 5 (2015) 68796–68805.
[10] P. Humpolíček, V. Kašpárková, J. Stejskal, Z. Kuceková, P. Ševčíková, Cell proliferation on a conducting polymer (Polyaniline), Chem. Listy 106 (2012) 380–383.
[11] M. Li, Y. Guo, Y. Wei, A.G. MacDiarmid, P.I. Lelkes, Electrospinning polyaniline-contained gelatin nanofibers for tissue engineering applications, Biomaterials 27 (2006) 2705–2715.
[12] P. Humpolíček, Z. Kuceková, V. Kašpárková, J. Pelková, M. Modic, I. Junkar, M. Trchová, P. Bober, J. Stejskal, M. Lehocký, Blood coagulation and platelet adhesion on polyaniline films, Colloid Surf. B 133 (2015) 278–285.

[13] K.G. Alves, E.F. de Melo, C.A. Andrade, C.P. de Mělo, Preparation of fluorescent polyaniline nanoparticles in aqueous solutions, J. Nanopart. Res. 15 (2013) 1–11.
[14] Z. Kucekova, P. Humpolicek, V. Kasparkova, T. Perecko, M. Lehocký, I. Hauerlandová, P. Sáha, J. Stejskal, Colloidal polyaniline dispersions: antibacterial activity, cytotoxicity and neutrophil oxidative burst, Colloids Surf. B 116 (2014) 411–417.
[15] J. Stejskal, I. Sapurina, On the origin of colloidal particles in the dispersion polymerization of aniline, J. Colloid Interface Sci. 274 (2004) 489–495.
[16] C.C. Liang, A.Y. Park, J.L. Guan, *In vitro* scratch assay: a convenient and inexpensive method for analysis of cell migration in vitro, Nat. Protoc. 2 (2007) 329–333.
[17] OECD, Test No. 439: *In Vitro* Skin Irritation: Reconstructed Human Epidermis Test Method, Organisation for Economic Co-operation and Development, 2015.
[18] A. Riede, M. Helmstedt, I. Sapurina, J. Stejskal, *In situ* polymerized polyaniline films. 4. Film formation in dispersion polymerization of aniline, J. Colloid Interface Sci. 248 (2002) 413–418.
[19] K. Crowley, M.R. Smyth, A.J. Killard, A. Morrin, Printing polyaniline for sensor applications, Chem. Pap. 67 (2013) 771–780.
[20] T. Syrový, P. Kuberský, I. Sapurina, S. Pretl, P. Bober, L. Syrová, A. Hamáček, J. Stejskal, Gravure-printed ammonia sensor based on organic polyaniline colloids, Sens. Actuators B: Chem. 225 (2016) 510–516.
[21] L. Yu, J.I.I. Lee, K.W. Shin, C.E. Park, R. Holze, Preparation of aqueous polyaniline dispersions by micellar-aided polymerization, J. Appl. Polym. Sci. 88 (2003) 1550–1555.
[22] B.J. Kim, S.G. Oh, M.G. Han, S.S. Im, Synthesis and characterization of polyaniline nanoparticles in SDS micellar solutions, Synth. Met. 122 (2001) 297–304.
[23] A. Kuczynska, A. Uygun, A. Kaim, H. Wilczura-Wachnik, A.G. Yavuz, M. Aldissi, Effects of surfactants on the characteristics and biosensing properties of polyaniline, Polym. Int. 59 (2010) 1650–1659.
[24] M. Trchová, Z. Moravková, I. Šeděnková, J. Stejskal, Spectroscopy of thin polyaniline films deposited during chemical oxidation of aniline, Chem. Pap. 66 (2012) 415–445.
[25] M. Trchová, Z. Morávková, M. Bláha, J. Stejskal, Raman spectroscopy of polyaniline and oligoaniline thin films, Electrochim. Acta 122 (2014) 28–38.
[26] H.M. Kowalczyńska, M. Nowak-Wyrzykowska, Modulation of adhesion, spreading and cytoskeleton organization of 3T3 fibroblasts by sulfonic groups present on polymer surfaces, Cell Biol. Int. 27 (2003) 101–114.

Article VIII.

Humpolicek, P.; Kasparkova, V.; Pachernik, J.; Stejskal, J.; Bober, P.; **Capakova, Z**.; Radaszkiewicz, K. A.; Junkar, I.; Lehocky, M. The Biocompatibility of Polyaniline and Polypyrrole: A Comparative Study of Their Cytotoxicity, Embryotoxicity and Impurity Profile. Mater. Sci. Eng. C-Mater. Biol. Appl. 2018, 91, 303–310. https://doi.org/10.1016/j.msec.2018.05.037.

Materials Science & Engineering C 91 (2018) 303–310

Contents lists available at ScienceDirect

Materials Science & Engineering C

journal homepage: www.elsevier.com/locate/msec

The biocompatibility of polyaniline and polypyrrole: A comparative study of their cytotoxicity, embryotoxicity and impurity profile

Petr Humpolíček[a,*], Věra Kašpárková[a], Jiří Pacherník[b], Jaroslav Stejskal[c], Patrycja Bober[c], Zdenka Capáková[a], Katarzyna Anna Radaszkiewicz[b], Ita Junkar[d], Marián Lehocký[a]

[a] Centre of Polymer Systems, Tomas Bata University in Zlin, 760 01 Zlin, Czech Republic
[b] Institute of Experimental Biology, Faculty of Science, Masaryk University, 625 00 Brno, Czech Republic
[c] Institute of Macromolecular Chemistry, Academy of Sciences of the Czech Republic, 162 06 Prague 6, Czech Republic
[d] Josef Stefan Institute, Jamova 39, Ljubljana 1000, Slovenia

ARTICLE INFO

Keywords:
Polyaniline
Polypyrrole
Biocompatibility

ABSTRACT

Conducting polymers (CP), namely polyaniline (PANI) and polypyrrole (PPy), are promising materials applicable for the use as biointerfaces as they intrinsically combine electronic and ionic conductivity. Although a number of works have employed PANI or PPy in the preparation of copolymers, composites, and blends with other polymers, there is no systematic study dealing with the comparison of their fundamental biological properties. The present study, therefore, compares the biocompatibility of PANI and PPy in terms of cytotoxicity (using NIH/3T3 fibroblasts and embryonic stem cells) and embryotoxicity (their impact on erythropoiesis and cardiomyogenesis within embryonic bodies). The novelty of the study lies not only in the fact that embryotoxicity is presented for the first time for both studied polymers, but also in the elimination of inter-laboratory variations within the testing, such variation making the comparison of previously published works difficult. The results clearly show that there is a bigger difference between the biocompatibility of the respective polymers in their salt and base forms than between PANI and PPy as such. PANI and PPy can, therefore, be similarly applied in biomedicine when solely their biological properties are considered. Impurity content detected by mass spectroscopy is presented. These results can change the generally accepted opinion of the scientific community on better biocompatibility of PPy in comparison with PANI.

1. Introduction

The impact of bioelectricity on physiological processes can be observed either on the level of individual cells, *e.g.,* the stem cell differentiation [1] and cell movement [2], or on the level of tissues, *e.g.*, the physiology of electro-sensitive tissues or wound healing [3]. In the preparation of a biocompatible biointerface, the combination of electronic and ionic conductivity is one of the key parameters; in this respect, conducting polymers (CP) are considered to be an excellent solution as they inherently combine both of these types of conductivities [4]. Though polyaniline (PANI) and polypyrrole (PPy) are the most studied conducting polymers, and there are a number of studies dealing with their preparation, characterization, and physico-chemical properties, the works which focus on their comparison are scarce as regards their chemistry [5,6] and especially their biological properties [7,8].

Both PANI and PPy have been used extensively for the preparation of composites with other materials and subsequently tested in terms of their biological properties, such as their *in vivo* capacities to cause reactions in tissues [9,10]. In spite of this, however, there are few studies describing the biological properties of pure PANI (*e.g.* in the form of powder [11]; colloids [12] or films [13,14]) or PPy [15]. This lack of knowledge is critical if biologically-oriented applications are to be considered.

The crucial characteristic of any material used in tissue engineering is its biocompatibility. It is very well known that biocompatibility is a complex characteristic combining a range of individual biological properties which are preferably tested using alternative *invitro* methods. Although *invitro* experiments can provide valuable information, its interpretation still presents a challenge, as any model (such as different cell lines) can behave differently and different conclusions can therefore be drawn. When comparing results published in literature, inter-laboratory variations in assay performance must also be considered, as the number of tests is not validated and each laboratory can apply a slightly different experimental set-up. For example, such variation and

* Corresponding author.
E-mail address: humpolicek@utb.cz (P. Humpolíček).

https://doi.org/10.1016/j.msec.2018.05.037
Received 14 November 2017; Received in revised form 9 May 2018; Accepted 10 May 2018
Available online 16 May 2018

inconsistency can occur as a result of the procedures for handling embryonic stem cells in individual laboratories. The presented work is, therefore, aimed at performing and discussing a complex comparative study of the fundamental biological impacts of PANI and PPy on NIH/3T3 fibroblasts, embryonic stem cells (ESc), and embryoid bodies (EBs) observed under the same conditions. Fibroblasts were chosen as they are the most frequently used line for the determination of cytotoxicity; ESc are a lineage with considerable potential for application in biomedicine and tissue engineering thanks to their naive phenotype and ability to differentiate into a variety of cell lineages; and the choice of EBs was motivated by the fact that their interaction with materials can be used as a marker of embryotoxicity.

The motivation for this study emerged from long term experience with CP and because PPy is understood by the scientific community to be more biocompatible than PANI even though the supposed superiority of PPy is not based on any experimental data.

2. Material and methods

2.1. Preparation and characterization of polymers

Polyaniline salt (PANI-S) was prepared using a standard procedure [16]. Specifically, a 0.2 M aqueous solution of aniline hydrochloride (Penta, Czech Republic) was oxidized with 0.25 M ammonium peroxydisulfate (APS; Penta, Czech Republic). Polymerization was carried out at room temperature for 12 h. The resulting green solids of polyaniline salt were collected on a filter, rinsed with 0.2 M hydrochloric acid, and similarly with acetone, and dried at room temperature over silica gel.

Polypyrrole salt (PPy-S) was synthetized by oxidizing 0.2 M pyrrole (Sigma-Aldrich) with 0.5 M iron (III) chloride hexahydrate (Sigma-Aldrich) in an aqueous environment. The oxidant to pyrrole mole ratio was 2.5. The mixture was left to polymerize at room temperature for 12 h. The black solids were collected on a filter and, similarly to PANI-S, rinsed with 0.2 M hydrochloric acid followed by acetone, and dried at room temperature over silica gel.

A part of both, PANI-S and PPy-S were deprotonated to polyaniline base (PANI-B) and polypyrrole base (PPy-B) by immersing the solids in an excess of 1 M aqueous ammonium hydroxide. SEM photomicrographs were captured using a JEOL 6400 microscope.

2.2. Preparation of polymer extracts

Samples were extracted according to a modification of protocol ISO 10993-12. The modification of the standard procedure involved the ratio between the mass of the extracted samples and the volume of the extraction medium. The standard procedure employs 0.2 g polymer per 1 mL cultivation medium. As the PPy samples were very fluffy and extremely difficult to separate from the medium after extraction, the ratio of 0.05 g of powder per 1 mL of cultivation medium was used for all tested samples. In this way a sufficient volume of each polymer extract was obtained for testing. Extraction was performed in chemically inert closed containers using an aseptic technique at 37 ± 1 °C under stirring for 24 h. The extracts were separated from the powders by double centrifugation at 1000 g for 15 min. The parent extracts (100%) were then diluted in a complete medium to obtain a series of dilutions with concentrations of 1, 5, 10, 25, and 50%. All extracts were used within 24 h. Prior to *in-vitro* testing, the samples were disinfected by means of sterile filtration through a 0.22 μm syringe filter (Millipore). Each of the concentrations was tested in quadruplicates, in four separate sets of experiment.

For mass spectroscopy analyses, the polymers were extracted using the procedure described above, but with deionized water as the extraction medium.

2.3. Characterization of polymer extracts

Aqueous polymer extracts were analysed using a 1260 Series liquid chromatography system (Agilent Technologies, Santa Clara, CA) coupled to a 6520 Accurate-Mass Q-TOF mass spectrometer (Agilent Technologies, Santa Clara, CA) equipped with a dual-spray electrospray ionization source. Aliquots of 5 μL were injected as an infusion into the system with no column installed. Compounds were eluted at 30 °C with an isocratic flow rate of 0.3 mL min^{-1} of 1% (v/v) formic acid in water. The positive ion mode mass spectrometry conditions were as follows: gas temperature, 300 °C; fragmentor voltage, 75 V; capillary voltage, 3.000 V; nozzle voltage, 2000 V; scan range m/z 50 to 1700; 1 scan/s. The internal mass reference ions m/z 121.050873 and m/z 922.009798 were used to keep the mass axis calibration stable during the analysis.

2.4. Cell lines and media

2.4.1. Mouse embryonic fibroblast cell line NIH/3T3 (ATCC CRL-1658TM)

ATCC–formulated Dulbecco's Modified Eagle's Medium, catalogue no. 30-2002, with added calf serum (BioSera, France) to a final concentration of 10% and penicillin/streptomycin, 100 U mL^{-1} (GE Healthcare HyClone, UK) was used as the culture medium.

The *embryonic stem cell ES R1* line (ESc) [17] was propagated in an undifferentiated state by culturing on gelatinized tissue culture dishes in complete media. The gelatinization was performed using 0.1% porcine gelatine. Complete media containing Dulbecco's Modified Eagle's Medium (DMEM), 15% fetal calf serum, 100 U mL^{-1} penicillin, 0.1 mg mL^{-1} streptomycin, 1 × non-essential amino acids solution (all from Gibco-Invitrogen; USA), 0.05 mM 2-mercaptoethanol (Sigma–Aldrich; USA), and 1000 U mL^{-1} leukemia inhibitory factor (Chemicon; USA) were used for the cultivation [13].

2.4.2. Cytotoxicity on ES R1 and NIH/3T3 cell lines

Cytotoxicity testing was performed according to ISO protocol 10 993-5. Cells were pre-cultivated for 24 h and seeded at a density of 5000 cells per cm^2 in the case of ESc or 12,000 per cm^2 in the case of NIH/3T3. The extracts were applied onto cells for 48 h (ESc) or 24 h (NIH/3T3). To assess the cytotoxic effects of PANI and PPy extracts on ESs, the mass of viable cells was determined as the level of ATP using Cellular ATP Kit HTS (Biothema, Sweden). Samples were prepared and analysed as published [18]. Before lyses, the morphology of the cells was observed and documented using an inverted Olympus phase contrast microscope (Olympus IX51, Japan) fitted up with a digital camera (Olympus E-450, Japan). To assess the viability of NIH/3T3 cells, MTT assay was used [19]. As a reference giving 100% cell viability, cells cultivated in pure complete media were used. The results are presented in two different ways. In addition to the strict processing of data according to the requirements of ISO 10 993-5 standard, statistical evaluation was also conducted using one-way analysis of variance ANOVA. ATP and MTT assays were evaluated using a Luminometer Infinite m200pro (Tecan, Switzerland).

2.4.3. Embryotoxicity

Embryotoxicity was determined as the likelihood of the formation of beating foci (the impact on cardiomyogenesis) and erythroid (red) clusters/colonies (the impact on erythropoiesis) within spontaneous differentiating ESc after exposure to the studied extracts. ESc differentiation was induced through the formation of embryoid bodies (EBs) by hanging drop techniques (400 cells per one 35 μL drop) in leukemia-inhibitory-free complete media described in ([20]. After 5 days, EBs were transferred to a gelatinized 24-well plate (one EB per well) in serum-free medium for the next 15 days and the medium was replaced with fresh medium every three days. Serum-free medium contained DMEM-F12 medium (1:1), 100 U mL^{-1} penicillin, 0.1 g mL^{-1} streptomycin, and 1 × insulin-transferrin-selen (ITS) supplement (all from

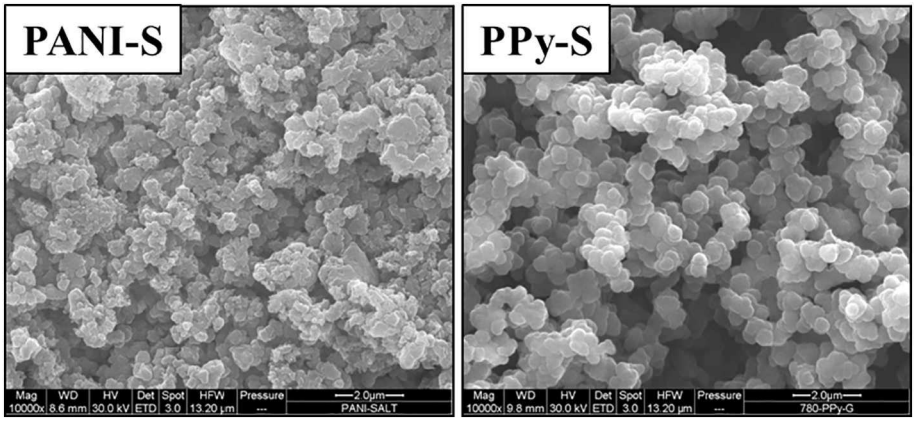

Fig. 1. The morphology of PANI-S and PPy-S visualized by SEM.

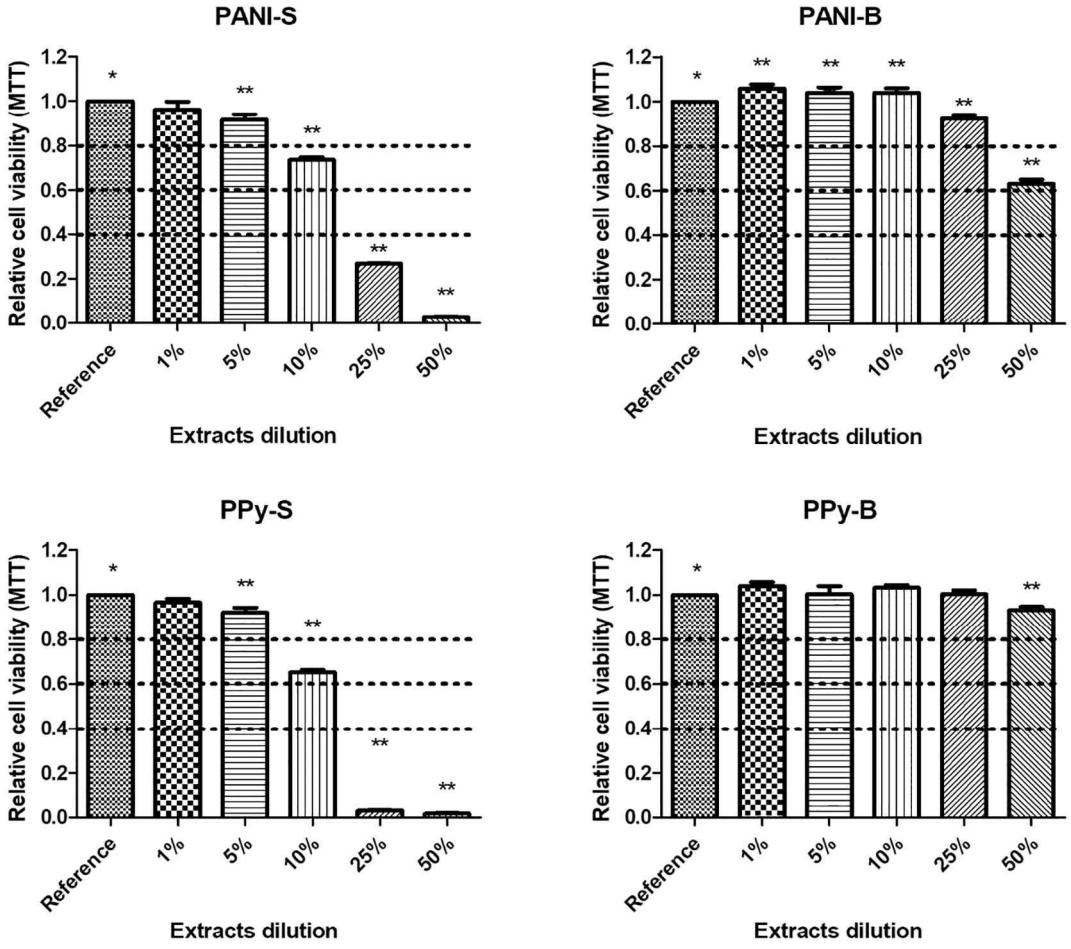

Fig. 2. Cytotoxicity of extracts of PANI and PPy towards NIH/3T3 cells determined by MTT assay. The different superscripts correspond to significant differences ($P \leq 0.05$) compared to the reference. The dashed lines highlight the limits of viability according to EN ISO 10993-5: viability > 0.8 corresponds to no cytotoxicity, > 0.6–0.8 mild cytotoxicity, > 0.4–0.6 moderate cytotoxicity and < 0.4 severe cytotoxicity.

Gibco-Invitrogen; USA). Differentiating cells were observed and documented using an inverted Olympus phase contrast microscope (Olympus IX51, Japan) equipped with digital camera (Olympus E-450, Japan) [13].

3. Results and discussion

Each of the studied polymers was synthesized using the most common preparation procedure employed within the chemical oxidation routes. Therefore, PANI was synthetized using the oxidation of aniline hydrochloride with ammonium persulfate according to the respective IUPAC protocol [16], and PPy was prepared *via* the oxidation of pyrrole with iron(III) chloride, which is the oxidant of first choice in the preparation of this polymer (Fig. 1) [21,22].

There is a common opinion in the scientific community and literature that PPy is more biocompatible than PANI. This generally accepted opinion is, however, based on indirect comparisons of studies conducted on these polymers [23]. The present study is the first to compare

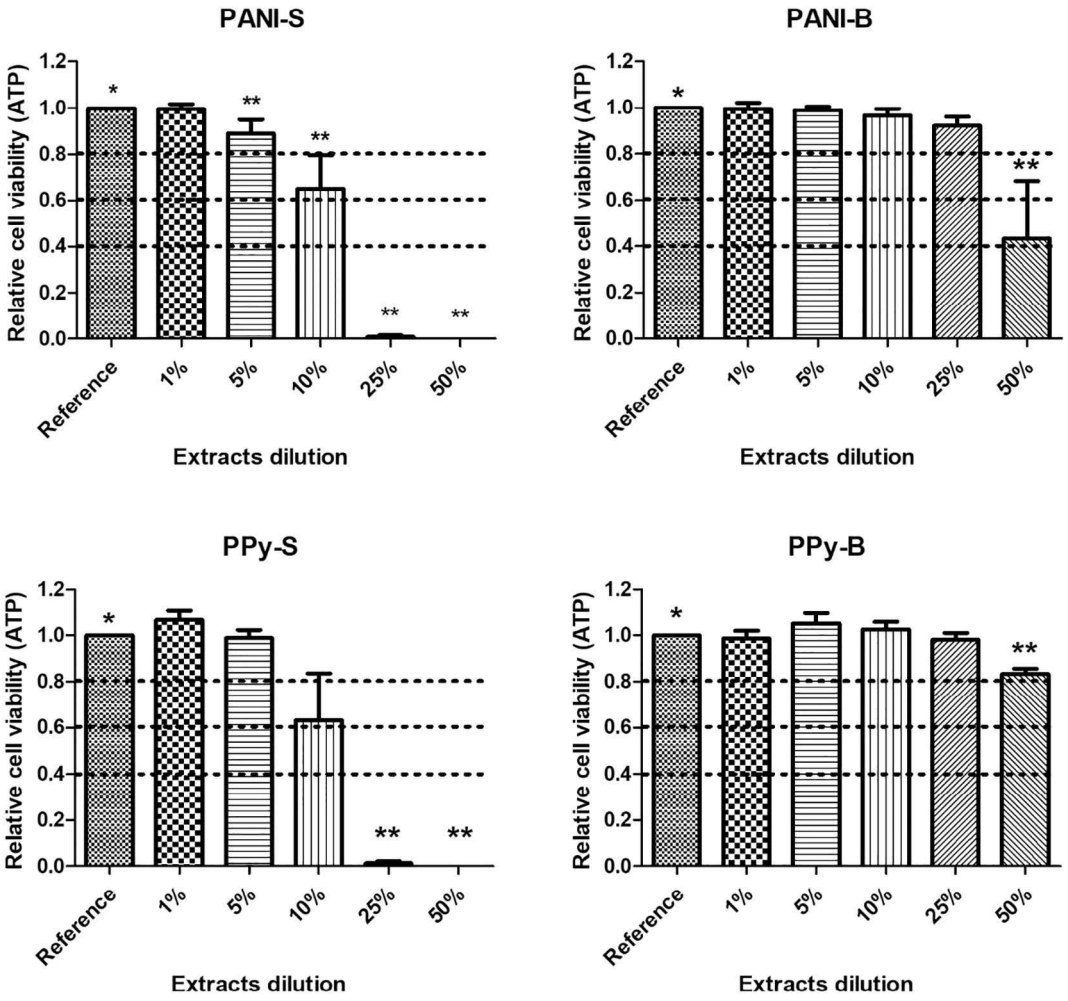

Fig. 3. Cytotoxicity of extracts of PANI and PPy on ESc determined by the relative level of ATP compared to the reference. The different superscripts correspond to significant differences ($P \leq 0.05$) compared to the reference. The dashed lines highlight the limits of viability according to EN ISO 10993-5: viability > 0.8 corresponds to no cytotoxicity, > 0.6–0.8 mild cytotoxicity, > 0.4–0.6 moderate cytotoxicity and < 0.4 severe cytotoxicity.

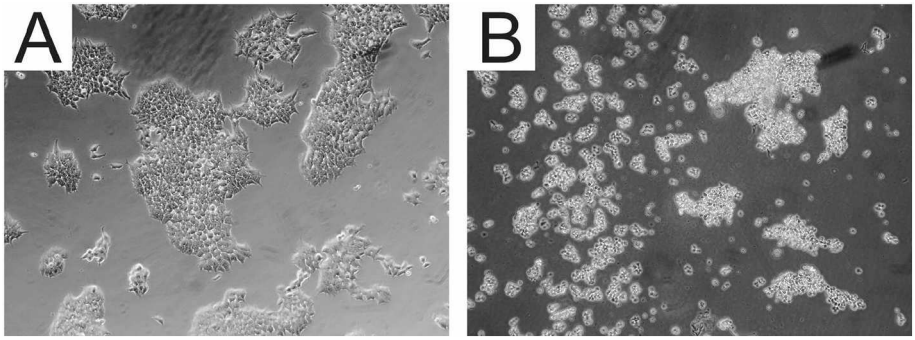

Fig. 4. The cytotoxicity of a tested sample towards ESc. A) reference, B) cytotoxic effect observed after the application of the 5% extract of PPy-S. Cell destruction after the application of PPy extract is obvious. Magnification: 100×.

the biological properties of these two most important CP determined under the same conditions, using the same cell lineages and methodology, and performed in the same laboratory. The results are therefore unique and difficult to compare meaningfully with those published in any previous works. Previous studies mainly investigated these polymers separately, using different methodologies, test protocols, and ways of processing the results obtained. Moreover, most of these works do not examine these CP alone, but their composites or blends with other thermoplastic polymers [24,25].

Therefore, the motivation of this study was to provide a comprehensive view of the biological properties of PANI and PPy as a base line for additional advanced studies dealing with the exploitation of these promising CP in biomedicine, regenerative medicine, and biosensors in electro-sensitive tissues.

Cytotoxicity tests are the test of first choice when the biocompatibility of materials, including polymers, is evaluated. According to the EN ISO 10993 protocol, mouse fibroblasts are the cells most commonly used to determine the cytotoxicity of polymers after the application of their extracts. Due to advances in the biomaterial sciences, ESc are also frequently used to determine and evaluate the biocompatibility of

Table 1
Cardiomyogenesis or erythropoiesis observed after contact of ES R1 ECs with PANI and PPy extracts. Results are expressed as a number of beating foci or erythroid clusters relative to the reference.

	Formed beating foci [%]			
Extract concentration [%]	PANI-S	PANI-B	PPy-S	PPy-B
Reference	100	100	100	100
1	100	100	100	100
5	50	100	75	100
25	0	100	0	100

	Formed erythroid clusters [%]			
Reference	100	100	100	100
1	100	100	75	100
5	13	100	50	100
25	0	100	0	100

materials and products. Thus, the cytotoxicities of PANI and PPy were determined not only using NIH/3T3 fibroblasts but also ESc. The results regarding NIH/3T3 cells are presented in Fig. 2 and illustrate that the extracts of both salts, PANI-S and PPy-S, lost their cytotoxicity at concentrations of 5% and below. In contrast, PPy-B did not induce any cytotoxicity, even when NIH/3T3 cells were cultivated in the presence of 50% extract; in the case of PANI-B the corresponding effect was observed at an extract concentration of 25%. The results unambiguously illustrate that PANI and PPy in their base form are notably less cytotoxic than both polymers in the form of salts. With respect to ECs (Figs. 3 and 4), the results were very similar to those for NIH/3T3 cells. That is, both bases exhibited notably lower cytotoxicity in comparison with the corresponding salts.

The embryotoxicity of PANI and PPy was studied with respect to the spontaneous differentiation of ES R1 cells using two parameters, namely the formation of beating foci, which is a marker of cardiomyogenesis, and the formation of erythroid clusters as a marker of erythropoiesis.

The results of the embryotoxicity test summarised in Table 1 show only minor differences within the two sets of samples, namely when the PANI-S with PPy-S and PANI-B with PPy-B are compared. Both PANI-B and PPy-B performed equally and the levels of formation of beating foci and erythroid clusters even corresponded to the reference. Therefore, it was not possible to determine the threshold concentration of extract at which cardiomyogenesis or erythropoiesis were influenced by these polymer extracts. The impacts of the PANI-S and PPy-S were, however, different, and their extracts terminated cardiomyogenesis and erythropoiesis in all EBs at a concentration of 25% in cultivation medium. The example of erythroid clusters formation is shown on the Fig. 5. The most adverse effect on erythropoiesis was exhibited by the PPy-S, which was capable of terminating 25% EB at an extract concentration of 1%. Similarly to cytotoxicity, bigger differences were observed between the behaviours of the respective salts and bases than between the pure forms of PANI and PPy.

To the best the authors' knowledge, there is only one previously published comprehensive study focused on the cytotoxicity of PANI in its native globular form [11] and one study dealing with the cytotoxicity of PPy prepared by the standard oxidation method [10] including both *in-vitro* and *in-vivo* investigations. In both of these studies, biocompatibility was assessed using extracts of polymers in culture medium or saline. There are also other studies concerning the cytotoxicity of PPy, but focused on their nanoparticle form [26,27], which make their results non-comparable to ours as the methodology of preparation is different. It is also well known that cytotoxicity of nanoparticles is different from that of the polymer in globular form and, in addition to chemical composition, it depends also on size and shape of the nanoparticles.

As mentioned above when describing the methods used for investigating the biological properties of PANI and PPy, a ratio of 0.05 g to 1 mL^{-1} of cultivation medium instead of the ISO-defined ratio of 0.2 g to 1 mL^{-1} was used to prepare the extracts of all samples in the test. The reason for this modification was the difficulty of separating PPy from the supernatant (medium) after polymer extraction. For the sake of comparison, PANI extracts were prepared in the same manner. The different starting concentrations of extracts obtained in this work make meaningful comparison of our results with those in literature somewhat complicated. Nevertheless, the comparison was performed and the current results were correlated with those reported by Humpolíček et al. [11] who investigated cytotoxicity of standard extracts (0.2 g to mL^{-1}) of PANI salt and PANI base. For comparison purposes, it can be considered that concentrations of extracts from current work are one-fourth of the concentrations prepared by standard procedure. In the work of Humpolíček, the cytotoxicity towards HaCaT and HepG2 cells was determined, revealing non-cytotoxic threshold concentrations of 1% for PANI-salt and 10% for PANI-base. These results are in accord with those observed for NIH/3T3 and ESc in the current study, which showed an absence of cytotoxicity at extract concentrations of 5% for PANI-S and 25% for PANI-B. When considering the use of different cell lines in both studies and fact that correlation of cytotoxicity with concentrations of impurities in an extract may not always be strictly linear, it can be concluded that the cytotoxicities of PANI-S and PANI-B, as determined in the current study, are similar.

The biocompatibility of PPy was determined by Wang et al. [10] using PPy-salt extracted at a ratio of 1 g to 10 mL saline, according to ISO protocol 10,993. Their work demonstrated that the viability and proliferation rates of Schwann cells in the presence of PPy extract in culture medium at a concentration of 25% (in the original article, referred to as 100 µL of 50% extract and 100 µL of cultivation medium) even improved in comparison with the control sample containing a corresponding amount of saline solution in medium, and equalled the cell behaviour in plain medium. The authors hence concluded that the polymer extract exhibited the absence of cytotoxicity. The current study, however, showed that PPy-S samples were cytotoxic down to a concentration of 5% and that cytotoxicity was reduced by transferring PPy-S to its base form (PPy-B), which was non-cytotoxic in the presence

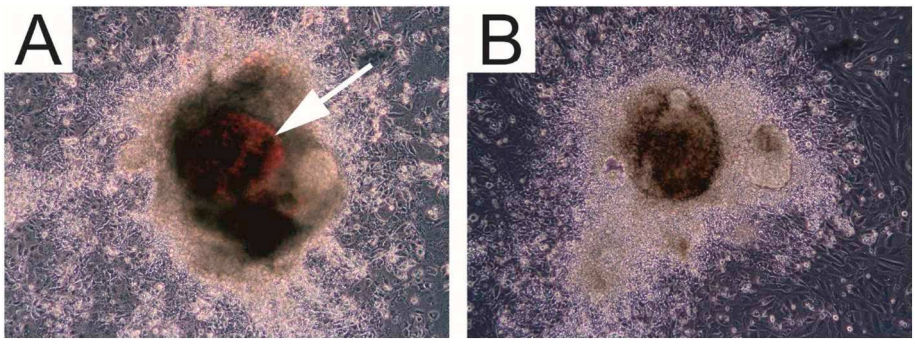

Fig. 5. The formation of erythroid clusters (red cluster marked with arrow) within the embryoid body. A) positive reference; B) absence of the red erythroid cluster after cultivation in the presence of 25% extracts of PANI-S. Magnification 100×. (For interpretation of the references to color in this figure legend, the reader is referred to the web version of this article.)

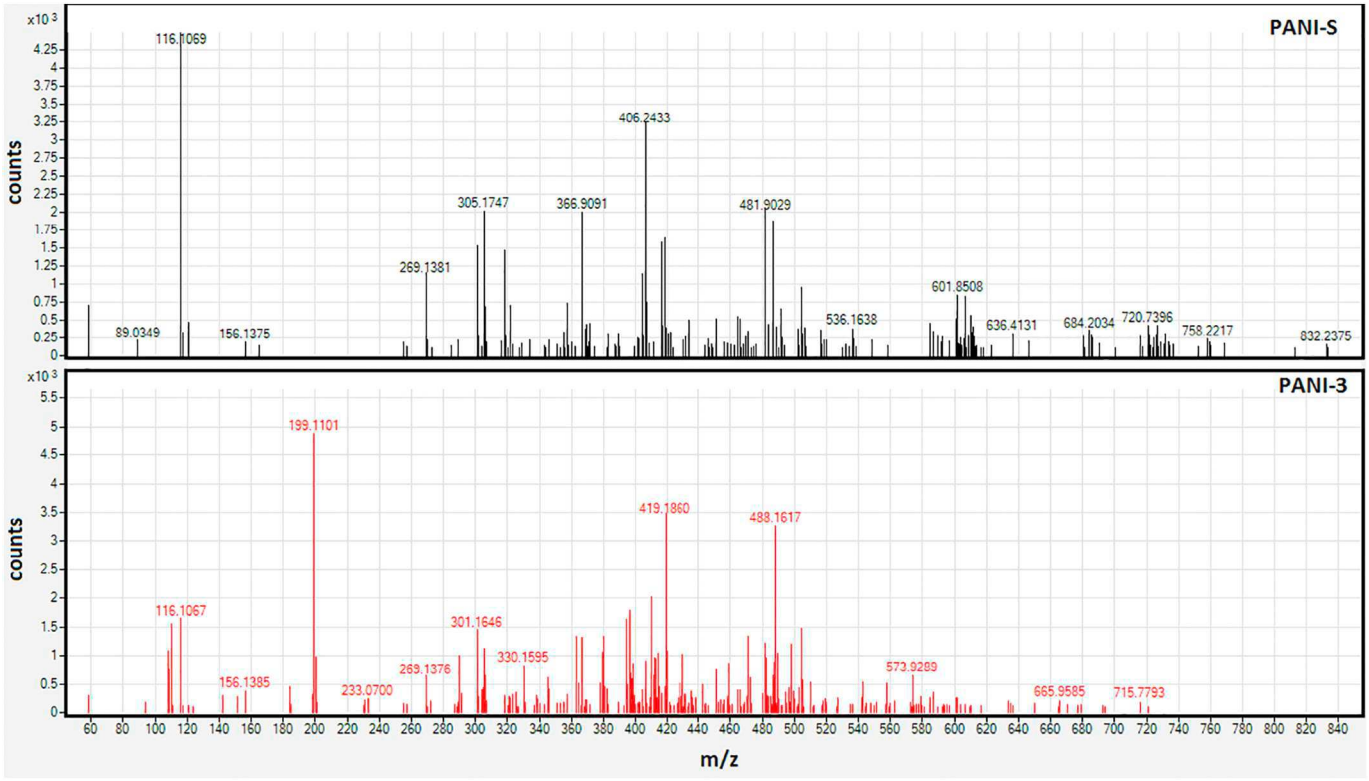

Fig. 6. Mass spectra of PANI-S and PANI-B samples.

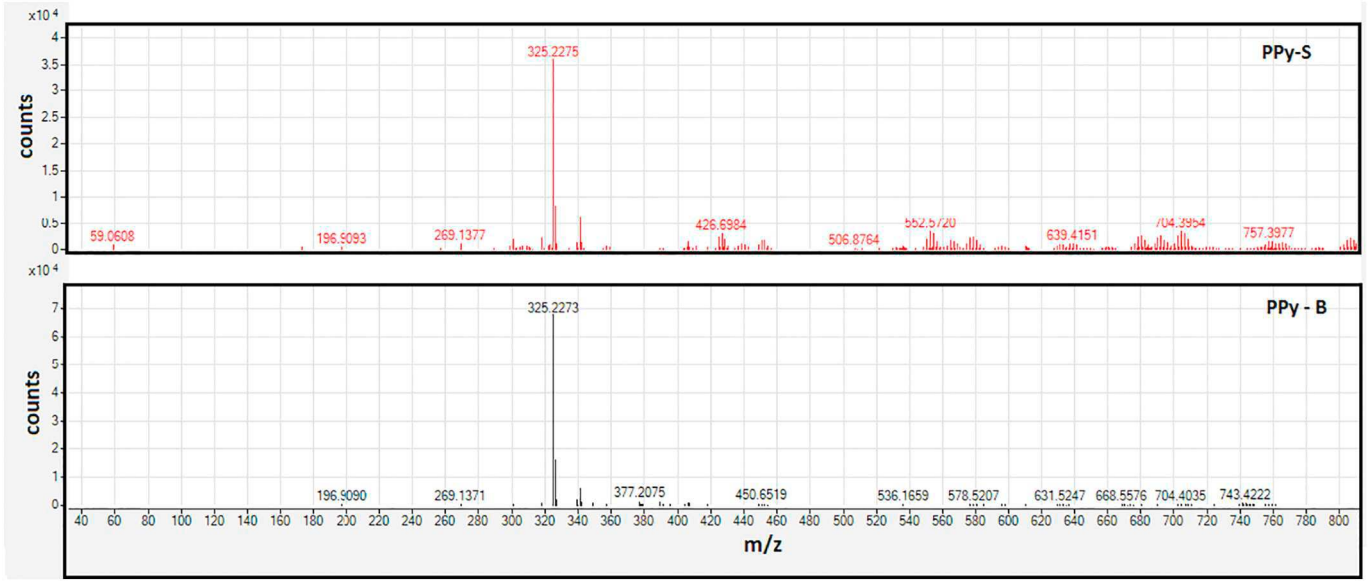

Fig. 7. Mass spectra of PPy-S and PPy-B samples.

of 50% extract. Though the polymers from these two studies were prepared by the oxidation of pyrrole with $FeCl_3$, different concentrations and ratios of individual monomers were used during syntheses; moreover, Wang et al. provided no information on the purification of the polymer used.

It is, however, much more important that, according to the results in Figs. 2 and 3, the cytotoxicities of PANI and PPy in their respective forms are comparable. To be more specific, the cytotoxicity depends more on the form of PANI or PPy (salt *vs* base) than on the type of polymer (PANI *vs* PPy). It should, however, be stressed that the current work covers only the most commonly used ways of synthesizing these conducting polymers. Considering other possible oxidation agents, whether of chemical or biological origin, the situation with respect to cytotoxicity might be different.

The impact of PANI and PPy on erythropoiesis and cardiomyogenesis has never been studied before. Nevertheless, it can be concluded that the threshold concentrations at which embryogenesis processes are influenced correlate with the cytotoxicities of individual polymer extracts. Similarly to cytotoxicity, embryogenesis and cardiomyogenesis depends more on the form of polymer (salt *vs* base) than on its type (PANI *vs* PPy).

As already mentioned, systematic work was previously undertaken

to determine the reasons for the cytotoxicity of PANI. Based on the work of Stejskal et al. [28] and Kašpárková et al. [29] it can be assumed that such cytotoxic effects are mainly connected with the presence of low-molecular-weight impurities. In order to improve our view of the correlation between biocompatibility and the contents of impurities, mass spectroscopy analyses of the studied samples were conducted with the aim of obtaining an insight into the structures of impurities extracted from polymers that might be responsible for their cytotoxic effects. The mass spectra of PANI-S and PANI-B are presented in Fig. 6. As can be seen, the samples contain a relatively rich mass profile with several major molecular ions $(M^+H)^+$. By comparison, it can be noticed that the PANI-S sample comprises slightly more fractions with molecular weights higher than 700 g mol^{-1} than the PANI-B sample. On the other hand, PANI-B exhibits a more complicated mass profile especially in the region 300–550 m/z. Although many signals of various intensities are present in both samples, it is obvious that PANI-B contains masses not found in PANI-S, such as those in the low m/z region – for example, 199.1101 and 233.0700. Of all the masses present, only the following were identified in PANI-S: aniline (m/z = 94.0645), *p*-benzoquinone imine (m/z = 108.0682), and *p*-aminophenol (m/z = 110.0599). Also tetramer (m/z = 290.1297, [30]) and quinoneiminoid structure (m/z = 290.1297) proposed by Kříž et al. [31], and Stejskal and Trchová [32] were assigned as possible impurities present in the extract.

As shown in Fig. 7, both PPy extracts exhibited much simpler mass spectra than extracts of PANI. In PPy-S and PPy-B, one dominant ion, m/z = 325.2275, was found, while higher masses were detected only with low intensities, in particular in PPy-S extracts. The substance corresponding to this mass, however, is probably non-cytotoxic as it is present in both samples. An interesting question therefore arises as to which of the substances present in PPy-S are involved in cytotoxic effects.

After careful inspection of MS data, it can be concluded that it was not possible to detect linear oligomers as possible impurities, as they were probably absent from the samples. The exact masses calculated, however, indicate that the impurities extracted from the samples comprise oxygen and that, therefore, oxygen containing by-products are probably the most frequent impurities in the samples.

In spite of the limited success of MS in identifying impurities in PANI and PPy, these spectroscopic analyses showed that both PANI-B and PPy-B contain lower numbers and amounts of impurities and have relatively simple impurity profiles. The reduced contents of impurities logically reflect the process to which both polymers are subjected during the transformation from salt to base. The process of re-protonation can, therefore, be considered as an additional purification step removing substances with potentially cytotoxic effects.

4. Conclusion

It is generally accepted in the scientific community that polypyrrole shows more favourable biological properties than polyaniline, which is reflected by prevalence of publications dealing with the first mentioned polymer. Until now, however, no study provided direct comparison of these two polymers in terms of their biological properties recorded under the same conditions. Therefore, both polypyrrole and polyaniline were synthetized by the most common procedures and studied within one laboratory to eliminate the inter-laboratory differences. Two parameters of biocompatibility were studied; the first, basic one - cytotoxicity was investigated using common fibroblasts NIH/3T3 cell line and embryonic stem cells. The second, advanced parameter - embryotoxicity was studied in terms of the impact of each of the polymers on the erythropoiesis and cardiomyogenesis within the embryonic bodies. The direct comparison of both polymers using the same methodology showed that the form of the polymer (salt *vs* base) is more important than its type (polypyrrole *vs* polyaniline) when cytotoxicity and embryotoxicity are taken into consideration. Especially the polymers in the form of bases proved low cytotoxicity and embryotoxicity. To clarify the reasons for determined differences in biological properties of polyaniline and polypyrrole, the mass spectroscopy was used to determine their impurity profiles. The detected impurities can't, however, fully explain observed differences. For example, with respect to presence of major molecular ions, the extract of polypyrrole base exhibited simpler mass spectra in comparison with extract of polyaniline base. However, as it was already mentioned their biological properties were similar. Therefore, the presented results should mainly provoke the scientific community to compare also other biological properties of both conducting polymers as, according to currently presented results, they are more similar than previously assumed and their application potential can be, at least, comparable.

Acknowledgments

This work was supported by the Czech Science Foundation (17-05095S) and by the Ministry of Education, Youth and Sports of the Czech Republic – Program NPU I (LO1504). Authors thank to Pavel Kucharczyk for help with LC-MS analysis.

References

[1] J.A. Genovese, C. Spadaccio, J. Langer, J. Habe, J. Jackson, A.N. Patel, Electrostimulation induces cardiomyocyte predifferentiation of fibroblasts, Biochem. Biophys. Res. Commun. 370 (2008) 450–455.
[2] C.D. McCaig, A.M. Rajnicek, B. Song, M. Zhao, Controlling cell behavior electrically: current views and future potential, Physiol. Rev. 85 (2005) 943–978.
[3] L.C. Kloth, Electrical stimulation for wound healing: a review of evidence from in vitro studies, animal experiments, and clinical trials, Int. J. Low. Extrem. Wounds 4 (2005) 23–44.
[4] B. Weng, J. Diao, Q. Xu, Y. Liu, C. Li, A. Ding, J. Chen, Bio-interface of conducting polymer-based materials for neuroregeneration, Adv. Mater. Interfaces 2 (2015) (1500059).
[5] J. Stejskal, M. Omastová, S. Fedorova, J. Prokeš, M. Trchová, Polyaniline and polypyrrole prepared in the presence of surfactants: a comparative conductivity study, Polymer 44 (2003) 1353–1358.
[6] J. Kim, S.D. Deshpande, S. Yun, Q. Li, A comparative study of conductive polypyrrole and polyaniline coatings on electro-active papers, Polym. J. 38 (2006) 659–668.
[7] N.K. Guimard, N. Gomez, C.E. Schmidt, Conducting polymers in biomedical engineering, Prog. Polym. Sci. 32 (2007) 876–921.
[8] A. Bendrea, L. Cianga, I. Cianga, Progress in the field of conducting polymers for tissue engineering applications, J. Biomater. Appl. 26 (2011) 3–84.
[9] T.H. Qazi, R. Rai, A.R. Boccaccini, Tissue engineering of electrically responsive tissues using polyaniline based polymers: a review, Biomaterials 35 (2014) 9068–9086.
[10] X. Wang, X. Gu, C. Yuan, S. Chen, P. Zhang, T. Zhang, J. Yao, F. Chen, G. Chen, Evaluation of biocompatibility of polypyrrole in vitro and in vivo, J. Biomed. Mater. Res. A 68 (2004) 411–422.
[11] P. Humpolíček, V. Kašpárková, P. Sáha, J. Stejskal, Biocompatibility of polyaniline, Synth. Met. 162 (2012) 722–727.
[12] Z. Kuceková, P. Humpolíček, V. Kašpárková, T. Perecko, M. Lehocký, I. Hauerlandová, P. Sáha, J. Stejskal, Colloidal polyaniline dispersions: antibacterial activity, cytotoxicity and neutrophil oxidative burst, Colloids Surf. B Biointerfaces 116 (2014) 411–417.
[13] P. Humpolíček, K.A. Radaszkiewicz, V. Kašpárková, J. Stejskal, M. Trchová, Z. Kuceková, H. Vicarova, J. Pacherník, M. Lehocký, A. Minařík, Stem cell differentiation on conducting polyaniline, RSC Adv. 5 (2015) 68796–68805.
[14] P. Humpolíček, Z. Kuceková, V. Kašpárková, J. Pelková, M. Modic, I. Junkar, M. Trchová, P. Bober, J. Stejskal, M. Lehocký, Blood coagulation and platelet adhesion on polyaniline films, Colloids Surf. B Biointerfaces 133 (2015) 278–285.
[15] A. Ramanaviciene, A. Kausaite, S. Tautkus, A. Ramanavicius, Biocompatibility of polypyrrole particles: an in-vivo study in mice, J. Pharm. Pharmacol. 59 (2007) 311–315.
[16] J. Stejskal, R.G. Gilbert, Polyaniline. Preparation of a conducting polymer (IUPAC technical report), Pure Appl. Chem. 74 (2002) 857–867.
[17] A. Nagy, J. Rossant, R. Nagy, W. Abramow-Newerly, J.C. Roder, Derivation of completely cell culture-derived mice from early-passage embryonic stem cells, Proc. Natl. Acad. Sci. U. S. A. 90 (1993) 8424–8428.
[18] R. Konopka, M. Hýzdalová, L. Kubala, J. Pacherník, New luminescence-based approach to measurement of luciferase gene expression reporter activity and adenosine triphosphate-based determination of cell viability, Folia Biol. 56 (2010) 66–71.
[19] C. Della Pina, Z. Capáková, A. Sironi, P. Humpolíček, P. Sáha, E. Falletta, On the cytotoxicity of poly(4-aminodiphenylaniline) powders: effect of acid dopant type and sample posttreatment, Int. J. Polym. Mater. Polym. Biomater. 66 (2017) 132–138.
[20] K.A. Radaszkiewicz, D. Sýkorová, L. Binó, J. Kudová, M. Bébarová, J. Procházková, H. Kotasová, L. Kubala, J. Pacherník, The acceleration of cardiomyogenesis in embryonic stem cells in vitro by serum depletion does not increase the number of

developed cardiomyocytes, PLoS One 12 (2017) e0173140.
[21] S.P. Armes, Optimum reaction conditions for the polymerization of pyrrole by iron (III) chloride in aqueous solution, Synth. Met. 20 (1987) 365–371.
[22] S. Machida, S. Miyata, A. Techagumpuch, Chemical synthesis of highly electrically conductive polypyrrole, Synth. Met. 31 (1989) 311–318.
[23] E. Jabbari, D. Kim, L.P. Lee, Handbook of Biomimetics and Bioinspiration: Biologically-Driven Engineering of Materials, Processes, Devices, and Systems, World Scientific, 2014.
[24] J. Jang, H. Yoon, Multigram-scale fabrication of monodisperse conducting polymer and magnetic carbon nanoparticles, Small 1 (2005) 1195–1199.
[25] J. Hong, H. Yoon, J. Jang, Kinetic study of the formation of polypyrrole nanoparticles in water-soluble polymer/metal cation systems: a light-scattering analysis, Small 6 (2010) 679–686.
[26] S. Kim, W. Oh, Y.S. Jeong, J. Hong, B. Cho, J. Hahn, J. Jang, Cytotoxicity of, and innate immune response to, size-controlled polypyrrole nanoparticles in mammalian cells, Biomaterials 32 (2011) 2342–2350.
[27] A. Ramtin, A. Seyfoddin, F. Coutinho, G. Waterhouse, I. Rupenthal, D. Svirskis, Cytotoxicity considerations and electrically tunable release of dexamethasone from polypyrrole for the treatment of back-of-the-eye conditions, Drug Deliv. Transl. Res. 6 (2016) 793–799.
[28] J. Stejskal, M. Hajná, V. Kašpárková, P. Humpolíček, A. Zhigunov, M. Trchová, Purification of a conducting polymer, polyaniline, for biomedical applications, Synth. Met. 195 (2014) 286–293.
[29] V. Kašpárková, P. Humpolíček, J. Stejskal, J. Kopecká, Z. Kuceková, R. Moučka, Conductivity, impurity profile, and cytotoxicity of solvent-extracted polyaniline, Polym. Adv. Technol. 27 (2016) 156–161.
[30] Z. Ding, T. Sanchez, A. Labouriau, S. Iyer, T. Larson, R. Currier, Y. Zhao, D. Yang, Characterization of reaction intermediate aggregates in aniline oxidative polymerization at low proton concentration, J. Phys. Chem. B 114 (2010) 10337–10346.
[31] J. Kříž, L. Starovoytova, M. Trchová, E.N. Konyushenko, J. Stejskal, NMR investigation of aniline oligomers produced in the early stages of oxidative polymerization of aniline, J. Phys. Chem. B 113 (2009) 6666–6673.
[32] J. Stejskal, M. Trchová, Aniline oligomers versus polyaniline, Polym. Int. 61 (2012) 240–251.

Article IX.

Capakova, Z.; Radaszkiewicz, K. A.; Acharya, U.; Truong, T. H.; Pachernik, J.; Bober, P.; Kasparkova, V.; Stejskal, J.; Pfleger, J.; Lehocky, M.; Humpolicek, P. The Biocompatibility of Polyaniline and Polypyrrole 2(1): Doping with Organic Phosphonates. Mater. Sci. Eng. C-Mater. Biol. Appl. 2020, 113, 110986. https://doi.org/10.1016/j.msec.2020.110986.

Materials Science & Engineering C 113 (2020) 110986

Contents lists available at ScienceDirect

Materials Science & Engineering C

journal homepage: www.elsevier.com/locate/msec

The biocompatibility of polyaniline and polypyrrole 2[1]: Doping with organic phosphonates

Zdenka Capáková[a], Katarzyna Anna Radaszkiewicz[b], Udit Acharya[c], Thanh Huong Truong[a], Jiří Pacherník[b], Patrycja Bober[c], Věra Kašpárková[a,d], Jaroslav Stejskal[c], Jiří Pfleger[c], Marián Lehocký[a,d], Petr Humpolíček[a,d,*]

[a] Centre of Polymer Systems, Tomas Bata University in Zlin, 760 01 Zlin, Czech Republic
[b] Department of Experimental Biology, Faculty of Science, Masaryk University, 625 00 Brno, Czech Republic
[c] Institute of Macromolecular Chemistry, Academy of Sciences of the Czech Republic, 162 06 Prague 6, Czech Republic
[d] Faculty of Technology, Tomas Bata University in Zlin, 760 01 Zlin, Czech Republic

ARTICLE INFO

Keywords:
Polyaniline
Polypyrrole
Conducting polymers biocompatibility
Phosphonates
Embryonic stem cells

ABSTRACT

Conducting polymers (CP) can be used as pH- and/or electro-responsive components in various bioapplications, for example, in 4D smart scaffolds. The ability of CP to maintain conductivity under physiological conditions is, therefore, their crucial property. Unfortunately, the conductivity of the CP rapidly decreases in physiological environment, as their conducting salts convert to non-conducting bases. One of the promising solutions how to cope with this shortcoming is the use of alternative "doping" process that is not based on the protonation of CP with acids but on interactions relying in acidic hydrogen bonding. Therefore, the phosphonates (dimethyl phosphonate, diethyl phosphonate, dibutyl phosphonate, or diphenyl phosphonate) were used to re-dope two most common representatives of CP, polyaniline (PANI) and polypyrrole (PPy) bases. As a result, PANI doped with organic phosphonates proved to have significantly better stability of conductivity under different pH. It has also been shown that cytotoxicity of studied materials determined on embryonic stem cells and their embryotoxicity, determined as the impact on cardiomyogenesis and erythropoiesis, depend both on the polymer and phosphonate types used. With the exception of PANI doped with dibutyl phosphonate, all PPy-based phosphonates showed better biocompatibility than the phosphonates based on PANI.

1. Introduction

Compared with metals that exhibit solely electronic conductivity, the combined electronic and ionic conductivity of CP is one of their most attractive properties when the applications in regenerative medicine, tissue engineering or bio-sensing are considered [1,2]. Ionic conductivity of CP is fundamental for the communication with biological objects, as it relies on ionic fluxes. PANI and PPy are two members of CP family, which are intensively studied for biological applications, [3,4]; however, their conductivity depends strongly on environmental conditions. Besides the impact of pH, which will be discussed below, the conductivity of PANI is notably influenced by temperature during polymerization [5,6]. The study of Bláha et al. [6] showed that the increase of temperature from −20 to 40 °C during PANI synthesis played the key role in controlling its molecular structure, morphology and crystallinity, and it strongly affects the conductivity. Similarly as in PANI, conductivity of PPy is also influenced by preparation temperature. Ready-synthetized PPy changes its conductivity with temperature variation [7] and different temperatures applied during PPy synthesis have impact on its resulting conductivity as well [8]. Influence of various doping agents, *e.g.*, chlorine or dodecylsulfate anions [9] or *p*-toluenesulfonic, itaconic and fumaric acids on PPy conductivity cannot be ignored, either [10].

As mentioned above, the critical factor limiting the use of CP in a number of biomedical applications is the decrease of their conductivity under physiological pH, as the conducting salts are converted to non-conducting bases already below this pH region [11]. There have been outlined, and even tested, several approaches how to improve the pH stability of CPs including, for example, electrochemical polymerization or re-protonation with perfluorooctanesulfonic [11] or poly(2-acrylamido-2-methyl-1-propanesulfonic acids) [12]. The perspective approach to solve this limitation can be the use of alternative "doping"

* Corresponding author at: Centre of Polymer Systems, Tomas Bata University in Zlin, 760 01 Zlin, Czech Republic.
E-mail address: humpolicek@utb.cz (P. Humpolíček).
[1] For Part 1, see Humpolíček et al. [20].

https://doi.org/10.1016/j.msec.2020.110986
Received 14 January 2020; Received in revised form 31 March 2020; Accepted 17 April 2020
Available online 20 April 2020
0928-4931/

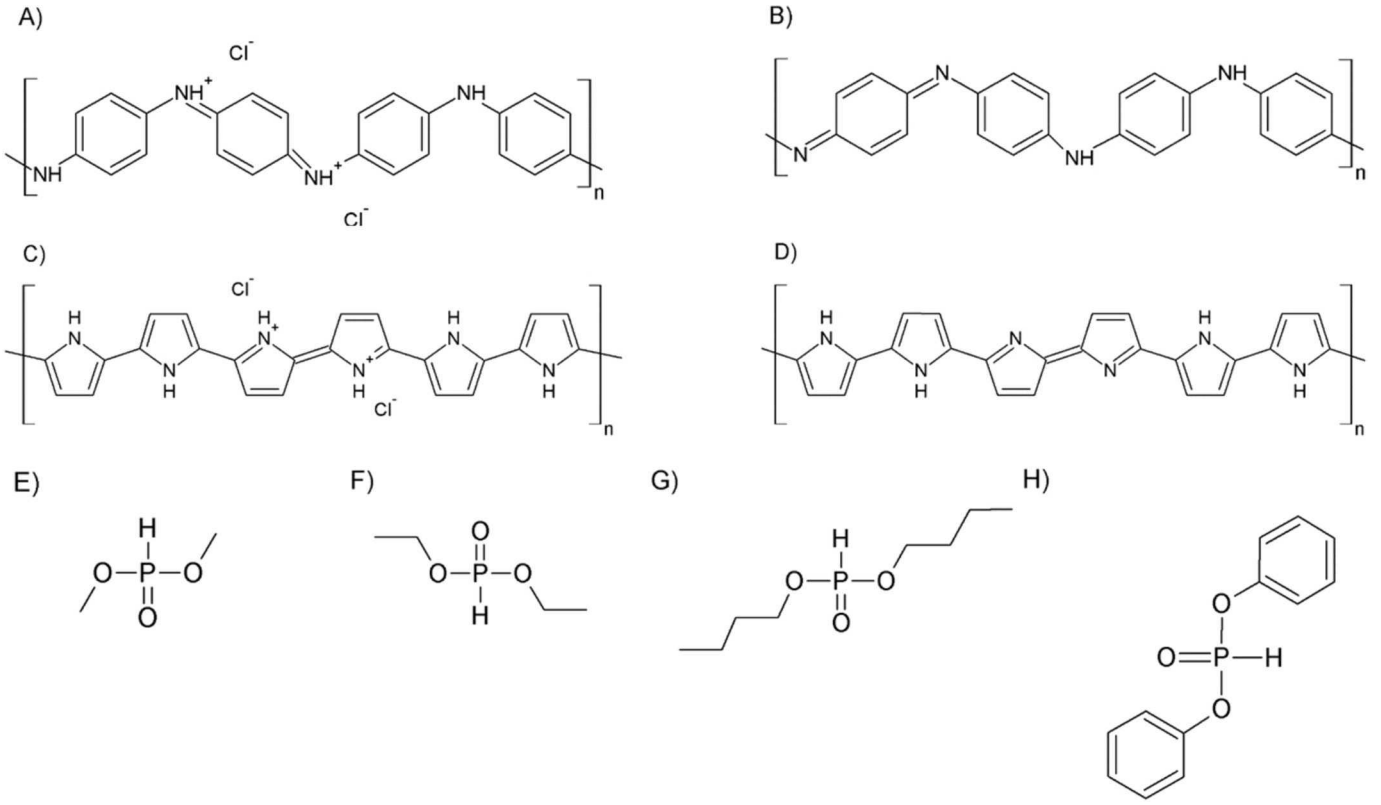

Fig. 1. Formulae of A) polyaniline salt (PANI-S); B) polyaniline base (PANI-B); C) polypyrrole salt (PPy-S); D) polypyrrole base (PPy-B); E) dimethyl phosphonate (DMPH); F) diethyl phosphonate (DEPH); G) dibutyl phosphonate (DBPH); H) diphenyl phosphonate (DPPH), the precursors of studied samples.

methods, which are not based on the classical protonation but on the application of acidic hydrogen atoms [13]. Several papers recently published show the possibility of this alternative doping to prepare the PANI with the organic phosphonates, which demonstrate interesting properties depending on the type of phosphonate used [13–15]. The present study extends the previous work to PPy and uses these organic phosphonates as a novel approach how to improve the stability of conductivity of PANI and PPy at various pH, mainly at the physiological pH. The work also discusses the biological properties of these new promising CP, primarily with respect to influence of phosphonate type used for CP modification.

2. Materials and methods

2.1. Sample preparation

Polyaniline, emeraldine salt (Fig. 1A), was prepared by standard oxidation of 0.2 M aniline hydrochloride (Penta, Czech Republic) with 0.25 M ammonium peroxydisulfate (Lach-Ner, Czech Republic) in aqueous medium at room temperature [16]. Globular polypyrrole (Fig. 1C) was synthetized by the oxidation of 0.2 M pyrrole (Sigma-Aldrich) with 0.5 M iron(III) chloride hexahydrate (Sigma-Aldrich) in water. The respective mixtures were left to react at room temperature for 24 h. Then the solids were collected on a filter, rinsed with 0.2 M hydrochloric acid and ethanol and dried in air and over silica gel.

Both solids were subsequently converted to PANI and PPy bases in 1 M ammonium hydroxide (Fig. 1B, D), rinsed with ethanol and dried as above. PANI and PPy bases were suspended in dimethyl phosphonate (DMPH, Fig. 1E), diethyl phosphonate (DEPH; Fig. 1F), dibutyl phosphonate (DBPH; Fig. 1G), or diphenyl phosphonate (DPPH; Fig. 1H) (all from Sigma Aldrich) without using any diluent. After 3 days, the solids were collected on a filter, rinsed with ethanol, and dried in air and then over silica gel. The samples were denoted according to their composition, with CP and phosphonate components as follows: PANI-DMPH, PANI-DEPH, PANI-DBPH, PANI-DPBH, PPy-DMPH, PPy-DEPH, PPy-DBPH and PPy-DPBH.

2.2. Cell lines

The embryonic stem cell ES R1 line (ESC) [17] was propagated in an undifferentiated state by culturing on gelatinized tissue culture dishes in complete media. The gelatinization was performed using 0.1% porcine gelatin solution in water. Complete media containing Dulbecco's Modified Eagle's Medium (DMEM), 15% fetal calf serum, 100 U mL^{-1} penicillin, 0.1 mg mL^{-1} streptomycin, 1× non-essential amino acids solution (all from Gibco-Invitrogen; USA), 0.05 mM 2-mercaptoethanol (Sigma–Aldrich; USA) and 1000 U mL^{-1} of leukemia inhibitory factor (Chemicon; USA) were used for the cultivation [18].

2.3. Preparation of extracts of PANI, PPy and their respective phosphonates

The testing of cytotoxicity was performed on polymer extracts obtained according to ISO 10993-5 protocol. Samples were extracted according to ISO 10993-12 with the following modification: the ratio 0.05 g polymer per 1 mL of cultivation medium was used instead of ISO defined 0.2 g polymer per 1 mL. Extraction was conducted in chemically inert closed containers using aseptic techniques at 37 ± 1 °C under stirring for 24 h. Subsequently, the extract was separated from the polymer powder by centrifugation at 1000 *g* for 15 min followed by second centrifugation of supernatant liquid under the same conditions. The parent extracts (100%) were then diluted in a complete medium to obtain a series of dilutions. All extracts were used within 24 h. Prior to *in-vitro* testing, the extracts were sterilized by filtration through the 0.22 μm filter (Millipore, USA). All tests were performed in quadruplicates, in four separates sets.

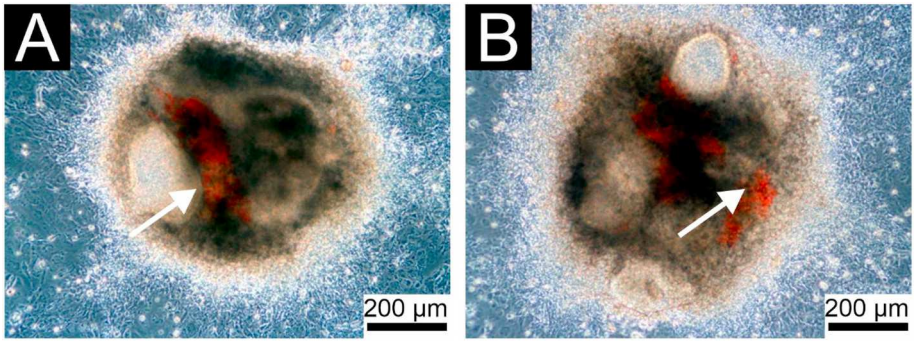

Fig. 2. The formation of erythroid clusters (red cluster marked with arrow) within the embryoid bodies. A) Positive reference, B) in the presence of 25% extracts of PPy-DBPH. (For interpretation of the references to colour in this figure legend, the reader is referred to the web version of this article.)

2.4. Cytotoxicity on ESC

The cells have been seeded at density of 5000 cells per cm^2 24 h before treatment. As a reference giving 100% cell viability, the cells cultivated in the pure complete medium were used. The cells were treated by extracts for 48 h. To assess cytotoxic effects, mass of viable ESC was determined as a level of adenosine triphosphate (ATP) using Cellular ATP Kit HTS (BioThema, Sweden). Samples were prepared and analysed as published previously [19]. Before lyses, the morphology of the cells was observed and documented using an inverted Olympus phase contrast microscope (Olympus IX51, Japan) supplemented with digital camera (Olympus E-450, Japan).

2.5. Embryotoxicity

The embryotoxicity was determined as the ratio of the formation of embryoid bodies (EBs) with beating foci (impact on cardiomyogenesis) and erythroid (in Fig. 2 shown in red) clusters/colonies (impact on erythropoiesis) within spontaneously differentiating ES R1 cells compared to reference. The ESC differentiation was induced through the formation of EBs by hanging drop techniques (400 cells per 35 μL drop) in leukemia inhibitory factor-free complete medium mentioned above, which was also used for sample extraction. After 5 days, EBs were transfer to gelatinized 24-wells plate (one EB per well) to serum-free media for next 15 days. Medium was replaced by fresh one each three days of cell culturing. Serum-free media contained DMEM-F12 media (1:1), 100 U mL^{-1} penicillin, 0.1 mg mL^{-1} streptomycin and 1× insulin-transferrin-selen (ITS) supplement (all from Gibco-Invitrogen; USA). Differentiating cells were observed as above.

2.6. Conductivity measurements

The DC conductivity was measured employing van der Pauw method on compressed polymer pellets having 13 mm diameter and thickness of 1.0 ± 0.2 mm. A Keithley 230 Programmable Voltage Source in serial connection with a Keithley 196 System DMM was used as current source and a Keithley 617 Programmable electrometer was used for the potential difference measurement. Measurements were carried out at stable ambient conditions at temperature 24 ± 1 °C and relative humidity 35 ± 5%. The conductivity was calculated from the linear part of the current-voltage characteristics, and is reported as an average value from measurements performed in two perpendicular directions conducted with the aim to reduce influence of the sample inhomogeneity.

3. Results and discussion

Recently, CP have received considerable attention due to their possible applications in regenerative medicine or tissue engineering of electro-sensitive tissues [2,20–22]. One of the studies conducted by Humpolíček et al. [20] compared the biocompatibility of PANI and PPy. The results demonstrated significant differences between biocompatibilities of the polymers in salt and base forms (Fig. 1). However, the differences between PANI and PPy in their respective forms (PPy-S *vs* PANI-S, PPy-B *vs* PANI-B) were negligible. In the present study, the PANI and PPy were prepared according to the procedure used in that study with a modification consisting in using phosphonates as dopants. The results obtained on the here-tested materials can be therefore compared and discussed with the results obtained on non-modified PANI and PPy in the mentioned study [20].

Here, the cytotoxicity was determined in accordance to ISO 10993-5 with the modification consisting in the use of different cell type, namely ESC. In addition to the cytotoxicity, embryotoxicity was also determined. Commonly, the embryotoxicity can be tested by using two main groups of methods: *in vivo* and *in vitro*. Here, the *in-vitro* testing of ESC differentiation processes of cardiomyogenesis and erythropoiesis were performed. The *in-vitro* cardiomyogenesis from ESC illustrates processes in the developing of embryo and helps to elucidate the mechanisms of differentiation of the cardiac cells. *In-vitro* erythropoiesis is observed by the formation of EBs with erythroid clusters (Fig. 2). These two processes are among the first steps of determining embryonic development [23].

One of the early studies dealing with cytotoxicity of PANI was published in 2012 by Humpolíček et al. [24] who used a standard protocol of ISO 10993-5 and NIH/3 T3 cells. However, in the already-mentioned work of the same authors from 2018 [20], cytotoxicities of PANI and PPy were determined using ESC (Fig. 4B) and are, therefore, comparable with a current study conducted on PANI-phosphonates (Figs. 3 and 4A). The cell morphology after exposition to the extracts is shown in the Fig. 3. It can be concluded that neither of the extracts influence the morphology of ESC. In the comparison with pristine PANI, the PANI-DPPH and PANI-DEPH show similar cytotoxicity towards ESC as polyaniline salt (PANI-S), while cytotoxicity of PANI-DBPH and PANI-DMPH are close to that of polyaniline base (PANI-B). Closer inspection of data revealed that the PANI-DPPH and PANI-DEPH were strongly cytotoxic even at very low extract concentrations (1%) in the cultivation medium. The embryotoxicity data expressed in percentage of formation of EBs with beating foci or erythroid clusters are presented in Table 1. The PANI-DPPH and PANI-DEPH exhibit embryotoxic effect in all tested concentrations and their embryotoxicities are even higher than that of PANI-S. On the other hand, PANI-DBPH and PANI-DMPH do not induce any embryotoxicity in any of the tested concentrations and induce the same, zero level, of cytotoxicity as PANI-B.

The cytotoxicity of all tested PPy phosphonates was low and, surprisingly, it was even lower than that of pristine polypyrrole salt (PPy-S) [20]. As in the case of PANI phosphonates, extracts of PPy phosphonates have no influence on cell morphology (Fig. 5). The lowest cytotoxicity exhibited PPy-DBPH and especially PPy-DEPH. It is thus evident that the biological properties of PPy-S improved by the treatment with phosphonates (Fig. 6). The embryotoxicity of PPy modified

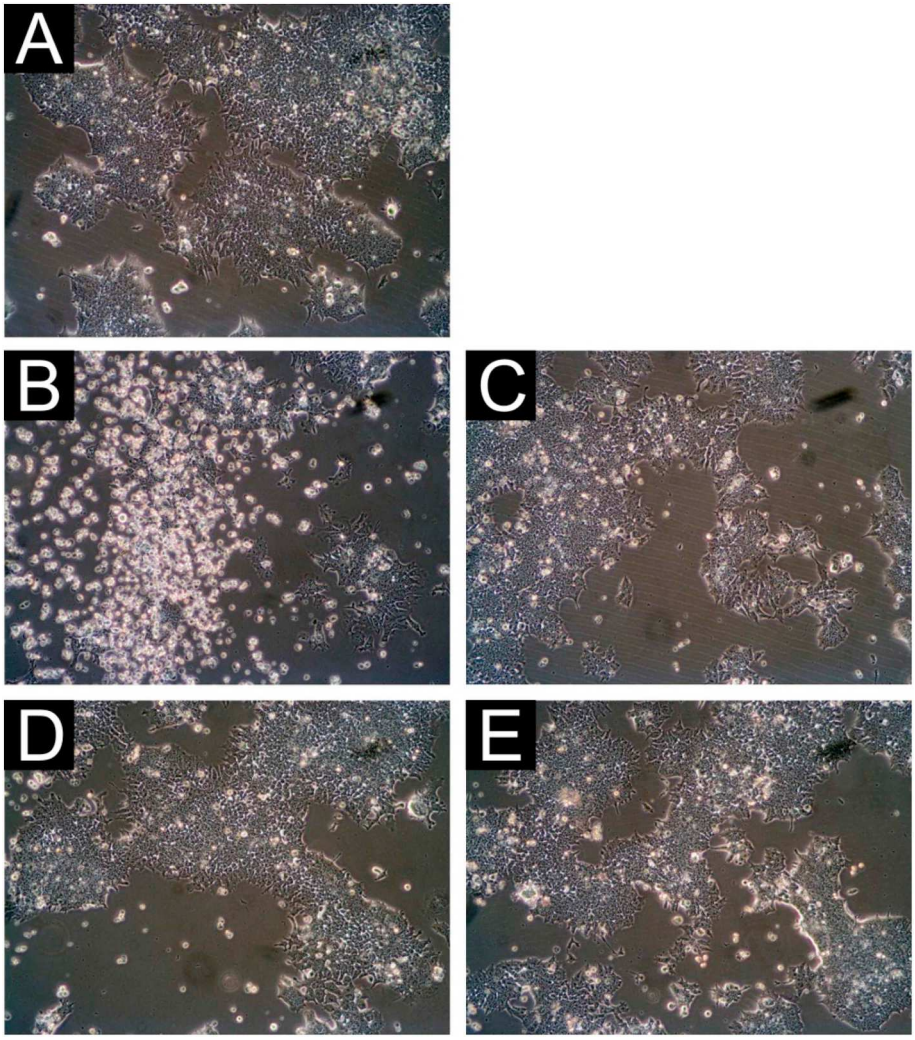

Fig. 3. The morphology of ESC after exposition to the extracts. A) Reference; B) PANI-DPPH 10%; C) PANI-DBPH 50%; D) PANI-DEPH 1%; E) PANI-DMPH 25%. Magnification 40 ×.

with phosphonates were even lower than their cytotoxicities. In fact, mild decrease (to 88%) of formation of EBs with erythroid clusters was observed only for PPy-DMPH and only in case of the highest tested extract concentration (50%). Formation of EBs with beating foci was not affected by the studied extracts at all, and no decrease in the percentage of EBs with clusters was detected (Table 2).

Cytotoxicity data obtained on ESC in current study obviously demonstrated that PPy-phosphonates exhibit much lower cytotoxicity than their corresponding PANI analogues. Interestingly, in the contrast to PPy where doping with DPPH and DEPH produced only negligible cytotoxic effect, the same phosphonates were significantly cytotoxic when combined with PANI. However, with exception of the PANI-DPPH and PANI-DEPH, all samples exhibited lower cytotoxicity than pristine polymer salts, PANI-S and PPy-S, and were comparable with cytotoxicity of both bases, PANI-B and PPy-B [20].

Based on the results from embryotoxicity testing, it can be concluded that all tested PPy-phosphonates and PANI-DBPH and PANI-DMPH do not show any harmful effect in terms of cardiomyogenesis and erythropoiesis. On the other hand, PANI-DPPH and PANI-DEPH significantly decreased the formation of EBs with beating foci or erythroid clusters in comparison with the reference. In fact, only 50% of EBs with beating foci and clusters were formed after treatment with only 1% extract of PANI-DPPH, and no EBs with beating foci or clusters formed in contact with higher concentrations of the PANI-DPPH extracts, as well as with the whole range of extract concentrations prepared of PANI-DEPH. Here, similarly as for cytotoxicity, all phosphonate-doped samples, except the PANI-DPPH and PANI-DEPH, showed lower embryotoxicity than pristine PANI-S and PPy-S, and were absent of embryotoxic effect as the PANI-B and PPy-B samples [20].

The most varying performance after being used as a dopant was observed in the case of DEPH. This phosphonate showed the highest cytotoxicity among all samples when used together with PANI; on the contrary, PPy with the same phosphonate had no cytotoxic effect in the whole range of extract concentrations tested. The corresponding effect was confirmed also by embryotoxicity testing, where PANI-DEPH exhibited the severe embryotoxicity whilst for PPy-DEPH the embryotoxic effect was absent.

The Fig. 7 summarizes the results of the conductivity measurements of CP doped with organic phosphonates under study at various pH. These results provide further insight into relation of conductivity and pH in the interval of pH 3–9. It can be clearly seen that there was a decrease in the conductivity with the increasing pH value from 3 to 9 in both of the examined samples of PANI-S and PPy-S. While the conductivity decrease in PANI is dramatic and limits the use of this polymer under physiological conditions, the reduction of the conductivity of PPy is marginal. Several differences can be found between polymers doped with different phosphonates: (1) At low pH values, both polymers show the highest conductivity when doped with DPPH. Based on the combination of Raman and EPR spectroscopy the higher conductivity of PANI-DPPH compared to other samples has been explained by a higher

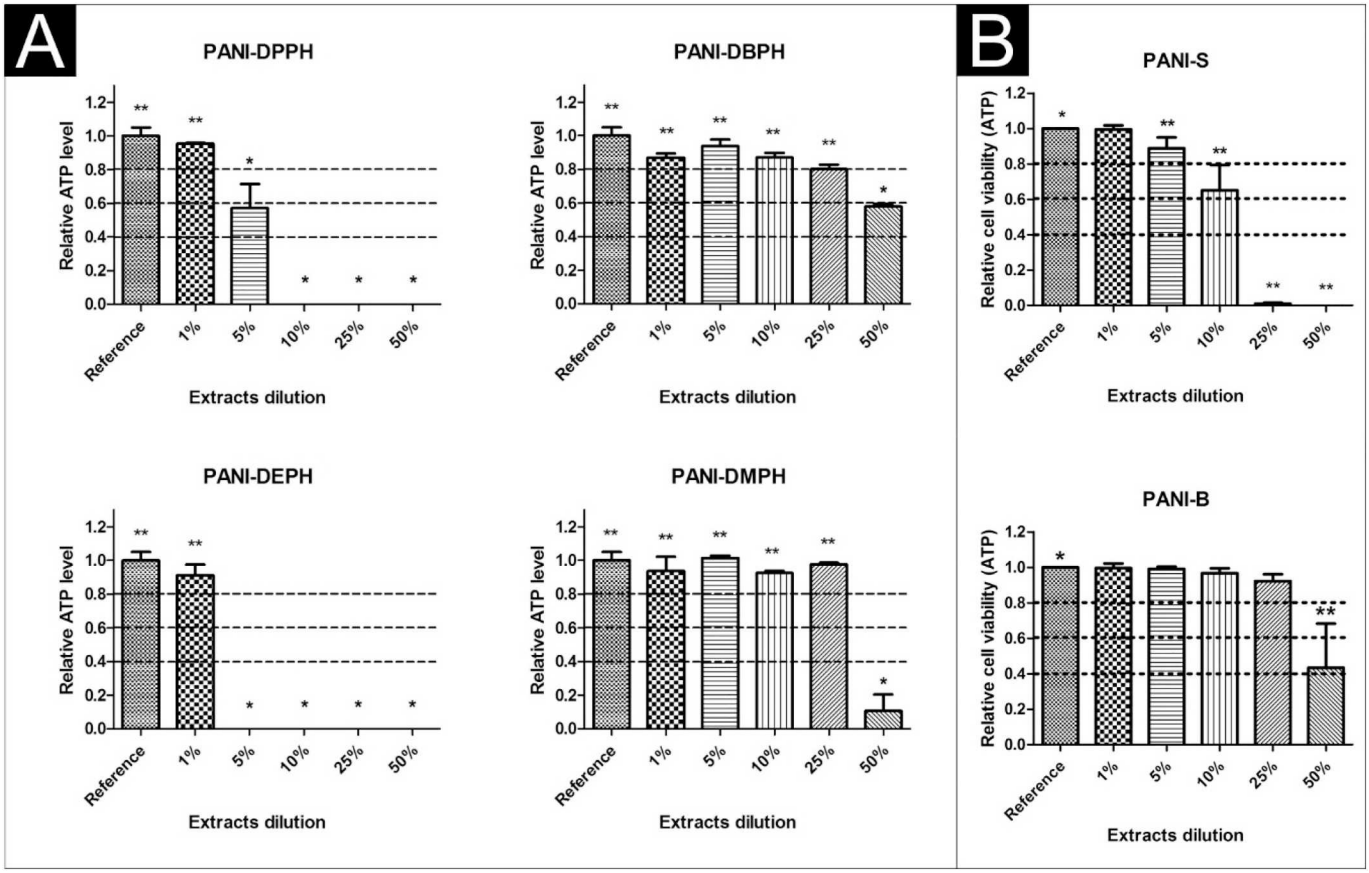

Fig. 4. Cytotoxicity of extracts of PANI on ESC. (A) PANI doped with phosphonates, (B) pristine PANI salt (PANI-S) and base (PANI-B) prepared according to IUPAC technical report [16]. Reproduced from [20]. The different superscripts correspond to significant differences ($P \leq 0.05$) compared to the reference. The dashed lines highlight the limits of viability according to EN ISO 10993-5 with modification: viability > 0.8 corresponds to no cytotoxicity, > 0.6–0.8 mild cytotoxicity, > 0.4–0.6 moderate cytotoxicity and < 0.4 severe cytotoxicity.

polaron delocalization and mobility [13]. Particularly large increase of conductivity (4 orders of magnitude higher than other systems under study) was found for PANI-DPPH. PPy-DPPH had also higher conductivity compared to other systems at pH 3 but the difference was much smaller, less than one order of magnitude. (2) With increasing pH, the conductivity was found to decrease in all systems but for PANI-DPPH and PANI-DEPH the decrease was smaller for pH < 5. On the other hand, the behaviour of PPy-DPPH is different: there is a steep decrease of conductivity when going from pH 3 to 4.

The trends in conductivity development with pH agree well with data reported in previous study dealing with PANI doped with the same organophosphonate dopants [13]. However, with the exception of PANI-DPPH the conductivities determined in current work are markedly lower in comparison with those reported in [25]. The reason could be fact that the measurements in our work started first at pH 3, compared to lower starting pH value used in the study of Bláha et al. [13] where the measurements were performed at more acidic state after doping with phosphonates. The increase in the conductivity of PANI with the doping using various phosphonates correlates well with their expected increasing acidity from DMPH through DEPH, DBPH and DPPH, as evaluated from the chemical shift in the ^{31}P NMR spectra [26]. The higher values of conductivity found for PANI-DPPH and

Table 1
The impact of extracts of PANI-phosphonates on cardiomyogenesis (expressed as percentage of EBs with beating foci) and erythropoiesis (expressed as percentage of EBs with erythroid clusters). Comparison with pristine PANI-S and PANI-B.

		EBs with formed foci or clusters [%]					
	Extract dilution [%]	DPPH	DBPH	DEPH	DMPH	PANI-S [a]	PANI-B [a]
EBs with beating foci	Reference	100	100	100	100	100	100
	1	50	100	0	100	100	100
	5	0	100	0	100	50	100
	25	0	100	0	100	0	100
EBs with erythroid clusters	Reference	100	100	100	100	100	100
	1	50	100	0	100	100	100
	5	0	100	0	100	13	100
	25	0	100	0	100	0	100

[a] Reproduced from Humpolíček et al. [20].

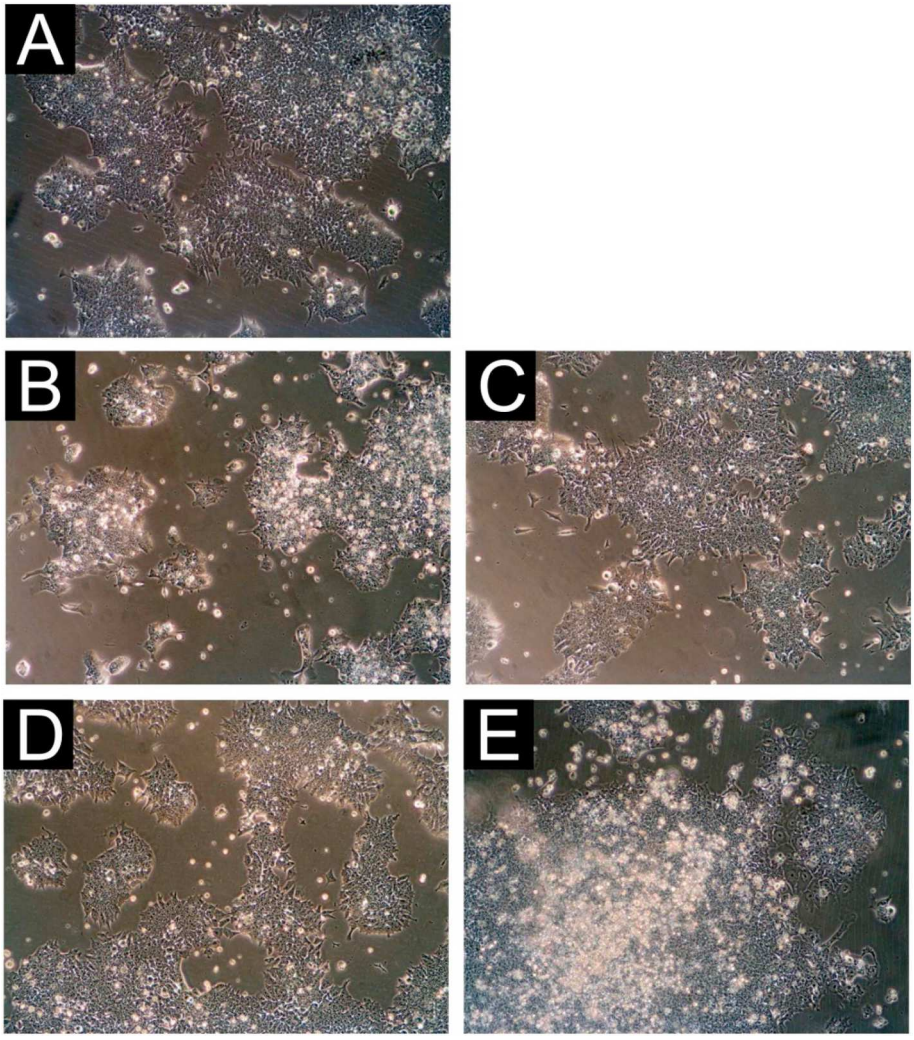

Fig. 5. The morphology of ESC after exposition to the extracts. A) Reference; B) PPy-DPPH 50%; C) PPy-DBPH 50%; D) PPy-DEPH 50%; E) PANI-DMPH 50%. Magnification 40×.

PANI-DEPH correlate also well with the increased level of their cytotoxicity. Since the conductivity depends on the type and dopant content, both the higher cytotoxicity and higher conductivity might be explained by higher content of the phosphonate dopants [8]. It is, however important, that in case of PANI the doping by phosphonates, especially by DPPH improves the pH stability of PANI, including the stability in physiological pH region. In the case of PPy, both the PPy-S and phosphonate doped PPy systems shoved better stability in increased pH compared to the respective systems with PANI but no further improvement of the stability with the phosphonate dopants was observed.

Humpolíček et al. [20] proved in their work similar cytotoxicity for PANI-S and PPy-S extracts. It is, therefore worth recording that these polymers when re-doped with phosphonates exhibit notably lower cytotoxicities. In this respect it can be mentioned that pyrrole, a monomer used for polypyrrole synthesis, is an interesting bioactive molecule and has numerous applications in therapeutically active compounds including fungicides, antibiotics, anti-inflammatory drugs [27], cholesterol reducing drugs [28] or antitumor agents. Therefore, the combination of this active molecule with phosphonates might be the reason for better biological activity of PPy samples in the comparison with polymers where the precursor of PANI, aniline, is employed, as it is known for its cytotoxicity.

4. Conclusions

The results demonstrate that the major barrier of practical use of CP and mainly of PANI, the limited conductivity under physiological conditions, can be overcome by their doping with organic phosphonates. Though published studies report on several ways of improving pH stability of conductivity, none of the studies provided an insight into the biocompatibility of these polymers. The findings from this study suggest that PPy in combination of DPPH, DEPH, DBPH, DPPH and PANI in combination of DBPH, and partially with DMPH provide attractive properties for applications in biomedicine thanks to their low cytotoxicity and reasonable high level of conductivity at physiological pH. Regrettably, PANI-DPPH and PANI-DEPH exhibit rather high cytotoxicity but their conductivities were reported to be higher than those of other tested samples. There was a significant correlation between high cytotoxicity and high values of conductivity of PANI doped with DPPH and DEPH. An extended study with more focus on investigation of interactions between phosphonates and CP can be, therefore, of high interest. We conclude that especially PPy doped with phosphonates with improved properties could be considered as a novel biomaterial with added conductivity value.

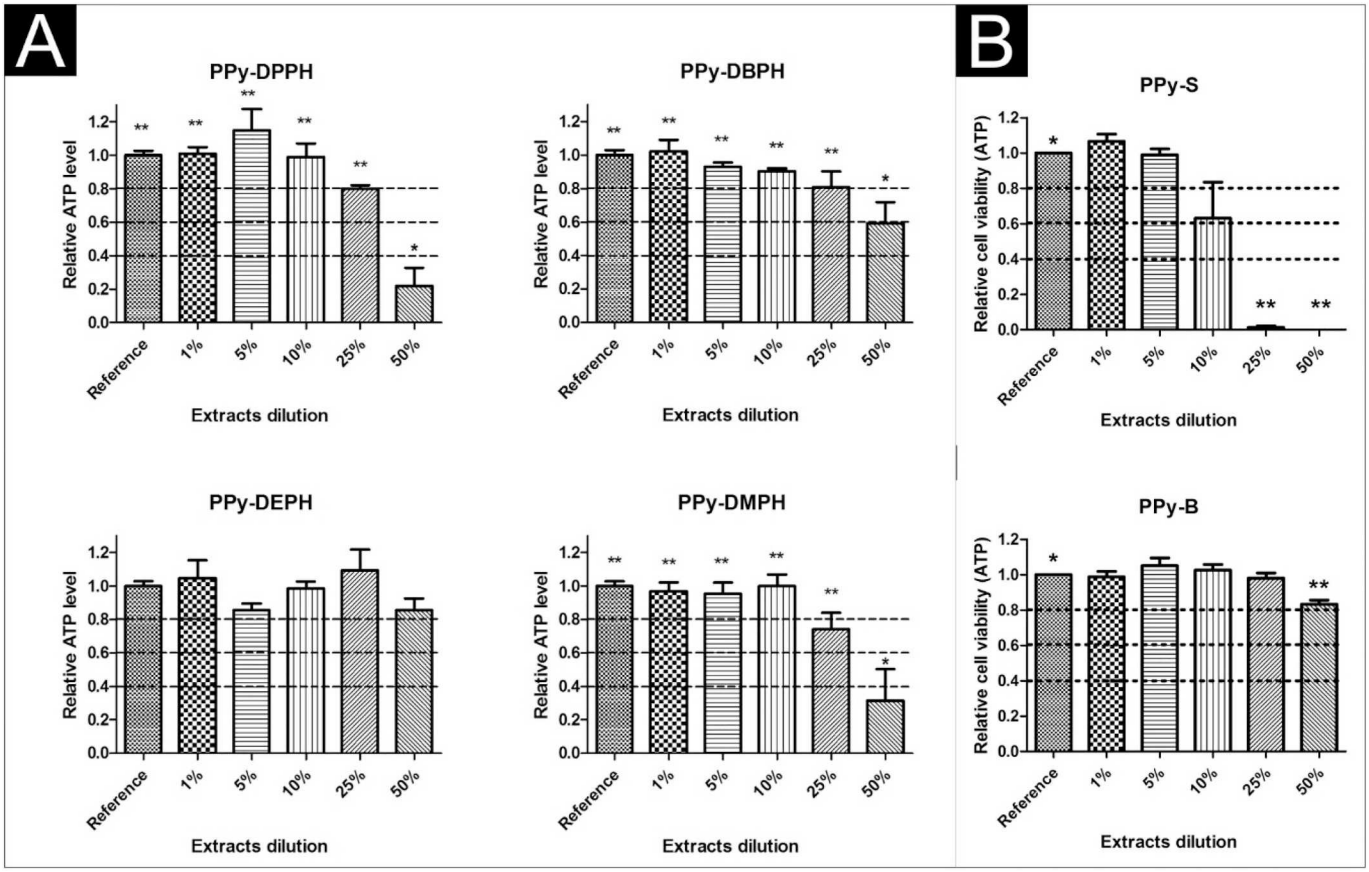

Fig. 6. Cytotoxicity of extracts of PPy determined on ESC. (A) PPy doped with phosphonates, (B) pristine polypyrrole salt (PPy-S) and base (PPy-B) prepared according to [20] and reproduced from the same study. The different superscripts correspond to significant differences ($P \leq 0.05$) compared to the reference. The dashed lines highlight the limits of viability according to EN ISO 10993-5 with modification: viability > 0.8 corresponds to no cytotoxicity, > 0.6–0.8 mild cytotoxicity, > 0.4–0.6 moderate cytotoxicity and < 0.4 severe cytotoxicity.

Table 2
The impact of extracts of PPy-phosphonates on cardiomyogenesis (percentage of EBs with beating foci) and erythropoiesis (percentage of EBs with erythroid clusters). Comparison with pristine PPy-S and PPy-B.

		EBs with formed foci or clusters [%]					
	Extract dilution [%]	DPPH	DBPH	DEPH	DMPH	PPy-S [a]	PPy-B [a]
EBs with beating foci	Reference	100	100	100	100	100	100
	1	100	100	100	100	100	100
	5	100	100	100	100	75	100
	25	100	100	100	100	0	100
EBs with erythroid clusters	Reference	100	100	100	100	100	100
	1	100	100	100	100	75	100
	5	100	100	100	100	50	100
	25	100	100	100	88	0	100

[a] Reproduced from Humpolíček et al. [20].

Funding

This work was funded by the Czech Science Foundation (19-16861S) and the Ministry of Education, Youth and Sports of the Czech Republic (NPU I, LO1504). One of us, T. H. T., acknowledges the support of an internal grant from TBU in Zlín (IGA/CPS/2020/001) financed from funds of specific academic research.

CRediT authorship contribution statement

Zdenka Capáková: Conceptualization. **Katarzyna Anna Radaszkiewicz:** Methodology. **Udit Acharya:** Methodology. **Thanh Huong Truong:** Methodology, Writing - original draft. **Jiří Pacherník:** Methodology. **Patrycja Bober:** Conceptualization, Writing - original draft, Writing - review & editing. **Věra Kašpárková:** Writing - original draft, Writing - review & editing. **Jaroslav Stejskal:** Writing - review & editing. **Jiří Pfleger:** Writing - review & editing. **Marián Lehocký:** Writing - review & editing. **Petr Humpolíček:** Conceptualization, Writing - original draft, Writing - review & editing, Supervision.

Declaration of competing interest

The authors declare no conflict of interest. The funders had no role

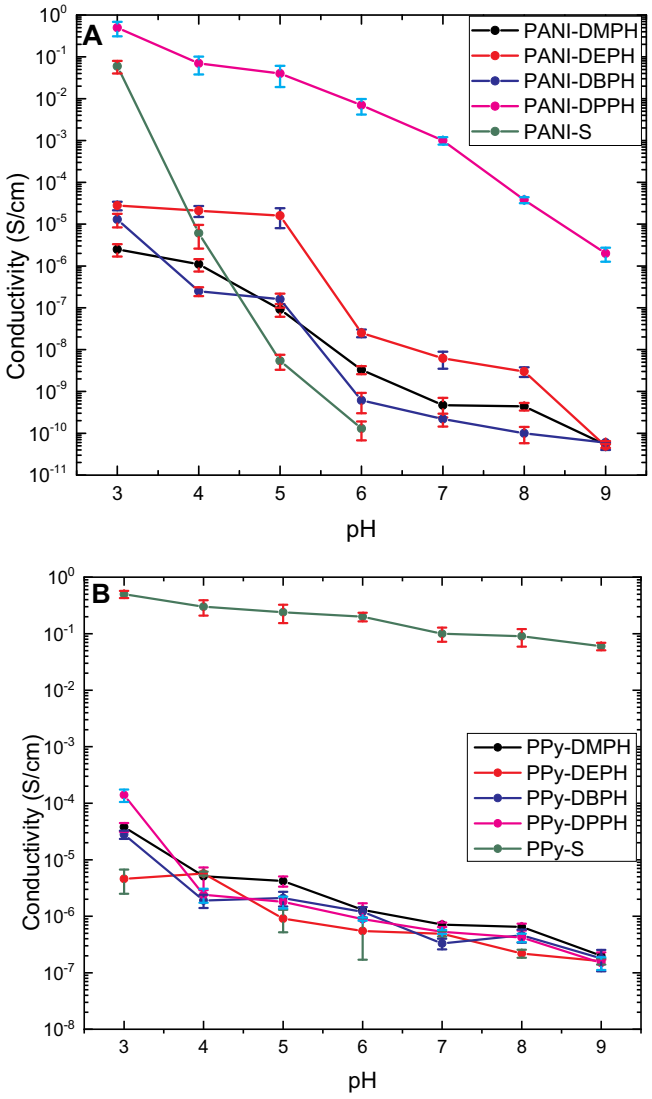

Fig. 7. The conductivity of A) PANI and B) polypyrrole doped with organic phosphonates under various pH and the comparison with pristine PANI-S and PPy-S.

in the design of the study, in the collection, analyses, or interpretation of data, in the writing of the manuscript, or in the decision to publish the results.

References

[1] B.D. Paulsen, K. Tybrandt, E. Stavrinidou, J. Rivnay, Organic mixed ionic–electronic conductors, Nat. Mater. 19 (2020) 13–26 https://doi.org/10.1038/s41563-019-0435-z.

[2] B. Guo, P.X. Ma, Conducting polymers for tissue engineering, Biomacromolecules 19 (2018) 1764–1782 https://doi.org/10.1021/acs.biomac.8b00276.

[3] R. Dong, P.X. Ma, B. Guo, Conductive biomaterials for muscle tissue engineering, Biomaterials 229 (2020) 119584https://doi.org/10.1016/j.biomaterials.2019.119584.

[4] X. Zhao, H. Wu, B. Guo, R. Dong, Y. Qiu, P.X. Ma, Antibacterial anti-oxidant electroactive injectable hydrogel as self-healing wound dressing with hemostasis and adhesiveness for cutaneous wound healing, Biomaterials 122 (2017) 34–47, https://doi.org/10.1016/j.biomaterials.2017.01.011.

[5] J. Stejskal, A. Riede, D. Hlavatá, J. Prokeš, M. Helmstedt, P. Holler, The effect of polymerization temperature on molecular weight, crystallinity, and electrical conductivity of polyaniline, Synth. Met. 96 (1998) 55–61, https://doi.org/10.1016/S0379-6779(98)00064-2.

[6] M. Bláha, M. Varga, J. Prokeš, A. Zhigunov, J. Vohlídal, Effects of the polymerization temperature on the structure, morphology and conductivity of polyaniline prepared with ammonium peroxodisulfate, Eur. Polym. J. 49 (2013) 3904–3911, https://doi.org/10.1016/j.eurpolymj.2013.08.018.

[7] M. Ahlskog, M. Reghu, A.J. Heeger, The temperature dependence of the conductivity in the critical regime of the metal–insulator transition in conducting polymers, J. Phys. Condens. Matter 9 (1997) 4145–4156, https://doi.org/10.1088/0953-8984/9/20/014.

[8] T.H. Le, Y. Kim, H. Yoon, Electrical and electrochemical properties of conducting polymers, Polymers 9 (2017) 150, https://doi.org/10.3390/polym9040150.

[9] A. Michalska, K. Maksymiuk, On the pH influence on electrochemical properties of poly(pyrrole) and poly(*N*-methylpyrrole), Electroanalysis 10 (1998) 177–180 https://doi.org/10.1002/(SICI)1521-4109(199803)10:3 < 177::AID-ELAN177 > 3.0.CO;2-G.

[10] H. Song, T. Li, Y. Han, Y. Wang, C. Zhang, Q. Wang, Optimizing the polymerization conditions of conductive polypyrrole, J. Photopolym. Sci. Technol. 29 (2016) 803–808, https://doi.org/10.2494/photopolymer.29.803.

[11] P. Bober, T. Lindfors, M. Pesonen, J. Stejskal, Enhanced pH stability of conducting polyaniline by reprotonation with perfluorooctanesulfonic acid, Synth. Met. 178 (2013) 52–55, https://doi.org/10.1016/j.synthmet.2013.07.002.

[12] P. Bober, P. Humpolíček, J. Pacherník, J. Stejskal, T. Lindfors, Conducting polyaniline based cell culture substrate for embryonic stem cells and embryoid bodies, RSC Adv. 5 (2015) 50328–50335, https://doi.org/10.1039/C5RA07504A.

[13] M. Bláha, M. Trchová, P. Bober, Z. Morávková, Z.D. Zujovic, S.K. Filippov, J. Prokeš, J. Pilař, J. Stejskal, Structure and properties of polyaniline interacting with H-phosphonates, Synth. Met. 232 (2017) 79–86, https://doi.org/10.1016/j.synthmet.2017.07.022.

[14] Z. Morávková, M. Trchová, J. Dybal, M. Bláha, J. Stejskal, The interaction of thin polyaniline films with various H-phosphonates: spectroscopy and quantum chemical calculations, J. Appl. Polym. Sci. 135 (2018) 46728, , https://doi.org/10.1002/app.46728.

[15] I. Šeděnková, M. Trchová, J. Dybal, J. Stejskal, Interaction of polyaniline film with dibutyl phosphonate versus phosphite: enhanced thermal stability, Polym. Degrad. Stab. 134 (2016) 357–365, https://doi.org/10.1016/j.polymdegradstab. 2016.11.005.

[16] J. Stejskal, R.G. Gilbert, Polyaniline. Preparation of a conducting polymer (IUPAC technical report), Pure Appl. Chem. 74 (2002) 857–867, https://doi.org/10.1351/pac200274050857.

[17] A. Nagy, J. Rossant, R. Nagy, W. Abramow-Newerly, J.C. Roder, Derivation of completely cell culture-derived mice from early-passage embryonic stem cells, Proc. Natl. Acad. Sci. U. S. A. 90 (1993) 8424–8428, https://doi.org/10.1073/pnas.90.18.8424.

[18] P. Humpolíček, K.A. Radaszkiewicz, V. Kašpárková, J. Stejskal, M. Trchová, Z. Kuceková, H. Vičarová, J. Pacherník, M. Lehocký, A. Minařík, Stem cell differentiation on conducting polyaniline, RSC Adv. 5 (2015) 68796–68805, https://doi.org/10.1039/C5RA12218J.

[19] R. Konopka, M. Hýzdalová, L. Kubala, J. Pacherník, New luminescence-based approach to measurement of luciferase gene expression reporter activity and adenosine triphosphate-based determination of cell viability, Folia Biol. 56 (2010) 66–71.

[20] P. Humpolíček, V. Kašpárková, J. Pacherník, J. Stejskal, P. Bober, Z. Capáková, K.A. Radaszkiewicz, I. Junkar, M. Lehocký, The biocompatibility of polyaniline and polypyrrole: a comparative study of their cytotoxicity, embryotoxicity and impurity profile, Mater. Sci. Eng. C Mater. Biol. Appl. 91 (2018) 303–310, https://doi.org/10.1016/j.msec.2018.05.037.

[21] E.N. Zare, P. Makvandi, B. Ashtari, F. Rossi, A. Motahari, G. Perale, Progress in conductive polyaniline-based nanocomposites for biomedical applications: a review, J. Med. Chem. 63 (2020) 1–22, https://doi.org/10.1021/acs.jmedchem.9b00803.

[22] M. Talikowska, X. Fu, G. Lisak, Application of conducting polymers to wound care and skin tissue engineering: a review, Biosens. Bioelectron. 135 (2019) 50–63, https://doi.org/10.1016/j.bios.2019.04.001.

[23] D.A.F. Loebel, C.M. Watson, R.A. De Young, P.P.L. Tam, Lineage choice and differentiation in mouse embryos and embryonic stem cells, Dev. Biol. 264 (2003) 1–14, https://doi.org/10.1016/S0012-1606(03)00390-7.

[24] P. Humpolicek, V. Kasparkova, P. Saha, J. Stejskal, Biocompatibility of polyaniline, Synth. Met. 162 (2012) 722–727, https://doi.org/10.1016/j.synthmet.2012.02.024.

[25] P. Humpolíček, Z. Kuceková, V. Kašpárková, J. Pelková, M. Modic, I. Junkar, M. Trchová, P. Bober, J. Stejskal, M. Lehocký, Blood coagulation and platelet adhesion on polyaniline films, Colloids Surf. B: Biointerfaces 133 (2015) 278–285, https://doi.org/10.1016/j.colsurfb.2015.06.008.

[26] K.D. Troev, Chemistry and Application of H-Phosphonates, Elsevier, 2006.

[27] W.W. Wilkerson, R.A. Copeland, M. Covington, J.M. Trzaskos, Antiinflammatory 4,5-diarylpyrroles. 2. Activity as a function of cyclooxygenase-2 inhibition, J. Med. Chem. 38 (1995) 3895–3901, https://doi.org/10.1021/jm00020a002.

[28] R.P. Wurz, A.B. Charette, Doubly activated cyclopropanes as synthetic precursors for the preparation of 4-nitro- and 4-cyano-dihydropyrroles and pyrroles, Org. Lett. 7 (2005) 2313–2316, https://doi.org/10.1021/ol050442l.

Article X.

Rejmontova, P.; Kovalcik, A.; Humpolicek, P.; **Capakova, Z**.; Wrzecionko, E.; Saha, P. The Use of Fractionated Kraft Lignin to Improve the Mechanical and Biological Properties of PVA-Based Scaffolds. RSC Adv. 2019, 9 (22), 12346–12353. https://doi.org/10.1039/c8ra09757g.

RSC Advances

PAPER

View Article Online
View Journal | View Issue

Cite this: *RSC Adv.*, 2019, **9**, 12346

The use of fractionated Kraft lignin to improve the mechanical and biological properties of PVA-based scaffolds

Petra Rejmontová,[ab] Adriana Kovalcik,*[cd] Petr Humpolíček, *[ab] Zdenka Capáková,[a] Erik Wrzecionko[ae] and Petr Sáha[ab]

Received 27th November 2018
Accepted 13th April 2019

DOI: 10.1039/c8ra09757g

rsc.li/rsc-advances

The mechanical properties of poly(vinyl alcohol) (PVA)-based scaffolds were successfully improved. The improvements in mechanical properties correlated with the amount of Kraft lignin in PVA matrices. The critical property for any scaffold is its capacity to allow cells to ingrow and survive within its internal structure. The ingrowth of cells was tested using bioreactors creating simulated *in vivo* conditions. In the context of all the mentioned parameters, the most advantageous properties were exhibited by the scaffold containing 99 wt% PVA and 1 wt% Kraft lignin. The composites with 1 wt% Kraft lignin exhibited sufficient mechanical stability, a lack of cytotoxicity, and mainly the ability to allow the ingrowth of cells into the scaffold in a rotation bioreactor.

1. Introduction

The rapidly evolving field of regenerative medicine has created a constant demand for the development of new three-dimensional scaffolds with mandatory biological properties (*e.g.*, biocompatibility or a bio-interface) and material properties (*e.g.*, elasticity or porosity). For this purpose, many polymers, natural as well as synthetic, have proven to be suitable matrix materials. Various polymer-based scaffolds have been used for bone,[1,2] heart,[3–6] and cartilage[7,8] regeneration. Particular attention is devoted to, among others, poly(vinyl alcohol) (PVA). This synthetic polymer is already widely utilized in biomedicine.[9] A wide variety of PVA-based biomaterials have been used for cartilage,[10,11] vascular,[12] cardiovascular,[13,14] and also bone[15] tissue replacement. The use of PVA hydrogel as a dermal filler has also been proposed.[16] The mechanical properties of PVA, however, are not entirely satisfactory.[17]

In contrast to PVA, the biological properties of Kraft lignin (KL) have not yet been satisfactorily described. It is a renewable industrial biopolymer, which has already been tested as an additive and filler for various polymers.[18,19] The purpose of using KL as an additive to polymers is mainly to exploit its stiffening effect[20] and antioxidant efficiency.[21] Both properties are beneficial for tissue engineering and can be especially advantageous for PVA-based devices. As both inflammatory responses and correlated oxidative stress are typical side effects of implantation, the latter mentioned property of KL is more than desirable for materials utilized as scaffolds in regenerative medicine. Another favourable feature which KL can bring to the final product is antibacterial activity. However, the antibacterial activity of industrial lignins within polymer composites is questionable.[22] The antibacterial properties of isolated lignins have been discussed in some recent papers. For example, Medina *et al.* reported the antibacterial efficiency of hydrolyzed lignin (derived from oil palm empty fruit bunches) against *E. coli*, *S. typhimurium*, *B. subtilis*, and *S. aureus*.[23] Guo *et al.* reported the antibacterial activity of lignin extracts obtained from anhydrous ammonia-pretreated corn stover after enzymatic hydrolysis.[24] As KL is a polydisperse compound, its utilization in biomedicine is challenging. However, the fractionation of KL (*e.g.*, using selective precipitation based on pH or organic solvent extraction) can improve its polydispersity index and lead to the derivation of specific lignin samples.[25]

In the light of the facts mentioned above, this work aimed to determine the improvement in the function of PVA scaffolds resulting from the incorporation of KL and the potential of these innovative scaffolds for use in regenerative medicine. Optimally, the novel material should exploit the advantages of lignin, especially its antibacterial activity, excellent mechanical properties, and biocompatibility with PVA. The methanol fraction of Kraft lignin (KL^f), obtained according to Gregorova and Sedlarik,[26] was used to prepare scaffolds. This fraction should

[a]*Centre of Polymer Systems, Tomas Bata University in Zlin, Trida Tomase Bati 5678, 76001 Zlin, Czech Republic. E-mail: humpolicek@utb.cz; Fax: +420-576-031-444; Tel: +420 576 038 035*

[b]*Polymer Centre, Faculty of Technology, Tomas Bata University in Zlin, Vavreckova 275, 760 01 Zlin, Czech Republic*

[c]*Institute for Chemistry and Technology of Materials, Graz University of Technology, Stremayrgasse 9, 8010 Graz, Austria*

[d]*Department of Food Chemistry and Biotechnology, Faculty of Chemistry, Brno University of Technology, Purkynova 118, 612 00 Brno, Czech Republic. E-mail: adriana.kovalcik@gmail.com*

[e]*Department of Physics and Materials Engineering, Tomas Bata University in Zlín, Vavrečkova 275, 760 01 Zlín, Czech Republic*

be more suitable for biomedical applications, as it exhibits lower polydispersity.[26]

2. Material and methods

2.1. Preparation of hydrogels

Mowiflex TC 232 (Kuraray Europe GmbH), a polyvinyl alcohol compound with an aliphatic polyol and calcium distearate, was used as the polymer matrix for hydrogels and is henceforth designated as PVA. Powdered lignin (KL) of the weight average molecular weight 2790 g mol^{-1} and polydispersity of 2.0 was obtained by methanol fractionation of Kraft lignin, which was isolated from black liquor (Zellstoff Pöls AG, Austria) by precipitation with 37% hydrochloric acid.[26] The methanol fraction KL^f was prepared as described by Gregorova and Sedlarik.[26]

1 g of PVA was fully dissolved in 20 mL of Mili-Q water at 80 °C by stirring in glass vials. Different concentrations of the methanol fraction of KL were uniformly dispersed in PVA solution. The pH was adjusted to 2.00 with 2.0 M HCl, and 200 μL of glutaraldehyde was added to the solution and stirred for 30 min. Subsequently, prepared solutions were densified by the repetition of six freeze-thawing cycles (freezing at −18 °C for 12 hours followed by thawing (gradual warming) at room temperature for 4 hours). Hydrogels were designated as PVA_*X*-KL^f, where *X* indicates the concentration of lignin (1, 5, 10, 15 and 20 wt%).

2.2. Mechanical and thermal stability of hydrogels

The mechanical stability of fully swollen hydrogels (15 mm in diameter and 10 mm in height) in water was tested by employing creep/creep recovery testing at 25 °C in air, using a DMA Q800 RH equipped with a submersion compression clamp (TA Instruments, USA). A force of 0.001 N, 5 minutes of isotherm, constant stress of 1 kPa for 5 minutes, and a relaxation time of 5 minutes were applied. Three parallel measurements were performed for each hydrogel.

Thermogravimetric analysis (TG) was performed using STA-449C Netzsch equipment. 5 mg of PVA hydrogels were spread in perforated alumina crucibles. Thermal behaviour was recorded from 25 °C to 550 °C at a heating rate of 10 °C min^{-1} under a nitrogen atmosphere (50 mL min^{-1} of nitrogen flow rate).

2.3. Internal structure of hydrogels and swelling ratio

The inner structures of the prepared scaffolds were observed using a Phenom Pro scanning electron microscope (SEM) (Phenom-World BV). The samples were studied at an acceleration voltage of 10 kV in the backscattered electron. Measurements were carried out on samples without prior metallization using a unique sample holder that allows the reduction of charges on nonconductive materials.

The internal structure of hydrogels was determined gravimetrically by estimation of the swelling behaviour in distilled water. The swelling ratio (Q) was calculated by the following equation:

$$Q = (W_s - W_d)/W_d,$$

where W_d and W_s are weights of dried hydrogel and swelled hydrogel after 24 hours in water, respectively.

2.4. Cytotoxicity and cytocompatibility

The cytotoxicity of scaffolds in direct contact with cells and the cytotoxicity of extracts from scaffolds were tested to reveal the fundamental biological properties of the scaffolds. Accordingly, the materials found to be most cytocompatible were tested for cytocompatibility using bioreactors creating simulated *in vivo* conditions. This testing allowed the ability of cells to grow into the scaffold's internal pores to be studied. Taken together, the results of the abovementioned tests provided a sophisticated view of the biological properties of the prepared scaffolds based on PVA and KL. All tests were performed using a mouse embryonic fibroblast cell line (ATCC CRL-1658 NIH/3T3, USA). ATCC-formulated Dulbecco's Modified Eagle's Medium (PAA Laboratories GmbH, Austria) containing 10% bovine calf serum (BioSera, France) and 100 U mL^{-1} of Penicillin/Streptomycin (GE Healthcare HyClone, United Kingdom) was used as the cultivation medium. The set-ups for individual tests were as follows:

Cytotoxicity in direct contact. Before testing the cytotoxicity of scaffolds in direct contact with cells, samples were disinfected by being submersed in 70% ethanol. The samples were left in 70% ethanol overnight; then the ethanol was removed with ultrapure water Milli-Q, which was further changed after 2 hours. The cytotoxicity test in direct contact was performed according to ISO 10993-5 with modifications. The cells were seeded in the presence of samples at a concentration of 10^5 cells per mL. Cell proliferation around the tested samples was evaluated after three days using an inverted Olympus phase contrast microscope (Olympus IX81, Japan). Cells seeded on tissue plastic were used as a reference.

The cytotoxicity of extracts. The test was performed according to ISO 10993-5 and samples were extracted according to ISO 10993-12 (0.2 g of sample per mL of cultivation medium). The extraction proceeded at 37 ± 1 °C with continuous stirring for 24 ± 1 h. The individual prepared extracts were then filtered through a 0.22 μm syringe filter and utilized within 24 hours. The parent extracts (100%) were diluted in the culture medium to obtain a series of dilutions with concentrations of 75, 50, 25, 10 and 5%. Cells were pre-cultivated for 24 h and the medium was then replaced with diluted extracts. Cells cultivated in the presence of the pure medium were used as a reference (giving 100% cell proliferation). Viable cells were counted after one day of cell cultivation (37 ± 0.1 °C) in the presence of sample extracts using a BD FACSCanto flow cytometer (BD Biosciences, Canada) employing SYTO^R 61 red fluorescent nucleic acid stain (Life Technologies, USA) to assess cytotoxic effects. First, the diluted extracts were sucked up, and the layer of cells was washed with phosphate buffered saline (PBS, BioSera, France). The adhered cells were released using trypsin and stained with SYTO at a final concentration of 30 nM. After 30 minutes, the viable cells were analyzed in the dark. All tests were performed

in quadruplicates, and Dixon's Q test was used to remove outlying values. The morphology of the cells was also observed using an inverted Olympus phase contrast microscope (Olympus IX81, Japan).

The ingrowth of cells through the scaffolds. Before testing, samples were disinfected with 70% ethanol as described earlier. One mL of cell suspension at a concentration of 1×10^6 cells per mL was gently injected by syringe into each scaffold [and 0.2 mL also onto the surface of the material], and the scaffolds were placed in a 24-well plate. After 2 hours, two mL of cultivation medium was added. The cells were cultivated in an incubator to allow them to adhere and subsequently began to proliferate inside the structure of the tested samples. After three days, the samples were placed into a bioreactor, where they were cultivated for the next 14 days. For this purpose, a Rotary Cell Culture systems™ RCCS-4 (Synthecon Incorporated, Texas) was used. Each sample was inserted separately inside the high aspect ratio vessel, and 50 mL of cultivation medium was added. The forward rotation was adjusted to 15.5 rpm. The medium was changed after seven days. After the cultivation period, the samples were fixed with 4% paraformaldehyde overnight and subsequently washed with PBS, permeabilized with 0.5% Triton X-100, and again washed with PBS three times. The fixed and permeabilized cells were stained using ActinRed™ 555 (Thermo Fisher Scientific, USA). The tested samples were sliced, and the cell morphology was observed using fluorescent microscopy.

2.5. Antibacterial properties

For antibacterial testing, two bacterial strains were utilized – *Staphylococcus aureus* CCM 4516 (ATCC; American Type Culture Collection 6538) and *Escherichia coli* CCM 4517 (ATCC; American Type Culture Collection 8739). Soybean Casein Digest Agar (Tryptone Soya Agar, HiMedia Laboratories, India) was used as nutrient agar.

To determine whether the amount of KL^f was sufficient to induce antibacterial properties in the selected scaffolds, the agar diffusion test with modifications was conducted. The amendment lay in the pouring of samples into agar instead of the placing of flat samples onto the surface of the agar. Samples were poured into the agar containing a bacterial suspension at a concentration of 5×10^5 CFU per mL of agar. The agar plates with inoculated bacteria were incubated at 35 °C for 24 hours. After this incubation period, inhibition zones were measured.

3. Results and discussion

All biomaterials must exhibit certain required properties and mainly low cytotoxicity. In the case of scaffolds, these include appropriate mechanical properties and advanced properties such as the capacity to allow cells to grow into the structure. Intrinsic antibacterial activity is another advanced and highly desired property which can decrease the risk of nosocomial infections. All of the properties mentioned above were determined for the PVA and KL^f-based scaffolds developed in this study.

PVA hydrogels with the addition of lignin at a concentration higher than 10 wt% were mechanically unstable and formless. The ability of hydrogels to withstand the mechanical stress was determined as a strain recovery after releasing the stress. Fig. 1 shows the record of creep behaviour of PVA hydrogel modified with 1 wt% of KL^f.

The maximum strain and strain recovery exhibited unfilled PVA hydrogel (see Table 1). The strain and strain recovery values decreased proportionally with the lignin addition. The reason is that lignin has a reinforcing effect and partially disrupts the homogeneity of the hydrogel. Lignin added at a concentration higher than 10 wt% resulted in mechanical instability, probably due to the inhibition of PVA cross-linking. Due to this insufficient cross-linking, hydrogels with 15 wt% and 20 wt% lignin were soft and formless and therefore unable to recover their original geometry after compression.

PVA_10-KL^f was hydrogel with the highest concentration of KL^f (10 wt%) and still well preserved mechanical stability. Fig. 2 shows the record of thermogravimetric analysis of neat PVA and PVA with 10 wt% of KL^f. The addition of 10 wt% of KL^f shifted the degradation onset about 2.5 °C to the lower temperature. The reason for an earlier degradation might be a lower cross-linking degree of the hydrogel.

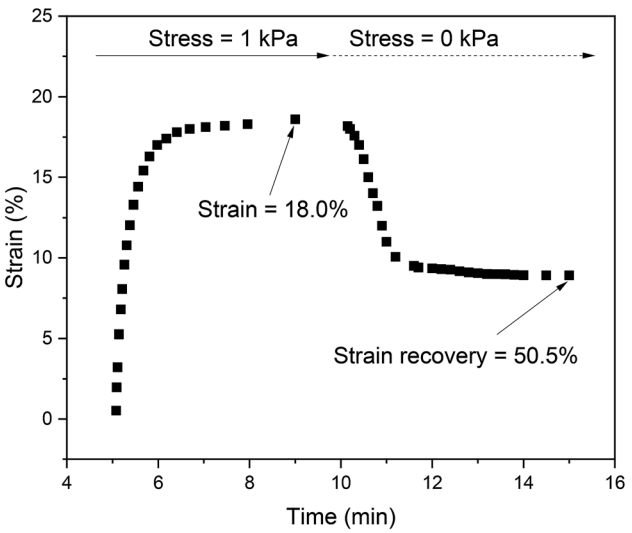

Fig. 1 Creep behaviour of PVA_1-KL^f hydrogel at 25 °C in air.

Table 1 Creep/recovery data for PVA hydrogels

Sample	[a]Compression strain after creep (%)	[b]Strain recovery after 5 min relaxation (%)
PVA	19.3 ± 2	54.2 ± 3
PVA_1-KL^f	18.0 ± 1	50.5 ± 3
PVA_5-KL^f	13 ± 5	45.2 ± 2
PVA_10-KL^f	8 ± 1	38.1 ± 2

[a] The value indicates a reduction in initial sample height due to stress of 1 kPa. [b] The value indicates the recovery of the original sample height after 5 min of relaxation without stress.

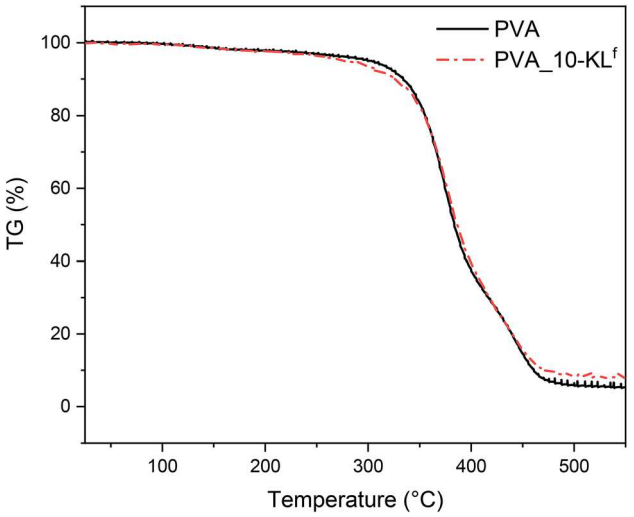

Fig. 2 TG curves of neat PVA hydrogel and PVA hydrogel with 10 wt% of KL^f.

The internal structures of the tested hydrogels were observed by SEM. The micrographs of PVA (referent sample) and selected samples are depicted in Fig. 3. The micrographs show the structure of PVA/KL^f scaffolds in dependence on the content of KL^f. The porosity and internal structures of neat PVA and PVA/KL^f scaffolds with lower lignin concentrations correspond to structures of scaffolds commonly utilized in tissue engineering. SEM micrographs show that the addition of lignin up to 5 wt% increased the density of PVA scaffold structures; Fig. 3B shows the longitudinal fibres of PVA_1-KL^f, while Fig. 3C depicts the cross-section of PVA_5-KL^f. However, as the amount of KL^f increased, the structure became less consistent, as shown in Fig. 3E, which depicts the disruption and mechanical instability of PVA_20-KL^f samples. The observed trend confirmed the changes in hydrogel properties with increasing contents of KL^f recorded during the testing of mechanical stability.

The differences in the internal structure in dependence on lignin concentration have been confirmed by the values of the swelling ratio (see Fig. 4). The changes in the swelling ratio values are following SEM micrographs. PVA hydrogels with 1–5 wt% KL^f are much denser as neat PVA hydrogel and show lower swelling ratio values. However, PVA hydrogels containing lignin in the concentration above 10 wt% show swelling ratio comparable with neat PVA, which correspond with the content of bigger pores and irregular inner structure.

The determination of cytotoxicity is the test of the first choice when the biocompatibility of any material is at issue. The cytotoxicity testing of scaffolds based on PVA and KL^f has not yet

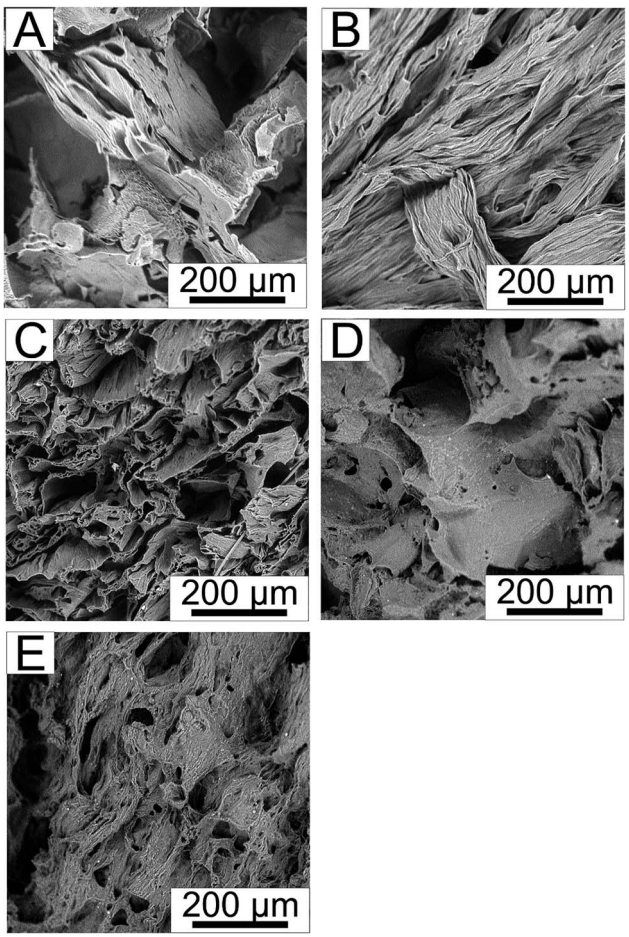

Fig. 3 The internal structure of (A) PVA, (B) PVA_1-KL^f, (C) PVA_5-KL^f, (D) PVA_15-KL^f, (E) PVA_20-KL^f.

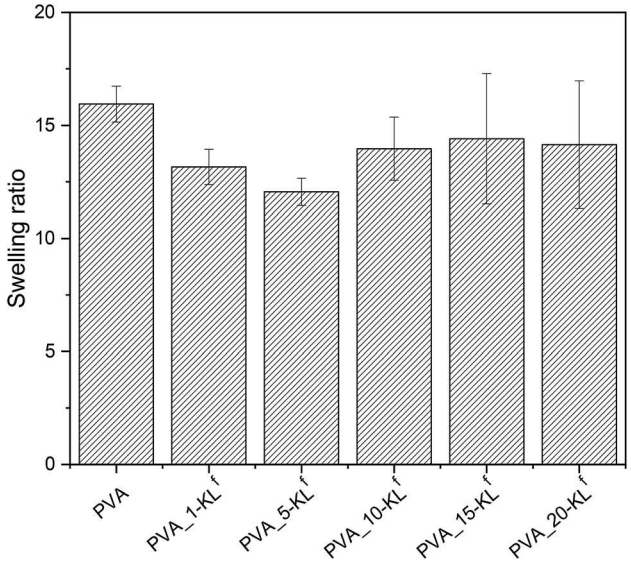

Fig. 4 Swelling ratio of neat PVA and PVA hydrogels modified with KL^f.

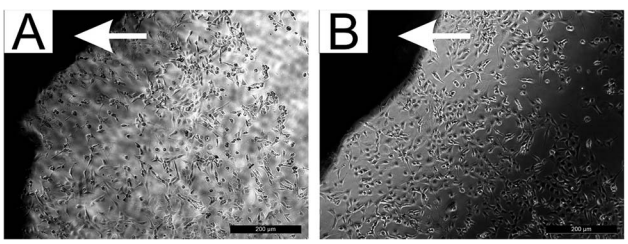

Fig. 5 The mass of NIH/3T3 cultivated in direct contact with (A) PVA_1-KL^f, (B) PVA_20-KL^f (dark regions marked with a white arrow).

been fully developed. For this reason, a preliminary method for determining scaffold cytotoxicity – that is, cytotoxicity testing in direct contact – was employed first.

It was found that cells were able to proliferate in direct contact with all samples. Moreover, no morphological changes were observed in comparison with reference cells. The obtained results, therefore, indicate no cytotoxic effect in direct contact. The micrographs in Fig. 5 show cells proliferating in direct contact with PVA_1-KL^f and PVA_20-KL^f.

For quantitative and more sensitive cytotoxicity assessments, extracts of the studied scaffolds were tested using flow cytometry and SYTO staining. First, the cytocompatibility of pure PVA material in the tested scaffolds, whose biocompatibility has already been described in previous studies,[27] was confirmed (see Fig. 6, where results for 50, 75 and 100% extracts are presented; lower extract concentrations exhibited no cytotoxic effect). Concerning the cytotoxicity of scaffold extracts, a significant dependence between the cytotoxic effect and the amount of KL^f in the tested samples was observed (Fig. 6).

Moreover, cell morphology supported the obtained results, confirming that a direct correlation existed between the cytotoxic effect and the amount of KL^f in the sample (see Fig. 7).

However, a comparison of the obtained results with the literature is problematic because of a lack of articles dealing

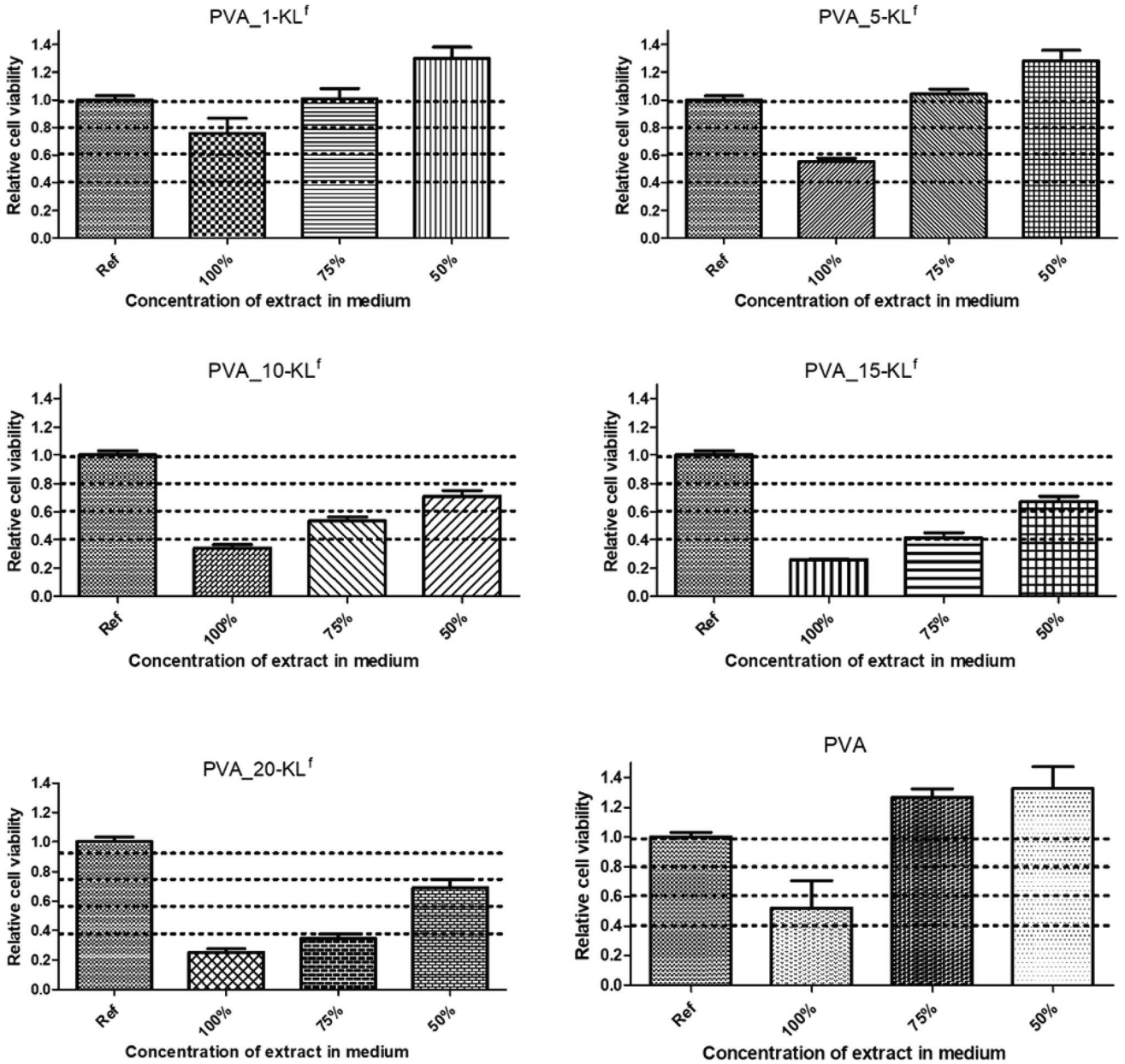

Fig. 6 Cytotoxicity of scaffold extracts of various concentrations presented as a relative number of viable cells ± the standard deviation compared to reference according to ISO 10993-5 standard. The dashed lines highlight the critical viabilities to be assessed according to requirements of EN ISO 10993-5, where viability > 0.8 means no cytotoxicity; 0.6–0.8, mild cytotoxicity; 0.4–0.6, moderate toxicity; and <0.4, severe cytotoxicity.

with the cytotoxicity and biocompatibility of KL in general and especially its fractionated form. The obtained results are discussed in the context of more general studies of lignin. Even though the fact that lignin-based copolymers are perceived as nontoxic,[28] it is necessary to mention that lignin could have an adverse impact on cell viability. The data presented in this article correlate well with the study by Kai *et al.*[29] They described limitations on the application of alkali lignin resulting from its cytotoxicity at high concentrations. A concentration of 6% by mass was evaluated as the optimal amount of alkali lignin in PLLA/PLA-lignin nanofibers.[29] Moreover, it was found that the cytotoxic effect of alkali lignin appeared to increase with time of exposure.[30] In light of the results obtained in our study, the highest possible concentration of KL^f that exhibits no or very low cytotoxicity was assessed to be around 5%.

The absence of cytotoxicity is one of the critical factors essential for the successful use of materials in tissue engineering. The ability of cells to ingrow and survive within the internal structure of scaffolds is another crucial parameter. Thus, NIH/3T3 cells were seeded inside the tested samples and cultivated in a Rotary Cell Culture systems™ RCCS-4 to evaluate the ability of cells to grow into the porous scaffolds. We found that the cells were able to grow into all the tested scaffolds (see Fig. 8, where only PVA, PVA_1-KL^f, PVA_5-KL^f, PVA_15-KL^f and PVA_20-KL^f are depicted as examples). However, a significant correlation was found between the ability of cells to grow into scaffolds and the amount of KL^f present. Greater cell growth into samples with lower amounts of KL^f was observed, similarly to what was seen during the cytotoxicity testing of extracts. The samples PVA_1-KL^f and PVA_5-KL^f are advantageous for mouse fibroblasts; therefore, the suggested amount of KL^f for tissue engineering scaffolds seems to be between 1 and 5%. However, according to the comparison of stained cell cytoskeletons inside scaffolds, cell growth was homogeneous only in the case of PVA_1-KL^f (Fig. 8B). In contrast, the cells inside the PVA_5-KL^f (Fig. 8C) scaffold created clusters. Growth is an important feature because a tissue-engineering scaffold should enable cells to grow homogeneously into its structure and gradually create continuous tissue. The creation of separate clusters is undesirable. From this point of view, a concentration of KL^f of about 1% should be optimal for use in tissue engineering.

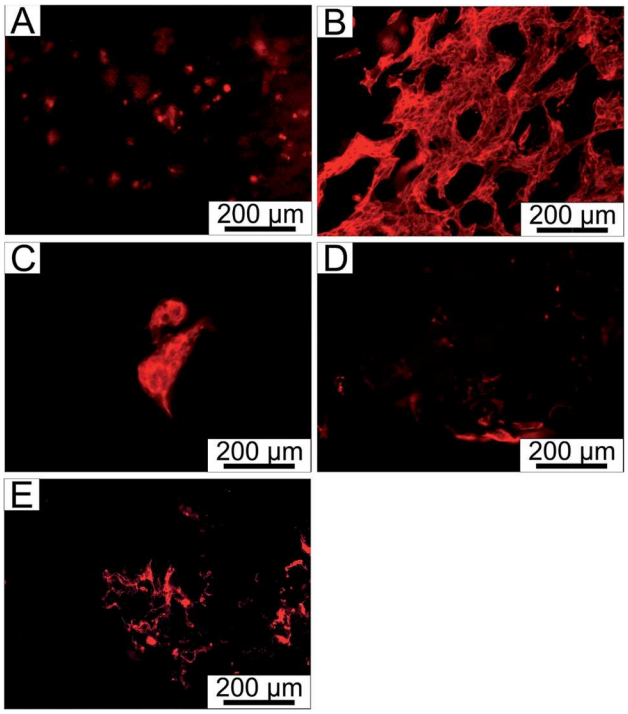

Fig. 8 NIH/3T3 fibroblasts stained with ActinRed™ 555 grown within (A) PVA, (B) PVA_1-KL^f, (C) PVA_5-KL^f, (D) PVA_15-KL^f, (E) PVA_20-KL^f.

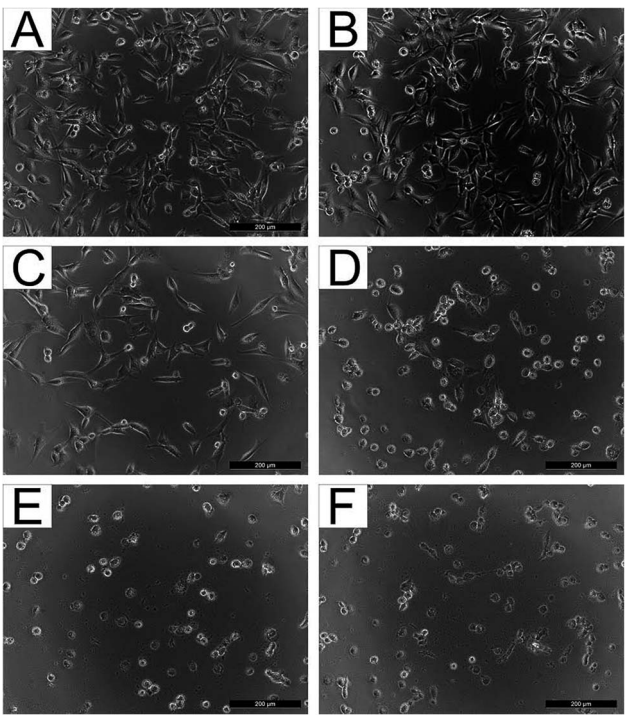

Fig. 7 NIH/3T3 cultivated in the presence of 75% extracts of (A) PVA, (B) PVA_1-KL^f, (C) PVA_5-KL^f, (D) PVA_10-KL^f, (E) PVA_15-KL^f, and (F) PVA_20-KL^f.

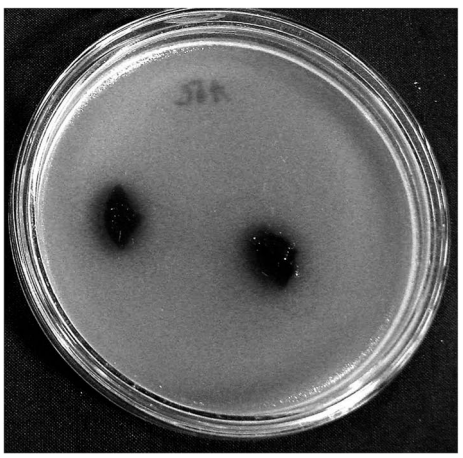

Fig. 9 The growth of *E. coli* in the presence of sample PVA_20-KL^f.

To determine whether the amount of KL^f was sufficient to induce antibacterial properties in the selected scaffolds, the agar diffusion test with modifications was conducted. However, no tested sample exhibited antibacterial properties (see Fig. 9, where no inhibition zones were detected). In this context, it should be mentioned that antibacterial properties of lignins depend on the nature of the lignin and the type of microorganisms. However, the antibacterial efficiency of lignin in polymer composites may be connected with their leaching into the environment. Thus, their antibacterial efficiency in composites in which lignins are chemically crosslinked with other constituents may be limited.

4. Conclusion

New scaffolds based on poly(vinyl alcohol) and KL^f in concentrations ranging from one to twenty wt% were prepared and biologically tested. Both materials, PVA and KL^f, are biopolymers exhibiting hypothetically high degrees of biocompatibility. KL^f was used as a stiffening additive with potential antibacterial properties. The determination of viscoelastic properties showed that all scaffolds based on PVA and KL^f up to 10 wt% demonstrated sufficient mechanical stability. However, on the basis of advanced biological testing (*i.e.*, according to the ingrowth of cells under simulated *in vivo* conditions in a bioreactor), it must be noted that only scaffolds containing 99 wt% PVA and one wt% KL^f can be proposed as advanced materials suitable for use in tissue engineering. Unfortunately, KL^f incorporated in PVA did not exhibit any antibacterial activity.

Conflicts of interest

There are no conflicts to declare.

Acknowledgements

This work was supported by the Czech Science Foundation (grant no. 17-05095S) and the Ministry of Education, Youth and Sports of the Czech Republic (Program NPU I, LO1504). Petra Rejmontová gratefully acknowledges support from the internal grant IGA/CPS/2018/001 of TBU in Zlin, financed from funds for specific academic research. Adriana Kovalcik is grateful for the support through the Brno University of Technology internal project FCH-S-18-5334 and project SoMoPro (project No. 6SA18032). This project has received funding from the European Union's Horizon 2020 research and innovation programme under the Marie Skłodowska-Curie, and it is co-financed by the South Moravian Region under grant agreement No. 665860. Authors confirm that the content of this work reflects only the author's view and that the EU is not responsible for any use that may be made of the information it contains.

References

1 B. P. Nair, D. Gangadharan, N. Mohan, B. Sumathi and P. D. Nair, *Mater. Sci. Eng., C*, 2015, **52**, 333–342, DOI: 10.1016/j.msec.2015.03.040.
2 H. Lee, H. Hwang, Y. Kim, H. Jeon and G. Kim, *Chem. Eng. J.*, 2014, **250**, 399–408, DOI: 10.1016/j.cej.2014.04.009.
3 M. R. Badrossamay, K. Balachandran, A. K. Capulli, H. M. Golecki, A. Agarwal, J. A. Goss, H. Kim, K. Shin and K. K. Parker, *Biomaterials*, 2014, **35**, 3188–3197, DOI: 10.1016/j.biomaterials.2013.12.072.
4 H. G. S. Ayaz, A. Perets, H. Ayaz, K. D. Gilroy, M. Govindaraj, D. Brookstein and P. I. Lelkes, *Biomaterials*, 2014, **35**, 8540–8552, DOI: 10.1016/j.biomaterials.2014.06.029.
5 S. Hinderer, J. Seifert, M. Votteler, N. Shen, J. Rheinlaender, T. E. Schaeffer and K. Schenke-Layland, *Biomaterials*, 2014, **35**, 2130–2139, DOI: 10.1016/j.biomaterials.2013.10.080.
6 S. Fleischer, R. Feiner, A. Shapira, J. Ji, X. Sui, H. D. Wagner and T. Dvir, *Biomaterials*, 2013, **34**, 8599–8606, DOI: 10.1016/j.biomaterials.2013.07.054.
7 S. J. Bryant and K. S. Anseth, *J. Biomed. Mater. Res., Part A*, 2003, **64**, 70–79, DOI: 10.1002/jbm.a.10319.
8 P. J. Martens, S. J. Bryant and K. S. Anseth, *Biomacromolecules*, 2003, **4**, 283–292, DOI: 10.1021/bm025666v.
9 T. S. Gaaz, A. B. Sulong, M. N. Akhtar, A. A. H. Kadhum, A. B. Mohamad and A. A. Al-Amiery, *Molecules*, 2015, **20**, 22833–22847, DOI: 10.3390/molecules201219884.
10 M. I. Baker, S. P. Walsh, Z. Schwartz and B. D. Boyan, *J. Biomed. Mater. Res., Part B*, 2012, **100**, 1451–1457, DOI: 10.1002/jbm.b.32694.
11 J. C. Hayes and J. E. Kennedy, *Mater. Sci. Eng., C*, 2016, **59**, 894–900, DOI: 10.1016/j.msec.2015.10.052.
12 N. Alexandre, J. Ribeiro, A. Gaertner, T. Pereira, I. Amorim, J. Fragoso, A. Lopes, J. Fernandes, E. Costa, A. Santos-Silva, M. Rodrigues, J. D. Santos, A. C. Mauricio and A. L. Luis, *J. Biomed. Mater. Res., Part A*, 2014, **102**, 4262–4275, DOI: 10.1002/jbm.a.35098.
13 A. F. Leitao, S. Gupta, J. P. Silva, I. Reviakine and M. Gama, *Colloids Surf., B*, 2013, **111**, 493–502, DOI: 10.1016/j.colsurfb.2013.06.031.
14 S. Mishra, R. Bajpai, R. Katare and A. K. Bajpai, *J. Appl. Polym. Sci.*, 2006, **100**, 2402–2408, DOI: 10.1002/app.23177.
15 C. Shuai, Z. Mao, H. Lu, Y. Nie, H. Hu and S. Peng, *Biofabrication*, 2013, **5**, 015014, DOI: 10.1088/1758-5082/5/1/015014.
16 L. Dini, E. Panzarini, M. A. Miccoli, V. Miceli, C. Protopapa and P. A. Ramires, *Tissue Cell*, 2005, **37**, 479–487, DOI: 10.1016/j.tice.2005.09.002.
17 A. Karimi and M. Navidbakhsh, *Materials and Technology*, 2014, **29**, 90–100, DOI: 10.1179/1753555713Y.0000000115.
18 O. Gordobil, R. Delucis, I. Eguees and J. Labidi, *Ind. Crops Prod.*, 2015, **72**, 46–53, DOI: 10.1016/j.indcrop.2015.01.055.
19 A. T. R. Sugano-Segura, L. B. Tavares, J. G. F. Rizzi, D. S. Rosa, M. G. Salvadori and D. J. dos Santos, *Radiat. Phys. Chem.*, 2017, **139**, 5–10, DOI: 10.1016/j.radphyschem.2017.05.016.
20 A. Naseem, S. Tabasum, K. M. Zia, M. Zuber, M. Ali and A. Noreen, *Int. J. Biol. Macromol.*, 2016, **93**, 296–313, DOI: 10.1016/j.ijbiomac.2016.08.030.
21 R. Kaur and S. K. Uppal, *Colloid Polym. Sci.*, 2015, **293**, 2585–2592, DOI: 10.1007/s00396-015-3653-1.

22 A. Gregorova, in *Encyclopedia of Biomedical Polymers and Polymeric Biomaterials, 11 Volume Set*, ed. M. Mishra, Taylor and Francis Group, New York, 2015.
23 J. D. Coral Medina, A. L. Woiciechowski, A. Zandona Filho, L. Bissoqui, M. D. Noseda, L. P. de Souza Vandenberghe, S. F. Zawadzki and C. R. Soccol, *Ind. Crops Prod.*, 2016, **94**, 630–637, DOI: 10.1016/j.indcrop.2016.09.046.
24 M. Guo, T. Jin, N. P. Nghiem, X. Fan, P. X. Qi, C. H. Jang, L. Shao and C. Wu, *Appl. Biochem. Biotechnol.*, 2017, **184**, 1–16.
25 X. Jiang, D. Savithri, X. Du, S. Pawar, H. Jameel, H. Chang and X. Zhou, *ACS Sustainable Chem. Eng.*, 2017, **5**, 835–842, DOI: 10.1021/acssuschemeng.6b02174.
26 A. Gregorova and V. Sedlarik, *Desalin. Water Treat.*, 2016, **57**, 10655–10663, DOI: 10.1080/19443994.2015.1036364.
27 A. Kumar and S. S. Han, *Int. J. Polym. Mater. Polym. Biomater.*, 2017, **66**, 159–182, DOI: 10.1080/00914037.2016.1190930.
28 D. Kai, Z. W. Low, S. S. Liow, A. A. Karim, H. Ye, G. Jin, K. Li and X. J. Loh, *ACS Sustainable Chem. Eng.*, 2015, **3**, 2160–2169, DOI: 10.1021/acssuschemeng.5b00405.
29 D. Kai, W. Ren, L. Tian, P. L. Chee, Y. Liu, S. Ramakrishna and X. J. Loh, *ACS Sustainable Chem. Eng.*, 2016, **4**, 5268–5276, DOI: 10.1021/acssuschemeng.6b00478.
30 V. Ugartondo, M. Mitjans and M. P. Vinardell, *Bioresour. Technol.*, 2008, **99**, 6683–6687, DOI: 10.1016/j.biortech.2007.11.038.

Article XI.

Munster, L.; **Capakova, Z**.; Fisera, M.; Kuritka, I.; Vicha, J. Biocompatible Dialdehyde Cellulose/Poly(Vinyl Alcohol) Hydrogels with Tunable Properties. Carbohydr. Polym. 2019, 218, 333–342. https://doi.org/10.1016/j.carbpol.2019.04.091.

Carbohydrate Polymers 218 (2019) 333–342

Contents lists available at ScienceDirect

Carbohydrate Polymers

journal homepage: www.elsevier.com/locate/carbpol

Biocompatible dialdehyde cellulose/poly(vinyl alcohol) hydrogels with tunable properties

Lukáš Münster[a], Zdenka Capáková[a], Miroslav Fišera[b], Ivo Kuřitka[a], Jan Vícha[a,*]

[a] Centre of Polymer Systems, Tomas Bata University in Zlín, tř Tomáše Bati 5678, 760 01, Zlín, Czech Republic
[b] Department of Food Analysis and Chemistry, Tomas Bata University in Zlín, nám. T.G. Masaryka 5555, 760 01, Zlín, Czech Republic

ARTICLE INFO

Keywords:
Poly(vinyl alcohol)
Crosslinking
Dialdehyde cellulose
Drug release
Biomaterials
Hydrogel

ABSTRACT

Solubilized dialdehyde cellulose (DAC), an efficient crosslinking agent for poly(vinyl alcohol) (PVA), provides less toxic alternative to current synthetic crosslinking agents such as glutaraldehyde, while simultaneously allowing for the preparation of hydrogels with comparably better characteristics. PVA/DAC hydrogels prepared using 0.5, 1 and 1.5 wt% of DAC were analyzed in terms of mechanical, swelling and cytotoxicity characteristics. Materials properties of PVA/DAC hydrogels range from stiff substances to soft viscoelastic gels capable of holding large amounts of water. Superior mechanical properties, porosity and surface area in comparison with analogical PVA/glutaraldehyde hydrogels were observed. Biological studies showed low toxicity and good biocompatibility of PVA/DAC hydrogels. Potential of PVA/DAC in mesh-controlled release of biologically active compounds was investigated using ibuprofen, rutin and phenanthriplatin. Hydrogel loaded with anticancer drug phenantriplatin was found effective against alveolar cancer cell line A549 under in vitro conditions.

1. Introduction

Hydrogels play an important role in industrial and biomedical sectors for more than half a century. (Wichterle & Lím, 1960; Yahia, 2015) They are receiving continuous attention due to their similarity with natural tissue, which rises from the high degree of flexibility and large content of water. Beside non-toxicity, suitable mechanical properties are one of the key criteria for successful application of hydrogels in biomedical sector. For example, hydrogels exhibiting polymer volume fraction ($v_{2,s}$) greater than 0.1 are probably the most important ones for biomedical applications as they possess improved mechanical stability. (Canal & Peppas, 1989) Besides, hydrogel-based artificial cartilage implants should possess relatively high compression stress profile from 0.5 to 10 MPa. (Park, Nicoll, Mauck, & Ateshian, 2008)

Other key properties of hydrogels, such as crosslink density, swelling capacity, equilibrium water content (EWC), gel fraction and mesh size (ξ), reflect the porosity of hydrogel and its ability to accommodate and subsequently release various substances. This makes hydrogels excellent materials for wide range of drug-delivery applications, from dermal patches and masks to implantable depots of anticancer drugs. Dermal absorption of biologically active compounds from hydrogels is widely used in both cosmetics and medicine, as it allows painless, sustained and controlled delivery of biologically active compounds over prolonged periods of time. (Caló & Khutoryanskiy, 2015) The localization of therapeutic agent via implantation of hydrogel-based drug delivery depots improves drug efficacy, limits the off-target side effects, increases its potency and thus decreases the required dose. This is particularly important for chemotherapeutics, as these substances are often constrained by dose-limiting toxicity. Therefore, clinicians have used intratumoral implantation of anticancer-drug depots to direct the biological effect to the target cells, reduce off-target toxicity and to lower the overall dose of chemotherapeutics. (Tibbitt, Dahlman, & Langer, 2016)

Current hydrogel materials are often prepared by using crosslinking agents of synthetic origin (epichlorhydrine, adipic acid, dihydrazide, glutaraldehyde etc.). (Gulrez, Al-Assaf, & Phillips, 2011) These low-molecular weight molecules are highly toxic (Kim et al., 2017) and can enter cells of living organism through various portals of entry. Hence, for biomedical applications, it would be more desirable to utilize crosslinking agents derived from naturally available biopolymers, particularly if they would have better properties than the synthetic ones.

Overall, the demand for new functional biopolymer derivatives, which would provide sustainable alternative to synthetic compounds while having better biocompatibility and biodegradability, worldwide availability and low cost, is growing rapidly. The selectively oxidized cellulose, 2,3-dialdehydecellulose (DAC), has received a lot of interest from scientific community due to a number of favorable properties. Firstly, its preparation is sustainable as various renewable sources of

* Corresponding author.
E-mail addresses: munster@utb.cz (L. Münster), capakova@utb.cz (Z. Capáková), fisera@utb.cz (M. Fišera), kuritka@utb.cz (I. Kuřitka), jvicha@utb.cz (J. Vícha).

https://doi.org/10.1016/j.carbpol.2019.04.091
Received 22 March 2019; Received in revised form 25 April 2019; Accepted 27 April 2019
Available online 02 May 2019
0144-8617/

cellulose, including fast growing plants like bamboo etc., may be used as starting material, (Yan et al., 2019) while the periodate salt used for oxidation of cellulose can be easily regenerated and re-used. (Koprivica et al., 2016; Liimatainen, Sirviö, Pajari, Hormi, & Niinimäki, 2013) Moreover, the possibility of DAC solubilization by hot water (Kim, Wada, & Kuga, 2004) greatly expands its utilization in aqueous chemistry, where raw cellulose cannot be used. The presence of reactive aldehyde groups in DAC structure then allows for a broad range of applications, such as preparation of micro beads and hollow microspheres, (Lindh, Carlsson, Strømme, & Mihranyan, 2014; Rocha, Ferraz, Mihranyan, Strømme, & Lindh, 2018; Yan et al., 2019), antibacterial agents (Ge, Zhang, Xu, Cao, & Kang, 2018; Kim et al., 2017) or other functional cellulose derivatives, e.g. 2,3-dicarboxycellulose (DCC), (Kim & Kuga, 2001; Suopajärvi, Liimatainen, Hormi, & Niinimäki, 2013) which exhibits large potential as an anticancer drug carrier. (Münster et al., 2019)

Last but not least, reactive aldehyde groups of DAC can serve as a crosslinking hotspots in the preparation of hydrogel materials. Pilot studies suggested a large potential of DAC in this area. Kim et al. noted low toxicity and high protein absorption capability of DAC-crosslinked chitosan hydrogels, (Kim et al., 2017) while we studied role of DAC aging in crosslinking of PVA. (Münster et al., 2018)

However, none of these proof-of-concept studies covered the scope of potential applications of DAC-crosslinked hydrogel materials, i.e. how they can be engineered for biomedical applications in the terms of mechanical properties or mesh density for controlled release of biologically active compounds. Therefore, mechanical and surface-related properties, toxicity and drug release characteristics of PVA/DAC hydrogels prepared using different amount of DAC are studied here to determine the full spectrum of their possible biomaterial applications. Tuning of material properties of PVA/DAC hydrogels from stiff substances resembling artificial cartilages to soft viscoelastic gels capable of holding large amounts of water, ideal for drug-delivery applications, is demonstrated. The factors influencing drug release, i.e. mesh density and size and charge of the released molecules, are investigated for (i) ibuprofen, one of the most broadly used nonsteroidal anti-inflammatory drugs acting as nonselective cyclooxygenase enzyme (COX) inhibitor. (ii) Rutin, a glycoside combining the flavonol quercetin and the disaccharide rutinose, abundant in buckwheat and tea, which is utilized in wound dressing and healing applications due to its antimicrobial and antiviral activity, cosmetics due to its antioxidant properties and has cytoprotective, vasoprotective, anticarcinogenic, neuroprotective and cardioprotective properties. (Ganeshpurkar & Saluja, 2017) (iii) Phenanthriplatin, the latest generation of chemotherapeutic with high potency, (Park, Wilson, Song, & Lippard, 2012) which would however greatly benefit from effective drug-delivery system. (Czapar et al., 2016) The biological compatibility of hydrogels is demonstrated using cell lines representing healthy tissues, while their drug-delivery capabilities are investigated using adenocarcinomic cells.

2. Methods

2.1. Materials and chemicals

Poly(vinyl alcohol) with 87–89% degree of hydrolysis (PVA), weight average molecular weight ($\bar{M}_w$) of 13–23 kDa and density of 1.269 g/cm^3 (Sigma Aldrich Co.) was used as source material. Its number average molecular weight ($\bar{M}_n$) employed in the calculation of network parameters was obtained by GPC (7.9 kDa). Crosslinking of PVA by dialdehyde cellulose or glutaraldehyde was performed under acidic conditions. Dialdehyde cellulose (DAC) was prepared by the periodate oxidation of alpha cellulose (Sigma Aldrich Co.) by sodium periodate ($NaIO_4$) supplied from Penta, Czech Republic. The weight average molecular weight ($\bar{M}_w$) of cellulose was estimated by gel permeation chromatography (GPC) to be 109 kDa (degree of polymerization 672). (Engel, Hein, & Spiess, 2012; Münster et al., 2017) Aqueous solution (50% w/w) of glutaraldehyde (GA) was supplied by Sigma Aldrich Co. The chemicals employed in DAC and hydrogel preparation and characterization include ethylene glycol, sodium hydroxide (NaOH), hydrochloric acid (HCl) (Penta, Czech Republic) and hydroxylamine hydrochloride ($NH_2OH \cdot HCl$) supplied from Sigma Aldrich Co. Prepared PVA/DAC hydrogels were loaded with ibuprofen, rutin (Sigma Aldrich Co.) and phenatriplatin synthesized according to Park et al. (Park et al., 2012) The release of active compounds was subsequently investigated.

Biological tests were performed on mouse embryonic fibroblast cell line (ATCC CRL-1658 NIH/3T3, USA), human keratinocyte cell line (HaCaT, CLS, Germany) and adenocarcinomic human alveolar basal epithelial cells (ATCC® CCL-185, A549, USA). The ATCC-formulated Dulbecco's Modified Eagle's Medium (PAA Laboratories GmbH, Austria) containing 10% of calf serum (BioSera, France) was used as a culture medium for NIH/3T3, while DMEM with 10% of fetal bovine serum (BioSera, France) was used for HaCaT and A549 cells. The 100 U/mL Penicillin/Streptomycin (GE Healthcare HyClone, United Kingdom) was added to all media. Phosphate buffer saline (PBS, (Invitrogen, USA) was used for washing cells. Cells were cultivated on Techno plastic products (TPP, Switzerland). Tetrazolium (MTT cell proliferation assay kit, Duchefa Biochemie, Netherlands) was used to determine the cell viability. For fluorescence microscopy the formaldehyde (Penta, Czech Republic), Triton X-100 (Sigma-Aldrich, USA), Hoechst, 33258 (Invitrogen, USA) and ActinRed™ 555 (Thermo Fisher Scientific, USA) were used.

2.2. Preparation of DAC and PVA/DAC hydrogels

The preparation of DAC follow well-established procedure of cellulose oxidation by periodate salt using 1:1.2 molar ratio of reactants (DAC:periodate salt). (Münster et al., 2017) Prepared solid DAC was immediately solubilized, purified and analyzed in the terms of reactive aldehyde group (−CHO) content. (Münster et al., 2018) Final product, which exhibited 93% degree of oxidation (11.6 mmol/g of –CHO groups), was kept under acidic conditions (pH = 3.5 ± 0.1) and was immediately used as crosslinking agent for PVA to prevent its degradation and other structural changes occurring during its aging. (Münster et al., 2017; 2018; Yan et al., 2019)

The PVA/DAC hydrogels were prepared by crosslinking of PVA by prepared DAC in the presence of diluted HCl serving as a catalyst. In brief, 40 g of PVA was dissolved in 170 mL of demineralized water overnight at 80 °C. Catalyst (12 mL of 1.33 M HCl) and solution containing 1 wt% of DAC (relative to PVA) were subsequently added to PVA solution. Volume was set to 200 mL by addition of water and reaction mixture was stirred vigorously to achieve good homogenization of all reactants. The same preparation process was repeated using 0.5 wt% and 1.5 wt% of DAC. The crosslinking reaction between PVA and DAC takes place during drying of reaction mixture, when DAC dehydration causes exposure of −CHO groups and subsequent formation of hemiacetals with hydroxyl groups of PVA. Therefore, the homogenized reaction mixtures were poured into the vessel with walls formed by semi-permeable membrane, which enables faster and more even evaporation of solvent from larger area in comparison to the casting of the reaction mixture into the solid form. After drying at 50 °C for several days, bulk PVA/DAC xerogels were swelled, thoroughly washed and cut to 5 × 5 × 5 mm cubes, which were sterilized by 70% ethanol solution.

Besides DAC, GA (11.1 mmol/g of −CHO groups, estimated by oxime reaction) was also employed for the crosslinking of PVA for comparative purposes. The PVA/GA hydrogel sample was prepared by the same process as PVA/DAC hydrogels. The amount of GA was chosen to be equivalent (in terms of −CHO group content) to the lowest concentration of DAC (0.5 wt%, n_{-CHO} per sample = 2.34 mmol/40 g of PVA), which corresponds to 185.6 µL of GA per 40 g of PVA. Designation of hydrogels based on PVA prepared using different

Table 1
Amount of reactive—CHO groups used for the sample crosslinking, n_{-CHO} (mmol), amounts of crosslinker used in their preparation and designation of prepared samples.

n_{-CHO} per sample (mmol)	DAC crosslinker		GA crosslinker	
	DAC (wt%)	PVA/DAC (#)	GA (μL)	PVA/GA (#)
2.34	0.5	PD1	185.6	PG1
4.68	1	PD2		
7.02	1.5	PD3		

amounts of crosslinking agents (DAC and GA) is noted in Table 1.

Hydrogels based on PVA were analyzed in the terms of mechanical properties in the equilibrium swelled state. They were subsequently lyophilized in order to determine their specific surface area and surface morphology. Resulting cryogels were used for determination of network parameters, swelling kinetics and for biological testing (after re-swelling in biological media). Selected samples were loaded with ibuprofen, rutin and phenanthriplatin (PhPt) and their drug-release profiles were evaluated. Cytotoxicity of PhPt-loaded hydrogels was evaluated on healthy and cancerous cell lines.

2.3. Mechanical and rheological analysis

Mechanical analysis was conducted on specimens in equilibrium swelled state using compression mode on tensile testing machine M350 5CT (Labor Chemie, Czech Republic). Highest strength, stress at highest strength and Young's modulus were recorded and calculated employing compression rate of 10 mm/min. Rheological measurements were performed on rotational rheometer Anton Paar MCR 502 (Anton Paar, Austria) equipped with D-CP/PP7 shaft using roughened aluminum plate with 5 mm diameter and bottom plate with glued sandpaper (P240) to prevent slipping. Specimens were cut to fit the chosen geometry. All experiments were done at room temperature in oscillation mode in frequency sweep from 1 to 10 Hz by applying constant strain of 1%.

2.4. BET and SEM analysis

Specific surface area (a_{BET}) of lyophilized PVA cryogel specimens was determined (three-times for each hydrogel) by multipoint Brunauer-Emmet-Teller (BET) analysis of adsorption and desorption isotherms recorded at 77 K utilizing high precision surface area analyzer Belsorp-mini II (BEL Japan Inc., Japan). Prior to the BET analysis, PVA cryogel specimens were degassed at 75 °C for 72 h. These materials were also analyzed by scanning electron microscopy (SEM) employing Nova NanoSEM 450 microscope (FEI, Czech Republic) operated at 5 kV accelerating voltage. Ahead of SEM imaging, PVA cryogels were sputtered with gold-palladium nanoparticles to suppress the charge accumulation effect.

2.5. Network parameters and swelling kinetics

Cryogel specimens were submerged in demineralized water, solutions gently shaken and weighted in at predetermined times (up to 96 h) to assess their swelling kinetics. The network parameters including swelling capacity and equilibrium water content (EWC) were estimated by weighting method. The average molecular weight between crosslinks ($\bar{M}_c$), crosslink density (ρ_c) and mesh size (ξ) were determined based on equilibrium swelling theory (Flory & Rehner, 1943) as follows:

$$\bar{M}_c = \left[\frac{2}{\bar{M}_n} - \frac{\left(\frac{\bar{v}}{V_1}\right)[\ln(1 - v_{2,s}) + v_{2,s} + \chi_1 (v_{2,s})^2]}{\left[(v_{2,s})^{\frac{1}{3}} - \frac{v_{2,s}}{2} \right]} \right]^{-1} \quad (1)$$

$\bar{M}_c$, the average molecular weight between crosslinks (g/mol), is determined by Eq. (1) (Peppas, Huang, Torres-Lugo, Ward, & Zhang, 2000), where $\bar{M}_n$ is the number average of molecular weight of initial uncrosslinked polymer, $\bar{v}$ is the specific volume of polymer (0.788 cm^3/g), V_1 is the molar volume of water at 25 °C (18.069 cm^3/mol), χ_1 is the polymer-solvent interaction parameter (0.464), (Peppas & Merrill, 1976) and $v_{2,s}$ is the polymer volume fraction, calculated according to Eq. (2):

$$v_{2,s} = \left[1 + \frac{\rho_p}{\rho_w} \left(\frac{M_s}{M_0} - 1 \right) \right]^{-1} \quad (2)$$

where M_s/M_0 is the weight swelling ratio of swollen hydrogel at equilibrium estimated by weighing method, ρ_p is the polymer density, and ρ_w is the density of water. Crosslink density ρ_c (mmol/cm^3) can be then calculated using Eq. (3). (Peppas, 1986)

$$\rho_c = (\bar{v}\bar{M}_c)^{-1} \quad (3)$$

Mesh size ξ (Å), defined by Eq. (4), (Canal & Peppas, 1989) can be estimated from the relation between polymer volume fraction $v_{2,s}$ and end-to-end distance of the unperturbed (solvent-free) state $(\bar{r}_0^2)^{1/2}$, which is defined by Eq. (5),

$$\xi = v_{2,s}^{-1/3} (\bar{r}_0^2)^{1/2} \quad (4)$$

$$(\bar{r}_0^2)^{1/2} = l \left(\frac{2\bar{M}_c}{M_r} \right)^{1/2} C_n^{3/2} \quad (5)$$

where l is the C—C bond length (1.54 Å), M_r is the molecular weight of the repeating unit (44 g/mol for PVA), and C_n is the characteristic ratio of PVA chain (8.9). (Flory & Volkenstein, 1969)

2.6. Drug loading and release

To estimate the role of hydrogel mesh density for drug release applications, the specimens of the least and the most crosslinked PVA-based hydrogels (PD1 and PD3) were prepared. The weight of the swollen specimens was optimized with respect to their different EWC (see Section 3.3) in a way that resulting samples would contain the same amount of liquid. Samples were loaded with ibuprofen by submerging in 20 mg/mL solution of the drug for a week at ambient temperature in the absence of light. This approach was chosen to minimize the differences in swelling capacity, EWC and gel fraction between the hydrogels and allow for loading of all hydrogel samples by equivalent amount of drug, which would enable for direct comparison of the role of hydrogel mesh density in the drug release.

The loaded specimens were subsequently placed in separate closed containers containing 20 mL of demineralized water and shaken gently at 37 °C in incubation box. Aliquots of 1 mL were collected at given times and replaced by 1 mL of demineralized water to conserve the volume. In analogy to ibuprofen, 0.1 mg/mL rutin solutions (limited by its solubility) was used for loading of the specimens and its release evaluated. Next, collected samples were analyzed using UV–vis spectrometer Perkin Elmer Lambda 1050 (Perkin Elmer Inc., USA) in the span of wavelengths from 250 to 400 nm. The release kinetics of ibuprofen and rutin were studied by using absorption peaks at 272 and 353 nm, respectively. The calibration curves were constructed by plotting absorption intensity vs. known concentration of prepared ibuprofen and rutin solutions.

The PhPt-loaded PD2 specimens were prepared using 0.125 mg/mL solution of PhPt in PBS, placed in 10 mL of neat PBS (pH 7.4), and aliquots of 1 mL were collected and replaced by 1 mL of PBS to conserve the volume. The amount of released PhPt was evaluated by inductively

coupled plasma mass spectrometry (ICP-MS).

The release of the drug is reported as a percentage of cumulative release, where the value of 100% corresponds to concentration of the drug in the system after the equilibrium between the hydrogel and the solution was reached (concentration curve reached plateau), which was within 96 h in all cases.

2.7. Determination of ^{195}Pt content using ICP-MS

Aliquots collected during the release of PhPt from the PD2 hydrogel (Section 2.6) were analyzed by ICP-MS analysis. Three isotopes of platinum, ^{194}Pt, ^{195}Pt and ^{196}Pt were investigated. The ^{195}Pt isotope was found the most sensitive (LOQ 0.001 ppb Pt) and was used for the measurements. Analyses were carried out with a quadrupole-based Thermo Scientific iCAP Qc inductively coupled plasma-mass spectrometer (ICP-MS) equipped with nickel cones, a Peltier-cooled, low-volume conical quartz spray chamber, concentric PFA nebulizer, a collision cell (QCell) with helium to remove undesirable molecule ions or by discrimination of their kinetic energy (CCT and KED mode), a peristaltic sample delivery pump, and a Cetac 520 autosampler. Mass calibration and detector cross-calibration were performed according to the instrument manufacturer's instructions before the sample measurements, using the prescribed solutions obtained from Thermo Fisher Scientific. A sensitivity check using a 10 µg/L Ba, Be, Bi, Ce, Co, In, Li, Ni, Pb and U tuning solutions was performed. The ICP-MS spectrometer was set to appropriate measurement parameters, calibrated in the range 0.1–20.0 µg/mL of Pt with Pt standard solution (ANALYTIKA® spol. s. r. o., Czech Republic) dissolved in PBS (pH 7.4) and samples were measured.

2.8. Biocompatibility and cytotoxicity and assays

The biocompatibility testing was performed in three ways: A) testing of cytotoxicity of extracts of pure hydrogels, B) cell growth and morphology in direct contact with pure hydrogels, C) the effect of hydrogels loaded with PhPt on cell viability.

A.) Cytotoxicity tests of the hydrogel extracts were performed using cell lines HaCaT and NIH/3T3. Extracts from PG1, PD1–PD3 specimens were prepared according to ISO standard 10993-12; in concentration 0.1 g/mL of media. The tested samples were extracted in culture medium for 24 h at 37 °C with stirring. The parent extracts (100%) were then diluted in culture medium to obtain a series of dilutions with concentrations of 75, 50, 25, 10, and 1% of the parent extract. Due to no observable cytotoxicity of diluted extracts, only those with concentrations above 50% are discussed in the following text. All extracts were used up within 24 h of preparation. Cytotoxicity testing itself was performed according to ISO protocol 10993-5. Cells were seeded at a density of 10^5 per mL in 96 well plates and pre-cultivated for 24 h. The extracts were applied onto cells for another 24 h. All tests were performed in quadruplicates. Tetrazolium (MTT cell proliferation assay kit, Duchefa Biochemie, Netherlands) was used to determine cell viability after exposure time. The absorbance was measured at 570 nm and the reference wavelength was adjusted to 690 nm. The results are presented as reduction of cell viability in relative values when compared to cell cultivated in medium without the extracts of tested materials, which corresponds to 1. Morphology of cells from the culture plates was observed using an inverted phase contrast microscope Olympus IX 81 (Olympus, Germany).

B.) The direct contact tests were performed according the ISO 10 993-5 using NIH/3T3 cells. Cells were seeded at a density of 10^5 per mL and pre-cultivated for 24 h to subconfluency. Afterwards, the tested samples (PD1, PD2) were carefully placed onto the cells with fresh medium and incubated for 5 days. After the incubation period, cell morphology was observed and recorded. Microphotographs were taken every 24 h. Firstly, cells were fixed using 4% formaldehyde (Penta, Czech Republic) for 15 min, washed by PBS and subsequently poured over with 0.5% Triton X-100 (Sigma-Aldrich, USA), left for 5 min to permeabilize and washed 3 times by PBS (Invitrogen, USA). Subsequently, cell nuclei were stained using Hoechst 33258 (Invitrogen, USA) and actin cytoskeleton was visualized using ActinRed™ 555 (Thermo Fisher Scientific, USA). Required amount of PBS, two drops per 1 mL of ActinRed™ 555 and 5 µg/mL of Hoechst,33258 were added and left to incubate for 30 min in the dark. Morphology of cells from the culture plates was recorded using an inverted phase contrast microscope Olympus IX 81 (Olympus, Germany). All tests were performed in triplicates.

C.) The effect of PhPt loaded on hydrogels was evaluated on A549 and NIH/3T3 cell lines. Cells were seeded at a density of 10^5 per mL to 24 well plates and pre-cultivated for 24 h. PD2 specimens were loaded with 0.5, 1 and 2.5 µg of PhPt and placed into the middle of the well. Fresh DMEM was added in a way that total volume (medium + hydrogel) was 1 mL, which results in concentrations of 1, 2 and 5 µM of PhPt in each well. The cells were incubated for 48 h and cell viability was determined through the MTT assay. All tests were performed in triplicates.

3. Results and discussion

3.1. Mechanical analysis

Compression tests of prepared PVA/DAC hydrogels showed expected increase in mechanical properties with the increasing amount of crosslinking agent. Fig. 1A shows the dependence of PVA/DAC highest strength, Young's modulus (*E*) and stress at highest strength on the amount of used crosslinker. Data for PVA/GA hydrogel are not shown as the test specimens were not able to withstand the compression tests and slowly broke apart under constant compression rate (10 mm/min) with no distinctive onset of irreversible deformation. In contrast to this, all PVA/DAC hydrogel specimens exhibit well defined transition between reversible and irreversible deformation, observable even by

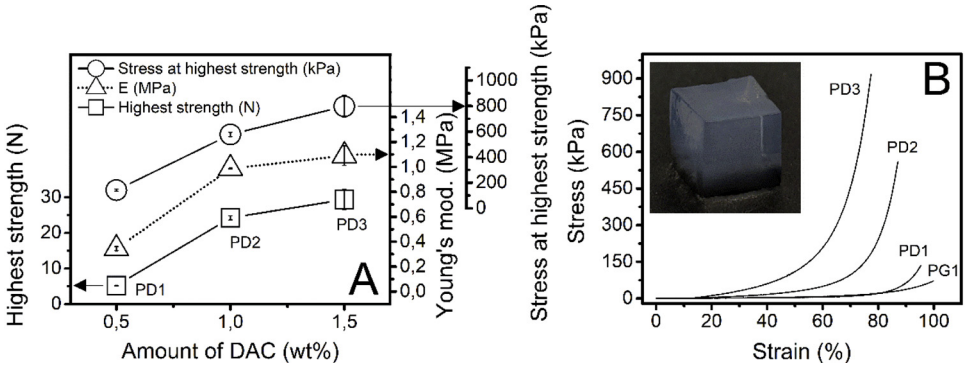

Fig. 1. Mechanical analysis in compression mode of prepared PVA/DAC hydrogels specimens (PD1, PD2 and PD3) plotting the dependence of highest strength, Young's modulus (*E*) and stress at highest strength on the amount of used crosslinking agent DAC (part A) and the examples of stress vs. strain curves of all hydrogels with the picture of PD1 hydrogel cube specimen (part B).

naked eye. The inability to obtain mechanical data for PG1 is the first indicator of inferior mechanical properties of PVA/GA hydrogels in comparison to those formed by DAC.

Utilizing the 0.5–1.5 wt% of DAC crosslinker (relative to PVA) enables preparation of PVA/DAC hydrogels whose Young's modulus lies in between 0.34–1.1 MPa. Measured values of stiffness for PD2 and PD3 samples correspond to materials mechanically suitable for artificial cartilage implants. (Park et al., 2008)

The stress vs. strain curves of all hydrogels based on PVA along with the picture of PD1 hydrogel cube specimen are depicted in Fig. 1B. The PVA/DAC hydrogel structure collapses at certain point, which enables to distinguish between reversible and irreversible deformation. As the amount of DAC crosslinker decreases, the hydrogels are able to withstand higher compression deformations without breakage.

It should be noted that mechanical characteristics obtained by compression test are influenced by so-called "barreling" artefact effect, a significant broadening of the middle cross-section of specimens when loaded with compression force. This horizontal deformation results in additional shear force influencing linear relation between stress and strain. (Meyvis et al., 2002) Thus, the calculated values of Young's modulus from such measurements cannot be treated as absolute. Nevertheless, they can serve for the relative comparison between the prepared specimens. To obtain more detailed information about the mechanical behavior of PVA-based hydrogels, rheological measurements were conducted.

3.2. Analysis of viscoelastic properties

All PVA-based hydrogel samples were analyzed using oscillatory shear rheometry utilizing frequency sweep from 1 Hz to 10 Hz and constant strain of 1%. The results are shown in the Fig. 2A and B. The dependence of storage modulus (*G'*) and loss modulus (*G"*) on angular frequency can be seen in the Fig. 2A. Both storage and loss moduli follow the same trends in all prepared PVA-based hydrogels. Generally, both *G'* and *G"* are higher for hydrogels containing larger amount of crosslinker. This is not surprising as the denser network of crosslinks is expected to possess higher elasticity oppose to the sparsely crosslinked one, which will rather dissipate energy. The PD3 and PD2 samples (1.5 and 1 wt% of DAC, respectively) exhibit relatively high *G'* around 121 Pa and 55.5 Pa in the selected span of oscillatory measurements, respectively. As the amount of DAC crosslinking agent decreases down to 0.5 wt%, the *G'* drops to approximately 9.5 Pa. However, this is still more than twice the value observed for PG1 (*G'* = 4.1 Pa). These results confirm previous observation from mechanical compression tests that the PVA-based hydrogels prepared by the use of DAC exhibit better mechanical properties when compared to those made by GA under the same conditions.

The Fig. 2B shows the dependence of dynamic modulus (*G**) and damping factor *tanδ* in the selected span of angular frequency. The dynamic modulus *G** can be calculated as the square root of the sum of the second powers of storage and loss modulus. It provides information about the complex modulus in the selected range of oscillatory measurement at ambient temperature. As the viscous component (*G"*) of dynamic modulus *G** is rather small in all cases, the trends follows those established for *G'*.

The parameter *tanδ*, defined as ratio between loss and storage modulus (*G"/G'*), gives a measure of viscous to elastic component of material. In other words, if the material is more elastic (i.e. stores mechanical energy) than viscous (i.e. dissipates energy), the *tanδ* value will limit to zero. From the data plotted in Fig. 2B it is evident that elastic component is increasing with the amount of DAC crosslinker. In contrast to this, PG1 possess highest damping factor which signifies more viscous-like behavior than PD1.

Overall, the materials properties of prepared PVA/DAC hydrogels are covering the area from stiff elastic gels (PD2 and PD3) to soft viscoelastic gels (PD1). In comparison with PD1, the PG1 sample exhibits inferior mechanical properties.

3.3. BET and SEM analysis

The PVA cryogels obtained by lyophilization were analyzed in terms of their specific surface area (a_{BET}). The example of lyophilized PD1 cryogels is depicted in Fig. 3A. The a_{BET} and the quantity of adsorbed volume of nitrogen (V_a) significantly grows with decreasing amount of DAC, see Fig. 3A and 3B. The a_{BET} for PD1 is by an order of the magnitude larger than that for PD3 (50 ± 2 m^2/g vs. 4.4 ± 0.2 m^2/g). This is closely related to the water absorption capability of the hydrogel, as the amount of absorbed water influences the extent of cavitation during lyophilization. Because the least crosslinked material has the highest water absorption capability, it also features the highest

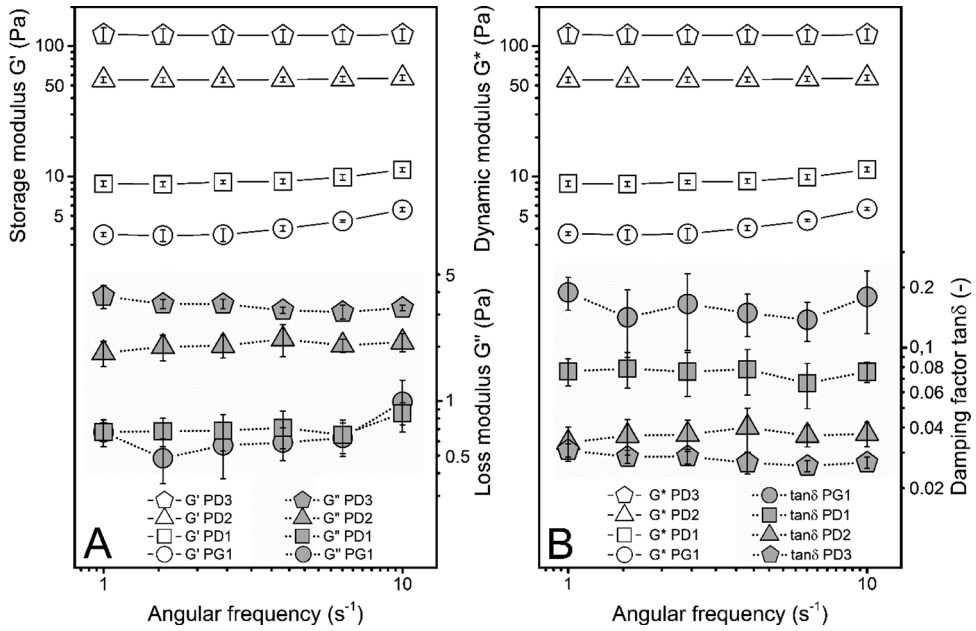

Fig. 2. Analysis of viscoelastic properties of PVA-based hydrogels with storage modulus (*G'*) and loss modulus (*G"*) plotted against angular frequency (part A) and calculated dynamic modulus *G** and damping factor *tanδ* dependence on angular frequency (part B). All measurements were carried at ambient temperature.

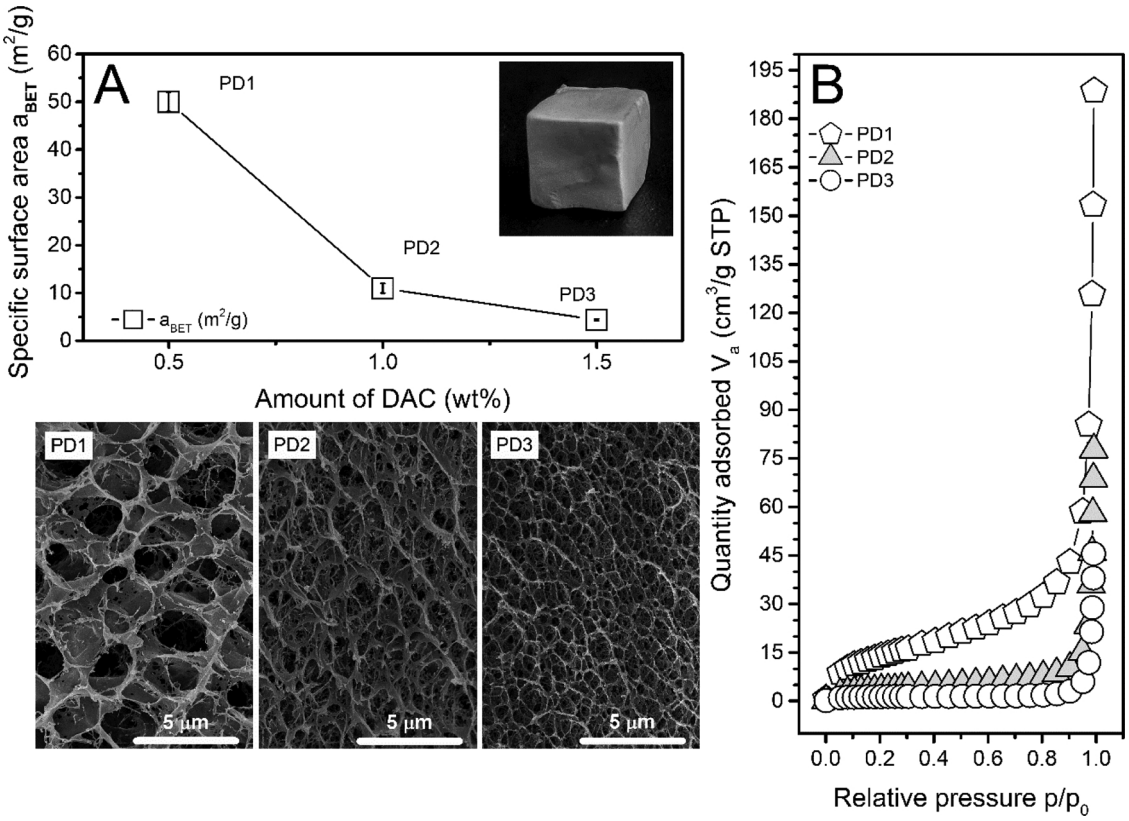

Fig. 3. Specific surface area a_{BET} of prepared PVA/DAC cryogels with depicted example of PD1 cryogel (part A), dependence of quantity of adsorbed volume of nitrogen per cryogel mass V_a on relative pressure p/p_0 obtained by BET analysis (part B) and SEM micrographs of prepared cryogels (bottom left).

porosity, as can be seen from the micrographs of PVA/DAC cryogels obtained by SEM (see bottom part of Fig. 3).

Notably, the specific surface area of PG1 (18 ± 2 m^2/g) is much lower than for its analog PD1 (50 ± 2 m^2/g), only somewhat higher than for PD2 (11 ± 1 m^2/g). The analogical DAC-crosslinked hydrogels thus possess not only superior mechanical properties, but also higher surface area and thus, presumably, better absorption capabilities in comparison with GA analog. This is another direct consequence of two-phase network topology of PVA/DAC hydrogels, (Münster et al., 2018) where the regions with very high crosslink density, formed by individual DAC macromolecules, are sparsely embedded and connected through physically entangled PVA matrix. Hence, PVA/DAC material contains larger fraction of chemically uncrosslinked PVA, which is washed away during preparation. The lyophilized PVA/DAC cryogels thus exhibit increased porosity and specific surface area compared to PVA/GA cryogels prepared using identical conditions.

3.4. Swelling kinetics and network parameters

The PVA cryogels were re-swelled in water and the swelling kinetics and network parameters were determined, Fig. 4. The equilibrium swollen state was achieved after 24 h for all PVA/DAC samples, see Fig. 4A. The main difference between prepared PVA/DAC materials is rapid water uptake and very high swelling capacity of PD1 (0.5 wt% of DAC) compared to PD2 (1 wt% of DAC), which well corresponds to significantly larger specific surface area and porosity of the former, as discussed in previous Section. While the swelling capacity of PD1 samples reaches 1630%, the PD2 and PD3 specimens exhibit swelling capacity of 344 and 242% after 96 h, respectively.

The network parameters (equilibrium water content EWC, mesh size ξ and crosslink density ρ_c, see Section 2.5 for more details) of prepared PVA/DAC hydrogels are plotted against amount of used DAC crossliker in Fig. 4B. As in mechanical and specific surface analysis, the network parameters are closely related to amount of used crosslinker. With increasing amount of DAC crosslinker (from PD1 to PD3), EWC drops from 94 to 71%, mesh size ξ decreases from 167 to 50 Å and the crosslink density ρ_c increases from 0.34 to 1.23 mmol/cm^3. The polymer volume fraction ($v_{2,s}$) increases from 0.05 to 0.25. Furthermore, dynamic modulus G^* shows almost linear dependence on estimated ρ_c (Fig. 4C) while there is also a linear correlation between the calculated ξ on measured specific surface area (Fig. 4D). The prepared materials thus obey classical theoretical framework, as both viscoelastic properties of hydrogels and specific surface area of cryogels prepared by various amounts of DAC are tightly correlated to parameters obtained by the means of equilibrium swelling theory. This makes them mutually predictable in the investigated range of crosslinker concentrations.

3.5. Drug release studies

The factors influencing drug release, i.e. mesh density and size and charge of released molecules, were investigated using ibuprofen, rutin and phenanthriplatin. Selection of compounds reflects the variability of potential hydrogel drug-delivery application, ranging from dermal masks for cosmetics to implantable depots of anticancer drugs.

The release profiles of rutin and ibuprofen were investigated for PD1 and PD3, which possess significantly different network parameters. Because drug release from hydrogel is essentially a mesh-controlled diffusion, it will be influenced by mesh size ξ and crosslink density ρ_c of the hydrogels as well as by the size of the released molecules. The release profiles of rutin and ibuprofen from the least (PD1) and the most (PD3) crosslinked PVA/DAC hydrogel specimens are shown in Fig. 5.

The influence of mesh parameters to release rates is evident in the both cases of tested PVA/DAC hydrogels, although the relative size of the molecules plays a role as well. Essentially, the denser the crosslinked network and the larger the released drug is, the slower is the release rate. The relatively small molecules of ibuprofen (M = 206 g/

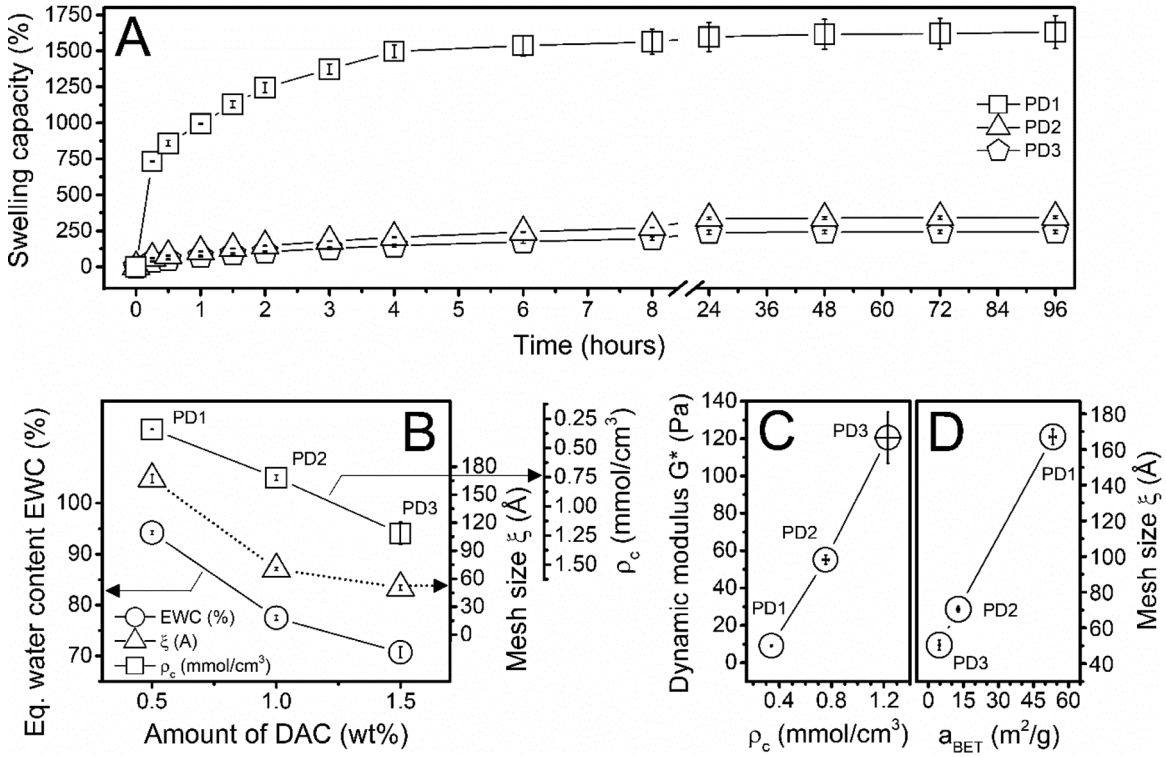

Fig. 4. Evaluation of swelling kinetics of prepared PVA/DAC hydrogels (part A), their calculated network parameters, namely equilibrium water content EWC, mesh size ξ and crosslink density ρ_c (part B), correlation between dynamic modulus G^* and calculated ρ_c (part C) and between mesh size ξ and specific surface area a_{BET} (part D).

mol) are released from the hydrogel matrix almost completely after only 2 h for PD1 but only after 6 h for PD3. The difference between PD1 and PD3 hydrogel matrices is thus visible mostly in early stages of release.

The larger molecules of rutin (610 g/mol) exhibits much slower release compared to ibuprofen (complete release takes up to 96 h). The role of mesh density parameters to the drug release rates is also much more pronounced. The initial burst release of rutin from denser PD3 is significantly reduced, being only about the half of that of PD1 (30% vs. 56% released after 1 h, respectively). This is followed by continuous release of rutin molecules from PD3 over the next four days. In comparison, the release of rutin from PD1 is completed in less than three days, Fig. 5.

Another property which might considerably influence the drug

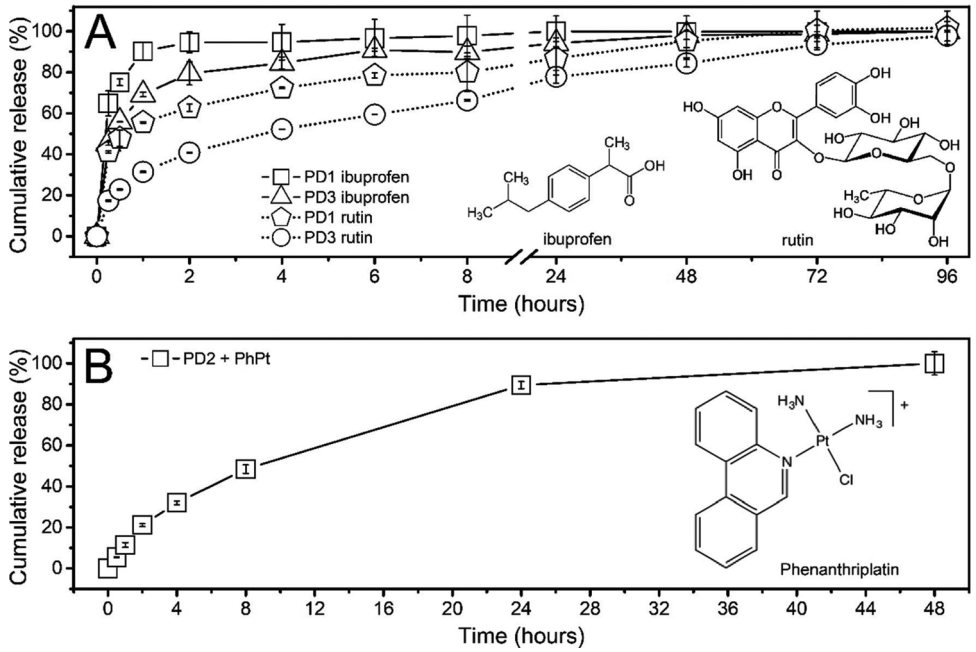

Fig. 5. A) Release profiles of ibuprofen and rutin from the least (PD1) and the most (PD3) crosslinked PVA/DAC hydrogel specimens. B) Release profile of PhPt from PD2.

release rates is the charge of the absorbed molecules. Both DAC and PVA chains are polar, with numerous −CHO and −OH groups bearing partial negative charges. Neither ibuprofen (negative charge) or rutin (neutral charge) are expected to be retained specifically by the matrix charge. Hence, phenanthriplatin (PhPt), positively charged monofunctional platinum(II) complex, (Park et al., 2012) was selected for the final experiment to complete the release study. It was assumed that attractive electrostatic interactions between PhPt and PVA/DAC matrix may increase the retention of PhPt in the hydrogels. With respect to the considerable synthetic costs and extremely high cytotoxicity of PhPt chemotherapeutic, which requires special handling, it was opted to study its release using only the PD2 hydrogel. This hydrogel sample also possesses suitable mechanical properties for the artificial implant applications. For the structure of PhPt and its release rates from PD2 see Fig. 5B.

The positive charge of the platinum complex seems to play a role particularly in early stages of PhPt release from PD2. Its initial release rate is considerably slower than those of rutin from PD3, despite smaller size of PhPt (M = 505 g/mol) and sparser hydrogel matrix of PD2. On the other hand, the release of PhPt from PD2 is fully accomplished after only two days, which is less than in case of rutin from PD3.

3.6. Biological testing

Three sets of tests were employed to determine the biocompatibility of PG1 and PD1-PD3 hydrogels: evaluation of cytotoxicity of extracts of pure hydrogels, cell growth and morphology in direct contact with pure hydrogels and the effect of hydrogels loaded with PhPt on cell viability.

Firstly, cytotoxicity of hydrogel extracts in culture media prepared according to ISO standard 10993-12 was investigated, using human aneuploid immortal keratinocyte cell line (HaCaT) and mouse embryo fibroblast cell line (NIH/3T3), Fig. 6A and B. Even the 100% extracts from PD1 and PD2 were non-cytotoxic towards both cell lines. The 100% extract of PD3 with 1.5 wt% of DAC shows only borderline cytotoxicity (about 80% cell viability). Despite very low amount of GA (corresponding to 0.5 wt% of DAC), the extracts from PG1 hydrogel, although overall non-cytotoxic, caused observable decrease in relative cell viability of both cell lines in comparison to its DAC-based counterpart PD1 (Fig. 6A and B). This correlates with previously noted higher cytotoxicity of GA at higher concentrations, (Kim et al., 2017; Mi et al., 2006) which may impair the biocompatibility of the GA-cross-linked products. Based on obtained results, further biological testing was limited only to PD1 and PD2 specimens.

Subsequently, effect of direct contact with pure hydrogels on cell growth and morphology was studied according the ISO 10 993-5, see Section 2.8 for more details. Cell growth and morphology were checked every 24 h for 5 days, after which cells become fully confluent and experiment was terminated. No negative effects of the hydrogel presence were observed during the test period. Cells incubated for 3 days in the presence of PD2 are visualized in Fig. 6C. It is clearly visible that there are no changes in cell quantity or morphology and fibroblasts held their typical oblong, triangular shape during the whole incubation time. Obtained data demonstrate good overall biocompatibility of PD1 and PD2.

The cytotoxicity of PD2 loaded by different amounts of PhPt, which corresponds to 1, 2 and 5 μM concentration of PhPt in the culture media, was evaluated using non-cancerous NIH/3T3 cells and cancer cell line A549 (Fig. 6D). Results were compared to equivalent amount of free PhPt tested at the same conditions using the same cell lines.

The adsorption of PhPt to the PD2 does not have any negative impact on drug cytotoxicity; quite the contrary in fact. Although the cytotoxicity of neat PD2 hydrogel towards non-cancerous immortalized cell line NIH/3T3 was negligible, pure PD2 is mildly cytotoxic towards A549 cancer cell line. This imply the possibility of synergy of cytotoxic effects of the hydrogel and carried compound. However, because PhPt was much more effective against A549 than against NIH/3T3, the A549 cell line results for PhPt-loaded PD2 are comparable with free PhPt.

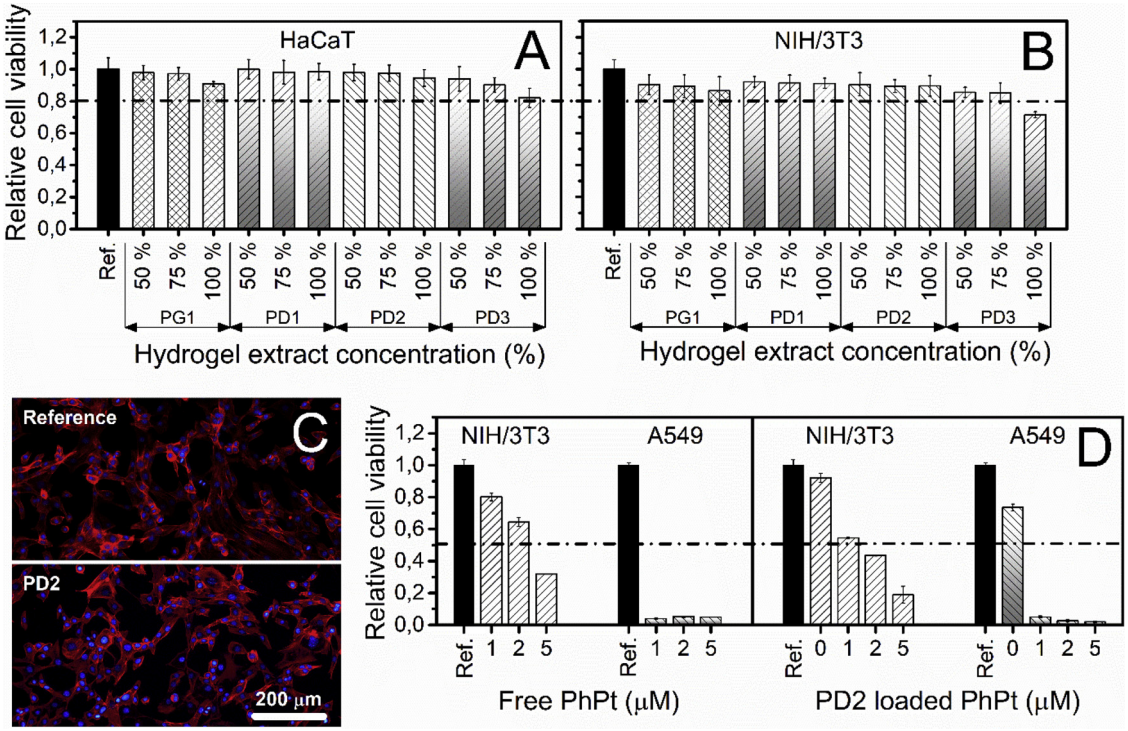

Fig. 6. Relative cell viability for all hydrogel extracts in different concentrations tested on A) human aneuploid immortal keratinocyte cell line (HaCaT) and B) mouse embryo fibroblast cell line (NIH/3T3). C) Micrographs of NIH/3T3 cell growth in the presence of neat PD2 hydrogel. D) Cytotoxicity of different concentrations of free PhPt, neat PD2 hydrogel and the PD2 loaded by various concentrations of PhPt tested against NIH/3T3 and adenocarcinomic human alveolar basal epithelial cell line (A549).

4. Conclusion

To summarize, the variation of DAC concentrations from 0.5wt% to 1.5wt% allows to prepare materials with mechanical characteristics ranging from soft viscoelastic (0.5wt%) to stiff elastic (1wt% and 1.5wt %). Resulting hydrogels thus have mechanical properties convenient for various pharmaceutical applications, from subcutaneous drug-delivery depots to artificial implants, i.e. cartilages. Amount of crosslinker also directly influences the swelling of the hydrogels, specific surface area, porosity and network parameters. The swelling capacity of hydrogel ranges from 200% to 1600% for the most and the least crosslinked hydrogel, respectively. The specific surface area decreases with increasing amount of crosslinker by an order of magnitude, i.e. from 50 m^2/g to ~4 m^2/g. Crosslink density is also increasing with the amount of crosslinker from 0.34 to 1.23 $mmol/cm^3$, while mesh size is simultaneously decreasing from 170 Å to 50 Å. Notably, network parameters (namely crosslink density and mesh size) exhibit almost linear correlation with measured dynamic modulus and specific surface area, respectively.

The PVA/DAC hydrogels were found to be superior in terms of mechanical characteristics (more than double values of dynamic modulus) and specific surface area (more than twice larger surface) to analogical material prepared using glutaraldehyde, probably due to the macromolecular character of DAC and resulting two-phase network topology, where the regions with very high crosslink density, formed by individual DAC macromolecules, are sparsely embedded and connected through physically entangled PVA matrix.

The drug release profiles from PVA/DAC hydrogels were found to be governed by the mesh parameters of hydrogels and the size and charge of released molecules. The available drug release rates range from very fast (2 h) for relatively small and negatively charged molecules of ibuprofen to rather slow (96 h) for larger and neutral molecules of rutin. Positively charged phenanthriplatin had slowest initial release rates, but was completely released already within 48 h.

The PVA/DAC hydrogels prepared using up to 1 wt% of DAC are entirely nontoxic, while higher amounts of crosslinker results in mild toxicity towards firbroblastic cell lines. However, to obtain stiffer PVA/DAC hydrogels with controlled mesh size-release profiles while maintaining the lowest possible level of toxicity, higher molecular weight PVA may be used. (Münster et al., 2018) Cytotoxicity studies suggests a possible synergic effect of DAC-crosslinked hydrogels and carried phenanthriplatin against adenocarcinomic human alveolar basal epithelial cell line and demonstrated the potential of PVA/DAC hydrogels for anticancer drug delivery applications, e.g. for localized release of chemotherapeutics after tumor resection.

Overall, the PVA/DAC has tunable materials and surface properties and drug release rates, good biocompatibility and no observable toxicity (up to 1 wt% of DAC). Thus, PVA/DAC hydrogel materials may be suitable for wide spectrum of potential biomedical applications such as intra-tumor drug delivery depots, artificial implants or dermal patches and masks. The DAC thus provides not only sustainable, cost effective and low toxic alternative to currently used synthetic crosslinking agents, but it can be simultaneously used for preparation of hydrogels with comparably better characteristics.

Competing interest

The authors declare no competing financial or other interest.

Acknowledgement

This work was supported by the Czech Science Foundation grant 16-05961S and Ministry of Education, Youth and Sports of the Czech Republic ProgramNPU I (LO1504).

References

Caló, E., & Khutoryanskiy, V. V. (2015). Biomedical applications of hydrogels: A review of patents and commercial products. *European Polymer Journal, 65*, 252–267. https://doi.org/10.1016/j.eurpolymj.2014.11.024.

Canal, T., & Peppas, N. A. (1989). Correlation between mesh size and equilibrium degree of swelling of polymeric networks. *Journal of Biomedical Materials Research, 23*(10), 1183–1193. https://doi.org/10.1002/jbm.820231007.

Czapar, A. E., Zheng, Y.-R., Riddell, I. A., Shukla, S., Awuah, S. G., Lippard, S. J., & Steinmetz, N. F. (2016). Tobacco mosaic virus delivery of phenanthriplatin for cancer therapy. *ACS Nano, 10*(4), 4119–4126. https://doi.org/10.1021/acsnano.5b07360.

Engel, P., Hein, L., & Spiess, A. C. (2012). Derivatization-free gel permeation chromatography elucidates enzymatic cellulose hydrolysis. *Biotechnology for Biofuels, 5*(1), 77. https://doi.org/10.1186/1754-6834-5-77.

Flory, P. J., & Rehner, J. (1943). Statistical mechanics of crosslinked polymer networks II. Swelling. *The Journal of Chemical Physics, 11*(11), 521–526. https://doi.org/10.1063/1.1723792.

Flory, P. J., & Volkenstein, M. (1969). Statistical mechanics of chain molecules. *Biopolymers, 8*(5), 699–700. https://doi.org/10.1002/bip.1969.360080514.

Ganeshpurkar, A., & Saluja, A. K. (2017). The pharmacological potential of rutin. *Journal of the Saudi Pharmaceutical Society, 25*(2), 149–164. https://doi.org/10.1016/j.jsps.2016.04.025.

Ge, H., Zhang, L., Xu, M., Cao, J., & Kang, C. (2018). Preparation of dialdehyde cellulose and its antibacterial activity. In H. Liu, C. Song, & A. Ram (Vol. Eds.), *Advances in applied biotechnology: Vol. 444*, (pp. 545–553). . https://doi.org/10.1007/978-981-10-4801-2_56.

Gulrez, S. K. H., Al-Assaf, S., & Phillips, G. O. (2011). Hydrogels: Methods of preparation, characterisation and applications. In A. Carpi (Ed.). *Progress in molecular and environmental bioengineering– From analysis and modeling to technology applications*. InTech.

Kim, U.-J., & Kuga, S. (2001). Ion-exchange chromatography by dicarboxyl cellulose gel. *Journal of Chromatography A, 919*(1), 29–37. https://doi.org/10.1016/S0021-9673(01)00800-7.

Kim, U.-J., Lee, Y. R., Kang, T. H., Choi, J. W., Kimura, S., & Wada, M. (2017). Protein adsorption of dialdehyde cellulose-crosslinked chitosan with high amino group contents. *Carbohydrate Polymers, 163*, 34–42. https://doi.org/10.1016/j.carbpol.2017.01.052.

Kim, U.-J., Wada, M., & Kuga, S. (2004). Solubilization of dialdehyde cellulose by hot water. *Carbohydrate Polymers, 56*(1), 7–10. https://doi.org/10.1016/j.carbpol.2003.10.013.

Koprivica, S., Siller, M., Hosoya, T., Roggenstein, W., Rosenau, T., & Potthast, A. (2016). Regeneration of aqueous periodate solutions by ozone treatment: A sustainable approach for dialdehyde cellulose production. *ChemSusChem, 9*(8), 825–833. https://doi.org/10.1002/cssc.201501639.

Liimatainen, H., Sirviö, J. A., Pajari, H., Hormi, O., & Niinimäki, J. (2013). Regeneration and recycling of aqueous periodate solution in dialdehyde cellulose production. *Journal of Wood Chemistry and Technology, 33*(4), 258–266. https://doi.org/10.1080/02773813.2013.783076.

Lindh, J., Carlsson, D. O., Strømme, M., & Mihranyan, A. (2014). Convenient one-pot formation of 2,3-dialdehyde cellulose beads via periodate oxidation of cellulose in water. *Biomacromolecules, 15*(5), 1928–1932. https://doi.org/10.1021/bm5002944.

Meyvis, T. K. L., Stubbe, B. G., Van Steenbergen, M. J., Hennink, W. E., De Smedt, S. C., & Demeester, J. (2002). A comparison between the use of dynamic mechanical analysis and oscillatory shear rheometry for the characterisation of hydrogels. *International Journal of Pharmaceutics, 244*(1–2), 163–168.

Mi, F.-L., Huang, C.-T., Liang, H.-F., Chen, M.-C., Chiu, Y.-L., Chen, C.-H., & Sung, H.-W. (2006). Physicochemical, antimicrobial, and cytotoxic characteristics of a chitosan film cross-linked by a naturally occurring cross-linking agent, aglycone geniposidic acid. *Journal of Agricultural and Food Chemistry, 54*(9), 3290–3296. https://doi.org/10.1021/jf0529868.

Münster, L., Vícha, J., Kloáč, J., Masař, M., Kucharczyk, P., & Kuřitka, I. (2017). Stability and aging of solubilized dialdehyde cellulose. *Cellulose, 24*(7), 2753–2766. https://doi.org/10.1007/s10570-017-1314-x.

Münster, L., Vícha, J., Kloáč, J., Masař, M., Hurajová, A., & Kuřitka, I. (2018). Dialdehyde cellulose crosslinked poly(vinyl alcohol) hydrogels: Influence of catalyst and crosslinker shelf life. *Carbohydrate Polymers, 198*, 181–190. https://doi.org/10.1016/j.carbpol.2018.06.035.

Münster, L.áš, Fojtů, M., Capáková, Z., Vaculovič, T., Tvrdoňová, M., Kuřitka, I., ... Vícha, J. (2019). Selectively oxidized cellulose with adjustable molecular weight for controlled release of platinum anticancer drugs. *Biomacromolecules, 20*(4), 1623–1634. https://doi.org/10.1021/acs.biomac.8b01807.

Park, G. Y., Wilson, J. J., Song, Y., & Lippard, S. J. (2012). Phenanthriplatin, a monofunctional DNA-binding platinum anticancer drug candidate with unusual potency and cellular activity profile. *Proceedings of the National Academy of Sciences U. S. A. 109*(30), 11987–11992. https://doi.org/10.1073/pnas.1207670109.

Park, S., Nicoll, S. B., Mauck, R. L., & Ateshian, G. A. (2008). Cartilage mechanical response under dynamic compression at physiological stress levels following collagenase digestion. *Annals of Biomedical Engineering, 36*(3), 425–434. https://doi.org/10.1007/s10439-007-9431-6.

Peppas, N. A. (Ed.). (1986). *Hydrogels in medicine and pharmacy*. Boca Raton: CRC Press.

Peppas, N. A., & Merrill, E. W. (1976). Determination of interaction parameter $\chi 1$, for poly(vinyl alcohol) and water in gels crosslinked from solutions. *Journal of Polymer Science: Polymer Chemistry Edition, 14*(2), 459–464. https://doi.org/10.1002/pol.1976.170140216.

Peppas, N. A., Huang, Y., Torres-Lugo, M., Ward, J. H., & Zhang, J. (2000).

Physicochemical foundations and structural design of hydrogels in medicine and biology. *Annual Review of Biomedical Engineering, 2*, 9–29. https://doi.org/10.1146/annurev.bioeng.2.1.9.

Rocha, I., Ferraz, N., Mihranyan, A., Strømme, M., & Lindh, J. (2018). Sulfonated nanocellulose beads as potential immunosorbents. *Cellulose, 25*(3), 1899–1910. https://doi.org/10.1007/s10570-018-1661-2.

Suopajärvi, T., Liimatainen, H., Hormi, O., & Niinimäki, J. (2013). Coagulation-flocculation treatment of municipal wastewater based on anionized nanocelluloses. *Chemical Engineering Journal, 231*, 59–67. https://doi.org/10.1016/j.cej.2013.07.010.

Tibbitt, M. W., Dahlman, J. E., & Langer, R. (2016). Emerging frontiers in drug delivery. *Journal of the American Chemical Society, 138*(3), 704–717. https://doi.org/10.1021/jacs.5b09974.

Wichterle, O., & Lím, D. (1960). Hydrophilic gels for biological use. *Nature, 185*(4706), 117–118. https://doi.org/10.1038/185117a0.

Yahia, L. (2015). History and applications of hydrogels. *Journal of Biomedical Sciencies, 04*(02), https://doi.org/10.4172/2254-609X.100013.

Yan, G., Zhang, X., Li, M., Zhao, X., Zeng, X., Sun, Y., ... Lin, L. (2019). Stability of soluble dialdehyde cellulose and the formation of hollow microspheres: Optimization and characterization. *ACS Sustainable Chemistry & Engineering, 7*(2), 2151–2159. https://doi.org/10.1021/acssuschemeng.8b04825.

Article XII.

Muchová, M.; Münster, L.; **Capáková, Z**.; Mikulcová, V.; Kuřitka, I.; Vícha, J. Design of Dialdehyde Cellulose Crosslinked Poly(Vinyl Alcohol) Hydrogels for Transdermal Drug Delivery and Wound Dressings. Materials Science and Engineering: C 2020, 116, 111242. https://doi.org/10.1016/j.msec.2020.111242.

Materials Science & Engineering C 116 (2020) 111242

Contents lists available at ScienceDirect

Materials Science & Engineering C

journal homepage: www.elsevier.com/locate/msec

Design of dialdehyde cellulose crosslinked poly(vinyl alcohol) hydrogels for transdermal drug delivery and wound dressings

Monika Muchová, Lukáš Münster, Zdenka Capáková, Veronika Mikulcová, Ivo Kuřitka, Jan Vícha*

Centre of Polymer Systems, Tomas Bata University in Zlín, tř. Tomáše Bati 5678, 760 01 Zlín, Czech Republic

ARTICLE INFO

Keywords:
Poly(vinyl alcohol)
Dialdehyde cellulose
Transdermal
Hydrogel
Drug delivery
Wound dressing

ABSTRACT

2,3-Dialdehyde cellulose (DAC) was used as an efficient and low-toxicity crosslinker to prepare thin PVA/DAC hydrogel films designed for topical applications such as drug-loaded patches, wound dressings or cosmetic products. An optimization of hydrogel properties was achieved by the variation of two factors – the amount of crosslinker and the weight-average molecular weight (M_w) of the source PVA. The role of each factor to network parameters, mechanical, rheological and surface properties, hydrogel porosity and transdermal absorption is discussed. The best results were obtained for hydrogel films prepared using 0.25 wt% of DAC and PVA with M_w = 130 kDa, which had a high porosity and drug-loading capacity (high water content), mechanical properties allowing easy handling, best adherence to the skin from all tested samples and improved transdermal drug-delivery. Hydrogel films are biocompatible, show no cytotoxicity and have no negative impact on cell growth and morphology in their presence. Furthermore, hydrogels do not support cell migration and attachment to their surface, which should ensure easy removal of hydrogel patches even from wounded or damaged skin after use.

1. Introduction

Hydrogel-based biomaterials receive steadily growing attention due to their similarity to living tissues in terms of mechanical properties, porosity and high content of water. The last two qualities allow hydrogels to accommodate, store, and later release various substances, making them excellent materials for a wide range of drug-delivery applications in both medicine and cosmetics, i.e. from injectable drug-delivery depots to dermal patches, or from drug-loaded wound dressings to hydrating masks. In contrast to implantable drug depots, topically applied hydrogels could be easily removed and replaced after their content is depleted, which is ideal for sustained, painless, and controlled delivery of biologically active compounds [1].

Hydrogel films are also excellent wound dressing materials as they naturally hydrate the skin and keep the wound zone moist and wettable, which accelerates healing [2], soothes and cools burns and reduces pain and inflammation [3]. Hydrogels loaded with antibiotics and anti-inflammatory agents can also deliver the active compounds directly to the wounded area, reducing the risk of infection.

Necessary characteristics of hydrogels intended for topical applications include: biocompatibility, large loading capacity (equilibrium water content), good adherence to the skin (bioadhesivity), which increases dermal absorption of compounds loaded in the hydrogel, [4] and mechanical stability sufficient for easy removal. Hydrogels intended as wound dressings should not interfere with the cell growth and formation of new tissues. Simultaneously, they should not support cell migration and attachment to their surface or bulk, which may complicate their removal from the wounded area and lead to the disturbance of tender healing tissue.

To successfully balance all these qualities is not an easy task. For instance, purely biopolymer-based hydrogels often have poor mechanical properties in the swollen state, which make them difficult to handle and to remove from skin. Hydrogels based on artificial polymers have well-defined structure and properties but may suffer from other disadvantages. For instance, hydrogels based on poly(vinyl alcohol), PVA, are used for preparation of immunotherapeutic anticancer gels and transdermal patches, [5,6] wound dressings [3], drug-delivery patches [7] and contact lenses [8]. However, properties of PVA hydrogels are difficult to optimize – they tend to have poor elasticity, high stiffness and relatively low hydrophilicity. Possible solution is to use hybrid hydrogels composed of two polymers of both natural and artificial origin [3]. Properties of hybrid hydrogels are generally better defined than in case of purely biopolymer-based analogs and their individual attributes can be more easily optimized than those of synthetic polymer-based hydrogels.

* Corresponding author.
E-mail address: jvicha@utb.cz (J. Vícha).

https://doi.org/10.1016/j.msec.2020.111242
Received 22 March 2020; Received in revised form 18 June 2020; Accepted 24 June 2020
Available online 26 June 2020

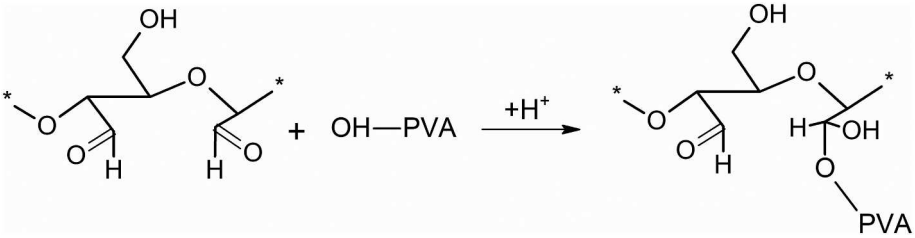

Fig. 1. Simplified reaction scheme between –CHO and –OH groups of 2,3-dialdehyde cellulose and PVA in an acidic environment.

In this work we investigate hydrogel films composed of PVA crosslinked by 2,3-dialdehydecellulose, DAC, which is prepared by regioselective periodate oxidation of hydroxyl groups of cellulose at C2 and C3 of pyranose cycle [9,10]. Structure of DAC and simplified reaction scheme between DAC and PVA is given in Fig. 1. Raw DAC is insoluble in aqueous media and must be solubilized by hot water prior to its utilization in solution-based processes [11]. DAC features two highly reactive aldehyde groups per each oxidized unit, which can be used for crosslinking of polymers bearing hydroxyl side groups (Fig. 1). However, DAC was deemed to be rather unstable in solution [12]. The presumed need to prepare a fresh crosslinker for every use reduced its potential in practical applications [13]. Only recently, we have shown that the stabilization of an aldehyde group content over a prolonged period can be achieved by decreasing the pH of the solution to 3.5 [10].

DAC has several advantages over currently used organic crosslinkers such as glutaraldehyde (GA). Firstly, DAC can be prepared using cellulose from renewable resources [14] and consumed periodate salt can be easily regenerated and re-used making the whole process sustainable [15]. Secondly, DAC is considerably less toxic than GA, [16] which is particularly important to the preparation of biomaterials for medical and cosmetic sector. Last but not least, DAC is more effective crosslinker than GA at the same concentration of aldehyde groups. [17] This is a result of "two-phase" network topology found in DAC hydrogels. [16–18] Briefly, while small GA molecules are uniformly distributed through the hydrogel network, much larger DAC macromolecules can crosslink numerous PVA chains simultaneously, thus creating regions with very high crosslink density, which are embedded in PVA matrix. Resulting PVA/DAC hydrogels thus have better mechanical properties than PVA/GA counterparts [18].

Here, DAC is used as a crosslinker for preparation of thin hydrogel films optimized for transdermal drug delivery, wound dressings and cosmetic products. The role of varied amount of crosslinker and different weight-average molecular weight (M_w) of PVA to the network parameters, porosity, viscoelastic properties, cytotoxicity and biocompatibility of prepared thin films is discussed together with release kinetics and transdermal absorption of two model drugs, rutin and caffeine.

Rutin is the glycoside composed of quercetin and rutinose (α-L-rhamnopyranosyl-(1 → 6)-β-D-glucopyranose). It is a flavonoid found in a wide variety of plants including buckwheat, tea and citrus fruit. It is highly versatile in its biological activity because it exhibits antioxidative, cytoprotective, vasoprotective, anticarcinogenic, neuroprotective and cardioprotective properties [19]. It finds numerous applications in cosmetics, because it stabilizes the vascular walls, prevents them from cracking and counteracts the manifestation of dilated veins. It is also utilized in wound dressing and healing applications because it shows anti-microbial and anti-inflammatory activity and reduces oxidative stress in the wounded area [20,21].

Caffeine is a stimulant of the central nervous system and is often used as a model drug for studying the penetration of hydrophilic substances across the skin barrier [22,23]. Caffeine-saturated hydrogels can stimulate the nervous system, support lymphatic system, prevent excessive fat accumulation in the skin and help to protect the skin from photodamage [22,23].

2. Experimental

2.1. Materials

Two types of poly(vinyl alcohol) (PVA) with 88% degree of hydrolysis with different M_w (130 and 31 kDa, respectively) were used (Sigma Aldrich Co.). Alpha cellulose (M_w = 109 kDa) [24] (Sigma Aldrich Co.), sodium periodate ($NaIO_4$) (Penta, Czech Republic), ethylene glycol, hydrochloric acid (HCl) (Penta, Czech Republic) were employed in the synthesis of 2,3-dialdehydecellulose (DAC) and in the subsequent preparation of hydrogels. The prepared PVA/DAC hydrogels were saturated with rutin and caffeine (Sigma Aldrich Co.). The mouse embryonic fibroblast cell line (NIH/3T3, ECACC) was used for the determination of biological properties. DMEM (Biosera, France) containing 10% of calf serum (Biosera, France) and 100 U/mL Penicillin/Streptomycin (Biosera, France) was used as a culture media. Cells were incubated at 37 °C in a 5% CO_2 humid atmosphere. Phosphate buffer saline (PBS) (Invitrogen, USA) was used for cells washing. Cells were cultured on Techno plastic (TPP, Switzerland), using Tetrazolium kit (MTT cell proliferation assay, Duchefa Biochemistry, The Netherlands). The other chemicals used in biological testing include formaldehyde (Penta, Czech Republic), Triton X (Sigma Aldrich Co.), Hoechst 33258 (Invitrogen, USA) and ActinRed™ 555 (Thermo Fisher Scientific, USA). For transdermal testing gentamicin sulfate (HiMedia Laboratories), formic acid (HCOOH), and methanol (Penta, Czech Republic) were used. All chemicals were of analytical purity and were used as received without further purification. Demineralized water was used throughout the experiments.

2.2. Preparation of crosslinked PVA/DAC hydrogels

In the first step, the 2,3-dialdehydecellulose (DAC) was prepared by oxidation of alpha cellulose by $NaIO_4$ using a 1:1.2 M ratio of reactants (DAC:periodate) following earlier works [10,17,18,25]. Briefly, to achieve high conversion of cellulose to DAC, 10 g of cellulose was suspended in 250 mL of water containing 16.5 g of sodium periodate. The mixture was then stirred in the dark for 72 h at 30 °C. The oxidation was stopped by addition of 10 mL of ethylene glycol and the product washed and filtered. Resulting raw DAC was suspended in 175 mL of water and solubilized at 80 °C for 7 h [11]. Next, the solubilized DAC was cooled, centrifuged (10 min, 10,000 RPM) and the solution was transferred to a 200 mL volumetric flask. The weight concentration of solubilized DAC was determined (42.3 ± 1.3 mg/mL) by simple weight analysis (i.e. solution evaporation and residue weighted). The prepared DAC solution of known concentration served for crosslinking of PVA.

In the second step, 10 g of each PVA type (M_w 31,000 or 130,000 g/mol) was dissolved in 80 mL of water at 90 °C. Subsequently, the catalyst (10 mL of 1.3 M HCl) and defined amount of DAC corresponding to 0.25 wt% and 1 wt% (with respect to the weight of PVA) was added. The prepared reaction mixtures were thoroughly stirred and poured onto Petri dishes (d = 140 mm) and left to dry at 30 °C until constant weight. The crosslinking reaction between PVA and DAC occurs during the drying of the reaction mixture, where dehydration of –CHO groups

Table 1
Designation of PVA/DAC samples, their composition and M_w of the PVA used.

Sample	PVA (g)	M_w PVA (kDa)	DAC (wt%)	DAC (g)
L-31	10	31	0.25	0.025
H-31	10	31	1	0.1
L-130	10	130	0.25	0.025
H-130	10	130	1	0.1

of DAC causes the formation of hemiacetals with hydroxyl groups of PVA. Simplified reaction scheme between –CHO of DAC and –OH group of PVA in an acidic environment is shown in Fig. 1.

The prepared thin films were then thoroughly washed in water to remove uncrosslinked material, and disc-shaped samples of 15 and 50 mm in diameter were cut out and stored in aseptic medium (70% ethanol solution) until used. A small part of the PVA/DAC samples was left unwashed for determination of network parameters (gel fraction). Designation and composition of the prepared PVA/DAC samples are listed in Table 1.

The estimation of network parameters, measurement of viscoelastic properties, BET and SEM analysis, drug release kinetics, cytotoxicity and transdermal absorption of prepared hydrogels were subsequently investigated.

2.3. Network parameters

The network parameters were estimated based on the measurements of swelling and weight change of prepared 15 mm disc-shaped PVA/DAC xerogel samples (6 specimens for each). Unwashed discs were weighed and then thoroughly washed for one week with regular changing of water. Subsequently, the swollen discs were gently dried to remove excess water, weighed and dried at 30 °C till constant weight. The network parameters were determined using equilibrium swelling theory suggested by Flory and Rehner [26]. The constants used for the calculation of network parameters include the specific volume of PVA polymer $\nu = 0.788\ cm^3/g$, the PVA density $\rho_p = 1.27\ g/cm^3$, the molar volume of water (V_1) at 25 °C = $18.069\ cm^3/mol$, the polymer-solvent interaction parameter (χ_1) = 0.464, the average bond length $l = 1.54$ Å, the characteristic ratio of PVA chain $C_n = 8.9$ and the molecular weight of PVA unit $M_r = 44$ g/mol. Following equations were used to calculate network parameters [10,27].

Equilibrium swelling (%) was obtained according to Eq. (1), where M_E is the mass of the hydrogel swollen to the equilibrium state, and M_0 is the mass of the washed and dried hydrogel [28].

$$\text{Equilibrium swelling (\%)} = \frac{M_E - M_0}{M_0} \times 100 \quad (1)$$

Equilibrium water content (*EWC*) describes the maximum amount of water absorbed by the hydrogel. M_s is the mass of the sample swelled under equilibrium conditions, and M_0 is the mass of the washed and dried hydrogel [29].

$$\text{EWC (\%)} = \frac{M_s - M_0}{M_s} \times 100 \quad (2)$$

The gel fraction was calculated using Eq. (3), where M_0 is the weight of the dried hydrogel after extraction of the soluble fraction in the hydrogel and M_{int} is the weight of the dry and non-washed hydrogel [28].

$$\text{Gel fraction (\%)} = \frac{M_0}{M_{int}} \times 100 \quad (3)$$

The average molecular weight between crosslinks (M_c), where M_n is the average number molecular weight of the initial uncrosslinked polymer, ν is the specific polymer volume, V_1 is the molar volume of water, $V_{2,s}$ is the polymer volume fraction and χ_1 is the polymer-solvent interaction parameter [26].

$$\mathrm{M_c\ (g/mol)} = \frac{M_n}{2} - \frac{\left[(V_{2,s})^{\frac{1}{3}} - \frac{V_{2,s}}{2} \right]}{\left(\frac{\nu}{V_1}\right)[\ln(1 - V_{2,s}) + V_{2,s} + \chi 1 (V_{2,s})^2\ ]} \quad (4)$$

Polymer fraction ($V_{2,s}$), where M_s/M_0 is the weight ratio of dry to swollen hydrogel at equilibrium, ρ_p is the density of the polymer and ρ_w is the density of water [30].

$$\mathrm{V_{2,s}} = \left[1 + \frac{\rho_p}{\rho_w} \left(\frac{M_s}{M_0} - 1 \right) \right]^{-1} \quad (5)$$

Calculation of the crosslink density (ρ_c) [26,31].

$$\rho_c\,(mol/cm^3) = \frac{1}{\nu M_c} \quad (6)$$

The mesh size (ξ):

$$\xi\ (\text{Å}) = V_{2,s}{}^{-1/3} (\bar{r}_0{}^2)^{1/2} \quad (7)$$

where $(\bar{r}_0{}^2)^{1/2}$ is the end-to-end distance of the unperturbed (solvent-free) state.

$$(\bar{r}_0{}^2)^{1/2} = l \left(\frac{2 \times M_c}{M_r} \right)^{1/2} \times C_n{}^{3/2} \quad (8)$$

2.4. Measurement of viscoelastic properties

Disc samples (d = 15 mm, 6 specimens per sample) were measured in an equilibrium swollen state using a rotational rheometer Anton Paar MCR 502 (Anton Paar, Austria) equipped with D-PP15 shaft using a roughened aluminium plate with 15 mm diameter and ground plate with glued sandpaper both used to prevent slipping of samples during measurement. The measurement was performed at laboratory temperature in oscillation mode in frequency sweep from 1 to 10 Hz by applying a constant strain of 1%.

2.5. BET and SEM analysis

Lyophilized PVA/DAC cryogels were initially degassed at 75 °C for 24 h. Specific surface area (α_{BET}), total pore volume (V_p) and mean pore diameter of cryogels was determined by multipoint Brunauer-Emmet-Teller (BET) analysis of adsorption isotherms recorded at 77 K utilizing high precision surface area analyzer Belsorp-mini II (BEL Japan Inc., Japan). The measurement was carried out in triplicates. These materials were also analyzed by scanning electron microscopy (SEM) employing Nova NanoSEM 450 microscope (FEI, Czech Republic) operated at 5 kV accelerating voltage. Ahead of SEM imaging, cryogels were sputtered with gold-palladium nanoparticles to suppress the charge accumulation effect.

2.6. Loading and release

H-31, L-130 and H-130 samples of approximately 500 mg and 15 mm in diameter were loaded by biologically active compound by submerging into a 50 mL of stock solution of 0.1 mg/mL (rutin) or 10 mg/mL (caffeine) and shaken for 72 h at 37 °C. Loaded samples were then used to study the drug release kinetics. For this purpose, three samples from each hydrogel were placed in separate closed containers containing 10 mL of demineralized water and shaken at 37 °C in the dark. Aliquots of 1 mL were collected in given times over 96 h and analyzed using UV-VIS spectrometer Perkin Elmer Lambda 1050 (Perkin Elmer Inc., USA) using characteristic peaks at 353 nm (rutin) and 273 nm (caffeine). The experiments were performed in triplicates.

2.7. Cytocompatibility of hydrogels

The cytocompatibility tests included 1) evaluation of cytotoxicity of hydrogel extracts and 2) cell growth in the presence of hydrogel and in direct contact with their surfaces. The cytotoxicity was tested according to ISO 10 993-5. All tests were performed in quadruplicates.

1) Extracts from L-130, H-130 and H-31 specimens were prepared according to ISO 10993-12 in the concentration of 0.1 g of swollen gels per 1 mL of culture media. The tested samples were extracted in culture medium for 24 h at 37 °C under constant shaking. The parent extracts (100%) were then diluted in culture medium to obtain a series of dilutions with concentrations of 75, 50, 25, 10, and 1%. The mouse embryonic fibroblast (NIH/3T3) cells were seeded into 96 well plates in concentration 10^5 cells per mL and placed to the incubator for pre-cultivation for 24 h at 37 °C. After the pre-incubation period, the extracts were added and cells incubated for another 24 h. Determination of cell viability after exposure time was performed by MTT assay. The reference wavelength was set to 570 and 690 nm, respectively. The results are presented as the relative cell viability compared to the reference (cells cultivated on tissue plastic only in culture medium), where reference corresponds to 1 (100% cell viability).
2) For the test of cell growth in the presence of hydrogels, cells were seeded on culture plastic plates in concentration 10^5 cells per mL and pre-incubated till they reached sub-confluence. The hydrogels were placed in the centre over the adherent cells. Cells were checked every day by an inverted phase-contrast microscope Olympus IX 81 (Olympus, Japan) until the reference reached full confluency (96 h). Cell viability was measured by MTT assay in the same conditions as in the cytotoxicity of hydrogel extracts after 48 and 96 h.

For the determination of cell adherence and growth on the surface of hydrogels, cells were seeded directly on the samples surfaces in concentration 5×10^4 cells per cm^2. After 48 h samples were fixed with 4% formaldehyde for 15 min, washed with PBS, permeabilized with 0.5% Triton X for 5 min and subsequently stained with Hoechst 33258 and ActinRed™ 555 for 30 min in the dark. Cells were observed using an inverted fluorescence phase-contrast microscope Olympus IX 81 (Olympus, Japan).

2.8. Transdermal absorption tests in vitro

Tests were conducted according to the OECD Test Guideline for Skin Absorption: In vitro method, using the skin from pig ear. The pig's ear lobe was shaved and the inner part of the auricle was separated from the underlying cartilage. Square skin samples of 3 × 3 cm were cut out from the separated skin. The skin samples were then placed in test cells and their skin integrity was determined using a UNI-T UT71D multimeter. Samples with a resistance below 5 mΩ were excluded.

Disc-shaped samples of individual hydrogels were added to the prepared skin samples. Prior to insertion, the hydrogels were loaded with caffeine by shaking for 120 h at 37 °C in 10 mg/mL caffeine. Testing was performed on an automated diffusion cell system with the continuous flow of receptor liquid through samples Fraction Collector FC33 (Permegear, USA). All experiments were performed in triplicates. The receptor fluid (PBS buffer and 0.05% gentamicin sulfate) was collected for 24 h at a constant flow rate of 2 mL/h. After completion of the measurements, the fractions obtained at pre-set times (1–24 h) were stored at −20 °C until analysis. The individual samples were then filtered and analyzed by liquid chromatography employing HPLC chromatograph Breeze 1525 with UV-VIS detector (Waters Corporation, USA). Chromatographic separation of the caffeine within the samples was carried out isocratically on a Kinetex C18 100A column (150 × 4.6 mm, 2.6 μm) (Phenomenex, USA). The mobile phase consisted of 0.2% HCOOH and methanol in a 75/25 ratio, the temperature was set to 30 °C, the flow rate 0.7 mL/min. The wavelength used for detection was 272 nm.

3. Results and discussion

Four types of hydrogel samples differing in concentrations of DAC and M_w of PVA were prepared, see Table 1. Only the network parameters were determined for the sample L-31 (L stands for lower amount of the DAC, 0.25 wt%, number 31 is the molecular weight of PVA in kDa, cf. Table 1) because of its poor physical properties caused by combination of low crosslinker concentration and low M_w of PVA. Sample L-31 teared and disintegrated even during gentle manipulation, which prevented meaningful characterization as certain techniques would be influenced by macroscopic faults in hydrogel structure, making obtained data unreliable. Other three types of hydrogel samples (L-130, H-31 and H-130, H stands for higher concentration of crosslinker – 1 wt%, number 130 is the molecular weight of PVA in kDa, cf. Table 1) were characterized by full set of methods described above.

3.1. Network parameters

Based on the equations given in Section 2.3, the network parameters of all types of PVA/DAC hydrogel samples (L-130, H-130, L-31, H-31) were determined, Table 2. Unsurprisingly, the swelling of hydrogel matrices and *EWC* depends on both the amount of DAC and the M_w of PVA. The lower the amount of crosslinker and the lower the M_w of PVA, the more the hydrogel swells. Thus, sample L-31 has the largest swelling, equal to almost 80-times of its dry mass. On the other side, sample H-130 swells only about 3.5-times. Conversely, the gel fraction increases with increasing amounts of DAC and M_w PVA, thereby sample H-130 shows the largest gel fraction and sample L-31 the smallest one.

The dependence of average molecular weight between crosslinks (M_c), crosslink density (ρ_c), and mesh size (ξ) on both observed factors is, however, not so straightforward. As one may expect, decreasing the amount of DAC results in higher separation of crosslinked regions (higher M_c), which reduces ρ_c and increase the ξ of respective samples. However, the influence of M_w of PVA on M_c and ρ_c actually differs for different the amounts of crosslinker. Increased M_w of PVA is causing a significant decrease of M_c (an increase of ρ_c) in H-series (1% of DAC), but the opposite trend was found in L-series (0.25% of DAC). Notably, the ξ is smaller for PVA with M_w = 130 kDa in both series.

The variation of M_c and ρ_c between series is likely related to the nature of PVA/DAC network, which is composed of two types of interactions – the PVA/DAC chemical crosslinks complemented by

Table 2
Network parameters (the equilibrium swelling, the equilibrium water content *EWC*, the gel fraction, the average molecular weight between crosslinks M_c, the crosslink density ρ_c and the mesh size ξ) calculated for the prepared hydrogel samples. Data represent average of six measurements with standard deviations.

Sample	Equilibrium swelling (%)	EWC (%)	Gel fraction (%)	M_c (g/mol)	ρ_c (μmol/cm^3)	ξ (Å)
L-31	7900 ± 800	98.7 ± 0.1	12 ± 0.8	12380 ± 20	103 ± 1	508 ± 17
H-31	710 ± 20	87.6 ± 0.3	47.7 ± 0.9	6410 ± 160	198 ± 5	169 ± 4
L-130	1150 ± 90	92 ± 0.6	58.8 ± 1.8	20660 ± 1880	62 ± 6	352 ± 25
H-130	350 ± 10	77.8 ± 0.3	88.8 ± 0.2	2890 ± 90	440 ± 14	93 ± 2

residual physical interactions (hydrogen bridge network and chain entanglements) between the PVA macromolecules [17]. It is reasonable to assume that chemical crosslinking is more pronounced in H-series hydrogels, particularly for H-130 sample, where longer PVA chains offer considerably more crosslinking hot-spots. Thus, the sample H-130 exhibits the smallest M_c and ξ and the highest ρ_c of all. In more sparsely crosslinked L series, the effect of residual physical crosslinking of longer PVA (130 kDa) chains provides additional stabilization to the hydrogel network. Hence, despite L-130 sample having the lowest-density network with highest M_c and lowest ρ_c from all samples, its ξ is lower than in case of L-31, and its physical properties are sufficient for easy handling in contrast to sample L-31, which had to be excluded from further analyses.

To summarize, although the role of the amount of the crosslinker governs the network parameters of hydrogels (i.e. four-times less of DAC results in up to 10-times the swelling in L-31 vs. H-31), it is further accentuated by changing the M_w of PVA, which influences the hydrogel network mainly at the (macro)molecular level.

3.2. Analysis of viscoelastic properties

Oscillatory shear rheometry utilizing frequency sweep from 1 Hz to 10 Hz and constant strain of 1% was used to study the viscoelastic properties of prepared hydrogels. The dependence of storage modulus (G') and loss modulus (G'') on angular frequency is given in Fig. 2A. The G' values of PVA/DAC hydrogel samples range from more than 2100 Pa for sample H-130 to about 150 Pa for sample L-130, see Fig. 2B. The G'' values range from about 190 Pa for sample H-130 to about 4.3 Pa for sample L-130. As expected, [18] the results follow the trend of ρ_c (see Table 2), because the denser mesh have a higher elasticity than the sparser one, which will, in turn, have more viscous-like behavior. Hence, the lowest G' and G'' values were observed for the L-130 sample with the lowest crosslink density. The effect of the M_w of PVA is observable for H series hydrogels, where four-times lower M_w of PVA results in decrease of both G' and G'' by approx. 75%.

Analogous correlations between the amount of crosslinker and the M_w of PVA were found for the complex dynamic modulus (G^*) and the damping factor (tan δ). The complex modulus G^* was calculated as the square root of the sum of the square of storage and loss moduli in the selected range of oscillatory measurement at ambient temperature, Fig. 2C. The range of G^* values is from more than ~2200 Pa for H-130 to ~150 Pa for sample L-130. The *tan δ* is defined as the ratio between loss and storage modulus (G''/G') and gives a measure of viscous to elastic component of the material. The damping factor ranges from 0.09 for sample H-130 (most elastic) to 0.03 for sample L-130 (the most viscous), Fig. 2D.

To summarize, the most viscous and the least elastic material is the least crosslinked sample L-130. The most elastic is sample H-130. Notably, viscoelastic properties of sample H-31 are generally closer to L-130 than to H-130 despite being prepared by using the same amount of crosslinker as the latter. This demonstrates a considerable influence of the PVA matrix on the rheological properties of the hydrogels.

3.3. BET and SEM analysis

Samples of PVA/DAC hydrogels were lyophilized, and their specific surface area (α_{BET}), total pore volume (V_p), mean pore diameter and adsorbed volume of nitrogen (V_a) measured, see Fig. 3. The α_{BET} value for sample L-130 (31.1 ± 0.9 m^2/g) is an order of the magnitude higher than the values for samples H-130 (2.0 ± 0.1 m^2/g) and H-31 (2.2 ± 0.1 m^2/g). The total pore volume (V_p) exhibits the same trend as α_{BET} being about ten times higher for L-130 (0.218 ± 0.007 cm^3/g) than for H-series hydrogels (H-130 = 0.021 ± 0.001 cm^3/g and H-31 = 0.031 ± 0.002 cm^3/g, see Fig. 3C). This difference is closely related to the extent of cavitation induced by the lyophilization and indirectly linked to the water absorption capability of the hydrogel. Interestingly, mean pore diameter do not follow described trend. Largest pore diameter was observed for H-31 sample (54.6 ± 3.3 nm), followed by H-130 sample (41.5 ± 2.1 nm) and L-130 sample (28.1 ± 0.8 nm). The H-series cryogels thus have fewer larger pores, while L-130 contains a larger number of smaller pores in its structure.

Cryogel samples were further analyzed by scanning electron microscopy (SEM). In agreement with α_{BET} values, surface of L-130 cryogel was found to be highly porous, see Fig. 3D, while the H-31 sample showed slightly larger surface pores than the H-130 sample, but the difference is not very significant.

To summarize, while both α_{BET}, V_p and V_a increase significantly with the decreasing amount of DAC, the M_w of PVA seems to influence the mean pore size. It should be noted that combination of the low amount of DAC and high-molecular-weight PVA allowed preparing highly

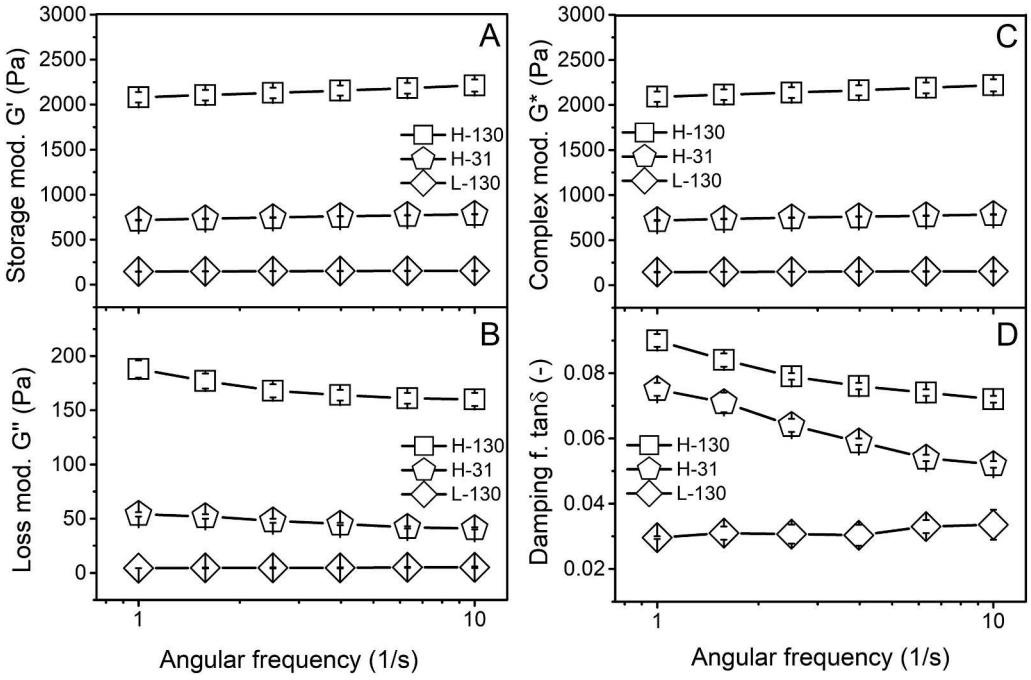

Fig. 2. Dependence of the storage modulus (G') and the loss modulus (G'') of PVA/DAC hydrogel samples on the angular frequency (part A and B), dependence of the calculated complex modulus (G^*, part C) and the damping factor ($tan\delta$, part D) on the angular frequency. Measurements were repeated six times; error bars express standard deviations.

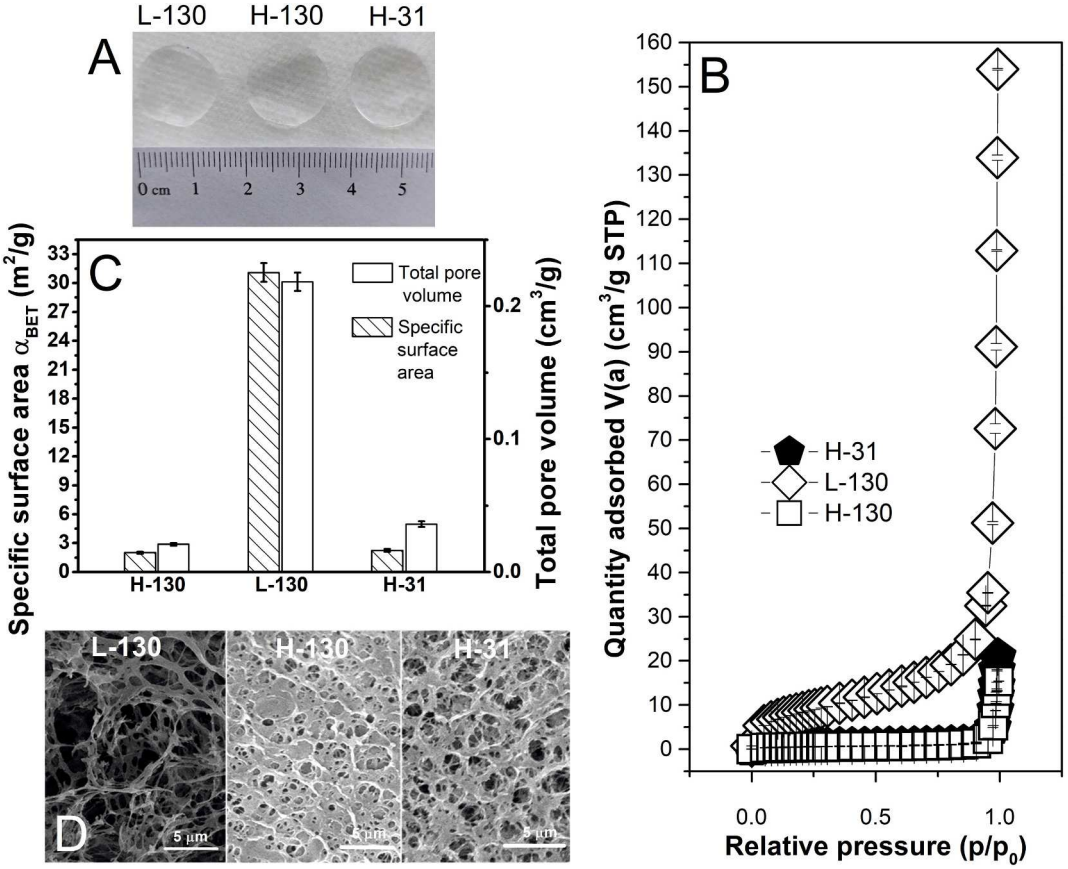

Fig. 3. Photographs of swollen hydrogel samples (part A), dependence of quantity of the adsorbed volume of nitrogen per cryogels mass (V_a) on the relative pressure p/p_0 (part B), the specific surface area α_{BET} and total pore volume (V_p) of prepared PVA/DAC cryogels (part C), and micrographs of individual PVA/DAC samples taken with SEM at 30.000× magnification (part D). Measurements were performed in triplicates; error bars represent standard deviations.

porous materials with mechanical properties allowing reasonable handling, which was not possible by using PVA with lower molecular weight (sample L-31).

3.4. Loading and release study

Samples of individual hydrogels were loaded with rutin or caffeine, see Section 2.6 for more details. The loaded hydrogel samples were subsequently put into separate containers containing 10 mL of water and release of rutin (Fig. 4A) and caffeine (Fig. 4B) evaluated by UV-VIS spectroscopy.

Release rates of relatively small caffeine molecules (M = 194 g/mol, Fig. 4B) from all three tested materials are identical within the experimental error. The effect of the network parameters is only observable for larger rutin (610 g/mol), where fastest release after 8 h was observed for H-31 sample, while both 130-series samples showed nearly identical release kinetics. This might be related to lower M_w of PVA influencing the pore size (see previous section), but the difference is relatively minor and more tests would be needed to confirm this observation.

Small overall differences in burst release kinetics are most likely caused by low thickness of prepared hydrogel films. Because most of the drug is situated in the vicinity of the thin film surface, the diffusion path is very short, which together with hydrogel mesh size being significantly larger than the diameter of studied molecules (100–350 Å, Table 2), minimizes the impact of hydrogel network to the drug release rate. This may be improved by employing thicker films or by modification of drug loading procedure.

Nevertheless, the observed burst release kinetics with up to 90% of compounds released in 8 h is considered to be suitable for topical drug delivery, where expected time of application is in order of hours rather than days.

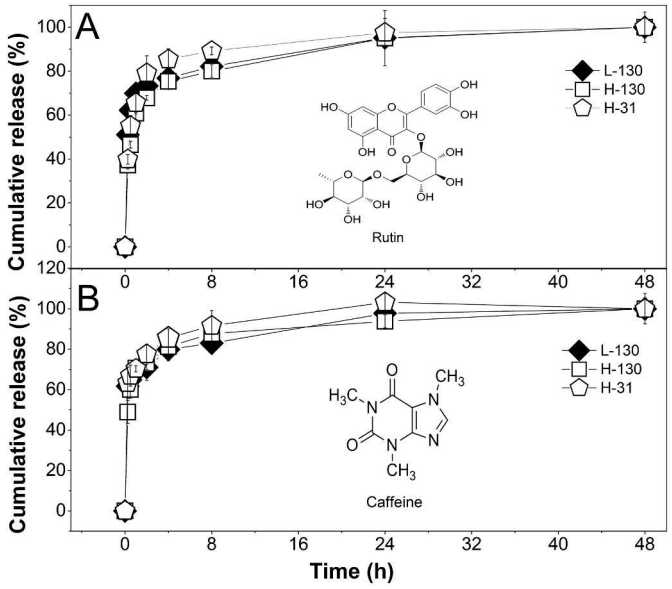

Fig. 4. Cumulative release of rutin (part A) and caffeine (part B) from L-130, H-31 and L-130 hydrogel samples. All experiments were performed in triplicates; error bars represent standard deviations.

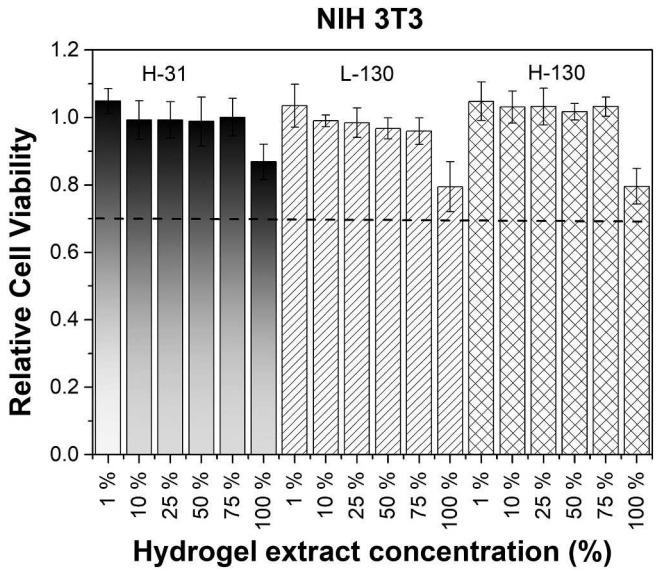

Fig. 5. Relative cell viability of mouse embryonic fibroblast cells (NIH/3T3) incubated with PVA/DAC hydrogel extracts of different concentrations (1–100%). Measurements were performed in quadruplicates; error bars represent standard deviations.

3.5. Biological testing

Biological evaluation included (i) determination of cytotoxicity of hydrogel extracts in culture media prepared according to ISO 10993-12 and (ii) observation of cell growth and morphology in the presence of hydrogels as well as directly on the gel surface. Cytotoxicity of hydrogel extracts was evaluated using mouse embryonic fibroblast cell line (NIH/3T3) according to ISO 10 993-5, see Fig. 5.

The amount of DAC did not have any observable impact to the cytotoxicity of hydrogel extracts and all materials can be considered non-toxic according to ISO 10933-5.

Subsequently, the cell growth and morphology in the presence of hydrogels was studied for 96 h. Cell viability was quantified by MTT assay, and qualitative analysis was done by observation under the microscope. Cell morphology was checked every day until reference reached confluency. Results are shown in Fig. 6, together with micrographs of cells cultivated in the presence of hydrogels for 96 h.

The presence of hydrogel samples has no observable effect on cell growth or morphology. Cells were growing at the same rate in the presence of hydrogels as in their absence and reached full confluency at the same time (Fig. 6, top). Likewise, the morphology was not affected by the hydrogels in any way, and fibroblasts retained their typical elongated shapes, see micrographs in Fig. 6. Cells were also seeded directly to the hydrogel surface in an attempt to observe they growth and morphology in direct contact with the hydrogel. However, cells did not adhere to hydrogel surface at all, making the evaluation impossible.

It should be also noted that no degradation of hydrogels was observed during the tests or when samples were kept under *in vitro* conditions (submerged to culture medium, seeded with NIH/3T3 cells, 37 °C) for one week. Surface of samples remained smooth, without signs of weathering or degradation and no difference in weight of the samples before and after the tests was observed.

To summarize, absence of cell migration/attachment to the hydrogel surface, no observable impact of hydrogel presence on the cell growth together with no observable degradation supports the suitability of hydrogel films as wound dressings. Additional tests are however required before biosafety in vivo can be claimed.

3.6. Transdermal absorption study

Transdermal absorption was studied using caffeine-loaded hydrogel samples. Caffeine was selected as a model substance for the study of transdermal absorption of hydrophilic compounds [22]. Hydrogel samples (1 cm in diameter) were loaded with caffeine and transdermal absorption of caffeine studied using skin from pig's earlobe, see Section 2.8 for more details. Amount of absorbed caffeine was determined by HPLC analysis.

The total amount of caffeine in the samples and calculated dose per 1 cm^2 skin is given in Table 3. All samples were loaded by the same method, but the total dose of caffeine differs between samples because of their different EWC, gel fractions and equilibrium swelling. The highest amount of caffeine was loaded in the sample L-130 (~900 μg), while sample H-130 was able to absorb the smallest amount (~500 μg).

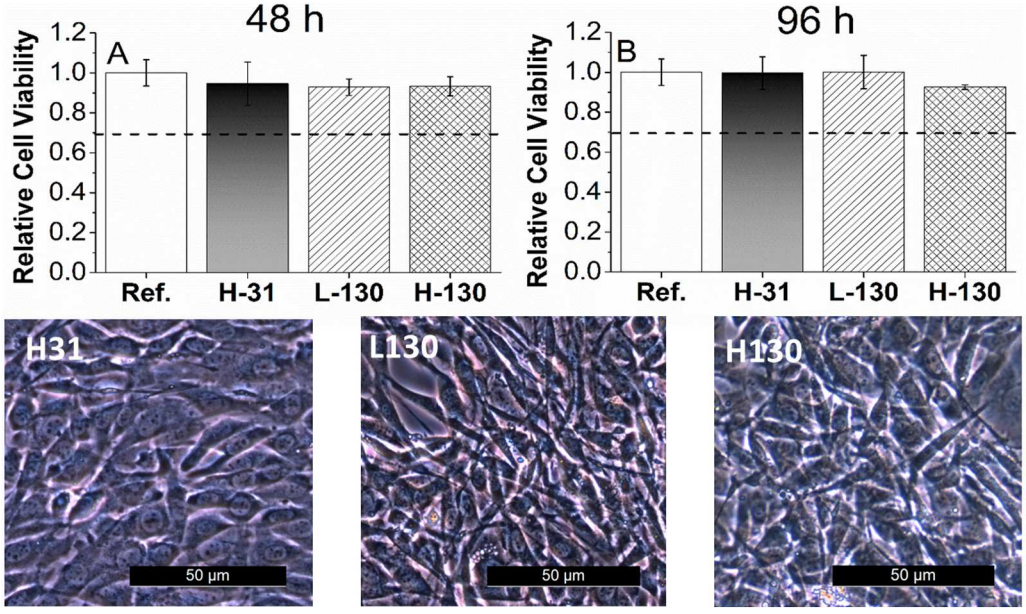

Fig. 6. Relative NIH/3T3 cell viability of cells incubated in the presence of hydrogel samples for 48 and 96 h, respectively, and micrographs of cells incubated for 96 h. Experiments were performed in quadruplicates; error bars represent standard deviations.

Table 3
The amount of caffeine in the samples (μg) and the dose of caffeine per cm^2 of skin.

Sample	Total dose of caffeine (μg)	Dose per cm^2 (μg/cm^2)
L-130	896 ± 8	1134 ± 10
H-31	660 ± 6	832 ± 7
H-130	495 ± 1	625 ± 1
Reference	250	320

The aqueous caffeine solution containing a total dose of 250 μg was used as a reference [23].

The total amount of transdermally absorbed caffeine (ng) is shown in Fig. 7A, the time profile of caffeine absorption (ng/mL) in Fig. 7B, total amount of transdermally absorbed caffeine relative to applied dose (%) in Fig. 7C and the time profile of caffeine absorption relative to applied dose (%) in Fig. 7D. Results show that caffeine penetrates the skin relatively slowly over the entire monitored time interval (24 h). According to Trauer et al. [23], this is a result of the absence of blood supply to the skin during the in vitro study because much faster absorption of caffeine through the skin of a living organism was observed. As a result, only between 0.07% and 0.2% of total caffeine dose crosses the skin barrier within 24 h under the employed setup (Fig. 7C and D). Caffeine hydrophilicity is thus clearly making its penetration through *stratum corneum* challenging [32]. This is in agreement with findings of other authors, including Trauer et al. [23], Bonina et al. [33], Santander-Ortega et al. [34] and Pilloni et al. [35] who also observed the transdermal caffeine absorption in the order of tenths of the percent of the applied dose using a variety of different carriers.

Despite the relatively low amount of transdermally absorbed caffeine, differences between the samples are clearly visible. The highest total amount of absorbed caffeine (1400 ng/0.15%) was observed for the L-130 sample, while only between 350 and 450 ng (0.06–0.07%) of caffeine was absorbed from H-series samples over 24 h. This corresponds to the average caffeine penetration of 72.1 ng·cm^2/h for L-130, 24.3 ng·cm^2/h for H-31, 19.3 ng·cm^2/h for H-130 and 18.1 ng·cm^2/h for caffeine solution. On the other hand, when the differences in applied dose are considered (Fig. 7C), only the sample L-130 overcomes the reference solution in terms of total caffeine absorption with respect to applied dose. However, while the amount of the drug absorbed from the caffeine solution linearly increases with time, the amount of caffeine absorbed from the hydrogels peaks between 8 and 12 h, respectively (Fig. 7B and D) showing higher effectivity of initial caffeine absorption from all hydrogels.

Comparing individual hydrogel samples, higher effectivity of caffeine absorption from L-130 stands out. The amount of caffeine permeated from the L-130 sample is approximately twice larger than from H-series samples, Fig. 7C, D. The higher efficiency of sample L-130 is assumed to be caused by its physical properties, namely the lowest elasticity among all tested materials. While more elastic H-series samples tend to keep their original shape on uneven skin surface, the L-130

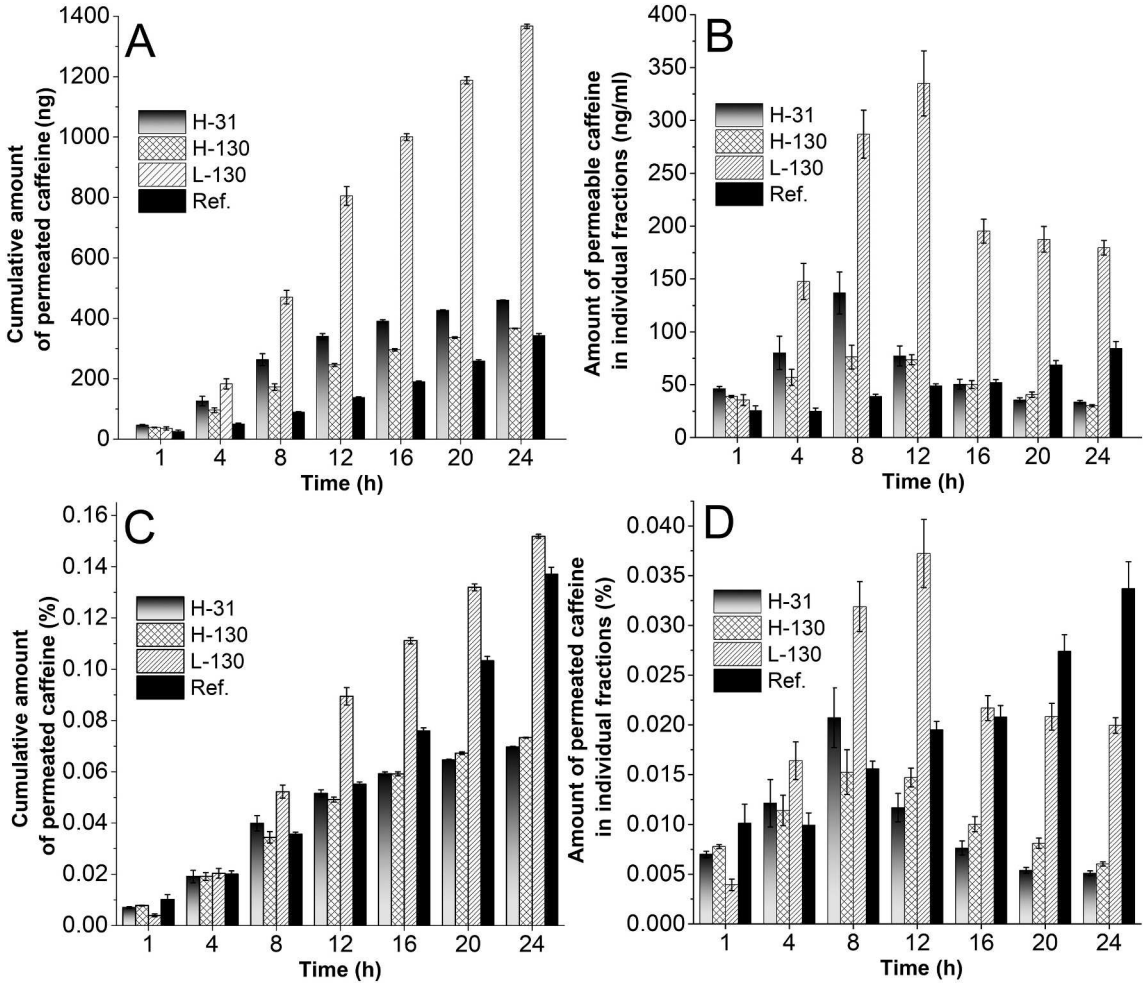

Fig. 7. The cumulative amount of permeated caffeine (ng) (part A), the time-dependent amount of permeated caffeine (ng/mL) (part B), total amount of transdermally absorbed caffeine relative to applied dose (%) (part C) and the time profile of caffeine absorption relative to applied dose (%) (part D). Ref. stands for the reference caffeine solution. Measurements were performed in triplicates; error bars represent standard deviations.

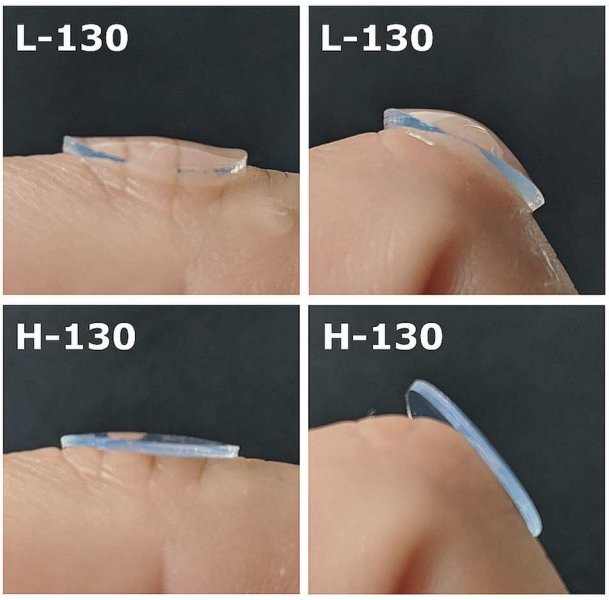

Fig. 8. The comparison of L-130 and H-130 hydrogels on the uneven skin surface.

adheres to the skin considerably better, see comparison of L-130 and H-130 hydrogel in Fig. 8. Because adherence to the skin is one of the key qualities dictating effectiveness of transdermal absorption, [4] this observation readily explain the improved transdermal delivery of caffeine from L-130 sample.

The hydrogel L-130 is thus assumed to be the most promising candidate for transdermal administration of biologically active substances from all tested materials without using any skin-penetration enhancers.

4. Conclusion

The combination of different concentration of crosslinker, 2,3-dialdehyde cellulose, DAC, and different molecular weight of the matrix, poly(vinyl alcohol), PVA, was used to optimize the properties of thin PVA/DAC hydrogel films towards topical applications. While changing the amount of crosslinker is a standard method for tuning the properties of hydrogels, simultaneous change of the molecular weight of the second hydrogel component provides another, yet often overlooked, degree of freedom which may be exploited to obtain the material with specific properties. Detailed analysis revealed that increased M_w of PVA influences hydrogel network parameters at (macro)molecular level (crosslink density, mesh size) providing additional stabilization. The impact of these molecular-scale changes on bulk properties of hydrogels is largest for equilibrium swelling capacity, viscoelastic characteristics and it also notably improves physical properties of L-130 films compared to L-31 ones (L-130 samples did not disintegrate during handling unlike the L-31). On the other hand, the specific surface area and the total pore volume of lyophilized samples is governed by the amount of crosslinker and does not depend on the type of PVA, which however influences the mean pore size. Neither the amount of crosslinker nor the molecular weight of PVA has a significant influence on drug release rates, likely because the role of hydrogel network density does not manifest in thin-film formulations. All hydrogels were non-cytotoxic under in vitro conditions, they did not affect the cellular growth and cell morphology or support the adherence of cells to their surface, which imply their suitability as biomaterials for transdermal drug delivery and wound dressings.

The best candidate for preparation of dermal patches and masks intended for transdermal delivery of biologically-active compounds is the hydrogel L-130, which is prepared using higher-molecular weight PVA matrix in combination with a lower concentration of crosslinker. It has high porosity and high water content (drug-loading capacity), physical properties allowing easy handling and the best adherence to the skin from all tested samples, which enhances its transdermal drug delivery properties. Conversely, a combination of higher M_w of PVA and a higher concentration of crosslinker leads to more elastic hydrogels with a denser network.

CRediT authorship contribution statement

Monika Muchová: Investigation, Visualization, Formal analysis, Writing - original draft. **Lukáš Münster**: Investigation, Visualization, Writing - original draft, Writing - review & editing. **Zdenka Capáková**: Investigation. **Veronika Mikulcová**: Investigation. **Ivo Kuřitka**: Resources, Funding acquisition. **Jan Vícha**: Conceptualization, Supervision, Writing - original draft, Writing - review & editing.

Declaration of competing interest

The authors declare that they have no known competing financial interests or personal relationships that could have appeared to influence the work reported in this paper.

Acknowledgement

This work was supported by the Ministry of Education, Youth and Sports of the Czech Republic Program NPU I (LO1504). M.M. was supported by the internal grant for specific research from Tomas Bata University in Zlín no. IGA/CPS/2020/003.

References

[1] E. Caló, V.V. Khutoryanskiy, Biomedical applications of hydrogels: a review of patents and commercial products, Eur. Polym. J. 65 (2015) 252–267, https://doi.org/10.1016/j.eurpolymj.2014.11.024.
[2] G.D. Winter, Formation of the scab and the rate of epithelization of superficial wounds in the skin of the young domestic pig, Nature 193 (1962) 293–294, https://doi.org/10.1038/193293a0.
[3] E.A. Kamoun, E.-R.S. Kenawy, X. Chen, A review on polymeric hydrogel membranes for wound dressing applications: PVA-based hydrogel dressings, J. Adv. Res. 8 (2017) 217–233, https://doi.org/10.1016/j.jare.2017.01.005.
[4] M.E. Parente, A.O. Andrade, G. Ares, F. Russo, Á. Jiménez-Kairuz, Bioadhesive hydrogels for cosmetic applications, Int. J. Cosmet. Sci. 37 (2015) 511–518, https://doi.org/10.1111/ics.12227.
[5] H. Ruan, Q. Hu, D. Wen, Q. Chen, G. Chen, Y. Lu, J. Wang, H. Cheng, W. Lu, Z. Gu, A dual-bioresponsive drug-delivery depot for combination of epigenetic modulation and immune checkpoint blockade, Adv. Mater. 31 (2019) 1806957, https://doi.org/10.1002/adma.201806957.
[6] C. Wang, J. Wang, X. Zhang, S. Yu, D. Wen, Q. Hu, Y. Ye, H. Bomba, X. Hu, Z. Liu, G. Dotti, Z. Gu, In situ formed reactive oxygen species–responsive scaffold with gemcitabine and checkpoint inhibitor for combination therapy, Sci. Transl. Med. 10 (2018), https://doi.org/10.1126/scitranslmed.aan3682.
[7] J.K. Li, N. Wang, X.S. Wu, Poly(vinyl alcohol) nanoparticles prepared by freezing–thawing process for protein/peptide drug delivery, J. Control. Release 56 (1998) 117–126, https://doi.org/10.1016/S0168-3659(98)00089-3.
[8] S.-H. Hyon, W.-I. Cha, Y. Ikada, M. Kita, Y. Ogura, Y. Honda, Poly(vinyl alcohol) hydrogels as soft contact lens material, J. Biomater. Sci. Polym. Ed. 5 (1994) 397–406, https://doi.org/10.1163/156856294X00103.
[9] U.-J. Kim, S. Kuga, M. Wada, T. Okano, T. Kondo, Periodate oxidation of crystalline cellulose, Biomacromolecules 1 (2000) 488–492, https://doi.org/10.1021/bm0000337.
[10] L. Münster, J. Vícha, J. Klofáč, M. Masař, P. Kucharczyk, I. Kuřitka, Stability and aging of solubilized dialdehyde cellulose, Cellulose 24 (2017) 2753–2766, https://doi.org/10.1007/s10570-017-1314-x.
[11] U.-J. Kim, M. Wada, S. Kuga, Solubilization of dialdehyde cellulose by hot water, Carbohydr. Polym. 56 (2004) 7–10, https://doi.org/10.1016/j.carbpol.2003.10.013.
[12] I. Sulaeva, K.M. Klinger, H. Amer, U. Henniges, T. Rosenau, A. Potthast, Determination of molar mass distributions of highly oxidized dialdehyde cellulose by size exclusion chromatography and asymmetric flow field-flow fractionation, Cellulose 22 (2015) 3569–3581, https://doi.org/10.1007/s10570-015-0769-x.
[13] J.A. Sirviö, H. Liimatainen, M. Visanko, J. Niinimäki, Optimization of dicarboxylic acid cellulose synthesis: reaction stoichiometry and role of hypochlorite scavengers, Carbohydr. Polym. 114 (2014) 73–77, https://doi.org/10.1016/j.carbpol.2014.07.

081.
[14] G. Yan, X. Zhang, M. Li, X. Zhao, X. Zeng, Y. Sun, X. Tang, T. Lei, L. Lin, Stability of soluble dialdehyde cellulose and the formation of hollow microspheres: optimization and characterization, ACS Sustain. Chem. Eng. 7 (2019) 2151–2159, https://doi.org/10.1021/acssuschemeng.8b04825.
[15] H. Liimatainen, M. Visanko, J.A. Sirviö, O.E.O. Hormi, J. Niinimaki, Enhancement of the nanofibrillation of wood cellulose through sequential periodate–chlorite oxidation, Biomacromolecules 13 (2012) 1592–1597, https://doi.org/10.1021/bm300319m.
[16] U.-J. Kim, Y.R. Lee, T.H. Kang, J.W. Choi, S. Kimura, M. Wada, Protein adsorption of dialdehyde cellulose-crosslinked chitosan with high amino group contents, Carbohydr. Polym. 163 (2017) 34–42, https://doi.org/10.1016/j.carbpol.2017.01.052.
[17] L. Münster, J. Vícha, J. Klofáč, M. Masař, A. Hurajová, I. Kuřitka, Dialdehyde cellulose crosslinked poly(vinyl alcohol) hydrogels: influence of catalyst and crosslinker shelf life, Carbohydr. Polym. 198 (2018) 181–190, https://doi.org/10.1016/j.carbpol.2018.06.035.
[18] L. Münster, Z. Capáková, M. Fišera, I. Kuřitka, J. Vícha, Biocompatible dialdehyde cellulose/poly(vinyl alcohol) hydrogels with tunable properties, Carbohydr. Polym. 218 (2019) 333–342, https://doi.org/10.1016/j.carbpol.2019.04.091.
[19] A. Ganeshpurkar, A.K. Saluja, The pharmacological potential of rutin, Saudi Pharm. J. 25 (2017) 149–164, https://doi.org/10.1016/j.jsps.2016.04.025.
[20] N.Q. Tran, Y.K. Joung, E. Lih, K.D. Park, In situ forming and rutin-releasing chitosan hydrogels as injectable dressings for dermal wound healing, Biomacromolecules 12 (2011) 2872–2880, https://doi.org/10.1021/bm200326g.
[21] J.K. Choi, S.-H. Kim, Rutin suppresses atopic dermatitis and allergic contact dermatitis, Exp. Biol. Med. (Maywood) 238 (2013) 410–417, https://doi.org/10.1177/1535370213477975.
[22] L. Luo, M.E. Lane, Topical and transdermal delivery of caffeine, Int. J. Pharm. 490 (2015) 155–164, https://doi.org/10.1016/j.ijpharm.2015.05.050.
[23] S. Trauer, A. Patzelt, N. Otberg, F. Knorr, C. Rozycki, G. Balizs, R. Büttemeyer, M. Linscheid, M. Liebsch, J. Lademann, Permeation of topically applied caffeine through human skin – a comparison of in vivo and in vitro data, Br. J. Clin. Pharmacol. 68 (2009) 181–186, https://doi.org/10.1111/j.1365-2125.2009.03463.x.
[24] P. Engel, L. Hein, A.C. Spiess, Derivatization-free gel permeation chromatography elucidates enzymatic cellulose hydrolysis, Biotechnol. Biofuels 5 (2012) 77, https://doi.org/10.1186/1754-6834-5-77.
[25] L. Münster, B. Hanulíková, M. Machovský, F. Latečka, I. Kuřitka, J. Vícha, Mechanism of sulfonation-induced chain scission of selectively oxidized polysaccharides, Carbohydr. Polym. 229 (2020) 115503, , https://doi.org/10.1016/j.carbpol.2019.115503.
[26] P.J. Flory, J. Rehner, Statistical mechanics of cross-linked polymer networks II. Swelling, J. Chem. Phys. 11 (1943) 521–526, https://doi.org/10.1063/1.1723792.
[27] N.A. Peppas, E.W. Merrill, Determination of interaction parameter $\chi 1$, for poly (vinyl alcohol) and water in gels crosslinked from solutions, J. Polym. Sci. Polym. Chem. Ed. 14 (1976) 459–464, https://doi.org/10.1002/pol.1976.170140216.
[28] S.K.H. Gulrez, S. Al-Assaf G.O, Hydrogels: methods of preparation, characterisation and applications, in: A. Carpi (Ed.), Progress in Molecular and Environmental Bioengineering - From Analysis and Modeling to Technology Applications, InTech, 2011, , https://doi.org/10.5772/24553.
[29] B.J. Tighe, The role of permeability and related properties in the design of synthetic hydrogels for biomedical applications, Brit. Poly. J. 18 (1986) 8–13, https://doi.org/10.1002/pi.4980180104.
[30] N.A. Peppas, Y. Huang, M. Torres-Lugo, J.H. Ward, J. Zhang, Physicochemical foundations and structural design of hydrogels in medicine and biology, Annu. Rev. Biomed. Eng. 2 (2000) 9–29, https://doi.org/10.1146/annurev.bioeng.2.1.9.
[31] H. Omidian, S.-A. Hasherni, F. Askari, S. Nafisi, Swelling and Crosslink Density Measurements for Hydrogels, (n.d.) 6.
[32] M. Dias, A. Farinha, E. Faustino, J. Hadgraft, J. Pais, C. Toscano, Topical delivery of caffeine from some commercial formulations, Int. J. Pharm. 182 (1999) 41–47, https://doi.org/10.1016/S0378-5173(99)00067-8.
[33] F. Bonina, S. Bader, L. Montenegro, C. Scrofani, M. Visca, Three phase emulsions for controlled delivery in the cosmetic field, Int. J. Cosmet. Sci. 14 (1992) 65–74, https://doi.org/10.1111/j.1467-2494.1992.tb00040.x.
[34] M.J. Santander-Ortega, T. Stauner, B. Loretz, J.L. Ortega-Vinuesa, D. Bastos-González, G. Wenz, U.F. Schaefer, C.M. Lehr, Nanoparticles made from novel starch derivatives for transdermal drug delivery, J. Control. Release 141 (2010) 85–92, https://doi.org/10.1016/j.jconrel.2009.08.012.
[35] M. Pilloni, G. Ennas, M. Casu, A.M. Fadda, F. Frongia, F. Marongiu, R. Sanna, A. Scano, D. Valenti, C. Sinico, Drug silica nanocomposite: preparation, characterization and skin permeation studies, Pharm. Dev. Technol. 18 (2013) 626–633, https://doi.org/10.3109/10837450.2011.653821.

Article XIII.

Humpolicek, P.; Radaszkiewicz, K. A.; **Capakova, Z**.; Pachernik, J.; Bober, P.; Kasparkova, V.; Rejmontova, P.; Lehocky, M.; Ponizil, P.; Stejskal, J. Polyaniline Cryogels: Biocompatibility of Novel Conducting Macroporous Material. Sci Rep 2018, 8, 135. https://doi.org/10.1038/s41598-017-18290-1.

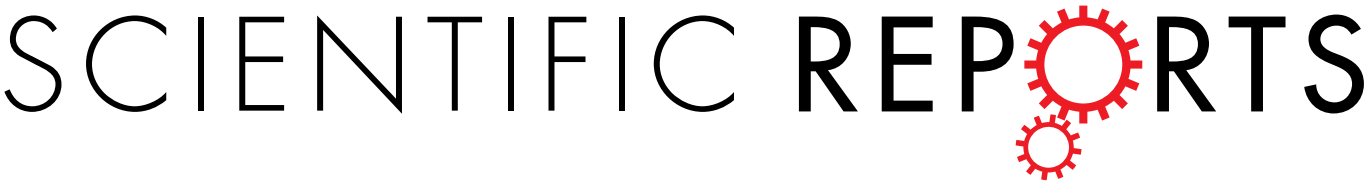

OPEN

Polyaniline cryogels: Biocompatibility of novel conducting macroporous material

Received: 8 August 2017
Accepted: 5 December 2017
Published online: 09 January 2018

Petr Humpolíček[1,2], Katarzyna Anna Radaszkiewicz[3], Zdenka Capáková[1], Jiří Pacherník[3], Patrycja Bober[4], Věra Kašpárková[1,2], Petra Rejmontová[1,2], Marián Lehocký[1,2], Petr Ponížil[1,2] & Jaroslav Stejskal[4]

Polyaniline cryogel is a new unique form of polyaniline combining intrinsic electrical conductivity and the material properties of hydrogels. It is prepared by the polymerization of aniline in frozen poly(vinyl alcohol) solutions. The biocompatibility of macroporous polyaniline cryogel was demonstrated by testing its cytotoxicity on mouse embryonic fibroblasts and *via* the test of embryotoxicity based on the formation of beating foci within spontaneous differentiating embryonic stem cells. Good biocompatibility was related to low contents of low-molecular-weight impurities in polyaniline cryogel, which was confirmed by liquid chromatography. The adhesion and growth of embryonic stem cells, embryoid bodies, cardiomyocytes, and neural progenitors prove that polyaniline cryogel has the potential to be used as a carrier for cells in tissue engineering or bio-sensing. The surface energy as well as the elasticity and porosity of cryogel mimic tissue properties. Polyaniline cryogel can therefore be applied in bio-sensing or regenerative medicine in general, and mainly in the tissue engineering of electrically excitable tissues.

It is no exaggeration to say that the impact of electricity on living subjects has been known at least since 1792, when Luigi Galvani noticed that an accidental spark discharge caused frog muscle fibres to contract. This was one of the first studies related to bioelectricity. Since that day, the knowledge on bioelectricity, which studies electrical signals from excitable tissues, has increased continuously. Today it is well known that bioelectricity plays a crucial role in a variety of cellular processes, such as cell division, cell signalling, and differentiation, as well as on the tissue level, e.g., in wound healing or angiogenesis. Knowledge of bioelectricity has led to the application of conducting materials in regenerative medicine and the tissue engineering of electrically excitable tissues, as well as in the field of bio-sensing.

Considering applications in bio-sensing, conventional materials such as platinum, gold or iridium oxide ensure good mechanical properties in sensors, e.g., hardness and shape; however, their properties are highly dissimilar to those of native tissues. This can lead to irritation, and adverse immune responses of tissues in contact with such materials. Because of this, conducting polymers (CP), such as polyaniline, polypyrrole or poly(3, 4-ethylenedioxythiophene), are considered as promising materials which can offer improved properties in comparison with conventional ones. The above-mentioned problems are very well described in the review by Jeong *et al.*[1] Moreover, it is known that the charge-transfer characteristics of the conventional metal electrodes used in bio-sensing are improved when coated with conducting polymers, which exhibit combined electronic and ionic conductivity[2–4].

The applicability of conducting polymers in tissue engineering is closely related to the preparation of corresponding 3D structures, ideally in a form combining appropriate biological as well as both mechanical and surface properties. As conducting polymers do not have the required bulk parameters, they have to be combined with other biopolymers or biomaterials[5–7]. Moreover, different routes for the preparation of 3D structures based on different types of CP can result in a broad variety of final materials which have different properties, this variability having a significant impact on biocompatibility and cell behaviour. Various preparation routes for CP-based

[1]Centre of Polymer Systems, Tomas Bata University in Zlin, 760 01, Zlin, Czech Republic. [2]Faculty of Technology, Tomas Bata University in Zlin, 760 01, Zlin, Czech Republic. [3]Institute of Experimental Biology, Faculty of Science, Masaryk University, 625 00, Brno, Czech Republic. [4]Institute of Macromolecular Chemistry, Academy of Sciences of the Czech Republic, 162 06, Prague 6, Czech Republic. Correspondence and requests for materials should be addressed to P.H. (email: humpolicek@utb.cz)

3D structures can involve, for example, conducting materials of a nanofibrous character prepared via electrospinning, which provide interconnected pores facilitating cell attachment and growth. The electrospinning of CP alone, however, is difficult because their backbones are rigid and they exhibit low solubility in solvents. Therefore, they are usually mixed with standard, thermoplastic polymers to achieve materials suitable for electrospinning[8,9]. The coating of independently prepared scaffolds by conducting polymer is another means of preparing conducting 3D structures[10,11]. All of the above-mentioned techniques, however, suffer from an inhomogeneous distribution of conducting components.

Polyaniline-based 3D cryogels are materials swollen with water, which contain a conducting polymer together with a supporting polymer as their constituents[12]. The polymerization takes place in the frozen state and the prefix "cryo" thus refers to the method of preparation; hydrogels are obtained after thawing. Polyaniline is the conducting part of hydrogels, while various water-soluble polymers can be used as the carriers providing the mechanical properties[13]. The utilization of CP-based cryogels is a novel approach affording a solution to the problem of the inhomogeneous distribution of conducting components in the bulk of common conducting hydrogels. It should be noted, however, that research into CP-based 3D materials is in its infancy, and studies dealing with their biological properties are rare despite the fact that cell responses are known to differ on planar and 3D materials.

Polyaniline is generally considered as a polymer with limited biocompatibility[14]. The term biocompatibility refers generally to the ability of a material to coexist with living organisms and tissues without harming them, and its testing can be conducted in a variety of ways. According to the prospective application of the material, defined sets of specific tests are used. As the prepared polyaniline cryogels are considered for applications in bio-sensing and tissue engineering, cytotoxicity, embryotoxicity, stem cell adhesion and growth, and the impact of CP on cardiomyogenesis and neurogenesis have been chosen in order to reveal the basic biocompatibility parameters of this novel and promising material.

Experimental Sections

The interaction of any material with cells or tissues depends on its surface and bulk properties. The surface energy, pore-size distribution, and elasticity expressed by Young moduli were determined for polyaniline cryogel. In addition, impurities leaching from polyaniline cryogel were characterized by chromatography. These characteristics, together with biological properties, provide a comprehensive view on the applicability of polyaniline cryogel in a variety of applications.

Preparation of Polyaniline cryogel. Polyaniline was prepared by the oxidation of the respective monomer with ammonium peroxydisulfate[15,16]. Aniline hydrochloride (2.59 g) was dissolved in a 5 wt.% aqueous solution of poly(vinyl alcohol) (PVAL; molecular weight 61,000; Sigma-Aldrich) to 50 mL volume, and ammonium peroxydisulfate (5.71 g) was also dissolved separately in the same solution to the same volume[12]. Both solutions were pre-cooled to 0 °C and mixed, then drawn into polyethylene syringes. The solutions were quickly frozen in a solid carbon-dioxide suspension in ethanol at −78 °C and subsequently placed in a freezer at −24 °C, and aniline was then left to polymerize for 7 days. The concentrations of reactants were 0.2 M aniline hydrochloride, 0.25 M ammonium peroxydisulfate, and 5 wt.% poly(vinyl alcohol)[12]. The originally white ice changed to dark green/black as polyaniline was produced. After thawing, the cryogels were removed[12] from the syringe and left in water for one week to remove any low-molecular-weight reactants or by-products. The cryogel was composed of ≈2 wt.% polyaniline, 5 wt.% poly(vinyl alcohol), and 93 wt.% water[12]. The cryogel thus has a composite nature where polyaniline affords the conductivity and poly(vinyl alcohol) the mechanical integrity[12].

Material Properties. *Thermal conductivity.* The thermal conductivity was measured by TCi Thermal Conductivity Analyzer (C-THERM Technologies, Ltd., Canada) with heat conductivity range 0.01–10 W m^{-1} K^{-1}, at 25 °C and instrument regime for porous materials. The cylindrical samples were prepared with diameter 1.5 cm and thickness 0.5 cm.

Surface energy. Contact angle measurements and the determination of surface energy were conducted with the aid of the Surface Energy Evaluation System (Advex Instruments, Czech Republic). For polyaniline cryogel, deionized water, ethylene glycol, and diiodomethane (Sigma-Aldrich) were used as test liquids. The droplet volume of the test liquids was set to 2 μL in all experiments, these conducted on a gently dried flat surface of polyaniline cryogel. Ten separate readings were averaged to obtain one representative contact angle. The substrate surface free energy was determined by the "acid–base" method and calculated according to procedure described in work of van Oss[17].

The acid-base theory enables the determination of the polar and dispersive contributions to the total surface free energy as well as the electron-donor and electron-acceptor components of the polar part of the surface free energy (equation 1).

$$\gamma^{TOT} = \gamma^{LW} + \gamma^{AB}, \tag{1}$$

where γ^{TOT} is the total surface energy, the superscript *LW* denotes the total dispersion Lifshitz-van der Walls interaction and *AB* refers to the acid-base interaction. According to Lewis, the acid-base interaction can be determined by equation (2).

$$\gamma^{AB} = 2\sqrt{\gamma^{+}\gamma^{-}}, \tag{2}$$

where γ^{+} is the electron-donor and γ^{-} is the electron-acceptor component of the acid-base part of the surface energy.

The surface free energy γ^{TOT} can be calculated using Young-Dupré equation (3).

$$(1 + \cos\theta_i)\gamma_i = 2\left(\sqrt{\gamma_i^{LW}\gamma_j^{LW}} + \sqrt{\gamma_i^{+}\gamma_j^{-}} + \sqrt{\gamma_i^{-}\gamma_j^{+}}\right). \quad (3)$$

Here j refers to the studied material, i the testing liquid and Θ is the measured contact angle.

Pore-size distribution. Pore size was estimated by analysis of scanning-electron micrographs of planar sections of freeze-dried polyaniline cryogel by the image analysis. The specific surface of the material was computed based on the assumption that the pores were closed; in reality, pores are partially open, and the real specific surface area is therefore slightly smaller than computed. It should be noted that the pore-size distribution in freeze-dried cryogels may differ somewhat from the pore-size distribution in native hydrogels. For calculation, method of chords recommended in ASTM E112-13 standard was employed. The system of random lines was drawn to planar section of image from which the lengths of individual chords were measured by automatic image analysis. From the mean chord length the mean pore size was subsequently estimated. For pore size estimation 10 images with magnification of 1000x were used and about 500 of chords were measured on each image.

The porosity was computed as $1-V_d/V_w$, where V_d is the volume of the polymer estimated from the mass density of the polymer and the mass of the dry sample, V_w is the total volume of the sample computed from the geometric parameters of the cylindrical sample and independently of the mass of the wet sample (difference was less than 5%).

Young modulus. Young modulus was determined on a Shimadzu Autograph AG-X tensile tester. The analyses were performed on four cylindrical samples with a length 10 mm and a diameter 9.2 mm. Each sample was inserted between two horizontal plates and deformed with a rate of 1 mm min^{-1}. Measurement time was of 3 min and within this short period of time the humidity of the sample was considered constant. The Young modulus was determined as a slope of the liner part of the stress-strain curve. The experiments were performed in compression.

Impurity profile. Concentrations of residual impurities were determined using a modular HPLC system consisting of a Waters 600E pump, a VD 040 vacuum degasser (Watrex, Czech Republic), and a UV200 ultraviolet detector (Watrex, Czech Republic). A reversed-phase C18 column X-select (300 mm × 7.8 mm; Waters) was employed. The analysis was performed in isocratic mode with an acetonitrile/acetate pH 4 buffer at a ratio of 60/40 (v/v) as the mobile phase. A flow rate of 0.8 mL min^{-1} and 20 μL injection volume were employed. Analytes were monitored at 235 nm by the UV detector. Data acquisition and analysis were performed using a Clarity Chromatography Station. For HPLC analysis, polyaniline samples were extracted in accordance with ISO 10993-12 in the ratio of 0.1 g of polyaniline cryogel per 1 mL of ultrapure water.

Biocompatibility. The study was approved by Committee on Animal Research and Ethics Faculty of Medicine Masaryk University.

Used cell lines. Primary mouse embryonic fibroblasts (MEF) were used to determine the cytotoxicity of individual extracts. They were isolated from 13.5 days post coitum (dpc) mouse embryo, mouse strain C57BL/6. Mice were obtained from the Laboratory Animal Breeding and Experimental Facility of the Faculty of Medicine, Masaryk University, Brno, Czech Republic and kept under controlled conditions; standardized diet pellets and UV light-treated tap water were available *ad libitum*. Experiments were performed in the accordance with national and international guidelines on laboratory animal care and with the approval of the Institute Ethical Committee. Embryos were washed in Phosphate Buffered Saline (PBS) and decapitated, and the inner organs removed. For the separation of fibroblasts, the embryos were trypsinized and mechanically disrupted by pipeting. A single-cell suspension was seeded onto a tissue culture dish in complete high glucose Dulbecco's modified Eagle's medium (DMEM) supplemented with 100 U mL^{-1} of penicillin, 0.1 mg mL^{-1} of streptomycin, 15% Foteal Bovine Serum (FBS) (all from Invitrogen-Gibco) and 0.05 mM 2-mercaptoethanol (Sigma-Aldrich). The first seeded MEFs were designated as passage 0. In our experiments, only MEFs up to passage 3 were employed.

The *embryonic stem cell ES R1* line[18] was propagated in an undifferentiated state by culturing on gelatinized tissue culture dishes in complete DMEM media. The gelatinization was performed using 0.1 wt% porcine gelatin in water. Dulbecco's Modified Eagle's Medium containing 15% fetal calf serum, 100 U mL^{-1} penicillin, 0.1 mg mL^{-1} streptomycin, 100 mM non-essential amino acids (all from Gibco-Invitrogen; USA), 0.05 mM 2-mercaptoethanol (Sigma Aldrich) and 1 000 U mL^{-1} of leukemia inhibitory factor (Chemicon; USA) was used for the cultivation.

Preparation of ESc R1 line-derived cardiomyocytes from the HG8 clone were described previously[19,20]. Purified cardiomyocytes were seeded onto reference tissue culture dishes and onto all tested polyaniline surfaces. DMEM:F12 (1:1) supplemented with 5% fetal calf serum, antibiotics as above, and insulin, transferrin, and selenium supplements (ITS; all from Gibco-Invitrogen) was used as the growth medium.

Neural progenitors were isolated from ganglionic eminences of embryonic brain (13.5 dpc)[19,21] and expanding in neurobasal media DMEM:F12 with B27 and N2 supplements, 100 U mL^{-1} penicillin, 0.1 mg mL^{-1} streptomycin (Gibco-Invitrogen; USA), 5 ng mL^{-1} of FGF-2 and 20 ng mL^{-1} of EGF (PeproTech; USA). Only cells up to passage 3 were used.

Cytotoxicity and embryotoxicity. The cytotoxicity testing of extracts of polyaniline cryogel was performed according to ISO 10 993-5. Samples were extracted according to ISO 10993-12 in the ratio of 0.2 g mL^{-1} of relevant cultivation medium. Extraction was performed in chemically inert closed containers using aseptic techniques at 37 ± 1 °C under stirring for 24 ± 1 h. The parent extracts (100%) were then diluted in a culture medium to obtain a series of dilutions with concentrations of 50, 25, 10, 5 and 1%. All extracts were used within 24 h. Cells were pre-cultivated for 24 h and the culture medium was subsequently replaced with polyaniline extracts. As a

γ^{tot} (mN m^{-1})	γ^{LW} (mN m^{-1})	γ^{AB} (mN m^{-1})	θ^{W} (deg)	θ^{E} (deg)	θ^{M} (deg)
47.6	20.5	27.1	1.66 (<15)	1.99 (<15)	74.2

Table 1. The surface energy of polyaniline cryogel. Total surface energy, γ^{tot}, dispersive component of surface energy, γ^{LW}, acid–base component of surface energy (polar), γ^{AB}, and contact angles, θ, determined using deionized water (W), ethylene glycol (E), and methylene iodide (M) as wetting agents.

reference giving 100% cell proliferation, cells cultivated in the pure medium were used. To assess cytotoxic effects, the MTT assay (Invitrogen Corporation, USA) was performed after one-day cell cultivation at 37 ± 0.1 °C. The absorbance was measured at 570 nm by an Infinite M200 PRO (Tecan, Switzerland). All tests were performed in quadruplicates. Dixon's Q test was used to remove outlying values. The morphology of the cells was observed using an inverted Olympus phase contrast microscope (Olympus IX81, Japan).

Polyaniline cryogel embryotoxicity was analysed as the likelihood of the formation of beating foci within spontaneous differentiating ES R1 cells carrying Nkx2.5-GFP reporter construct (NKX2-5-Emerald GFP BAC reporter), which mediated cardiomyocyte specific expression of green fluorescent protein (GFP) was used[22]. An 5-day-old EBs[20,23] derived from ES R1 cells clone NK4 were seeded onto polyaniline cryogel or tissue culture plastics coated with gelatin. After 13 days (day 18 of overall differentiation), the appearance of both GFP positive cells and beating foci was checked.

Cytocompatibility. *Adhesion and growth of stem cells*: ES R1 cells were seeded onto tissue culture plastics (reference) or onto polyaniline cryogel at a density of 4×10^4 cells per cm^2. They were uploaded by calcein AM (10 μM; Invitrogene) or after ES R1 cell growth for two days, then fixed by 2% formaldehyde and visualized through nuclei staining by 4′,6-diamidine-2′-phenylindole dihydrochloride (DAPI; 10 ng mL^{-1}, Sigma). The number of ESc was quantified by counting of viable cells (counterstained by calcein) visible on photomicrographs.

Adhesion and expansion of embryoid bodies (*EBs*): 5-day-old EBs were seeded onto tissue culture plastic (reference) or onto polyaniline cryogel. On day 20 of differentiation overall, expanding EBs were counterstained by calcein AM (10 μM, Invitrogene).

Adhesion and growth of cardiomyocytes: Purified ES-derived cardiomyocytes were seeded onto tissue culture plastics (reference) or onto polyaniline cryogel. After two days, cells were fixed by 2% formaldehyde and counterstained by antibody against cardiomyocite specific myosine heavy chain (MF20 antibody, developed by Donald and Fischman, was obtained from the Developmental Studies Hybridoma Bank developed under the auspices of the National Institute of Child Health and Human Development and maintained by the University of Iowa, Department of Biological Sciences). Anti-mouse IgG antibody conjugated to Alexa 568 fluorochrome (Invitrogen) was used as the secondary antibody. Cell nuclei were counterstained by DAPI (10 ng mL^{-1}, Sigma)[20]. When the visualization of viable cardiomyocytes was required, the ES R1 cell clone NK4 carrying Nkx2.5promotor-GFP reporter (RP11-88L12 NKX2-5-Emerald GFP BAC Reporter, from BACPAC Resources Children's Hospital and Research Center at Oakland), which is specifically expressed only in cardiomyocytes[24], was used[20]. The number of cardiomyocytes was quantified by counting of viable cells (counterstained by calcein) visible on micrographs.

Neural progenitors: Neural stem/progenitors cells (NSCs) were isolated from the embryonic ganglionic eminence (GE) of the forebrain of C57/BL6 mice at 13.5 dpc. C57BL/6 mice were obtained from the Laboratory Animal Breeding and Experimental Facility of the Faculty of Medicine, Masaryk University, Brno, Czech Republic. The mice were kept under controlled conditions; a standardized pelleted diet and HCl or UV light-treated tap water were available *ad libitum*. Experiments were performed in accordance with national and international guidelines on laboratory animal care and with the approval of the Institute's Ethical Committee conforming to the guidelines from Directive 2010/63/EU of the European Parliament on the protection of animals used for scientific purposes[21].

Three-day-old neurospheres were seeded onto tissue culture plastic with gelatin coating or onto polyaniline cryogel. Neurosphere differentiation was mediated by the withdrawal of neural supplements (B27, N2) and growth factors (EGF, FGF-2), and by supplementation with 2% bovine serum. Differentiating cells were stained by calcein AM (10 μM) or fixed by 2% formaldehyde, and F-actin was stained by phaloidin-FITC (Sigma-Aldrich). Nuclei were counterstained by DAPI (Sigma-Aldrich, 10 ng mL^{-1}). Cell pictures were taken using an Olympus digital camera (E-450) mounted onto an Olympus inverted microscope (IX51). The number of neural progenitors was quantified by counting of viable cells (counterstained by calcein) present on micrographs.

A fluorescent pictures or videos of cells were taken using an Olympus E-450 digital camera (photos) or INFINITYLite camera (videos) mounted onto an Olympus inverted epifluorescent microscope IX51.

Results and Discussion

Material Properties. Materials properties of cryogel can be classified into surface and bulk properties. While surface properties are crucial with respect to the first contact of a material with biological fluids and cells, bulk properties, such as porosity and elasticity, play a crucial role in its long-term interaction with cells and tissues. The coefficient of thermal conductivity for swollen cryogel sample was (1.3 ± 0.1) W m^{-1} K^{-1}.

Surface energy, as a basic surface characteristic of polyaniline cryogel is shown Table 1. The obtained values indicate that the surface of the cryogel is extremely hydrophilic as the only value of contact angle, which can be taken into consideration refers to the methylene iodide. The other liquids created sessile drops below the adequate level. This result is in agreement with expected data for PVAL systems. Cell adhesion is a process that is affected by the properties of the surfaces to which the cells adhere. These include a broad range of characteristics

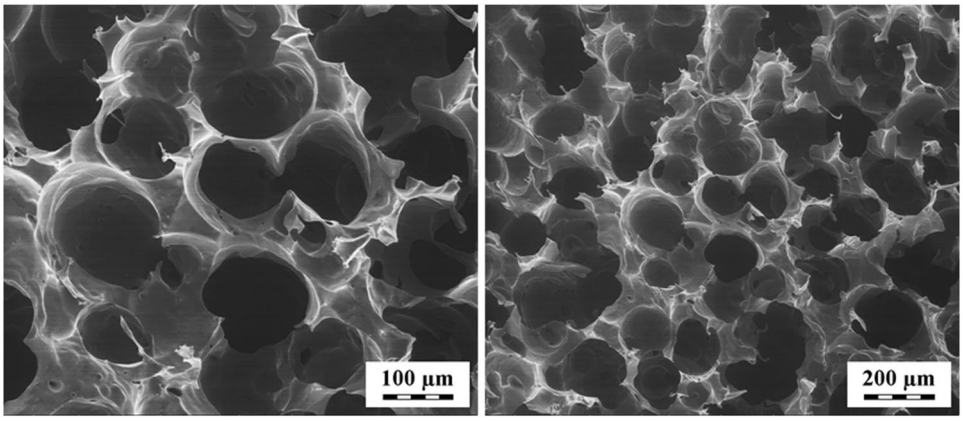

Figure 1. Scanning electron micrographs of cryogel (2 magnifications).

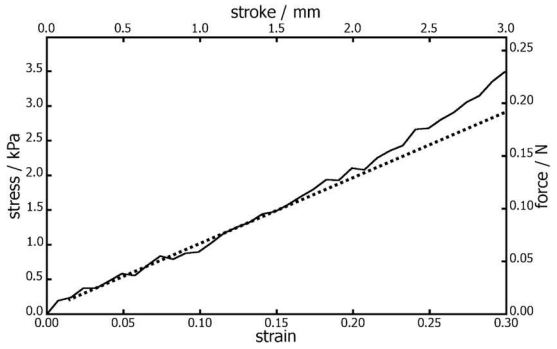

Figure 2. Stress-strain curve used for calculation of Young modulus of PVA-PANI cryogel measured under confined conditions. The experiments were performed in compression.

such as topography, porosity wettability, softness, roughness microstructure as well as presence of characteristic functional groups on the material surface[25]. Key role in the cell response plays protein adsorption, which exhibits the first step preceding attachment of cells. Thanks to their amphiphilic character, proteins can absorb on both hydrophilic and hydrophobic surfaces. On the hydrophobic surfaces they adsorb through hydrophobic patches present on their surface. In the case the surfaces are hydrophilic, they interact with the polar and charged functional groups[26]. Hence the protein composition and conformation are critical characteristics with respect to subsequent cell adhesion and influence also nature of cells to be adsorbed on the surfaces. Detailed description of mechanism of adsorption of proteins on polymers surface is beyond the scope of the current manuscript. However taking into account the published studies the hydrophilicity of the polymer is considered preferable for adsorption of the cells[27].

Porosity is a crucial factor not only influencing the ability of cells to migrate and grow within the structure but also providing biomechanical stimuli and influencing the microenvironment (e.g., with respect to the release of biofactors or efficient nutrient exchange). Moreover, porosity affects vascularization and facilitates mechanical interlocking between scaffolds and surrounding tissue[28]. As can be seen from the scanning-electron micrographs (Fig. 1), polyaniline cryogel has a highly macroporous structure. The mean pore size obtained from the image analysis of planar sections of cryogel was estimated to 159 µm and corresponding specific surface area to $0.020\,m^2\,cm^{-3}$. Pore size distribution was not computed; however, from images it can be concluded that it is quite narrow and covers sizes from tens to hundreds of microns.

The porosity of sample estimated from comparison of swollen and dry mass of cryogels reveals value of 95.5 vol%. Therefore, polyaniline cryogel meets the criteria for scaffolds.

Elasticity is the second important bulk property influencing tissue reactions to the scaffold. Metallic neural interfaces can serve as a good example as their mechanical and structural properties are highly dissimilar to those of neuronal tissue, a situation which can lead to irritation and adverse immune responses[1]. Polyaniline cryogel has properties much closer to those of native soft tissues than for example mentioned metallic devices. The mean value of Young modulus of polyaniline cryogel was determined to (9.7 ± 0.5) kPa; the example of stress-strain curve recorded on the cryogel is given in Fig. 2. With respect to obtained value of Young modulus and the fact that typical soft tissues have a Young modulus $\approx$1 MPa[29] or even lower, it can be concluded that the cryogel exhibits properties of elastic material. Moreover, the elasticity of swollen polyaniline cryogel is demonstrated in Fig. 3.

Figure 3. Polyaniline cryogel mimicking the properties of native tissue. Polyaniline is green in transparent thin films but appears black in thick layers or in powder form[16].

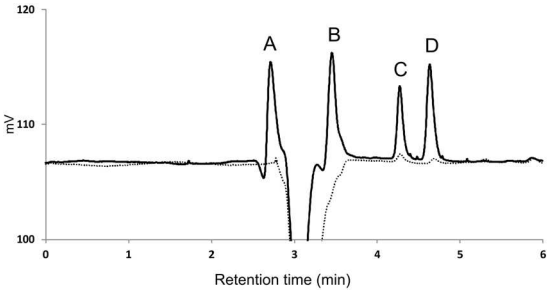

Figure 4. HPLC chromatogram of impurities detected in extracts of native (solid line) and purified (dotted line) polyaniline cryogels. Residuals of A – ammonium peroxydisulfate, B –hydroquinone, C – *p*-benzoquinone, D – aniline hydrochloride.

Impurity Profile. With respect to the preparation procedure, residual aniline hydrochloride and ammonium peroxydisulfate are the main expected impurities in polyaniline cryogel. Both of these substances are considered as potentially harmful[30,31]. Chromatographic analyses revealed that the concentrations of residual aniline hydrochloride and ammonium peroxydisulfate in native polyaniline cryogel were $12.8 \pm 0.5\,\mu g\,g^{-1}$ and $2.3 \pm 0.3\,mg\,g^{-1}$ of the cryogel, respectively. In addition to these two impurities, two other unknown peaks were observed on chromatogram. With the aid of appropriate standards and their retention times, these two peaks were identified to be oxidation products of aniline, namely hydroquinone and *p*-benzoquinone[32]. Their concentrations were of $8.4 \pm 0.3\,\mu g\,g^{-1}$ and $36 \pm 3\,mg\,g^{-1}$ of the cryogel, respectively.

Chromatogram of impurities detected in cryogel extract is presented in Fig. 4. It can be assumed that the cryogels also contain residual ammonium sulfate originating from polymer synthesis[11,15]. However, this impurity can't be detected by UV detector and, moreover it falls to a group of substances generally recognized as safe (GRAS) by U.S. Food and Drug Administration[33] and hence it is not expected to have any significant harmful effect to the cells. To reveal if the additional purification can lead to elimination of low molecular impurities the polyaniline cryogel was further purified by the repeated extraction of 5 g of cryogel with 50 mL ultrapure water for 24 h until a pH 7 of the extract was achieved. Additional purification of the sample through its extraction with ultrapure water further reduced the content of impurities leached from it. The concentrations of aniline hydrochloride and *p*-benzoquinone were lower than $1\,\mu g\,g^{-1}$ of cryogel and ammonium peroxydisulfate and hydroquinone were not detected. Additionally purified cryogel was used only for determination of impurities and cytotoxicity. All the other tests, however, were performed on native cryogel without additional purification not to bias the biocompatibility of native polyaniline cryogel.

Biocompatibility. *Cytotoxicity and embryotoxicity.* Cytotoxicity is the basic parameter of biocompatibility, which demonstrates the ability of cells to survive in the presence of foreign materials – in present case, the extracts of the tested polyaniline cryogel. It is known that polyaniline powder displays significant toxicity[14,19]. Cytotoxicity is mainly connected with the presence of low-molecular-weight impurities[34]. Cryogel contains of 2 wt.% of polyaniline in the matrix; thus its toxicity should be lower than in the case of polyaniline powders, which was confirmed in the current work.

As described above, the cytotoxicity tests on MEF were performed not only on native but also on additionally purified polyaniline cryogels. Cell viability was similar for native and purified samples, and 5, 10, 25, 50 and 75% extracts caused no cytotoxicity (cell survival was higher than 80%, compared to the reference). Only the parent 100% extracts showed mild cytotoxicity (cell survival 60 to 80%). The cytotoxicity of extracts is clearly illustrated in Fig. 5. It can be concluded that although purification leads to a decrease in the amount of low-molecular-weight impurities present in polyaniline cryogel, the impact of washing on cytotoxicity is negligible. In all the other tests,

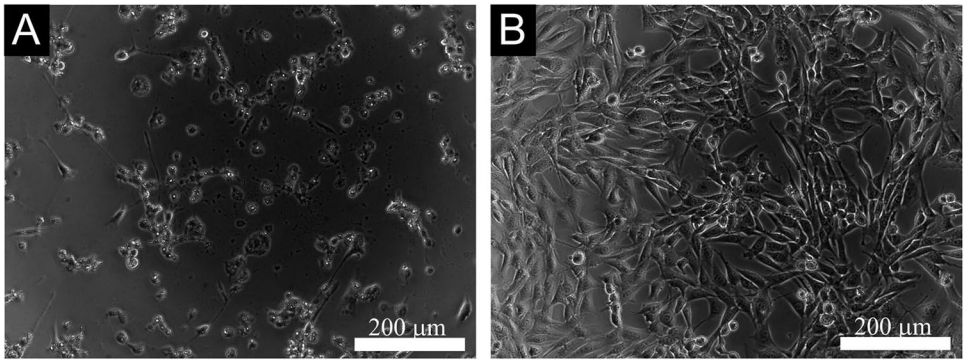

Figure 5. Cytotoxicity of extracts of native (**A**) or purified (**B**) polyaniline cryogel determined as relative number of viable MEF cells cultivated in the presence of extracts for 24 h. The dashed lines highlight the limits of viability according to EN ISO 10993-5: viability >0.8 corresponds to no cytotoxicity, >0.6–0.8 mild cytotoxicity, >0.4–0.6 moderate toxicity and <0.4 severe cytotoxicity.

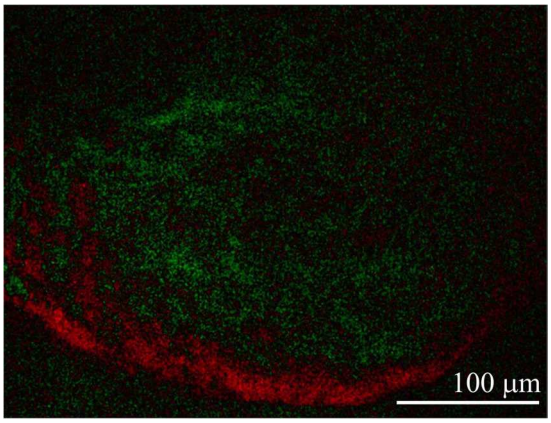

Figure 6. Beating foci within spontaneous differentiating ESc on polyaniline cryogel. The difference between microscopy images taken with a 0.3 s time shift. Red spots correspond to the movement of cells to the right. Green spots indicate no difference between the images (see the supplement for video of the beating foci). The video was taken on day 18 of differentiation overall.

the native non-purified polyaniline cryogel was used to demonstrate the properties of native polyaniline cryogel as a new material.

The appearance of beating cardiomyocytes in EB outgrowths is used as one of toxicological end-points to assess the embryotoxic potential of tested samples. In this experiment, beating foci within spontaneous differentiating ES R1 cells through formation of EBs were observed both on tissue culture plastics and on polyaniline cryogel, the foci beating in the same manner and frequency. The beating is presented in micrographs of beating foci on polyaniline cryogel (Fig. 6) and in a supplementary video. Combining the results of cytotoxicity testing on differentiated fibroblasts with visual assessment of the morphology of beating cardiomyocytes in differentiating embryonic stem cells is considered as a standard procedure for the evaluation of embryotoxicity[35]. It can therefore be concluded that polyaniline cryogels do not exhibit embryotoxicity.

Cyto-compatibility. The application of any material in regenerative medicine, tissue engineering, or biomedicine presumes that its surface will be in contact with cells. Although the adhesion of cells on surfaces *in vivo* depends on the adhesion of proteins, which can significantly alter the surface properties of the material, the adhesion of cells under *in-vitro* conditions is the technique generally accepted for evaluating the interaction between surfaces and cells. It is well known that cell types require different surface properties for their growth. Therefore, the responses of cells related to electro-sensitive tissues were tested on polyaniline cryogel. Namely, stem cells, embryoid bodies, cardiomyocytes, and neural progenitors were used.

Stem cells are generally considered for application in regenerative medicine and tissue engineering. In general, ES R1 cells were able to adhere, grow and form compact colonies on tissue culture plastics (Fig. 7A,B). A slightly different situation arose on the surface of polyaniline cryogel. Thanks to DAPI counterstaining, which visualizes the nuclei of cells (Fig. 7C,D), it can be seen that the number of stem cells on the cryogel surface was lower in comparison with the reference. This was confirmed by counterstaining with calcein which determined only viable cells (Fig. 7). On the cryogel, ES R1 cells formed more compact colonies, which was probably the result of their

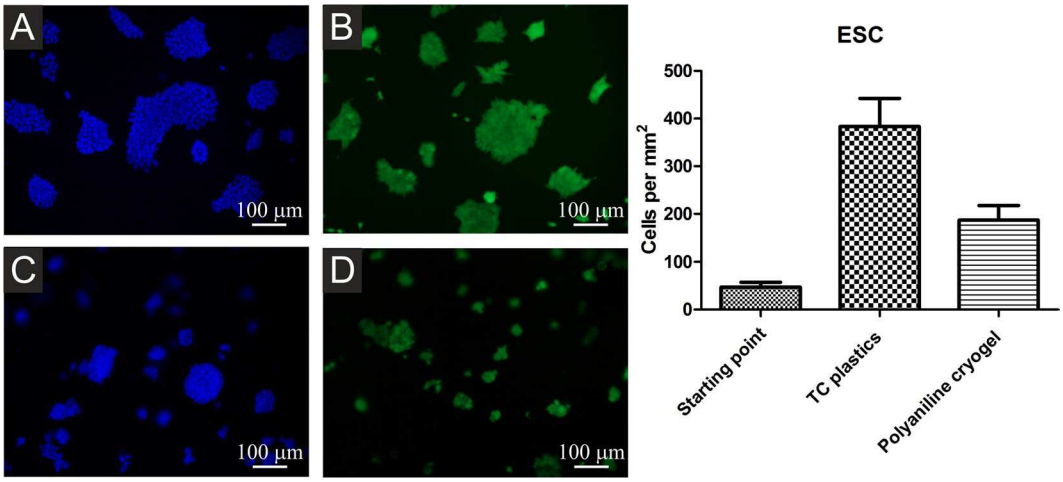

Figure 7. ESc growing on TC plastics (**A**,**B**) or polyaniline cryogel (**C**,**D**). Viable cells are visualized by calcein AM (**B**,**D**), all cells through nuclei counterstain by DAPI (**A**,**C**). Starting point is defined as a number of adherent cells 4 h hours after seeding. The ESc adhered and proliferated on the cryogel to a lesser extent than on the TC plastic. The micrographs were taken on day 2 after seeding.

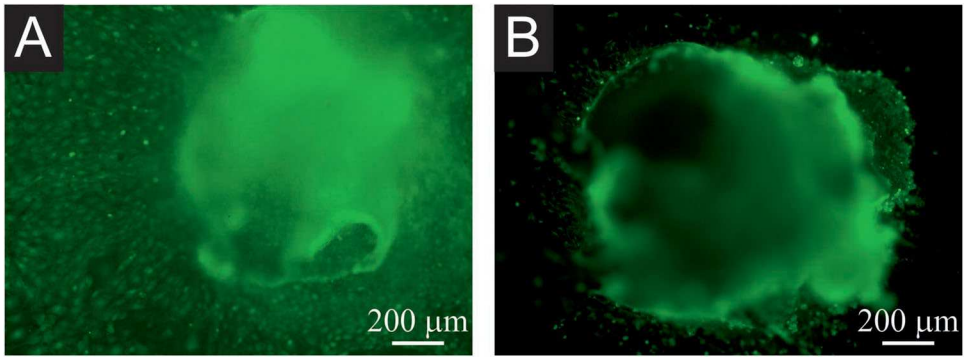

Figure 8. EB growth on TC plastics (**A**) and polyaniline cryogel (**B**). Only viable cells are visualized by calcein. The migration of cells (represented by individual spots) is weaker on polyaniline cryogel (**B**) than on TC plastic. The micrographs were taken on day 20 of differentiation overall.

lower capacity to adhere to its surface. This was also demonstrated by the presence of more compact colonies and also by the smaller number of viable cells.

A similar situation was encountered after previously formed EBs were seeded on the polyaniline cryogel (Fig. 8). After the seeding the EBs either attached on the surface or stayed floating. The number of attached and floating EBs were similar in case of TC plastic or polyaniline cryogel. The floating EBs were removed when cultivation medium was changed. From the EBs which attached to the surface, the cells can further migrate and proliferate. As can be seen from Fig. 8A,B, where only viable cells are visualised, the migration and proliferation of cells from EBs is more intense in case the EBs are attached to TC plastic than to polyaniline cryogel. This is depicted by the green spots visible outside the EBs which are present in higher quantity on TC plastic than on cryogel. EBs seeded onto polyaniline cryogel maintained their compact morphology better, and cell growth outside EB boundaries was relatively rare (Fig. 8B). Comparison of cell behaviour visualized in Fig. 8A and B indicates that polyaniline cryogel allows for the adhesion of EBs, but the migration is less intensive than on reference TC plastics.

The weakest interaction between the cryogel surface and cells was observed in the case of cardiomyocytes and neural progenitors. Cardiomyocytes seeded onto TC plastics adhered well to this surface. In contrast, they were not able to adhere to polyaniline cryogel (Fig. 9). The differences in the responses of ES R1 cells, EBs, and cardiomyocytes can be explained by the specific properties of cardiomyocytes. In comparison with the other types of cells used, cardiomyocytes were already beating when they came into the contact with the surface of the cryogel. In general, such beating can have an impact on their ability to adhere to surfaces. The behavior of EBs, however, shows that cardiomyocytes can spontaneously differentiate within the EB on the cryogel. It can therefore be expected that spontaneously differentiating cardiomyocytes will probably be able to grow on the cryogel surface.

Differentiating neural progenitors were seeded onto TC plastics or polyaniline cryogel and visualized using phalloidin-FITC (binding to F-actin), or by calcein AM (determined viable cells). The micrographs show that neural progenitors formed compact colonies of well-spread cells on tissue plastic both with and without gelatin

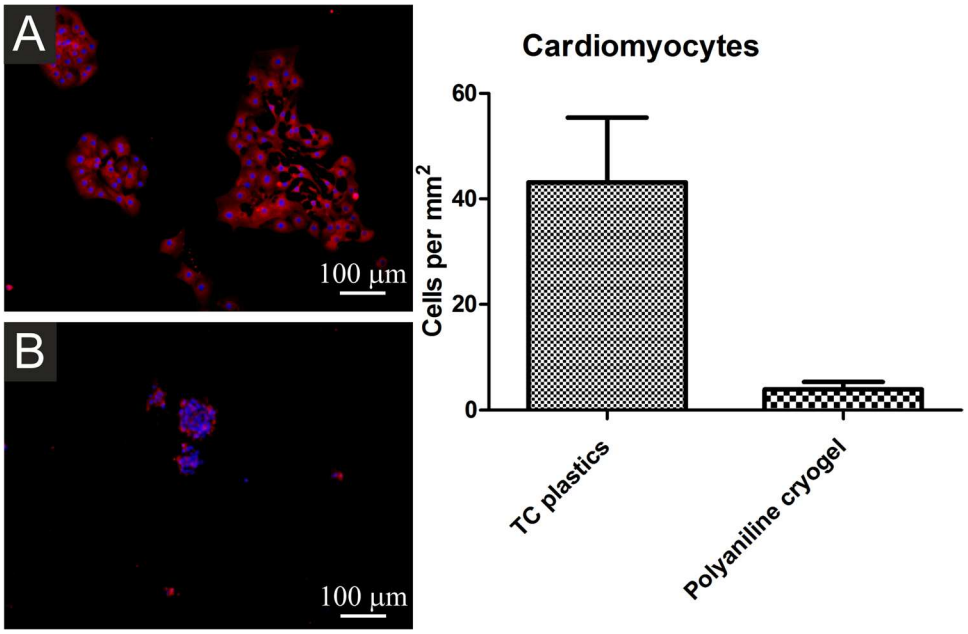

Figure 9. Isolated cardiomyocytes seeded onto TC plastics (**A**) and polyaniline cryogel (**B**). Cardiomyocytes were visualised using antibody against cardiomyocyte-specific myosine heavy chain (red). Individual cells were visualised through nuclei counterstaining by DAPI (blue). Number of cells at the starting point is not presented as the cardiomyocytes did not proliferate after the seeding. The number of cardiomyocytes adhered on the cryogel was significantly smaller than on TC plastic. The micrographs were taken on day 2 after seeding.

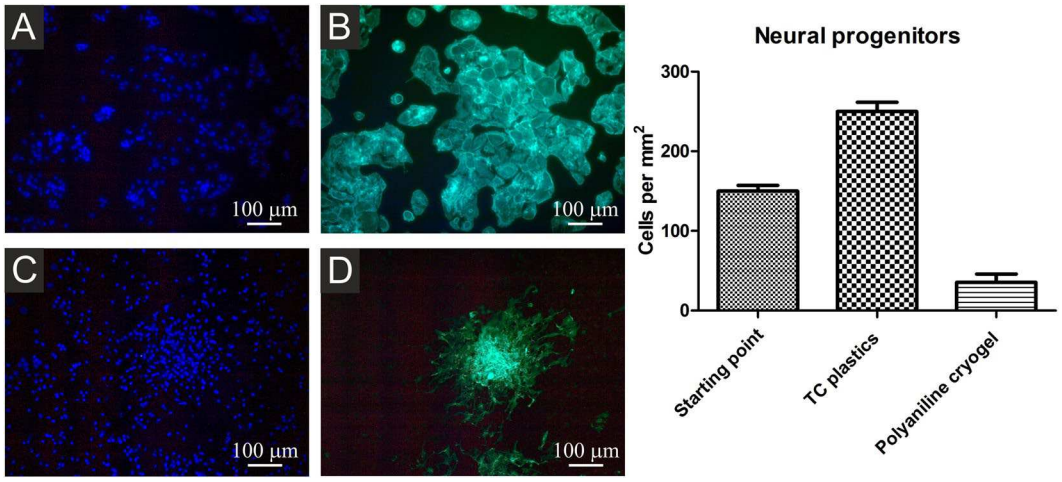

Figure 10. Neural progenitors differentiating on TC plastics (**A**,**B**) and on polyaniline cryogel (**C**,**D**). Cells were visualized by F-actin detection using DAPI (**A**,**C**). Cell nuclei were counterstained by phalloidin FITC (**B**,**D**). Starting point is defined as number of adherent cells 12 h hours after seeding. The number of adhered neural progenitors on the cryogel was significantly lower than on TC plastic, thus also the proliferation of neural progenitors on the polyaniline cryogel is low. The micrographs were taken on day 4 of differentiation overall.

coating (Fig. 10A,B). When seeded onto polyaniline cryogel, rare colonies of poorly-spread cells were observed (Fig. 10C,D). Corresponding results were also observed for cells stained with calcein AM, which visualizes only viable cells (not shown).

Any polymer intended for application in regenerative medicine or biosensors must fulfil a number of criteria including good biocompatibility, the presence of appropriate bulk and surface properties and, in particular cases, also the presence of more specific properties, such as conductivity. Some of these properties can be achieved through the use of conducting polymers; however, such polymers do not possess appropriate bulk properties as they can only be prepared in the form of thin films (in case of polyaniline 40–400 nm thick)[36], powders, and colloidal dispersions, which all have only limited application potential. Due to these shortcomings, it is advantageous to combine conducting polymers with other polymer biomaterials. The efficacy of this strategy has recently

been confirmed by a number of research studies[9,37–40]. Here, the bulk properties of the studied polyaniline cryogel correspond to those of hydrogels and are ideal for contact with soft tissues. One of the advantages of using polyaniline is the ability to modify its surface properties by a variety of simple methods including reprotonation with various acids, the grafting of functional groups, and copolymerization with various co-monomers, etc. It is also well known that any type of cell requires specific surface properties, as was unambiguously confirmed by the different behaviours of PC12 cells on polyaniline-grafted with bioactive peptides[41]. The limited ability of ESc, EBs, cardiomyocytes, and neural progenitors to adhere, grow and proliferate on polyaniline cryogel corresponds to previously published findings[41] and confirms that polyaniline-based materials require post-preparation surface modification, which is tailored to the specific cells used in order to improve such materials' cyto-compatibility.

Polyaniline cryogel is a new form of biomaterial. The purpose of present study is therefore to describe basic biological properties of its native form. In context of future studies, the cytotoxicity and embryotoxicity of native polyaniline cryogel is more important than surface properties influencing the cell adhesion, proliferation and migration, as surface properties can be easily modified by various techniques to achieve the desired interaction with concrete cell lines. Polyaniline cryogels combine poly(vinyl alcohol) and conducting polyaniline. To determine the cytotoxicity of polyaniline, it is best to study polyaniline powder, as it has the highest content of potentially hazardous components compared to thin films or colloidal dispersions. A previously published study dealing with the biocompatibility of standard powder polyaniline hydrochloride prepared by the IUPAC-approved procedure[15,16] through the oxidative polymerization of aniline hydrochloride with ammonium persulfate indicated that cytotoxicity can be related to low-molecular-weight compounds accompanying the polymer[14]. A reduction in cytotoxicity was observed after purification procedures aimed at the removal of impurities found in pristine powder polymer. Whether such procedures involved reprotonation/deprotonation[14], reprecipitation[42] or Soxhlet extraction[34], all such purification methods pointed to residual monomers or low-molecular-weight by-products as being responsible for cytotoxicity. In standard polyaniline powder, impurities related to residual precursors used for polymerization, i.e. aniline hydrochloride and ammonium peroxydisulfate, were determined in the respective extracts. HPLC analyses showed that polyaniline hydrochloride polymer leached out residual aniline hydrochloride and ammonium peroxydisulfate in concentrations of $0.95 \pm 0.03\,mg\,g^{-1}$ and $96.1 \pm 1.9\,mg\,g^{-1}$ of polymer powder, respectively. The sample exhibited cytotoxicity against two different cell lines, human immortalized non-tumorogenic keratinocyte cell line (HaCaT) and human hepatocellular carcinoma cell line (HepG2). In both cases, the cytotoxicity was dependent on the concentration of impurities in the extract and the type of cells to which the extract was applied. When graded according to the requirements of EN ISO 10993-5, the cytotoxicity of parent 100% extract of polymer was assigned as severe for HaCaT cells (a survival rate lower than or equal to 40%) and moderate for HepG2 (a survival rate of 40–60%). After the parent extract was diluted, the first entirely non-cytotoxic concentration appeared in the case of 1% extract, with cell survival higher than 80% for both cell lines. Interestingly, the impurity profile of polyaniline gel was completely different compared to standard polyaniline powder.

The fact that polyaniline cryogel does not express significant cytotoxicity or embryotoxicity, that various cell types are able to adhere and grow on its surface, and that it can undergo simple surface modification in order to improve its biointerfacial cytocompatibility opens the door to its potential application in regenerative medicine and biosensing.

Concluding remark. Electrical conductivity, based on the presence of conducting polymer, is an important parameter of cryogels. Though not reported or discussed in the present study, preliminary results suggest that the conductivity of native polyaniline/poly(vinyl alcohol) cryogel swollen with water is of the order of $10^{-3}\,S\,cm^{-1}$ [12]. In the solutions of electrolytes, especially of acids, such conductivity will be higher due to the contribution of ionic charge-transport. In contrast, polyaniline becomes non-conducting under alkaline conditions when the salt converts to a base, and the contribution of electronic conductivity becomes negligible.

Conclusions

Polyaniline cryogels supported by poly(vinyl alcohol) are novel macroporous soft conducting materials. They not only have good mechanical integrity represented by Young modulus of 9.7 ± 0.5 kPa but they are also macroporous and highly hydrophilic. All these properties are prerequisites for any application in tissue engineering or biosensing. On the basis of the results of cytotoxicity testing and stem cell differentiation, it can be concluded that polyaniline cryogel also has appropriate biological properties and is therefore suitable for application in tissue engineering and biomedicine in general, where the electrical monitoring or stimulation of tissue is required.

References

1. Jeong, J. *et al*. Soft materials in neuroengineering for hard problems in neuroscience. *Neuron* **86**, 175–186 (2015).
2. Cui, X. *et al*. Surface modification of neural recording electrodes with conducting polymer/biomolecule blends. *J. Biomed. Mater. Res.* **56**, 261–272 (2001).
3. Cui, X. & Martin, D. Fuzzy gold electrodes for lowering impedance and improving adhesion with electrodeposited conducting polymer films. *Sens. Actuators A-Phys.* **103**, 384–394 (2003).
4. Abidian, M. R., Corey, J. M., Kipke, D. R. & Martin, D. C. Conducting-polymer nanotubes improve electrical properties, mechanical adhesion, neural attachment, and neurite outgrowth of neural electrodes. *Small* **6**, 421–429 (2010).
5. Petrov, P., Mokreva, P., Kostov, I., Uzunova, V. & Tzoneva, R. Novel electrically conducting 2-hydroxyethylcellulose/polyaniline nanocomposite cryogels: Synthesis and application in tissue engineering. *Carbohydr. Polym.* **140**, 349–355 (2016).
6. Sirivisoot, S., Pareta, R. & Harrison, B. S. Protocol and cell responses in three-dimensional conductive collagen gel scaffolds with conductive polymer nanofibres for tissue regeneration. *Interface Focus* **4**, 20130050 (2014).
7. Vishnoi, T. & Kumar, A. Conducting cryogel scaffold as a potential biomaterial for cell stimulation and proliferation. *J. Mater. Sci. Mater. Med.* **24**, 447–459 (2013).
8. Subramanian, A., Krishnan, U. M. & Sethuraman, S. Axially aligned electrically conducting biodegradable nanofibers for neural regeneration. *J. Mater. Sci. Mater. Med* **23**, 1797–1809 (2012).

9. Prabhakaran, M. P., Ghasemi-Mobarakeh, L., Jin, G. & Ramakrishna, S. Electrospun conducting polymer nanofibers and electrical stimulation of nerve stem cells. *J. Biosci. Bioeng.* **112**, 501–507 (2011).
10. Gelmi, A. *et al*. Direct mechanical stimulation of stem cells: a beating electromechanically active scaffold for cardiac tissue engineering. *Adv. Healthc. Mater.* **5**, 1471–1480 (2016).
11. Stejskal, J. Conducting polymer hydrogels. *Chem. Pap.* **71**, 269–291 (2017).
12. Stejskal, J. *et al*. Polyaniline cryogels supported with poly(vinyl alcohol): soft and conducting. *Macromolecules* **50**, 972–978 (2017).
13. Guiseppi-Elie, A. Electroconductive hydrogels: synthesis, characterization and biomedical applications. *Biomaterials* **31**, 2701–2716 (2010).
14. Humpolíček, P., Kašpárková, V., Sáha, P. & Stejskal, J. Biocompatibility of polyaniline. *Synth. Met.* **162**, 722–727 (2012).
15. Stejskal, J. & Gilbert, R. G. Polyaniline. Preparation of a conducting polymer (IUPAC technical report). *Pure Appl. Chem.* **74**, 857–867 (2002).
16. Stejskal, J. & Sapurina, I. Polyaniline: Thin films and colloidal dispersions - (IUPAC technical report). *Pure Appl. Chem.* **77**, 815–826 (2005).
17. van Oss, C. J. Hydrophobicity of biosurfaces — Origin, quantitative determination and interaction energies. *Colloids Surf. B: Biointerfaces* **5**, 91–110 (1995).
18. Nagy, A., Rossant, J., Nagy, R., Abramow-Newerly, W. & Roder, J. C. Derivation of completely cell culture-derived mice from early-passage embryonic stem cells. *Proc. Natl. Acad. Sci. USA* **90**, 8424–8428 (1993).
19. Humpolíček, P. *et al*. Stem cell differentiation on conducting polyaniline. *RSC Adv.* **5**, 68796–68805 (2015).
20. Radaszkiewicz, K. A. *et al*. Simple non-invasive analysis of embryonic stem cell-derived cardiomyocytes beating *in vitro*. *Rev. Sci. Instrum.* **87**, 024301 (2016).
21. Bartova, E. *et al*. The level and distribution pattern of HP1 beta in the embryonic brain correspond to those of H3K9me1/me2 but not of H3K9me3. *Histochem. Cell Biol.* **145**, 447–461 (2016).
22. Hsiao, E. C. *et al*. Marking embryonic stem cells with a 2A self-cleaving peptide: A NKX2-5 emerald GFP BAC reporter. *Plos One* **3**, e2532 (2008).
23. Vesela, I., Kotasova, H., Jankovska, S., Prochazkova, J. & Pachernik, J. Leukaemia inhibitory factor inhibits cardiomyogenesis of mouse embryonic stem cells via STAT3 activation. *Folia Biol. (Praha)* **56**, 165–172 (2010).
24. Sepulveda, J. *et al*. GATA-4 and Nkx-2.5 coactivate Nkx-2 DNA binding targets: Role for regulating early cardiac gene expression. *Mol. Cell. Biol.* **18**, 3405–3415 (1998).
25. Engler, A. J., Sen, S., Sweeney, H. L. & Discher, D. E. Matrix elasticity directs stem cell lineage specification. *Cell* **126**, 677–689 (2006).
26. Patel, A. J. *et al*. Sitting at the edge: How biomolecules use hydrophobicity to tune their interactions and function. *J. Phys. Chem. B* **116**, 2498–2503 (2012).
27. Latour, R. A. Biomaterials: protein-surface interactions. *Encyclopedia of biomaterials and biomedical engineering* **1**, 270–278 (2005).
28. Loh, Q. L. & Choong, C. Three-dimensional scaffolds for tissue engineering applications: role of porosity and pore size. *Tissue Eng. Part B-Rev.* **19**, 485–502 (2013).
29. Akhtar, R., Sherratt, M. J., Cruickshank, J. K. & Derby, B. Characterizing the elastic properties of tissues. *Mater. Today* **14**, 96–105 (2011).
30. Jenkins, F. P., Robinson, J. A., Gellatly, J. B. & Salmond, G. W. The no-effect dose of aniline in human subjects and a comparison of aniline toxicity in man and the rat. *Food Cosmet. Toxicol* **10**, 671–679 (1972).
31. Signorin, J., Ulrich, C., Butt, M. & D'Amato, E. 13-Week inhalation toxicity study (including 6-and 13-week recovery periods) with ammonium persulfate dust in Albino rats. *Inhal. Toxicol.* **13**, 1033–1045 (2001).
32. Stejskal, J. & Trchová, M. Aniline oligomers versus polyaniline. *Polym. Int.* **61**, 240–251 (2012).
33. GRAS 2011. Select Committee on GRAS Substances (SCOGS) Opinion: Ammonium sulfate". U.S. Food and Drug Administration. August 16, 2011).
34. Kašpárková, V. *et al*. Conductivity, impurity profile, and cytotoxicity of solvent-extracted polyaniline. *Polym. Adv. Technol.* **27**, 156–161 (2016).
35. Seiler, A. E. M. & Spielmann, H. The validated embryonic stem cell test to predict embryotoxicity *in vitro*. *Nature Protocols* **6**, 961–978 (2011).
36. Stejskal, J., Sapurina, I., Prokeš, J. & Zemek, J. *In-situ* polymerized polyaniline films. *Synth. Met.* **105**, 195–202 (1999).
37. Kim, H., Hobbs, H. L., Wang, L., Rutten, M. J. & Wamser, C. C. Biocompatible composites of polyaniline nanofibers and collagen. *Synth. Met.* **159**, 1313–1318 (2009).
38. McKeon, K. D., Lewis, A. & Freeman, J. W. Electrospun poly(D,L-lactide) and polyaniline scaffold characterization. *J. Appl. Polym. Sci.* **115**, 1566–1572 (2010).
39. Rahman, N. A. *et al*. Functional polyaniline nanofibre mats for human adipose-derived stem cell proliferation and adhesion. *Mater. Chem. Phys.* **138**, 333–341 (2013).
40. Li, L., Ge, J., Guo, B. & Ma, P. X. *In situ* forming biodegradable electroactive hydrogels. *Polym. Chem.* **5**, 2880–2890 (2014).
41. Bidez, P. R. *et al*. Polyaniline, an electroactive polymer, supports adhesion and proliferation of cardiac myoblasts. *J. Biomater. Sci. Polym. Ed.* **17**, 199–212 (2006).
42. Stejskal, J. *et al*. Purification of a conducting polymer, polyaniline, for biomedical applications. *Synth. Met.* **195**, 286–293 (2014).

Acknowledgements

This work was supported by the Czech Science Foundation (17-05095S), and by the Ministry of Education, Youth and Sports of the Czech Republic – Program NPU I (LO1504). The European Regional Development Fund (Grant CZ.1.05/2.1.00/19.0409) is thanked for thermal conductivity analyser (C-term technologies, model TCi).

Author Contributions

P.H. was the author and has designed the tests. K.A.R. and J.P. were testing biocompatibility using embryonic stem cells, embryoid bodies, cardiomyocytes, and neural progenitors. Z.C. and P.R. were determined the cytotoxicity of primary mouse embryonic fibroblasts. P.B. and J.S. developed and prepared the cryogels. V.K. evaluated the impurity profile. M.L. and P.P. have assessed the materials properties.

Additional Information

Supplementary information accompanies this paper at https://doi.org/10.1038/s41598-017-18290-1.

Competing Interests: The authors declare that they have no competing interests.

Publisher's note: Springer Nature remains neutral with regard to jurisdictional claims in published maps and institutional affiliations.

Article XIV.

Bober, P.; **Capakova, Z.**; Acharya, U.; Zasonska, B. A.; Humpolicek, P.; Hodan, J.; Hromadkova, J.; Stejskal, J. Highly Conducting and Biocompatible Polypyrrole/Poly(Vinyl Alcohol) Cryogels. Synth. Met. 2019, 252, 122–126. https://doi.org/10.1016/j.synthmet.2019.04.015.

Synthetic Metals 252 (2019) 122–126

Contents lists available at ScienceDirect

Synthetic Metals

journal homepage: www.elsevier.com/locate/synmet

Highly conducting and biocompatible polypyrrole/poly(vinyl alcohol) cryogels

Patrycja Bober[a,*], Zdenka Capáková[b], Udit Acharya[a,c], Beata A. Zasońska[a], Petr Humpolíček[b], Jiří Hodan[a], Jiřina Hromádková[a], Jaroslav Stejskal[a]

[a] Institute of Macromolecular Chemistry, Academy of Sciences of the Czech Republic, 162 06 Prague 6, Czech Republic
[b] Centre of Polymer Systems, Tomas Bata University in Zlin, 760 01 Zlin, Czech Republic
[c] Faculty of Mathematics and Physics, Charles University, 121 16 Prague 2, Czech Republic

ARTICLE INFO

Keywords:
Polypyrrole
Cryogel
Conductivity
Biocompatibility
Mechanical properties

ABSTRACT

Conducting macroporous soft cryogels were prepared by the oxidation of pyrrole within the frozen aqueous solutions of 5–8 wt.% poly(vinyl alcohol) at −24 °C. Mechanical properties of cryogels were independent of poly (vinyl alcohol) concentration, Young moduli were ≈20 kPa. The conductivity of compressed freeze-dried composites reached 18 S cm^{-1} thus exceeding the conductivity of polypyrrole alone. This level of conductivity was also preserved after long-term treatment with water, *i.e.* close to physiological conditions. *In-vitro* determined cytotoxicity demonstrated high potential applications due to low cytotoxicity. Moreover, compared to the steel based materials, the cryogels mimic the properties of soft tissues. All these properties are a prerequisite for the utilization in biomedical applications.

1. Introduction

Polypyrrole (PPy) is a conducting polymer which possesses unique chemical and physical properties, such as high electrical conductivity, redox properties, environmental stability, ease of preparation and biocompatibility [1–3]. These particular properties enable PPy to be used in widely differing applications, such as in supercapacitors [4–6], batteries [7,8], sensors [9–11], as adsorbents [12,13], electroactive separation membranes [14], anti-corrosion coatings [15,16], and others. In recent years, however, PPy has attracted great attention as a functional material in biological and biomedical applications, including cardiac and neural-tissue engineering [17–19], drug delivery [20,19], and biosensors [21,22]. Due to its poor processability, owing to the insolubility and infusibility, the use in practical applications is limited and various composite forms have been sought to overcome this problem [4,5,7,12,23], *viz.* colloids [24,25] and hydrogels [18,26].

The last form, conducting hydrogels, became the most prospective material in biomedicine due to their soft texture, biocompatibility, mixed electron and proton conductivity and good mechanical properties [27]. Conducting polymer hydrogels can be obtained in two basic ways [26]: (1) by the preparation of conducting polymer within hydrogel matrix [10,17], or (2) by the preparation of hydrogels in the presence of a conducting polymer [28]. The former approach dominates in the literature. The resulting hydrogels, however, suffer usually from uneven distribution of conducting polymer phase.

New class of conducting polyaniline materials, cryogels, have recently been developed [29–33]. Unlike the current approaches, the conducting polymer and supporting hydrogel phase have been produced in a single step. The polymerization of aniline was conducted in the presence of water-soluble polymer, poly(vinyl alcohol) (PVAL), in a frozen reaction mixture and cryogels were obtained after thawing [29]. Composite polyaniline/PVAL cryogels are three-dimensional, macroporous, conducting polymeric networks combining electrical properties of polyaniline with mechanical properties of PVAL-based cryogels. The term "cryogel" refers to the way of preparation [34]; a "hydrogel" is the final product.

In the present work, the facile, one-step procedure of the preparation of multifunctional macroporous conducting hydrogel was extended to polypyrrole/poly(vinyl alcohol) (PPy/PVAL) (Fig. 1). The resulting composite cryogels are macroscopically homogeneous and possess high electrical conductivity, which is preserved even upon deprotonation in water under physiological conditions. In addition, their biocompatibility has been investigated with the promising result.

* Corresponding author.
E-mail address: bober@imc.cas.cz (P. Bober).

https://doi.org/10.1016/j.synthmet.2019.04.015
Received 6 March 2019; Received in revised form 12 April 2019; Accepted 13 April 2019
Available online 23 April 2019
0379-6779/

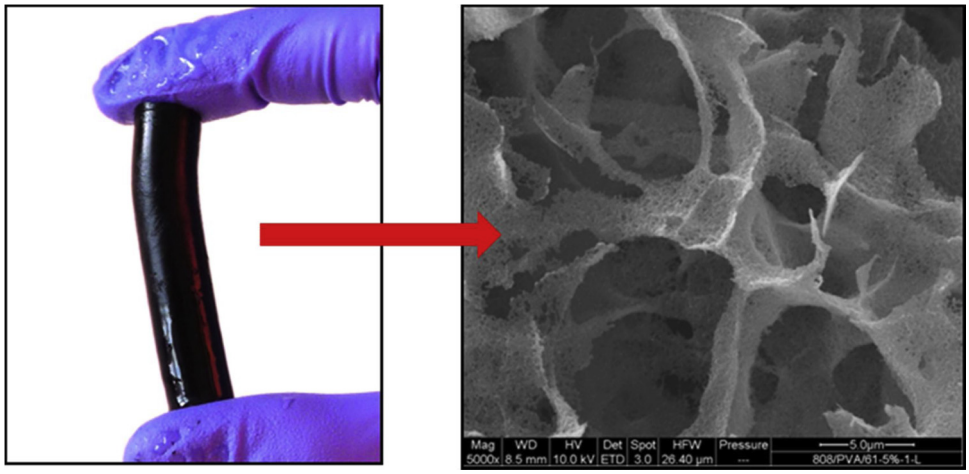

Fig. 1. Composite polypyrrole/poly(vinyl alcohol) cryogel prepared with 5 wt% of poly(vinyl alcohol) (left) and illustration of macroporous morphology of corresponding aerogel (right).

2. Experimental

2.1. Preparation

Polypyrrole/poly(vinyl alcohol) cryogels were prepared by the oxidation of pyrrole (0.2 M; Sigma-Aldrich) with iron(III) chloride hexahydrate (0.5 M; Sigma-Aldrich) in the presence of various concentrations, 5–8 wt%, of poly(vinyl alcohol) (Mowiol® 10–98, molecular weight 61,000; Sigma-Aldrich) in water. The fresh mixture of pyrrole and oxidant in poly(vinyl alcohol) solutions was quickly sucked into a plastic syringe, frozen in solid carbon dioxide/ethanol suspension at −78 °C, and then left in a freezer at −24 °C for 7 days to allow pyrrole to polymerize. After thawing at room temperature, cryogels were removed from syringe and immersed in excess of water or 0.2 M hydrochloric acid to extract any residual reactants and by-products. The corresponding PPy/PVAL aerogel was obtained by freeze-drying of cryogels.

2.2. Characterization

Morphology of freeze-dried PPy/PVAL cryogels was studied by scanning electron microscope (SEM) Vega Plus TS 5135. Static mechanical properties of hydrogels were analyzed on electromechanical testing device Instron 6025/5800R equipped with a 10 N load cell at room temperature and with a cross-head speed of 10 mm min^{-1}. Cylindrical specimens with diameter 3 mm and length 60 mm were employed in the environment of deionized water. At least 3 measurements had been performed and the results were averaged.

DC electrical conductivity was obtained by a van der Pauw method on dried cryogels compressed to pellets (diameter 13 mm, thickness ≈1 mm) at 530 MPa using a hydraulic press Trystom H-62. A Keithley 230 Programmable Voltage Source in serial connection with a Keithley 196 System DMM served as a current source, the potential difference between the potential probes was measured with a Keithley 617 Programmable Electrometer. The conductivity was obtained as an average value from the measurements in two perpendicular directions at room temperature 23 °C and relative humidity 35 ± 5%.

The specific surface area of the samples was determined by Brunauer-Emmett-Teller (BET) method using a Gemini VII 2390 (Micromiretics, Instruments Corp, Norcross, USA) with nitrogen as the sorbate. The samples were vacuum-dried at 130 °C for 50 h.

The cytotoxicity was assessed by the procedure reported earlier [3,30]. In brief, the Mouse embryonic fibroblast cell line (ATCC CRL-1658 NIH/3T3, USA) was used for testing according to the ISO 10-993-5 and 10-993-12 standards. The cell viability was determined using colorimetric MTT assay. MTT cell-proliferation assay is a colorimetric reaction based on the reduction of a tetrazolium component (MTT; 3-[4,5-dimethylthiazole-2-yl]-2,5-diphenyltetrazolium bromide) into an insoluble formazan product by the mitochondria of viable cells.

3. Results and discussion

3.1. Cryogel characterization

Polypyrrole is usually prepared by the polymerization of pyrrole with iron(III) chloride [10,35,36]. When the same polymerization is carried out in aqueous medium in the presence of PVAL in the frozen state, *i.e.* in ice, black PPy/PVAL cryogels are obtained (Fig. 1). Elemental analysis of freeze-dried cryogel revealed that they contain from 41 to 49 wt.% of PPy for various amount of PVAL used for their synthesis. Scanning electron microscopy images revealed that cryogels have an interconnected, uniform, three-dimensional macroporous network with macropore diameters from 5 to 100 µm (Fig. 2). It can be observed that pore size does not depend on the concentration of PVAL used for the preparation of cryogels. Similar pore size was observed previously when the same preparation technique was applied to polyaniline/poly(vinyl alcohol) cryogels [29]. This confirmed the hypothesis that pore size in cryogels is given by the size of ice crystals formed during the freezing of the polymerization mixture [29]. The pore walls are microporous and seem to be composed of globules of PPy incorporated in ultra-thin layer of PVAL matrix (Fig. 1). However, the specific surface area of PPy/PVAL cryogel is rather low, from 0.45 to 14 m^2g^{-1} (Table 1) and only slightly changes with amount of PVAL.

Various concentrations of poly(vinyl alcohol) do not have influence on the stiffness of the PPy/PVAL cryogel (Table 1), so the mechanical properties are controlled by PPy phase. Despite a low Young modulus, ≈20 kPa, these soft and macroporous cryogels are easy to handle and manipulate (Fig. 1).

The conductivity of PPy/PVAL cryogel was analyzed on pressed pellets from freeze-dried material before and after deprotonation with water (Table 1). The conductivity of protonated composite cryogel is ≈18 S cm^{-1}, which is higher than neat PPy prepared by oxidation of pyrrole with iron(III) chloride (units S cm^{-1}) [37]. This is explained by different PPy chain organization in various morphologies [38]. Similar polymerization of aniline in the presence of PVAL in frozen state, however, led to polyaniline/PVAL cryogel with conductivity much lower than that of corresponding polyaniline [29]. When the composite materials of PPy with non-conducting component are prepared, the conductivity is usually expected to decrease by a few orders of magnitude (Table 2). The fact that their conductivity maintained at the

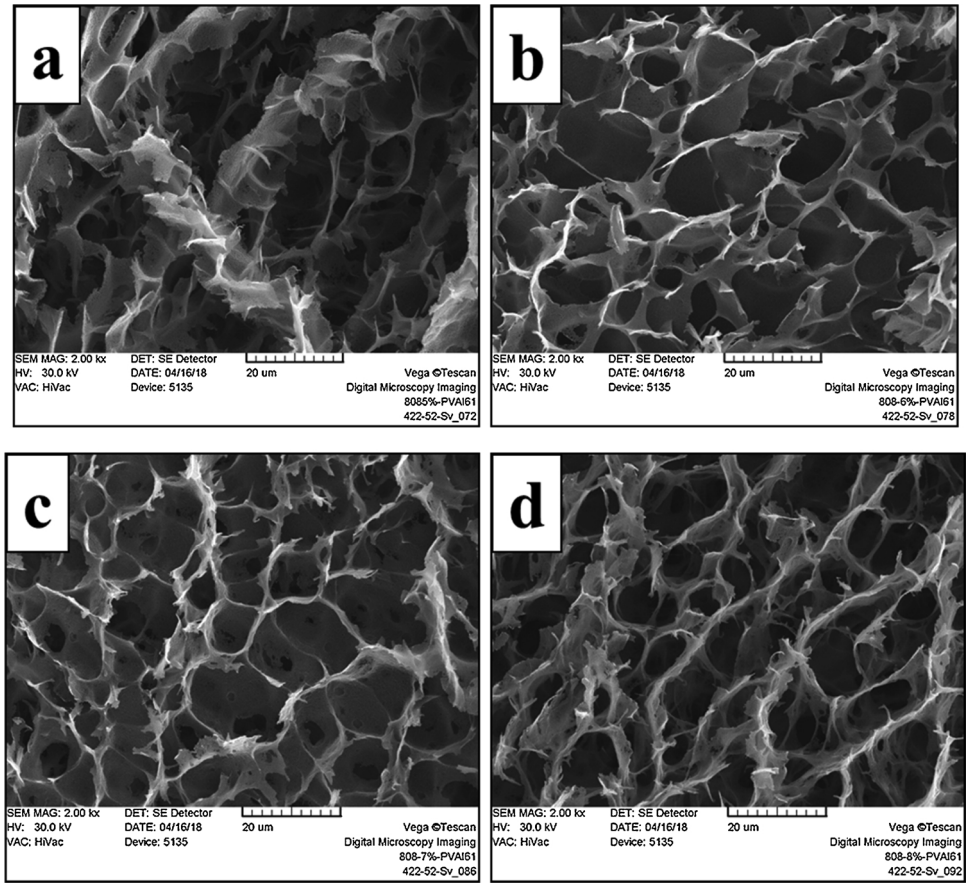

Fig. 2. Scanning electron micrographs of freeze-dried polypyrrole/poly(vinyl alcohol) cryogels prepared in the presence of (a) 5, (b) 6, (c) 7 and (d) 8 wt% of poly (vinyl alcohol).

Table 1
Mechanical properties of polypyrrole/poly(vinyl alcohol) cryogels, and conductivity and surface area of corresponding freeze-dried material.

Poly(vinyl alcohol) concentration, wt%	Young modulus (kPa)	Tensile strength (kPa)	Tensile strain at break (%)	Conductivity (cryogels washed with acid) (S cm^{-1})	Conductivity (cryogels washed with water) (S cm^{-1})	BET surface area (m^2g^{-1})
5	18.8 ± 3.0	1.5 ± 0.1	9.3 ± 0.1	14.8	6.1	0.45
6	22.1 ± 0.9	2.0 ± 0.2	9.9 ± 0.2	18.4	6.8	14.1
7	22.8 ± 2.8	2.4 ± 0.5	13.0 ± 0.5	12.9	7.1	11.1
8	16.2 ± 2.1	2.4 ± 0.4	15.0 ± 0.4	8.2	7.4	3.4

Table 2
Conductivity, σ, and biological properties or intended application of polypyrrole and its composite hydrogels and cryogels.

Polypyrrole/hydrogel support	σ (S cm^{-1})	Biological properties	Ref.
Globular polypyrrole reference	0.3	–	[37]
Alginate	1×10^{-4}	*In vitro* – supported human mesenchymal stem cells attachment and proliferation	[17]
Poly(amino ester)	6×10^{-4}	*In vivo* – efficiently promoted the cardiac function and enhanced the conduction of electrophysiological signal and revascularization of the infarct myocardium	[18]
Chitosan/polyacrylic acid/magnetite	1.9×10^{-4}	–	[40]
Sodium alginate/carboxymethylchitosan	8×10^{-3}	*In vitro* – rat adrenal pheochromocytoma cells (PC12), Schwann cell lines (RSC96) and bone marrow mesenchymal stem cells exhibited good adhesion and proliferation *In vivo* – without inflammatory reaction after 5 weeks and can be support for peripheral nerve regeneration	[41]
Polyacrylamide (cryogel)	1.5×10^{-4}	–	[42]
	–	*In vitro* – Human hepatoma derived cell line (HepG2) and rat glial cells (C6) indicated good biocompatibility	[43]
Poly(acrylic acid) (cryogel)	3.5×10^{-4}	–	[42]
Poly(4-vinylpyridine) (cryogel)	2.5×10^{-4}	–	[42]
Chitosan	–	*In vitro* – neonatal cardiomyocyte exhibited good adhesion and proliferation *In vivo* – can improve electrical conduction across a fibrotic scar in the injured heart	[44]

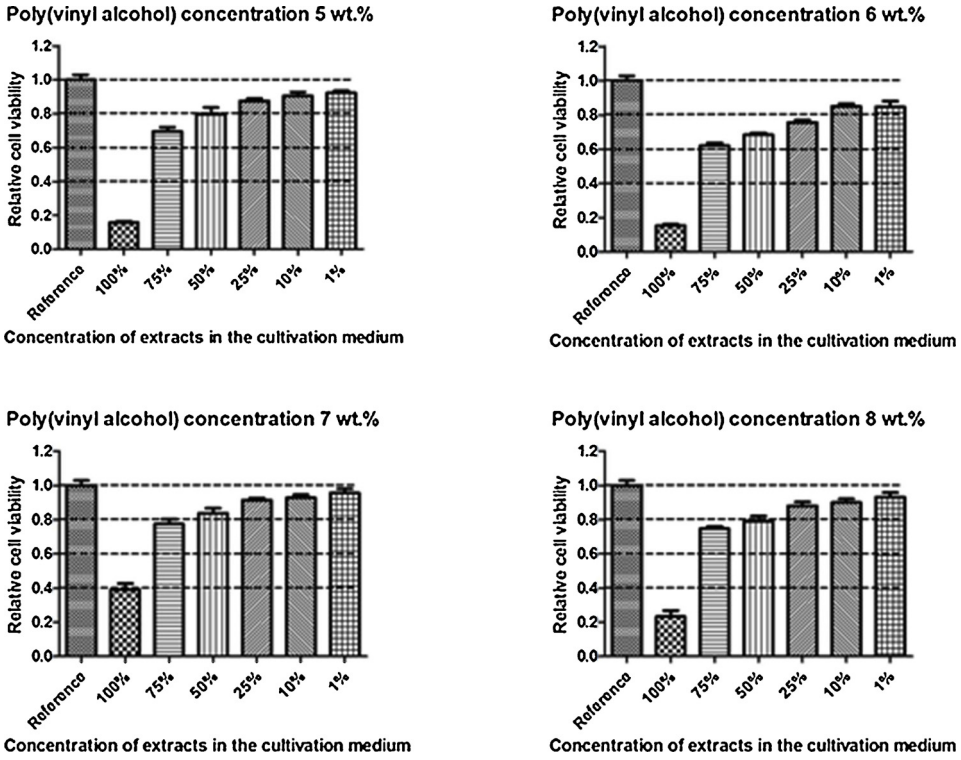

Fig. 3. Cytotoxicity of extracts of PPy/PVAL cryogels towards NIH/3T3 cells determined by MTT assay. The dashed lines highlight the limits of viability according to EN ISO 10993-5 where viability > 0.8 means no cytotoxicity, 0.6–0.8 mild cytotoxicity, 0.4–0.6 moderate toxicity, < 0.4 severe cytotoxicity.

same level after extensive washing of such cryogels with water for 3 months makes PPy in general [39] and PPy/PVAL cryogel in particular promising materials for potential biomedical applications.

3.2. Cytotoxicity

Considering the cytotoxicity of PPy/PVAL cryogels, the only moderate correlation of cytotoxicity to the different concentrations of PVAL was found (Fig. 3). In fact, the cytotoxicity of PPy/PVAL cryogel was observed only in the case of 100% concentration of extracts in cultivation medium. Adverse effect of 100% extracts is moreover connected to the change of acidity of cultivation medium due to releasing of residual acids from preparation procedure of cryogels (the testing was performed on native samples, without any additional purification). In the case of any application, the determined low cytotoxicity can be regarded as negligible because for lower concentration of extract the cytotoxicity is eliminated, especially for 7 and 8 wt% of PVAL in cryogel.

PVAL is generally considered as biocompatible material, thus the observed slight impact of extracts of PPy/PVAL cryogels on cell viability can be connected mainly to the presence of PPy. According to the study of Humpolíček et al. [3], the cytotoxicity as well as the embryotoxicity of PPy is closely connected to its form, salt *vs* base, and it is associated with the presence of low-molecular-weight impurities and not to the polymer itself. Observed biological properties of PPy/PVAL correspond to the generally good biocompatibility of PPy-based hydrogels (Table 2). There are, moreover, the studies demonstrating the superior properties of PPy-based materials towards the use in electrosensitive tissues, *e.g.*, cardiac patches [18]. The porous cryogels are thus promising for application as bio-interfaces.

4. Conclusions

The soft macroporous conducting cryogels were prepared by a single-step polymerization of pyrrole in the frozen aqueous solutions of poly(vinyl alcohol). Compressed freeze-dried composites have conductivity exceeding the conductivity of standard polypyrrole alone and the conductivity is maintained even when cryogels was washed with water (pH close to physiological conditions). The cryogels are soft with good mechanical properties and biocompatibility sufficient to make them suitable for potential biomedical applications.

Conflict of interest

The authors have declared no conflict of interest.

Acknowledgment

The authors wish to thank the Czech Science Foundation (17-05095S) for the financial support.

References

[1] B.G. Yan, Y. Wu, L. Guo, Recent advances on polypyrrole electroactuators, Polymers 9 (2017) 446.
[2] T.H. Le, Y.Y. Kim, H.S. Yoon, Electrical and electrochemical properties of conducting polymers, Polymers 9 (2017) 150.
[3] P. Humpolíček, V. Kašpárková, J. Pacherník, J. Stejskal, P. Bober, Z. Capáková, K.A. Radaszkiewicz, I. Junkar, M. Lehocký, The biocompatibility of polyaniline and polypyrrole: a comparative study of their cytotoxicity, embryotoxicity and impurity profile, Mater. Sci. Eng. C 91 (2018) 303–310.
[4] K.W. Shu, Y.F. Chao, S.L. Chou, C.Y. Wang, T. Zheng, S. Gambhir, G.G. Wallace, A "tandem" strategy to fabricate flexible graphene/polypyrrole nanofiber film using the surfactant-exfoliated graphene for supercapacitors, ACS Appl. Mater. Interfaces 10 (2018) 22031–22041.
[5] H.W. Gao, X.H. Wang, G.H. Wang, C. Hao, S.S. Zhou, C.X. Huang, An urchin-like $MgCo_2O_4$@PPy core–shell composite grown on Ni foam for a high-performance all-solid-state asymmetric supercapacitor, Nanoscale 10 (2018) 10190–10202.
[6] J.G. Wang, H.Y. Liu, H.Z. Liu, W. Hua, M.H. Shao, Interfacial constructing flexible V_2O_5@polypyrrole core − shell nanowire membrane with superior supercapacitive performance, ACS Appl. Mater. Interfaces 10 (2018) 18816–18823.
[7] W.L. Wei, P.C. Du, D. Liu, Q. Wang, P. Li, Facile one-pot synthesis of well-defined coaxial sulfur/polypyrrole tubular nanocomposites as cathodes for long-cycling lithium–sulfur batteries, Nanoscale 10 (2018) 13037–13044.
[8] Y. Liu, W.Y. Yan, X.W. An, X. Du, Z.D. Wang, H.L. Fan, S.B. Liu, X.G. Hao,

G.Q. Guan, A polypyrrole hollow nanosphere with ultra-thin wrinkled shell: Synergistic trapping of sulfur in Lithium-Sulfur batteries with excellent elasticity and buffer capability, Electrochim. Acta 271 (2018) 67–76.
[9] R. Jain, N. Jadon, A. Pawaiya, Polypyrrole based next generation electrochemical sensors and biosensors: A review, Trends Analyt. Chem. 97 (2017) 363–373.
[10] Z.D. Gu, Y.C. Xu, L. Chen, R.C. Fang, Q.F. Rong, X. Jin, L. Jiang, M.J. Liu, Macroporous conductive hydrogels with fatigue resistance as strain sensor for human motion monitoring, Macromol. Mater. Eng. 303 (2018) 1800339.
[11] Y.L. He, Q.Y. Gui, Y.X. Wang, Z. Wang, S.G. Liao, Y.P. Wang, A polypyrrole elastomer based on confined polymerization in a host polymer network for highly stretchable temperature and strain sensors, Small 14 (2018) 1800394.
[12] M.M. Ayad, W.A. Amer, S. Zaghlol, I.M. Minisy, P. Bober, J. Stejskal, Polypyrrole-coated cotton textile as adsorbent of methylene blue dye, Chem. Pap. 72 (2018) 1605–1618.
[13] N. Ballava, R. Dasb, S. Girib, A.M. Muliwac, K. Pillaya, A. Maity, L-Cysteine doped polypyrrole (PPy@L-Cyst): A super adsorbent for the rapid removal of Hg^{+2} and efficient catalytic activity of the spent adsorbent for reuse, Chem. Eng. J. 345 (2018) 621–630.
[14] A. Uma Devi, K. Divya, D. Rana, M. Sri Abirami Saraswathi, A. Nagendran, Highly selective and methanol resistant polypyrrole laminated SPVdF-*co*-HFP/PWA proton exchange membranes for DMFC applications, Mater. Chem. Phys. 212 (2018) 533–542.
[15] N. Aravindan, M.V. Sangaranarayanan, Influence of solvent composition on the anti-corrosion performance of copper–polypyrrole (Cu–PPy) coated 304 stainless steel, Prog. Org. Coat. 95 (2016) 38–45.
[16] L.L. Zhang, S.J. Liu, H.C. Han, Y. Zhou, S.C. Hu, C. He, Q.X. Yan, Studies on the formation process and anti-corrosion performance of polypyrrole film deposited on the surface of Q235 steel by an electrochemical method, Surf. Coat. Technol. 341 (2018) 95–102.
[17] S. Yang, L.K. Jang, S. Kim, J. Yang, K. Yang, S.W. Cho, J.Y. Lee, Polypyrrole/alginate hybrid hydrogels: Electrically conductive and soft biomaterials for human mesenchymal stem cell culture and potential neural tissue engineering applications, Macromol. Biosci. 16 (2016) 1653–1661.
[18] S. Liang, Y.Y. Zhang, H.B. Wang, Z.Y. Xu, J.G. Chen, R. Bao, B.Y. Tan, Y.L. Cui, G.W. Fan, W.X. Wang, W. Wang, W.G. Liu, Paintable and rapidly bondable conductive hydrogels as therapeutic cardiac patches, Adv. Mater. 30 (2018) 1704235.
[19] B. Tandon, A. Magaz, R. Balint, J.J. Blaker, S.H. Cartmell, Electroactive biomaterials: vehicles for controlled delivery of therapeutic agents for drug delivery and tissue regeneration, Adv. Drug Deliv. Rev. 129 (2018) 148–168.
[20] A.P. Tiwari, T.I. Hwang, J.M. Oh, B. Maharjan, S.G. Chun, B.S. Kim, M. Kumar Joshi, C.H. Park, C.S. Kim, pH/NIR-Responsive polypyrrole-functionalized fibrous localized drug-delivery platform for synergistic cancer therapy, ACS Appl. Mater. Interfaces 10 (2018) 20256–20270.
[21] R. Ramya, P. Muthukumaran, J. Wilson, Electron beam-irradiated polypyrrole decorated with Bovine serum albumin pores: Simultaneous determination of epinephrine and L-tyrosine, Biosens. Bioelectron. 108 (2018) 53–61.
[22] H. Karimi-Maleh, A. Bananezhad, M.R. Ganjali, P. Norouzi, A. Sadrnia, Surface amplification of pencil graphite electrode with polypyrrole and reduced graphene oxide for fabrication of a guanine/adenine DNA based electrochemical biosensors for determination of didanosine anticancer drug, Appl. Surf. Sci. 441 (2018) 55–60.
[23] P. Bober, J. Stejskal, I. Šeděnková, M. Trchová, L. Martinková, J. Marek, The deposition of globular polypyrrole and polypyrrole nanotubes on cotton textile, Appl. Surf. Sci. 356 (2015) 737–741.
[24] M. Omastová, P. Bober, Z. Morávková, N. Peřinka, M. Kaplanová, T. Syrový, J. Hromádková, M. Trchová, J. Stejskal, Towards conducting inks: polypyrrole-silver colloids, Electrochim. Acta 122 (2014) 296–302.
[25] Y. Li, P. Bober, D.H. Apaydin, T. Syrový, N.S. Sariciftci, J. Hromádková, I. Sapurina, M. Trchová, J. Stejskal, Colloids of polypyrrole nanotubes/nanorods: A promising conducting ink, Synth. Met. 221 (2016) 67–74.
[26] J. Stejskal, Conducting polymer hydrogels, Chem. Pap. 71 (2017) 269–291.
[27] A. Guiseppi-Elie, Electroconductive hydrogels: Synthesis, characterization and biomedical applications, Biomaterials 31 (2010) 2701–2716.
[28] L.C. Lopes, F.F. Simas-Tosin, T.R. Cipriani, L.F. Marchesi, M. Vidotti, I.C. Riegel-Vidotti, Effect of low and high methoxyl citrus pectin on the properties of polypyrrole based electroactive hydrogels, Carbohydr. Polym. 155 (2017) 11–18.
[29] J. Stejskal, P. Bober, M. Trchová, A. Kovalcik, J. Hodan, J. Hromádková, J. Prokeš, Polyaniline cryogels supported with poly(vinyl alcohol): soft and conducting, Macromolecules 50 (2017) 972–978.
[30] P. Humpolíček, K.A. Radaszkiewicz, Z. Capáková, J. Pacherník, P. Bober, V. Kašpárková, P. Rejmontová, M. Lehocký, P. Ponížil, J. Stejskal, Polyaniline cryogels: biocompatibility of novel conducting macroporous material, Sci. Rep. 8 (2018) 135.
[31] J. Stejskal, P. Bober, Conducting polymer colloids, hydrogels, and cryogels: common start to various destinations, Colloid Polym. Sci. 296 (2018) 989–994.
[32] P. Bober, M. Trchová, J. Kovářová, U. Acharya, J. Hromádková, J. Stejskal, Reduction of silver ions to silver with polyaniline/poly(vinyl alcohol) cryogels and aerogels, Chem. Pap. 72 (2018) 1619–1628.
[33] K.A. Milakin, U. Acharya, J. Hodan, M. Trchová, J. Stejskal, P. Bober, Effect of 1,3-phenylenediamine concentration on the properties of poly(aniline-*co*-1,3-phenylenediamine) cryogels, Mater. Lett. 229 (2018) 68–70.
[34] V.I. Lozinsky, Cryostructuring of polymeric systems. 50. Cryogels and cryotropic gel-formation: terms and definitions, Gels 4 (2018) 77.
[35] M. Omastová, M. Trchová, J. Kovářová, J. Stejskal, Synthesis and structural study of polypyrroles prepared in the presence of surfactants, Synth. Met. 138 (2003) 447–455.
[36] J. Kopecká, D. Kopecký, M. Vrňata, P. Fitl, J. Stejskal, M. Trchová, P. Bober, Z. Morávková, J. Prokeš, I. Sapurina, Polypyrrole nanotubes: mechanism of formation, RSC Adv. 4 (2014) 1551–1558.
[37] N.V. Blinova, J. Stejskal, M. Trchová, J. Prokeš, M. Omastová, Polyaniline and polypyrrole: a comparative study of the preparation, Eur. Polym. J. 43 (2007) 2331–2341.
[38] U. Acharya, P. Bober, M. Trchová, A. Zhigunov, J. Stejskal, J. Pfleger, Synergistic conductivity increase in polypyrrole/molybdenum disulfide composite, Polymer 50 (2018) 130–137.
[39] J. Stejskal, M. Trchová, P. Bober, Z. Morávková, D. Kopecký, M. Vrňata, J. Prokeš, M. Varga, E. Watzlová, Polypyrrole salts and bases: Superior conductivity of nanotubes and their stability towards the loss of conductivity by deprotonation, RSC Adv. 6 (2016) 88382–88390.
[40] A.M. Youssef, M.E. Abdel-Aziz, E.S.A. El-Sayed, M.S. Abdel-Aziz, A.A. Abd El-Hakim, S. Kamel, G. Turky, Morphological, electrical & antibacterial properties of trilayered Cs/PAA/ PPy bionanocomposites hydrogel based on Fe_3O_4-NPs, Carbohydr. Polym. 196 (2018) 483–493.
[41] Y. Bu, H.-X. Xu, X. Li, W.-J. Xu, Y.-X. Yin, H.-L. Dai, X.-B. Wang, Z.-J. Huang, P.-H. Xu, A conductive sodium alginate and carboxymethyl chitosan hydrogel doped with polypyrrole for peripheral nerve regeneration, RSC Adv. 8 (2018) 10806–10817.
[42] N. Sahiner, S. Demirci, N. Aktas, Superporous cryogel/conductive composite systems for potential sensor applications, J. Polym. Res. 24 (2017) 126.
[43] S. Saha, P. Sarkar, M. Sarkar, B. Giri, Electroconductive smart polyacrylamide–polypyrrole (PAC–PPY) hydrogel: a device for controlled release of risperidone, RSC Adv. 5 (2015) 27665–27673.
[44] Z. Cui, N.C. Ni, J. Wu, G.Q. Du, S. He, T.M. Yau, R.D. Weisel, H.W. Sung, R.K. Li, Polypyrrole-chitosan conductive biomaterial synchronizes cardiomyocyte contraction and improves myocardial electrical impulse propagation, Theranostics 8 (2018) 2752–2764.